UNIVERSITAT DE BARCELONA

The Contribution of the Polyamine Spermine to Plant Defense

Chi Zhang

UNIVERSITAT DE BARCELONA

The Contribution of the Polyamine Spermine to Plant Defense

Chi Zhang

2024

UNIVERSITAT DE BARCELONA

FACULTAT DE FARMÀCIA I CIÈNCIES DE L'ALIMENTACIÓ

DOCTORAT EN BIOTECNOLOGIA

The Contribution of the Polyamine Spermine to Plant Defense

Memòria presentada per Chi Zhang per optar al títol de doctor per la

Universitat de Barcelona

Rubén Alcázar Hernández

Director i Tutor

Chi Zhang

Doctorand

ACKNOWLEDGEMENTS

ACKNOWLEDGEMENTS

First and foremost, I express my gratitude to my supervisor Dr. Rubén Alcázar Hernández for guiding me throughout my doctoral project. He has been supportive since I applied for a doctoral scholarship. His knowledge and patience during my doctoral project deeply moved and impressed me, leading to significant benefits on my part.

Next, I extend my thanks to my colleagues, including Ester Murillo, Lucía Díaz, Kostadin E. Atanasov, Changxin Liu, Ana Fleitas, Nazanin Arafaty, Cristina Noguera, Anna Valls, Cuiyun Deng, Jiaqi Zhao, and others. I appreciate their collaborative efforts, and the friendly and efficient atmosphere within our work team. Special gratitude goes to Edgar Perez, Miguel Angel, Diego Alberto, and Ainoa Escrich for the enjoyable time we spent together.

I am thankful to University of Barcelona for providing an excellent learning platform, particularly to the Section of Plant Physiology, Department of Biology, Healthcare & Environment, and Faculty of Pharmacy and Food Sciences.

Acknowledgments also go to Dr. Francesc Viladomat Meya, the head of our department, for signing of a lot of documents in my work. I appreciate the strong support from the department secretary, Mari Carmen Molina, and Angel Gutiérrez.

I want to convey my appreciation to the Servei de Camps Experimentals de la Universitat de Barcelona for their assistance in facilitating my work, particularly in the cultivation of most of my experimental model plant, *Arabidopsis thaliana*. A special acknowledgment is extended to Xavier Aranda, Josep Matas, and Francesc Prenyanosa for their dedicated and hard work.

Furthermore, I am delighted to have made new Chinese friends during my time here, including Jiaqi Xu, Meijian Zhang, Ting Zhou, and others. Our exploration of beautiful places in Europe and exposure to diverse cultures and climates have been memorable.

I express my appreciation to the China Scholarship Council (CSC) for their financial support, the Education Section of the Chinese Embassy in Barcelona for documentary assistance in my renewal Spain residency, and the annual Spring Festival gift pack.

Last but not least, heartfelt thanks to my family for their unwavering support, my parents for their love, and my brothers and sisters for their understanding. Their unwavering love, support, and encouragement for me have been invaluable.

Chi Zhang

Barcelona

March 11, 2024

Summary

Polyamines are essential in plant defense, with putrescine (Put), spermidine (Spd), and spermine (Spm) being the most abundant ones. In response to various pathogens, including *Pseudomonas syringae pv. tomato* DC3000 (*Pst* DC3000), polyamine levels increase, highlighting their importance in immune responses.

Our research compared the effects of Put and Spm on pathogen-associated molecular pattern (PAMP)-triggered immunity (PTI) responses in *Arabidopsis*. While Put enhances the production of reactive oxygen species (ROS) triggered by PAMPs like flg22, Spm exhibits an inhibitory effect on ROS burst dependent on *RBOHD (RESPIRATORY BURST OXIDASE HOMOLOG D)*. It also attenuates cytosolic calcium influx stimulated by flg22, suggesting a broader influence on PTI signaling. Genome-Wide Association Studies (GWAS) conducted in 136 *Arabidopsis* accessions from diverse populations aimed to unravel the genetic determinants underlying the Spm inhibitory effect on flg22-induced ROS production. This approach identified associated polymorphisms, shedding light on candidate genes involved in this process.

Additionally, we also found that *Pst* DC3000 stimulates Put biosynthesis through coronatine perception and jasmonic acid (JA) signaling, independently of salicylic acid (SA). Conversely, Spm deficiency resulted in heightened JA signaling and compromised SA-mediated defense responses, stimulating disease resistance to *Botrytis cinerea*. Moreover, Spm deficiency increased endoplasmic reticulum (ER) stress signaling in response to *Pst* DC3000, suggesting a role for Spm in buffering ER stress during defense.

In summary, this research provides valuable insights into the differential contributions of polyamines to plant defense.

Resumen

Las poliaminas son esenciales para la defensa de las plantas, siendo la putrescina (Put), la espermidina (Spd) y la espermina (Spm) las poliaminas más abundantes. En respuesta a diferentes patógenos, incluyendo *Pseudomonas syringae* pv. *tomato* DC3000 *(Pst* DC3000*)*, los niveles de poliaminas aumentan, destacando su importancia en las respuestas inmunitarias.

Nuestra investigación ha comparado los efectos de la Put y la Spm en las respuestas inmunes desencadenadas por patrones moleculares asociados a patógenos (PTI) en Arabidopsis. Mientras que la Put incrementa la producción de especies reactivas de oxígeno (ROS) desencadenadas por PAMPs como flg22, la Spm provoca un efecto inhibidor de la explosión oxidativa dependiente de *RBOHD (RESPIRATORY BURST OXIDASE HOMOLOG D)*. También atenúa el influjo de calcio citosólico estimulado por flg22, lo que sugiere una influencia más amplia en las vías de señalización de PTI.

Los estudios GWAS realizados utilizando 136 accesiones de Arabidopsis de diversas poblaciones, nos han permitido identificar los determinantes genéticos detrás del efecto inhibidor de la Spm en la producción de ROS inducida por flg22.

Además, también encontramos que *Pst* DC3000 estimula la biosíntesis de Put a través de la percepción de coronatina y la señalización del ácido jasmónico (JA), independientemente del ácido salicílico (SA). Por el contrario, la deficiencia de Spm resultó en una mayor señalización de JA y una inhibición de las respuestas de defensa mediadas por SA, estimulando la resistencia a la enfermedad causada por *Botrytis cinerea*. Además, la deficiencia de Spm se relacionó con un aumento de la señalización de estrés en el retículo endoplásmico (RE) en respuesta al *Pst* DC3000, lo que sugiere un papel de la Spm en la mitigación del estrés del ER durante la defensa.

En resumen, esta investigación proporciona valiosas contribuciones sobre las funciones diferenciales de las poliaminas en la defensa de las plantas.

Contents

List of Abbreviations

A. thaliana: Arabidopsis thaliana

ACAs: AUTOINHIBITED Ca $^{2+}$ -ATPases

ACC:1-aminocyclopropane-1-carboxylic acid

ACD6: *ACCELERATED CELL DEATH 6*

ACIF1: AVR9/CF-9-INDUCED F-BOX1

ACL5: *ACAULIS 5*

ACX: ACYL-COA OXIDASE

ADC: ARGININE DECARBOXYLASE

ADR1: ACTIVATED DISEASE RESISTANCE 1

AGD2: *ABERRANT GROWTH AND DEATH 2*

AIH: AGMATINE IMINOHYDROLASE

ALD1: *AGD2-LIKE DEFENSE RESPONSE PROTEIN 1*

APX: ASCORBATE PEROXIDASE

ATG8: AUTOPHAGY-RELATED (ATG) PROTEIN 8

AVR: Avirulence

BAK1: *BRASSINOSTEROID INSENSITIVE ASSOCIATED RECEPTOR KINASE 1*

bHLH: basic HELIX-LOOP-HELIX

BIK1: *BOTRYTIS-INDUCED KINASE 1*

BIR1: *BAK1-INTERACTING RECEPTOR-LIKE KINASE 1*

BSA: Bulk segregant analysis

BSMT1: *BENZOIC ACID/SA CARBOXYL METHYLTRANSFERASE 1*

bZIP: basic leucine ZIPPER

Cad: Cadaverine

CAMTA: CALMODULIN-BINDING TRANSCRIPTION ACTIVATOR

CAT: *CATALASE*

CAXs: *Ca^{2+} EXCHANGERS*

CBL-CIPKs: CBL - INTERACTING PROTEIN KINASES

CaMs: CALMODULIN PROTEINS

CBLs: CALCINEURIN B-LIKE PROTEINS

CC: Coiled coil

CC-NB-LRR: Coiled coil- Nucleotide binding- Leucine-rich repeat

Cd: Cadmium

cDAMPs: constitutive DAMPs

CDPKs: *CALCIUM-DEPENDENT PROTEIN KINASES*

CERK1: *CHITIN ELICITOR RECEPTOR KINASE1*

CMLs: CaM-LIKE PROTEINS

CMV: Cucumber mosaic virus

CNGCs: CYCLIC NUCLEOTIDE GATED CHANNELS

CNL: CC-NB-LRR

COI1: *CORONATINE INSENSITIVE 1*

COR: Coronatine

CPA: N-CARBAMOYLPUTRESCINE AMIDOHYDROLASE

CPR1: *CONSTITUTIVE EXPRESSER OF PATHOGENESIS RELATED GENES 1*

CRKs: CYSTEINE-RICH RECEPTOR-LIKE KINASES

cPTIO: 2-4-carboxyphenyl-4,4,5,5-tetramethylimidazoline-1-oxyl-3-oxide

CuAO: COPPER AMINO OXIDASE

CYP94: CYTOCHROME P450 94

DAB: 3, 3'-diaminobenzidine

DAMPs: Damage-associated molecular patterns

DFMA: DL-α-difluoromethylarginine

DMR6: *DOWNY MILDEW RESISTANT 6*

DMTU: 1,3-dimethyl-2-thiourea

DPI: Diphenylene iodonium

DREB: DEHYDRATION RESPONSIVE ELEMENT BINDING

ECAs: ER-type Ca^{2+} ATPases

ECD: Extracellular domain

EDR1: *ENHANCED DISEASE RESISTANCE 1*

EDS: *ENHANCED DISEASE SUSCEPTIBILITY*

EFR: EF-Tu RECEPTOR

EF-Tu: Elongation Factor Tu

EGF-like: Epidermal growth factor-like

EIL1: *EIN3-LIKE 1*

EIN2: *ETHYLENE INSENSITIVE 2*

EIN3: *ETHYLENE INSENSITIVE 3*

EMS: Ethyl methanesulfonate

EPS1: *ENHANCED PSEUDOMONAS SUSCEPTIBILITY 1*

ERF: *ETHYLENE RESPONSIVE FACTOR*

CBP60g: CALMODULIN BINDING PROTEIN 60-like g

ET: Ethylene

ETI: Effector-triggered immunity

ETS: Effector-triggered susceptibility

Flg22: Flagellin 22

FLS2: *FLAGELLIN SENSING* 2

FMO1: *FLAVIN-DEPENDENT-MONOOXYGENASE 1*

GLRs: GLUTAMATE RECEPTORS

GSL5: *GLUCAN SYNTHASE-LIKE* 5

GUS: β-glucuronidase

GWAS: Genome-Wide Association Studies

HCAAs: hydroxycinnamic acid amides

HPCA1: *HYDROGEN PEROXIDE INDUCED Ca^{2+} INCREASE 1*

HPLC: High performance liquid chromatography

HR: Hypersensitive response

IC-9-Glu: isochorismate-9-glutamate

ICS: *ISOCHORISMATE SYNTHASE*

iDAMPs: inducible DAMPs

iGluR: *IONOTROPIC GLUTAMATE RECEPTOR*

JA: Jasmonic acid

JA-Ile: JA-isoleucine

JAR1: *JASMONOYL-ISOLEUCINE SYNTHETASE 1*

KD: Kinase domain

LPO: Lipid peroxidation

LPS: Lipopolysaccharide

LRR: Leucine-rich repeat

LUC: Luciferase

LYK5: *LYSIN MOTIF-CONTAINING RECEPTOR-LIKE KINASE 5*

LysM: Lysine motif

MAPK: *MITOGEN-ACTIVATED PROTEIN KINASE*

MCA: MECHANOSENSITIVE PROTEIN CHANNEL

MCUC: *MITOCHONDRIAL CALCIUM UNIPORTER COMPLEX*

MeSA: methyl salicylate

MGDG: Monogalactosyldiacyl - glycerol

MS: Murashige & Skoog

MYB: *MYELOBLASTOSIS*

NAC: *Petunia NAM and Arabidopsis ATAF1, ATAF2, and CUC2*

NADPH: Nicotinamide adenine dinucleotide phosphate

NATA1: *N-ACETYL TRANSFERASE ACTIVITY 1*

NB: Nucleotide - binding

NDR1: *NON-RACE-SPECIFIC DISEASE RESISTANCE 1*

NHP: N-hydroxypipecolic acid

NINJA：*NOVEL INTERACTOR OF JAZ*

NLR: Nucleotide binding leucin rich repeat

NO: Nitric oxide

NPR1: NONEXPRESSOR OF PATHOGENESIS-RELATED GENES 1

ODC: *ORNITHINE DECARBOXYLASE*

OGs: Oligogalacturonides

ORA59: *OCTADECANOID-RESPONSIVE ARABIDOPSIS AP2/ERF 59*

ORM: OROSOMUCOID

OSCA: *HYPEROSMOLALITY-GATED CALCIUM-PERMEABLE CHANNEL*

OST1: *OPEN STOMATA 1*

P. syringae: Pseudomonas syringae

PA(s): Polyamine(s)

PAD4: *PHYTOALEXIN-DEFICIENT 4*

PAL: *PHENYLALANINE AMMONIA LYASE*

PAMP: Pathogen-associated molecular pattern

PAO: *POLYAMINE OXIDASE*

PBL1: *PBS1-LIKE 1*

PBS: *AvrPphB SUSCEPTIBLE*

PCD: Programmed cell death

PDF1.2: *PLANT DEFENSIN GENE 1.2*

PEPR1: PEPTIDES RECEPTOR 1

PGN: Peptidoglycan

Pip: Pipecolic acid

PLD: PHOSPHOLIPASE D

PM: Plasma membrane

PMR4: *POWDERY MILDEW RESISTANT 4*

PR1: *PATHOGENESIS-RELATED GENE 1*

PRRs: Pattern recognition receptors

PRXs: *PEROXIDASES*

PSII: photosystem II

Pst DC3000: Pseudomonas syringae pv tomato DC3000

PTI: PAMP-triggered immunity

PUB12 and *PUB13*: *PLANT U-BOX 12* and *13*

Put: Putrescine

QTL: Quantitative trait loci

RBO: *RESPIRATORY BURST OXIDASE*

RBOH: *RBO HOMOLOG*

RD29A: *RESPONSE-TO-DEHYDRATION 29A*

RLCK: *RECEPTOR-LIKE CYTOPLASMIC KINASE*

RLKs: *RECEPTOR LIKE KINASES*

RLPs: *RECEPTOR LIKE PROTEINS*

ROS: Reactive oxygen species

RPP1: *RECOGNITION OF PERONOSPORA PARASITICA 1*

RPW8: *RESISTANCE TO POWDERY MILDEW 8*

SA: Salicylic acid

SAA: Systemic acquired acclimation

SAC: *SUPPRESSOR-OF-ACL5*

SAG: Salicylic acid 2-O-β-d-glucose

SAM: S-adenosylmethionine

SAMDC: *SAM DECARBOXYLASE*

SAR: Systemic acquired resistance

SARD1: *SYSTEMIC ACQUIRED RESISTANCE DEFICIENT 1*

SID2: *SALICYLIC ACID (SA) INDUCTION DEFICIENT 2*

SLAC1: *SLOW ANION CHANNEL-ASSOCIATED 1*

SLAH3: *SLAC1 HOMOLOG 3*

SKL: Serine-lysine-leucine

SNC1: *SUPPRESSOR OF NPR1-1 CONSTITUTIVE 1*

SOBIR1: SUPPRESSOR OF BIR 1-1

SOD: *SUPEROXIDE DISMUTASE*

SON1: *SUPPRESSOR OF NIM1-1*

SPDS: *SPERMIDINE SYNTHASE*

TALE: Transcription-activator-like effector

TFs: Transcription factors

TIR: Toll/interleukin-1 receptor

TM: Transmembrane domain

TMV: *Tobacco mosaic virus*

TIR-NB-LRR: Toll/interleukin-1 receptor (TIR)- Nucleotide binding- Leucine-rich repeat

TPCs: *TWO PORE CHANNELS*

TSPMS: *THERMOSPERMINE SYNTHASE*

uORF: upstream Open Reading Frame

VIGS: Virus-induced gene silencing

VSP2: *VEGETATIVE STORAGE PROTEIN 2*

ZAR1: *HOPZ-ACTIVATED RESISTANCE 1*

General Introduction

1. Arabidopsis *thaliana*

1. 1 The history of *Arabidopsis thaliana*

A. thaliana belongs to the mustard (*Brassicaceae*) family, which includes cultivated species like cabbage and radish, and is widely distributed in natural habitats across Europe, Asia, and North America (Krämer, 2015; Meinke et al., 1998). The entire life cycle of *A. thaliana*, encompassing seed germination, rosette plant formation, main stem bolting, flowering, and the maturation of the first seeds, unfolds within 6 weeks (Meinke et al., 1998). *A. thaliana* exhibits a high frequency of self-pollination in the wild (Abbott & Gomes, 1989). This results in individuals being homozygous at most loci.

The advantages of using *A. thaliana* as a genetic model organism include its small genome size, short generation time, ease of hybridization, strong reproductive capability, and possible self-pollination, along with broad selection of accessions and mutant lines and the ability to perform saturated mutagenesis screens in the laboratory (Fridman et al., 2023; Laibach, 1943; Meyerowitz & Pruitt, 1985; Provart et al., 2016; Somssich, 2019). These factors have collectively led to a significant increase in the volume of research on this species.

Initially documented with the name of *Pilosella siliquata* by the physician Johannes Thal in the Harz Mountains of Northern Germany in 1577, this plant was featured, renamed, and placed into the genus Arabis in Carolus Linnaeus's *Species Plantarum II*, published in 1753 (Krämer, 2015; Woodward & Bartel, 2018). In 1842, Gustav Heynhold elevated *A. thaliana* to the generic level, designating *A. thaliana* as the exclusive representative of the genus (Al-Shehbaz & O'Kane, 2002; Woodward & Bartel, 2018).

In 1907, Friedrich Laibach noted that *A. thaliana* has only five pairs of chromosomes (Laibach, 1907). Laibach is acknowledged as the pioneer of *A. thaliana* research. In 1943, Laibach highlighted the advantages of using *A. thaliana* for scientific research: easy to grow, small genome, short lifecycle, high seed yield, can be crossed and mutagenized, and proposed considering *A. thaliana* as a model plant (Laibach, 1943, 1951). Additionally, in 1945, Erna Reinholz, Laibach's student, used X-ray treatment to isolate the first induced mutant of *A. thaliana* (Meyerowitz, 2001; Somssich, 2019).

In 1964, Gerhard Röbbelen collaborated with Laibach, Andreas Müller, George Rédei, and Jiri Veleminsky to publish the first *A. thaliana* Information Service (AIS) newsletter (Meyerowitz, 2001; Somerville & Koornneef, 2002). Röbbelen with Albert Kranz administered a seed stock center housing Röbbelen's own mutants and Laibach’s assortment of ecotypes (later referred to as accessions) alongside various induced mutants (Koornneef & Meinke, 2010; Somerville & Koornneef, 2002). Röbbelen orchestrated the inaugural International *Arabidopsis* Symposium in 1965 in Göttingen, Germany, which drew attendance from 25 participants (Koornneef & Meinke, 2010; Meyerowitz, 2001; Somerville & Koornneef, 2002).

In 1975, George Rédei published a notable review article in the *Annual Review of*

Genetics highlighting *A. thaliana* as a model genetic plant and reiterated the advantages as pointed out by Laibach over 30 years ago (Koornneef & Meinke, 2010; Rédei, 1975). In 1957, Rédei used X-ray to mutagenize Landsberg seeds which were originally from Laibach and screened for mutants of interest (Rédei, 1992; Somssich, 2019). During the mutant screening process, Rédei discovered that Landsberg was not homozygous and could be a mixture of multiple plants (Rédei, 1962, 1992; Somssich, 2022). Therefore, Rédei went back to the original Landsberg seeds that had not been treated with X-rays and established a new homozygous plant for subsequent research (Somssich, 2019, 2022). Following Laibach's rule of naming according to the place of discovery, Rédei named this accession *Columbia (Col)* (Rédei, 1975; Somssich, 2019, 2022).

In 1983, Maarten Koornneef et al. released the first comprehensive genetic linkage map of *A. thaliana,* which comprised 76 loci allocated in five linkage groups (Koornneef et al., 1983). In 1986, Elliot Meyerowitz et al. first reported the cloning of a gene coding for *ALCOHOL DEHYDROGENASE* (*ADH*) in *A. thaliana* (Chang & Meyerowitz, 1986). In 1988, the Meyerowitz lab published the first restriction fragment length polymorphism (RFLP) linkage map of the *A. thaliana* genome, which included 90 molecular markers randomly distributed across the genome (Chang et al., 1988).

In 2000, the *A. thaliana* complete genomic sequence was reported, marking the first fully sequenced eukaryotic plant genome, and holding immeasurable value for biological studies (The *Arabidopsis* Genome, 2000). *A. thaliana* carries five chromosomes of approximately 125 million base pairs (125 Mbp) and over 25,000 genes sorted in 11,000 families, of which only ~9% had been experimentally characterized with assigned functions (The *Arabidopsis* Genome, 2000). In contrast, the rice genome is approximately 400 to 430 Mb (Eckardt, 2000). In 2005, the map-based rice genome sequence was drawn, which showed that 71% of the total 37,544 non-transposable element-related protein-coding genes had putative homologs in *A. thaliana* (International Rice Genome Sequencing, 2005). In 2017, the *A. thaliana* genome annotation was updated (Cheng et al., 2017).

The completion of the *A. thaliana* genome significantly accelerated research involving mutants. The main collections of T-DNA insertion mutant lines currently include SALK, SAIL, GABI-Kat, and WiscDsLox. The three most used accessions in *A. thaliana* are *Landsberg erecta* (*Ler*)*, Columbia (Col)*, and *Wassilewskija* (*Ws*), with the *Col* accession being employed in most mutant collections. The SALK lines were constructed by the Salk Institute and developed in the lab of Joseph R. Ecker (Alonso et al., 2003), which is the most used collection worldwide. The SAIL (Syngenta *A. thaliana* Insertion Library) population was characterized by amplification of DNA fragments flanking the T-DNA left borders from approximately 100,000 transformed lines using the method of thermal asymmetric interlaced (TAIL)-PCR (Sessions et al., 2002). The GABI-Kat line was constructed by the Max Planck Institute for Plant Breeding Research in Germany (Rosso et al., 2003). The WiscDsLox collection developed by University of Wisconsin-Madison, comprises 10,459 T-DNA lines generated using the *A. thaliana* accession *Col* (Woody et al., 2007). Collectively, these lines encompass over 260,000 individual mutants, each representing at least one insertion mutation in almost every *A. thaliana* gene (O'Malley et al., 2015).

1.2 Forward and reverse genetics

In *A. thaliana* research, the most used genetic research strategies include forward and reverse genetics. The forward (from-phenotype-to-gene) method aims to identify the sequence changes underlying a specific mutant phenotype, starting from already available or specifically searched and predicted mutants with the phenotype of interest (Peters et al., 2003). For example, in 1999, Fletcher et al. used forward genetics to clone a small, predicted extracellular protein *CLAVATA 3* and identified that this gene could participate in the proliferation and differentiation of the shoot apical meristem tissue (Fletcher et al., 1999; Fletcher & Meyerowitz, 2000). Forward and reverse genetics approaches employed in plant research can be seen in figure 1.

The first step in forward genetics is to obtain mutants (Aklilu, 2021). There are three primary approaches to induce mutations: one involves employing the mutagen EMS (ethyl methanesulfonate) for chemical mutagenesis (Greene et al., 2003); another entail utilizing X-ray for physical mutagenesis; and the third method involves *Agrobacterium*-mediated T-DNA transformation to generate mutants (Alonso et al., 2003). Different populations can be used for gene mapping, including F2 populations, backcross (BC) populations, recombinant inbred lines (RILs), and double haploids (DH). Gene mapping can be performed through different methods such as bulk segregant analysis (BSA) (Zou et al., 2016), Quantitative trait loci (QTL) mapping (Sahu et al., 2020), Genome-wide association studies (GWAS) (Huang & Han, 2014; Miculan et al., 2021), and Mapping-Based Cloning (Peters et al., 2003).

Reverse genetics is a strategy to determine the function of a specific gene by studying the phenotype of individuals with alterations in the gene of interest (Sessions et al., 2002). For reverse genetics, it is required to obtain candidate genes using other approaches, those including different 'omics' such as transcriptomic, metabolomic and proteomic analyses (Weckwerth et al., 2020).

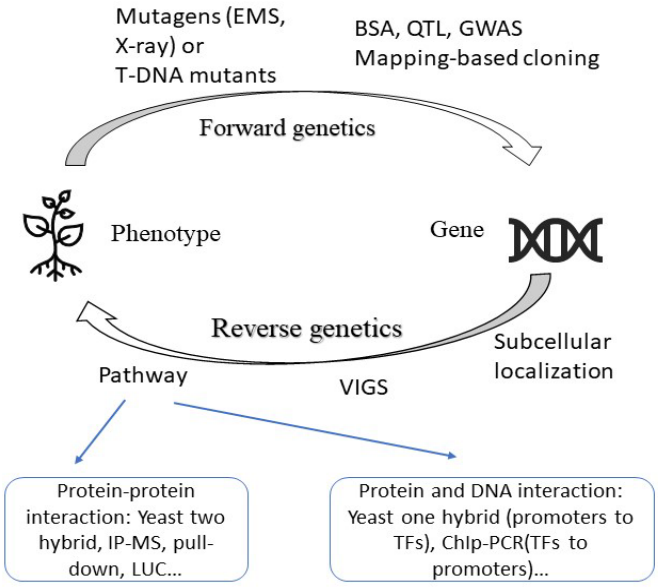

Figure 1. Forward and reverse genetics approaches employed in plant research. BSA: Bulk segregant

analysis, EMS: Ethyl methanesulfonate, QTL: Quantitative trait loci, GWAS: Genome-wide association studies, VIGS: Virus-induced gene silencing, TFs: Transcription factors, Chlp-PCR: Chromatin Immunoprecipitation-Quantitative Polymerase Chain Reaction, LUC: Luciferase, IP-MS: Immunoprecipitation-Mass Spectrometry.

2. The plant immune system

The term "innate immunity" was established by Charles Janeway (Janeway, 1989). In the 1990s, Janeway proposed the groundbreaking hypothesis about the occurrence of pathogen-associated molecular patterns (PAMPs) and pattern recognition receptors (PRRs) that recognize these PAMPs (Janeway, 1989). The first insights into innate immunity were established in animal models. In *Drosophila*, two primary pathways exist for recognizing microbes. The Toll pathway is responsible for recognizing fungal and gram-positive bacterial pathogens, while the Imd pathway is essential for recognizing and responding to Gram-negative bacterial infections (Medzhitov, 2001; Tanji et al., 2007). In 1996, Jules Hoffmann's team discovered Toll's role in *Drosophila*'s resistance to fungal infection, where Toll-activated mutants consistently produced antifungal peptides, contrasting with Toll-deletion mutants that lose their ability to combat fungal infections (Lemaitre et al., 1996,1997). Subsequently, Bruce Beutler's research team identified that *TLR4 (Toll-like receptor 4)*, a *Drosophila* protein Toll homolog, primarily evolved to aid in recognizing LPS (lipopolysaccharide) in mice (Beutler, 2002; Poltorak et al., 1998). Due to their groundbreaking work and significant contributions in the field of innate immunity, they jointly received the Nobel Prize in 2011 (Nüsslein-Volhard, 2022).

2.1 Introduction to the plant immune system

Unlike most animals, plants typically do not move, but some can persist for centuries. Plant natural immunity was established slightly later than animals. In the last two decades, studies using the plant-pathogen interaction model of *A. thaliana* and *Pseudomonas syringae* have revealed many components of plant immunity (Xin et al., 2018). In plants, two distinct strategies have been developed for detecting pathogens, namely PTI and ETI (Jones & Dangl, 2006).

The frontline of active plant defense is established by PRRs (pattern recognition receptors), which are cell surface receptors identifying PAMPs (pathogen associated molecular patterns) (Thomma et al., 2011). Activation of PRRs results in PAMP-triggered immunity (PTI) (Engelsdorf et al., 2018). In turn, effective pathogens utilize effectors that enhance pathogen virulence and disrupt PTI, leading to effector-triggered susceptibility (ETS) (Jones & Dangl, 2006). For example, the virulent pathogen of tomato and *A. thaliana, Pst DC3000* (*Pseudomonas syringae* pv. *tomato DC3000*), deploys virulence effector proteins into the plant cell host, via the type III secretion system (T3SS), thus inhibiting PTI immune responses (Guttman et al., 2014; Li et al., 2002).

Confronting the attack of pathogenic microorganisms, plants have intracellular receptor proteins known as NLRs (nucleotide-binding/leucine-rich-repeat receptors), which trigger the so-called effector-triggered immunity (ETI) upon detecting pathogenic

effectors, typically impeding the invasion of pathogens (Cui et al., 2015). ETI could lead to the establishment of the hypersensitive response (HR), leading to programmed cell death (PCD) (Coll et al., 2011). Plants have developed resistance (R) proteins that either directly or indirectly recognize certain effectors, which are referred to as avirulence (AVR) proteins (Dangl & Jones, 2001; Jones & Dangl, 2006; Petit-Houdenot & Fudal, 2017). Upon local activation of PTI and/or ETI, distant leaves can induce SAR (systemic acquired resistance), effectively limiting pathogen spread across the foliage (Zeier, 2021).

PTI involves the detection of PAMPs, but also danger-associated molecular patterns (DAMPs) that are derived from cellular damage (Zipfel, 2014). Various molecules, such as flg22 (flagellin22), EF-Tu (elongation Factor-Tu), and peptidoglycans derived from bacteria, have demonstrated immune-stimulating properties, serving as PAMPs (Ge et al., 2022) (Fishman & Shirasu, 2021; Kemen & Jones, 2012). In addition, host cell damage releases substances, such as extracellular ATP (Tanaka et al., 2014), that can behave like DAMPs (Ge et al., 2022). DAMPs are clasified as constitutive (cDAMPs) and inducible (iDAMPs) (Tanaka & Heil, 2021). The cDAMPs, such as oligosaccharides, nucleotides, and amino acids, carry out fundamental and conserved functions, manifesting a signaling role only in instances of cellular damage (Ge et al., 2022; Tanaka & Heil, 2021). In contrast, immunomodulatory peptides (also referred to as phytocytokines) serve solely as signals and, when subjected to injury, become activated as inducible DAMPs (iDAMPs). (Ge et al., 2022; Schilmiller & Howe, 2005; Tavormina et al., 2015).

PRRs are divided into *RECEPTOR LIKE KINASES* (*RLKs*) and *RECEPTOR LIKE PROTEINS* (*RLPs*) depending on the presence of the kinase domain (KD) (Tang et al., 2017). *RLKs* contain a ligand-binding extracellular domain (ECD), a single-pass transmembrane domain (TM), and an intracellular KD, whereas *RLPs* lack the KD (Macho & Zipfel, 2014). The family of *RLKs* comprises over 600 members, providing up to 60% of all kinases present in *A. thaliana* (Shiu & Bleecker, 2003). Based on variations in the ECD, PRRs can be categorized in leucine-rich repeat (LRR), lysine motif (LysM), lectin domain, epidermal growth factor-like (EGF-like) domain, domain of unknown function 26 (Duf26) and others (Gandhi & Oelmüller, 2023; Ngou et al., 2024; Tang et al., 2017; Wrzaczek et al., 2010; Yu et al., 2021).

The NLRs contain a N-terminal domain, a central NB-ARC (nucleotide-binding domain adapter shared by APAF-1, R proteins, and CED-4) and C-terminal LRR domain (Steele et al., 2019). According to the differences in N-terminal domains, NLRs can be divided into coiled-coil (CC)-NB-LRRs and Toll/interleukin-1 receptor (TIR)-NB-LRRs (Bentham et al., 2018). The NB-ARC domain engages in ATP/ADP exchange by undergoing conformational changes (Rafiqi et al., 2009; Tameling et al., 2006). NLRs, upon activation, often assemble into oligomeric complexes known as inflammasomes in animals and resistosomes in plants, subsequently triggering regulated cell death termed hypersensitive response (HR) (Bi et al., 2021). The HOPZ-*ACTIVATED RESISTANCE 1* (*ZAR1*), a typical CC-NB-LRR with a canonical CC domain, can detect various pathogen effector proteins, such as HopZ1a, HopF1, HopX1, HopO1, and HopBA1 from *Pseudomonas syringae* tomato, XopJ4 from *Xanthomonas perforans*, and AvrAC from *Xanthomonas campestris campestris* (Bi et al., 2021; Lewis

et al., 2013; Seto et al., 2017; Wang et al., 2015). The *RECOGNITION OF PERONOSPORA PARASITICA 1 (RPP1)* locus, identified in *A. thaliana* ecotype Ws, contains a complex resistance gene cluster (Krasileva et al., 2010; Ma et al., 2020). Several members of the *RPP1* gene family confer disease resistance against *Hyaloperonospora arabidopsidis* (Krasileva et al., 2010; Ma et al., 2020). *The ARABIDOPSIS THALIANA RECOGNIZED1 (ATR1)*, a simple locus in *H. arabidopsidis*, exhibits diverse allelic variants across different pathogen strains and proteins encoded by *RPP1* alleles are known to recognize the corresponding effector *ATR1* (Krasileva et al., 2010; Ma et al., 2020).

There is also an atypical NLR called *RESISTANCE TO POWDERY MILDEW 8* (*RPW8*), which sometimes is also considered as "helper NLR" (Duggan et al., 2021; Li et al., 2020; Saile et al., 2021). CC-NB-LRRs and TIR-NB-LRRs are "sensor NLRs" which possess the ability to directly or indirectly recognize effectors (Feehan et al., 2020; Maruta et al., 2022). *RPW8* proteins, which confer resistance to powdery mildew fungus, are characterized by a potential transmembrane domain at their N-terminus, followed by a specific truncated CC domain, but without NB or LRR domains (Barragan et al., 2019; Wang et al., 2009b; Xiao et al., 2001; Zhong & Cheng, 2016). The latest research indicates that *RPW8.1* boosts ethylene (ET) signaling, while ET dampens *RPW8.1* defenses by downregulating its expression (Zhao et al., 2021a). Another atypical NLR is *RESPONSE TO HOPBA1 (RBA1),* which only has a TIR domain, and exhibits a distinct immune response by specifically targeting the bacterial type III effector protein HopBA1(Nishimura et al., 2017).

Table 1. Examples of immune receptors characterized in *A. thaliana*

Receptors	Ligand	Receptor type	References
FLS2	Flg22	LRR-RLK	(Chinchilla et al., 2006; Gómez-Gómez & T. Boller, 2000)
EFR	EF-Tu	LRR-RLK	(Kunze et al., 2004; Zipfel et al., 2006)
PEPR1/2	Pep1-8 / Pep1-2	LRR-RLK	(Bartels et al., 2013; Krol et al., 2010; Yamaguchi et al., 2006b, 2010)
CEPK1	Chitin	LysM-RLK	(Cao et al., 2014; T. Liu et al., 2012; Miya et al., 2007)
LORE	LPS	Lectin-RLK	(Luo et al., 2020; Ranf et al., 2015)
WAK1	OGs	EGF-like-RLK	(Brutus et al., 2010; Wagner & Kohorn, 2001)
CRK13/36	?	Duf26-RLK	(Acharya et al., 2007; Lee et al., 2017; Wrzaczek et al., 2010; Zhang et al., 2023)
RLP23	NLPs	LRR-RLP	(Albert et al., 2015)
LYM1/3	PGN	LysM-RLP	(Willmann et al., 2011)
ZAR1	HopZ1a, AvrAC, XopJ4, HopF2	CC-NB-LRR	(Bi et al., 2021; Lewis et al., 2013; Seto et al., 2017; Wang et al., 2015)
RPP1	ATR1	TIR-NB-LRR	(Krasileva et al., 2010; Ma et al., 2020)
RBA1	HopBA1	Atypical NLR	(Nishimura et al., 2017)

The relationship between PTI and ETI is intricate. PTI is typically effective against non-adapted pathogens, a phenomenon known as non-host resistance, whereas ETI is specifically activated against adapted pathogens (Dodds & Rathjen, 2010). Furthermore, there is an overlap in the sets of genes activated during both PTI and ETI (Navarro et al., 2004). The PRRs activation of PTI strengthens the ETI-triggered HR to limit

pathogen proliferation, while ETI enhances PTI responses by elevating PTI signaling elements and regulating protein processes, amplifying defense mechanisms (Ngou et al., 2021; Yuan et al., 2021). Cooperation between PRRs and NLRs is necessary in plant immunity. Table 1 shows some examples of immune receptors characterized in *A. thaliana*, some of which are furtherly detailed in the following sections.

2.2 PAMP-triggered immunity (PTI)

The signaling mechanisms triggered by PRRs in PTI include Ca^{2+} influx, reactive oxygen species (ROS) burst, *MITOGEN-ACTIVATED PROTEIN KINASES* (*MAPK*) cascades, salicylic acid (SA) and ET production, callose deposition, and stomatal closure, among others (Bigeard et al., 2015; Li et al., 2016b).

2.2.1. PTI and Calcium signaling

The influx of extracellular Ca^{2+} into the cytosol, occurring approximately between 30 seconds to 2 min after PAMP perception, peaks at 4–6 min (Bigeard et al., 2015; Ranf et al., 2011). Ca^{2+} channel blockers like $LaCl_3$, inhibit Ca^{2+} signals and immune responses by preventing Ca^{2+} entry from the apoplast, indicating the crucial role of Ca^{2+} influx across the plasma membrane (PM) in both layers of immunity, despite its storage in intracellular organelles such as the ER and vacuole lumen (Bi et al., 2021; Jacob et al., 2021; Wang & Luan, 2024). The activation of PRRs like PAMP receptors *FLS2* (*FLAGELLIN SENSING* 2) and *EFR* (*EF-Tu RECEPTOR*), induces a rapid but transient spike in cytoplasmic calcium (Jeworutzki et al., 2010). Besides the Ca^{2+} fluxes induced by PAMPs flg22 and elf18, the plant derived pep1 (peptide 1) can also initiate calcium influx (Ranf et al., 2011). Apart from eliciting changes in calcium ions, flg22 triggers swift effluxes of Cl^-, NO_3^-, and K^+, alongside an influx of H^+ across the PM, often causing depolarization and extracellular alkalinization (Jeworutzki et al., 2010).

A common method to measure $[Ca^{2+}]_{cyt}$ levels in plants is using the bioluminescent calcium sensor apoaequorin from jellyfish *Aequorea victoria*, which emits light upon binding calcium ions, and the bioluminescence can be quantified using microplate readers (Knight et al., 1991; Ranf et al., 2012). In plant research, besides the calcium ion inhibitor $LaCl_3$, ionomycin can be used as a Ca^{2+} ionophore, inducing Ca^{2+} influx into the cell (Morgan & Jacob, 1994). For instance, ROS production by *RBOHD* (*RESPIRATORY BURST OXIDASE HOMOLOG D*) was induced by ionomycin in *A. thaliana*, facilitating the study of the correlation between Ca^{2+} influx and ROS burst (Ogasawara et al., 2008).

2.2.2. PTI and ROS burst

Another immediate reaction to PTI is the ROS burst (Torres et al., 2006). Upon sensing flg22 or other PAMPs, there is a rapid generation of ROS in the apoplast, which is typically detected utilizing chemiluminescence (Jabs et al., 1997), initiated within around 2 min and peaking at approximately 10 min (Chinchilla et al., 2007). The PAMP-triggered ROS burst is mainly mediated by the membrane NADPH (nicotinamide adenine dinucleotide phosphate) oxidase *RBOHD* in *A. thaliana* (Nühse et al., 2007; Ranf et al., 2011). Besides *RBOHD*, *PRXs* (*PEROXIDASES*) also contribute to ROS burst during PTI, as evidenced by decreased H_2O_2 levels via DAB

(3,3'-diaminobenzidine) staining in *prx33/prx34* mutants after different PAMP treatments, resembling the *rbohD* mutant (Daudi et al., 2012). *PRX33* and *PRX34* play crucial roles in SA-mediated gene expression like *PR1* (*PATHOGENESIS-RELATED GENE 1*), and subsequent defense responses (Bindschedler et al., 2006; Boudsocq et al., 2010). Ca^{2+} influx and ROS production create a positive loop, boosting the defense signal and enhancing immune responses (Köster et al., 2022; Tian et al., 2019; Yuan, et al., 2017a). For example, the ROS sensor *HPCA1* (*HYDROGEN PEROXIDE INDUCED Ca^{2+} INCREASE 1*) is an LRR-RLK located at the PM and becomes activated by H_2O_2 through covalent alteration of cysteine residues (Wu et al., 2020). *HPCA1* facilitates the opening of calcium channels in guard cells in response to H_2O_2 that is essential for the closure of stomata (Wu et al., 2020).

2.2.3. PTI and *MAPK* cascades

MAPK (*MITOGEN-ACTIVATED PROTEIN KINASES*) cascades consist of three tiers phosphorylation reactions (Meng & Zhang, 2013). The standard *MAPK* cascade comprises at least one *MAPK* (*MPK*), one *MAPK* kinase (*MAPKK, MKK,* or *MEK*), and one *MAPKK* kinase (*MAPKKK, MKKK,* or *MEKK*) (Zhang & Zhang, 2022). Based on sequence homology, the *A. thaliana* contains roughly 20 *MAPKs*, 10 *MAPKKs*, and around 60 *MAPKKKs* (Meng & Zhang, 2013). The PAMPs flg22 or elf18 can induce a strong but transient activation of *MAPKs* in *A. thaliana*, such as *MPK3* (Asai et al., 2002), *MPK6* (Nuhse et al., 2000), MPK4 (Suarez-Rodriguez et al., 2007), and MPK11 (Bethke et al., 2012; Bigeard et al., 2015). Flg22-induced *MAPK* activation in *A. thaliana* is independent of ROS burst, *BIK1(BOTRYTIS-INDUCED KINASE 1)*/*PBL1* (*PBS1-LIKE 1*), and SA/JA/ET signaling pathways (Bigeard et al., 2015). Especially *MPK3* and *MPK6* are engaged in both biotic and abiotic stress responses (Kumar et al., 2020; Ren et al., 2008).

In the plant immune signaling pathway, *MAPK* and *CDPK* (*CALCIUM-DEPENDENT PROTEIN KINASE*) can regulate the expression of plant immunity-related genes through phosphorylation modification of downstream TFs (Bredow & Monaghan, 2019; Sun & Zhang, 2022). For example, *A. thaliana CALMODULIN-BINDING TRANSCRIPTION ACTIVATOR 3* (*CAMTA3*), a transcription factor known for its negative regulatory role in plant immunity, is phosphorylated by *MPK3/6* upon flg22 treatment, leading to destabilization of *CAMTA3* protein and facilitation of its nuclear-to-cytoplasmic trafficking (Jiang et al., 2020). After flg22 treatment, *MPK3* phosphorylates the *bZIP* transcription factor *VIP1* (*VIRE2-INTERACTING PROTEIN 1*), causing its movement into the nucleus to activate *PR1* gene expression (Djamei et al., 2007). Following flg22 treatment, *MPK6* phosphorylates *ERF104*, leading to activation of defense genes (Bethke et al., 2009; Bigeard et al., 2015). On the other hand, *CPK5/CPK6* or *MPK3/MPK6* phosphorylate *WRKY33* to regulate camalexin biosynthesis in *A. thaliana* (Zhou et al., 2020).

2.2.4. PTI and transcription factors

Key TFs of plant immunity include *bZIP* (*basic leucine ZIPPER*), *bHLH* (*basic HELIX-LOOP-HELIX*), *MYB* (*MYELOBLASTOSIS*), *NAC* (*Petunia NAM and Arabidopsis ATAF1, ATAF2,* and *CUC2*), *CAMTA* (*CALMODULIN-BINDING TRANSCRIPTION ACTIVATOR*), *ERF* (*ETHYLENE RESPONSIVE FACTOR*), and *WRKY* gene families

(Bian et al., 2020; Xiao et al., 2021). *ERF* subfamily members exhibit high affinity for the GCC sequence (AGCCGCC) and play a role in regulating genes responsive to biotic stress, particularly those associated with the JA and ET signaling pathways (Tsuda & Somssich, 2015). Notable members of *ERF* subfamily include *ORA59* (*OCTADECANOID-RESPONSIVE ARABIDOPSIS AP2/ERF 59*), *ERF1*, *ERF6*, and *ERF104* (Tsuda & Somssich, 2015). In the *NAC* family, *ANAC019*, *ANAC055*, and *ANAC072* are direct targets of *MYC2* (*bHLH*) (Meraj et al., 2020; Zheng et al., 2012). *WRKY* gene family members are extensively involved in plant immunity (Pandey & Somssich, 2009). For example, *WRKY46* is a substrate of *MPK3*, and its overexpression enhances the expression of the immune-related gene *NHL10*, thereby boosting plant disease resistance (Sheikh et al., 2016).

2.2.5. PTI and hormone signaling

Synthesis of SA initiates between 3 to 6 h following flg22 treatment, reaching its maximum level after 9 h (Tsuda et al., 2008). Flg22 treatment leads to the accumulation of SA and activates the expression of typical SA-responsive genes such as *SID2* (*SALICYLIC ACID (SA) INDUCTION DEFICIENT 2*), *EDS5* (*ENHANCED DISEASE SUSCEPTIBILITY 5*), *NPR1 (NONEXPRESSOR OF PATHOGENESIS-RELATED GENES 1)*, and *PR1* (*PATHOGENESIS-RELATED GENE 1*) (Mishina & Zeier, 2007; Tsuda et al., 2008). The defense signaling pathways mediated by SA and ET/JA interact both synergistically and antagonistically (Li et al., 2019; Mur et al., 2006). Low concentrations of SA and JA lead to synergistic expression of SA target gene *PR1* and JA marker gene *PDF1.2 (PLANT DEFENSIN GENE 1.2)*, while higher concentrations result in antagonistic expression of these genes (Mur et al., 2006). Additionally, the activation of both SA and JA signaling pathways impacts the ROS burst and callose deposition triggered by flg22 (Yi et al., 2014).

ET production commences approximately 1 h post-flg22 treatment, reaching its peak around 4 h (Liu & Zhang, 2004). The TFs *EIN3* (*ETHYLENE INSENSITIVE 3*) and *EIL1* (*EIN3-LIKE 1*), activated by ET, interact with the promoter of *FLS2* to control the transcription of this gene (Boutrot et al., 2010). It is highly likely that ET and JA pathways coordinate during plant defense, while ET and SA pathways exhibit antagonism. JA signaling amplifies the activity of *EIN3* and *EIL1*, resulting in the elevation of *ERF1* and *ORA59* (*OCTADECANOID-RESPONSIVE ARABIDOPSIS AP2/ERF 59*) expression (Zhu et al., 2011). *EIN3* suppresses SA signaling by repressing *SID2* expression (Chen et al., 2009), while SA reduces *ORA59* accumulation (Van der Does et al., 2013) and the *ein3 eil1* double mutant or *ein2* single mutant accumulates more SA and is more resistant to *P. syringae* (*Pseudomonas syringae*) (Chen et al., 2009). Endoplasmic reticulum (ER) localized *ERFs* integrate ET signaling with key defense pathways (Müller & Munné-Bosch, 2015). *ERF6*, phosphorylated by *MPK3/MPK6*, induces the expression of *PR* genes like *PDF1.2*, thus enhancing resistance against *Botrytis cinerea* (Meng et al., 2013). *ERF96* overexpression increases the expression of JA/ET defense genes like *PDF1.2a*, *PR-3*, and *PR-4*, boosting resistance against *Botrytis cinerea* and *Pectobacterium carotovorum* (Catinot et al., 2015). *EIN2* (*ETHYLENE INSENSITIVE 2*) serves as a key membrane protein in ET signaling pathways, with *EIN3* and *EIL1* acting downstream as TFs to regulate hundreds of ET-responsive genes (Yang et al., 2015b).

2.2.6. PTI and callose deposition

After treating with flg22, and staining with aniline blue, there is significant fluorescence observed, indicating the presence of dense callose deposits in *A. thaliana* leaves (Gómez-Gómez et al., 1999). Callose, a (1,3)-β-glucan cell wall polymer with (1,6)-branches, is present in both multicellular green algae and higher plants (Ellinger & Voigt, 2014). The activity of callose synthase *GSL5* (*GLUCAN SYNTHASE-LIKE 5*) was essential for the induction of callose deposition triggered by flg22 (Jacobs et al., 2003; Luna et al., 2011). The role of callose in plant-bacteria interactions is still under debate (Ellinger & Voigt, 2014). It may act as a barrier against pathogens or help detoxify antimicrobial compounds (Ellinger & Voigt, 2014; Luna et al., 2011; Samardakiewicz et al., 2012). The *pmr4* (*gsl5*) mutant showed increased SA biosynthesis and constitutive expression of defense-related genes (Nishimura et al., 2003). Moreover, neither the absence nor the excess of callose deposition alone enhanced resistance to bacterial pathogens (Moreau et al., 2012). Callose deposition near plasmodesmata neck zone acts as a defense mechanism, controlling their permeability (Amsbury et al., 2018). Plasmodesmata closure and callose deposition induced by SA or pathogens necessitate an SA pathway dependent on *EDS1* (*ENHANCED DISEASE SUSCEPTIBILITY 1*) and *NPR1* and rely on the plasmodesma gating regulator *PDL5* (*PROTEIN DISULFIDE ISOMERASE-LIKE 5*) (Wang et al., 2013). Flg22, EF-Tu, LPS (lipopolysaccharide), and PGN (peptidoglycan) hairpins all induce callose deposition (Ellinger & Voigt, 2014). However, distinct signaling pathways regulate different PAMPs-induced callose deposition (Wang et al., 2021).

2.2.7. PTI and stomata regulation

Stomatal closure, as an early immune response, aims to restrict bacterial entry (Sakata & Ishiga, 2023). When leaves or epidermal peels are exposed to *Pst DC3000* suspension, stomata closes within 1 to 2 h, but reopens at 3 h (Melotto et al., 2006). PAMP-induced stomatal closure involves the buildup of ROS and NO, oscillations in cytosolic calcium levels, stimulation of S-type anion channels, and suppression of potassium (K^+) inward channels (Melotto et al., 2006, 2008,2017). Abscisic acid (ABA) also regulates stomatal movements during water-deficit conditions (Hsu et al., 2021). But stomatal closure induced by flg22 involves both *LOX1 (LIPOXYGENASE 1)* and *MPK3* and *MPK6*, along with SA, in an ABA-independent process (Montillet et al., 2013).

OSCA1.3 and *OSCA1.7* (*HYPEROSMOLALITY-GATED CALCIUM-PERMEABLE CHANNEL 1.3* and *1.7*) are indispensable for flg22-triggered stomatal immunity (Thor et al., 2020). Flg22 triggers the activation of *SLAC1* (*SLOW ANION CHANNEL-ASSOCIATED 1)* and *SLAH3* (*SLAC1 HOMOLOGUE 3*), which are S-type anion channels in guard cells, necessary for stomatal closure in *A. thaliana* (Geiger et al., 2011; Guzel Deger et al., 2015). *SLAC1* can be activated by *OST1* (*OPEN STOMATA 1*) in a Ca^{2+}-independent manner (Geiger et al., 2010) or Calcium Dependent Protein Kinases *CDPK3* and *CDPK21*, in a manner largely dependent of cytosolic calcium elevation (Geiger et al., 2010; Scherzer et al., 2012). *SLAH3* activation requires the co-expression of *CDPKs* and the *CBL* (*CALCINEURIN B-LIKE PROTEIN*) and *CIPKs* (*CBL-INTERACTING PROTEIN KINASES*) module but not *OST1* (Geiger et al., 2011; Maierhofer et al., 2014). *OST1* is essential for mediating stomatal closure induced by

flg22 (Guzel Deger et al., 2015; Melotto et al., 2006). Recent findings indicate that *BAK1* (*BRASSINOSTEROID INSENSITIVE ASSOCIATED RECEPTOR KINASE 1*) phosphorylates *OST1* in vitro and is necessary for ABA -induced ROS production in guard cells (Shang et al., 2016). However, the mechanism of *OST1* activation by flg22 needs further investigation.

2.2.8. PTI and Leucine-rich repeat receptors.

In addition to PTI triggered by LRR-PLKs like *FLS2* and *EFR*, other PRRs also induce PTI. The LysM -RLKs *CHITIN ELICITOR RECEPTOR KINASE 1* (*CERK1*), which may serve as a co-receptor of *LYSIN MOTIF-CONTAINING RECEPTOR-LIKE KINASE 5* (*LYK5*) (Cao et al., 2014), detects fungal chitin in cell walls using its extracellular LysM domains (Miya et al., 2007). The *cerk1* mutant, deficient in the chitin-triggered PTI pathway, showed weaker defense responses against *Fusarium oxysporum f. sp. cubense* (*Foc*) *B2*, including reduced gene expression, lack of stomatal closure, lower ROS levels, and decreased callose deposition compared to the wild-type (Huaping et al., 2017). *CERK1*, along with two LysM-RLPs (*LYM1* and *LYM3*) have been involved in PGN (peptidoglycan) ligand binding (Willmann et al., 2011). The *A. thaliana* receptor-like cytoplasmic kinase *PBS1-LIKE 27* (*PBL27*) is necessary for the activation of MAP kinases induced by chitin but is not involved in the generation of ROS (Shinya et al., 2014; Yamada et al., 2016; Zipfel & Oldroyd, 2017). When chitin is detected by *CERK1*/*LYK5* complexes, *PBL27* directly phosphorylates the anion channel *SLAC1 HOMOLOGUE 3* (*SLAH3*), which is important for stomatal immunity (Liu et al., 2019a).

In the early stage of *P. syringae* (*Pseudomonas syringae*) infection, LPS (lipopolysaccharide) perception leads to auto-phosphorylation of *LORE* (*LIPOOLIGOSACCHARIDE-SPECIFIC REDUCED ELICITATION*), a membrane localized S-domain receptor kinase that is involved in LPS sensing. *LORE* in turn phosphorylates the Receptor-like cytoplasmic kinases *PBL34/PBL35/PBL36* activating immune responses (Luo et al., 2020; Ranf et al., 2015). *WAK1*, known for its role in maintaining cell wall integrity (Rui & Dinneny, 2020; Wagner & Kohorn, 2001), responds to OGs (Oligogalacturonides) and functions in the later stages of PTI immunity, as evidenced by significantly reduced callose deposition in *wak1* mutants (Brutus et al., 2010). In response to avirulent strains of *P. syringae*, the expression of the *CYSTEINE-RICH RECEPTOR-LIKE KINASE 13* (*CRK13*) showed strong induction, and its overexpression resulted in increased resistance to *P. syringae* (Acharya et al., 2007). Another cysteine-rich receptor-like kinase, *CRK36*, has been shown to modulate PTI responses triggered by flg22 by interacting with *BIK1*(*BOTRYTIS-INDUCED KINASE 1*) (Lee et al., 2017). However, ligands for Duf26-RLK still remain unknown.

In *A. thaliana*, when the LRR receptor protein involved in PAMP mediated immunity *RLP23* (*RECEPTOR LIKE PROTEIN 23*) senses *NECROSIS- AND ETHYLENE-INDUCING PEPTIDE 1* (*NEP1*)*-LIKE PROTEINs* (*NLPs*), it triggers signaling through the leucine rich repeat transmembrane protein *SOBIR1 (SUPPRESSOR OF BIR1-1)* and leucine-rich receptor serine/threonine protein kinase *BAK1*, resulting in bacterial and fungal resistance (Albert et al., 2015; Liebrand et al., 2014; Ono et al., 2020). *Arabidopsis* plants with deficiencies in the *EDS1 (ENHANCED DISEASE*

SUSCEPTIBILITY 1)-PAD4 (*PHYTOALEXIN-DEFICIENT 4*)-*ADR1* (*ACTIVATED DISEASE RESISTANCE 1*) module exhibit decreased *RLP23*-dependent PTI stimulation such as ET production, ROS burst, callose deposition, and resistance to *Pst DC3000* (Pruitt et al., 2021). This suggests that PTI may also depend on elements associated with ETI signaling.

2.3 Flg22-triggered PTI

In *A. thaliana*, a widely recognized LRR-PRR is the kinase *FLS2*, which specifically detects a conserved 22-amino acid N-terminal sequence within the bacterial flagellin protein known as flg22 (Chinchilla et al., 2006; Felix et al., 1999; Gómez-Gómez et al., 2001). In 2001, the team of Thomas Boller used forward genetics to obtain the mutant *fls2* that was insensitive to flg22 (Gómez-Gómez & Boller, 2000; Gómez-Gómez et al., 2001). In 2006, Thomas Boller lab also used reverse genetics to identify the receptor *EFR* that recognizes EF-Tu from numerous receptor kinases (Zipfel et al., 2006). In contrast to *FLS2*, the genes encoding *EFR* are exclusively found in the *Brassicaceae* (Nekrasov et al., 2009). The most extensively studied PAMP/PRR pairs in plants are flg22-*FLS2* and elf18-*EFR* (Yu et al., 2021).

In *A. thaliana*, flg22 triggers callose deposition, ROS burst, and inhibits plant growth (Gómez-Gómez & Boller, 2000; Gómez‐Gómez et al., 1999). Flg22 also activates the MAP kinase cascade (*MEKK1*, *MKK4/MKK5*, and *MPK3/MPK6*) and *WRKY22/WRKY29* transcription factors (Asai et al., 2002; Suarez-Rodriguez et al., 2007).

At first, *FLS2* possibly forms homodimers in the absence of flg22 (Sun et al., 2012). In resting plants, *FLS2* interacts with both *BIK1* (*BOTRYTIS-INDUCED KINASE 1*) and *PBL1* (*PBS1-LIKE 1*) that belong to the group of cytoplasmic receptor-like kinases lacking extracellular domains (Liang & Zhou, 2018; Lu et al., 2010; Zhang et al., 2010a). In the absence of the ligand, *FLS2* and *BAK1* are typically found in close to the PM (Roux et al., 2011; Schulze et al., 2010; Yu et al., 2021).

Flg22 induces the formation of the immune receptor complex between *FLS2* and *BAK1* (Chinchilla et al., 2007; Schulze et al., 2010; Sun et al., 2013). The reduced sensitivity of *bak1-3* and *bak1-4* mutants to flg22, along with diminished ROS burst induced by flg22 and EF-Tu, and weakened *MAPK* signaling activation, indicates that *BAK1* serves as a positive regulator of PAMPs (Chinchilla et al., 2007). In vivo, the formation of the *FLS2* and *BAK1* complex is rapid, occurring within 2 min of flg22 treatment (Chinchilla et al., 2007).

Upon flg22 induction, *BIK1* undergoes rapid phosphorylation by *BAK1* and dissociates from the *FLS2* protein (Lin et al., 2014). After treatment with flg22, *bik1* mutants exhibit reduced ROS burst and immune gene expression compared to wild-type plants, suggesting *BIK1*'s involvement in positively regulating PTI signal transduction (Veronese et al., 2006; Zhang et al., 2010a). Subsequent in vivo Co-IP and in vitro pull-down assays confirmed the direct interaction of *RBOHD* with both *BIK1* and *FLS2*, and treatment with flg22 induced the dissociation of *RBHOD* from *FLS2* (Li et al., 2014). In addition, *BIK1* phosphorylates *RBOHD* (Kadota et al., 2014; Li et al., 2014) at Ser39 and Ser343, which is crucial for flg22-induced ROS production. The phosphorylation

at Ser39 is calcium independent (Li et al., 2014).

The NADPH oxidase *RBOHD*, located at the plasma membrane (PM), mediates the flg22-induced burst of ROS (Nühse et al., 2007; Zhang et al., 2007). NADPH oxidases generate $O_2^{\bullet -}$ from oxygen molecules in the apoplast, and the $O_2^{\bullet -}$ can quickly convert to H_2O_2 either spontaneously or through the action of *SUPEROXIDE DISMUTASE* (*SOD*), which enzymatically detoxifies $O_2^{\bullet -}$ (Chen & Yang, 2020). In *A. thaliana*, two putative *SODs*, *Mn-SOD* (*AT3G56350*) (Chen et al., 2022) and *Fe-SOD* (*AT4G00651*), are predicted to be secreted into the apoplastic space (Waszczak et al., 2018). H_2O_2 can activate Ca^{2+} influx in *A. thaliana* (Klusener et al., 2002; Pei et al., 2000). In turn, cytoplasmic Ca^{2+} binding to *RBOHD* N-terminal EF-hand domains are crucial for ROS production (Ogasawara et al., 2008).

PBL1 and *BIK1* play a crucial role in calcium signaling induced by flg22 (Li et al., 2014; Ranf et al., 2014). Upon flg22 stimulation, *BIK1* and *PBL1* become phosphorylated (Zhang et al., 2010a). The identity of the Ca^{2+} channel(s) involved in PTI remains unclear, but these results suggest that *BIK1* and *PBL1* may phosphorylate and activate Ca^{2+} channels or positive regulators, or that ROS plays a role in channel activation (Kadota et al., 2015).

BIK1 phosphorylates and activates the cyclic proteins *CNGC2* and *CNGC4 (CYCLIC NUCLEOTIDE-GATED CHANNEL 2* and *4*), and *HYPEROSMOLALITY-GATED CALCIUM-PERMEABLE CHANNELS 1.3* (*OSCA1.3*) channels for Ca^{2+} influx upon flg22 perception (Thor et al., 2020; Tian et al., 2019). Calcium channels, like *CNGC*s (*CYCLIC NUCLEOTIDE GATED CHANNELS*), *GLUTAMATE RECEPTOR-LIKE PROTEINS* (*GLRs*), *OSCAs*, *TWO-PORE CHANNELS* (*TPCs*), and *ANNEXINS* (*ANNs*), play crucial roles in modulating Ca^{2+} fluxes during plant immunity (Xu et al., 2022). Plant *CNGCs*, belonging to the superfamily of voltage-gated ion channels, are tetrameric proteins characterized by six transmembrane domains and possess cytosolic N-terminal and C-terminal regions per subunit (Dietrich et al., 2020; Jegla et al., 2018). In *A. thaliana*, the *OSCA* family, comprising 15 genes, exhibits structural characteristics including 11 transmembrane helices and a cytosolic domain, forming homodimers (Xu et al., 2022).

The entry of Ca^{2+} can potentially trigger the activation of *CDPKs*, which possess a dual calmodulin-like calcium sensor and a protein kinase effector domain (Kudla et al., 2010). Indeed, calcium-dependent protein kinases *CDPK4*, *CDPK5*, *CDPK6*, and *CDPK11* were found to undergo transient activation following flg22 treatment (Boudsocq et al., 2010). Flg22 triggers phosphorylation of *CDPK5*, which phosphorylates *RBOHD*, leading to the modulation of ROS (Dubiella et al., 2013). However, *CDPK* proteins have no impact on the activation of *MAPK* induced by flg22, indicating that *CDPK* and *MAPK* pathways may operate independently (Boudsocq et al., 2010).

BIK1 is dispensable for the activation of *MAP* kinases induced by flg22 (Feng et al., 2012; Zipfel & Oldroyd, 2017). Flg22-induced *MPK3/MPK6* activation is comparable between the quadruple mutant *dde2 ein2 pad4 sid2* and the wild-type (Tsuda et al., 2009). This could imply that *MAPK* activation occurs regardless of SA, ET and JA signaling pathways (Bigeard et al., 2015; Tsuda et al., 2009). The two response

pathways, *MAPKKK3/5 -MKK4/5-MPK3/6* (Asai et al., 2002; Sun, Nitta, et al., 2018) and *MEKK1-MKK1/2-MPK4* (Gao et al., 2008; Qiu et al., 2008; Suarez-Rodriguez et al., 2007) cascades, are rapidly activated in response to flg22 stimulation.

Upon treatment with flg22, perception by *FLS2* can trigger subsequent PTI responses, as well as to induce negative regulation. Two U-box E3 ubiquitin ligases, *PUB12* and *PUB13 (PLANT U-BOX 12* and *13)*, interact with *FLS2* under the mediation of *BAK1*, leading to ubiquitination modification of *FLS2* and ultimately resulting in its degradation (Lu et al., 2011). *FLS2* undergoes endocytosis upon ligand induction, transitioning from the PM to vesicles or vacuoles in plant cells, potentially leading to degradation (Mbengue et al., 2016; Robatzek et al., 2006; Smith et al., 2014). In the absence of flg22, *FLS2* can also undergo degradation. *A. thaliana ORM* (*OROSOMUCOID*) proteins, recognized as negative regulators of sphingolipid biosynthesis, act as selective autophagy receptors interacting with non-activated *FLS2* and the autophagy key protein *ATG8* (*AUTOPHAGY-RELATED PROTEIN 8*) to facilitate *FLS2* degradation (Yang et al., 2019).

2.4. NADPH oxidases

The NADPH (nicotinamide adenine dinucleotide phosphate) oxidase, referred to as the *RESPIRATORY BURST OXIDASE* (*RBO*), is sensitive to inhibition by diphenylene iodonium (DPI) but not by cyanide or azide (Torres et al., 2006). The key catalytic subunit of the phagocyte NADPH oxidase (phox) is gp91phox, a glycoprotein embedded within the membrane, exhibiting an apparent molecular mass of around 91 kDa (Keller et al., 1998; Sumimoto, 2008; Torres et al., 2002). *A. thaliana* possesses ten *RBO HOMOLOGS* (*RBOH*) (*RBOHA* to *RBOHJ*) that are analogous to gp91phox (Chapman et al., 2019; Torres et al., 1998, 2006).

In *A. thaliana*, *RBOHD* and *RBOHF* are vital for the buildup of reactive oxygen intermediates during plant defense reactions (Torres et al., 2002, 2005). Subsequent studies have found that *RBOHD* is the primary contributor to PAMP-induced ROS production, while *RBOHF* contributes less to this process (Nühse et al., 2007; Zhang et al., 2007). When *A. thaliana* is exposed to PAMPs such as flg22, elf18, and chitin, the promoter of *RBOHD* can cause excessive expression of GUS (β-glucuronidase) and LUC (luciferase) reporter genes (Morales et al., 2016). The upregulation of *RBOHD* promoters initiates 15 min after flg22 treatment, peaking at 1–1.5 h, whereas no activity of *RBOHF* promoter is detected (Morales et al., 2016). These findings confirmed that *RBOHD* is a key gene which expression is upregulated during pathogen infection, contributing to ROS production.

RBOHD is a protein located at the plasma membrane (PM), with cytosolic N and C termini, featuring six conserved transmembrane helices that anchor two heme groups (Kadota et al., 2015). The N terminus of *RBOHD* contains two Ca^{2+}-binding EF-hand motifs, a phosphatidic acid-binding motif, and multiple phosphorylation sites (Kadota et al., 2015). The Protein Kinase *PBL13* can directly phosphorylate conserved residues at the C-terminus of *RBOHD*, affecting its activity and promoting its degradation via E3 ligase under normal conditions (Lee et al., 2020).

BIK1 phosphorylates *RBOHD* at Ser39, Ser339, and Ser343 residues, specifically (Kadota et al., 2015; Li et al., 2014). *BIK1*, along with other *RECEPTOR-LIKE CYTOPLASMIC KINASE* (*RLCK*) members like *PBL1*, *PBL9*, and *PBL11*, promotes flg22-triggered ROS production (Li et al., 2021; Sun et al., 2022; Wu et al., 2023). Phosphorylation of Ser163 is contingent upon calcium levels (Kadota et al., 2015). The calcium-dependent protein kinase *CDPK5*, which signaling can improve salicylic acid (SA)-mediated resistance to the pathogen *Pst DC3000*, alter plant defense gene expression, and induce ROS synthesis, phosphorylates *RBOHD* at Ser148, Ser163, and Ser347 residues (Boudsocq et al., 2010; Dubiella et al., 2013). Treatment with calcium chelators and mutations in EF-hand motifs inhibit PAMP-induced ROS production, indicating the essential role of calcium in the regulation of *RBOHD* (Kadota et al., 2015; Kimura et al., 2012; Ogasawara et al., 2008).

The increased Ca^{2+} levels also lead to the activation of *CALCINEURIN B-LIKE PROTEIN 1* (*CBL1*) and *CBL9*, both of which bind to *CALCINEURIN B-LIKE PROTEIN (CBL)-INTERACTING PROTEIN KINASE 26* (*CIPK26*) to phosphorylate *RBOHF*, establishing a positive feedback loop for ROS generation (Drerup et al., 2013; Mittler & Blumwald, 2015). In addition, ET induces stomatal closure by generating H_2O_2 through *RBOHF* (Desikan et al., 2006).

2.5. Salicylic acid

SA signaling is mainly involved in response to biotrophic and hemibiotrophic pathogens, leading to SAR (systemic acquired resistance) (Ding et al., 2011; Klessig et al., 2018). SA is a phenolic compound synthesized from chorismate through two pathways involving *PHENYL ALANINE AMMONIA-LYASE* (*PAL*) and *ISOCHORYSMATE SYNTHASE* (*ICS*) enzymes (Peng et al., 2021). In *A. thaliana*, SA production during pathogen attack mainly relies on the *ICS* pathway, particularly through the induction of *ICS1 (ISOCHORISMATE SYNTHASE 1*) (Wildermuth et al., 2001).

ICS1 (also referred to as *SID2*) proteins are found in chloroplasts (Garcion et al., 2008). *PBS3 (AvrPphB SUSCEPTIBLE 3)*, located in the cytosol, is crucial for pathogen-triggered SA accumulation by catalyzing the conjugation of isochorismate (IC) to glutamate, forming IC-9-Glu (isochorismate-9-glutamate), which is an essential intermediate in SA production and can either spontaneously degrade into SA or be converted to SA by the BAHD acyltransferase *ENHANCED PSEUDOMONAS SUSCEPTIBILTY 1* (*EPS1*) (Rekhter et al., 2019; Torrens-Spence et al., 2019). The BAHD acyltransferases utilize CoA thioesters and catalyze the synthesis of a diverse range of plant metabolites, serving multiple biological functions within plants (D'Auria et al., 2006; Wang et al., 2023). The name "BAHD" originates from the initial letters of the first four characterized enzymes: BEAT, AHCT, HCBT, and DAT, encompassing benzylalcohol O-acetyl transferase, anthocyanin O-hydroxycinnamoyl transferase, N-hydroxycinnamoyl anthranilate benzoyl transferase, and deacetylvindoline 4-O-acetyltransferase (D'Auria, 2006; Luo et al., 2007; St-Pierre & De Luca, 2000; Wang et al., 2023).

Isochorismate must be transported from plastids to the cytosol for SA production, with

EDS5 (*ENHANCED DISEASE SUSCEPTIBILITY 5*) /*SID1* likely facilitating this process (Nawrath et al., 2002; Rekhter et al., 2019; Serrano et al., 2013). In *A. thaliana*, this *ICS1* pathway also depends on some other important proteins, including *EDS1* (*ENHANCED DISEASE SUSCEPTIBILITY 1*), *PAD4 (PHYTOALEXIN-DEFICIENT 4)*, *NDR1* (*NON-RACE-SPECIFIC DISEASE RESISTANCE 1*) and *ACD6* (*ACCELERATED CELL DEATH 6*) (Qi et al., 2018a). During PTI, lipase-like proteins *EDS1* and *PAD4* initiate SA biosynthesis (Pieterse et al., 2012). Upon ETI initiation by TIR-NBS-LRR type R proteins, SA biosynthesis is facilitated by *EDS1* and *PAD4* (Pieterse et al., 2012; Wiermer et al., 2005). However, when CC-NBS-LRR type R proteins trigger ETI, SA production onset is regulated by *NDR1* (Knepper et al., 2011; Pieterse et al., 2012). In *A. thaliana*, most SA is converted to 2,5-dihydroxybenzoic acid (2,5-DHBA), catalyzed by *DOWNY MILDEW RESISTANT 6* (*DMR6*) already in the absence of pathogen infection (Peng et al., 2021; Zhang et al., 2017).

Upon pathogen invasion, *ICS1* expression rapidly increases, causing a substantial rise in SA levels (Strawn et al., 2007; Wildermuth et al., 2001). *SARD1* (*SYSTEMIC ACQUIRED RESISTANCE DEFICIENT 1*) and *CBP60g* (*CALMODULIN BINDING PROTEIN 60-like g*) regulate *ICS1* expression and SA biosynthesis after flg22 treatment, with loss of both genes resulting in inhibited *ICS1* induction and SA accumulation (Wang et al., 2011b; Zhang et al., 2010b). The synthesis or signaling pathway of SA may also be associated with calcium ion concentration. *CBP60g* contains an essential N-terminal *CaM* (*CALMODULIN*)-binding domain which mediates SA signaling upon pathogen recognition (Wang et al., 2009a). On the contrary, three TFs *CAMTA1/2/3* play a role in suppressing the expression of *SARD1* and *CBP60g*, as well as SA biosynthesis (Jacob et al., 2018; Kim et al., 2013b; Sun et al., 2020). ChIP analysis indicated that *SARD1* and *CBP60g* also target *FMO1 (FLAVIN-DEPENDENT-MONOOXYGENASE 1)*, *ALD1(AGD2-LIKE DEFENSE RESPONSE PROTEIN 1)*, *SARD4* (*SYSTEMIC ACQUIRED RESISTANCE DEFICIENT 4*), *EDS5* (*ENHANCED DISEASE SUSCEPTIBILITY 5*) and *PBS3 (AvrPphB SUSCEPTIBLE 3)* (Sun, Busta, et al., 2018; Sun et al., 2015). Upon pathogen infection, *ALD1*, *SARD4*, and *FMO1* expression are significantly induced, leading to increased production of Pipecolic acid (Pip) and N-HydroxyPip, which both are crucial for SAR (Chen et al., 2018; Hartmann et al., 2018; Liu et al., 2020a). *MAPK* activation can increase Pip and NHP (N-hydroxypipecolic acid) levels (Wang, et al., 2018b). In *wrky33* mutant, *ALD1* expression, Pip accumulation, and SAR were impaired, with ChIP demonstrating *MPK3/6*-regulated transcription factor *WRKY33* binding to the *ALD1* promoter (Wang et al., 2018b). In addition, *WRKY70* binds to a specific motif in the *SARD1* promoter, suppressing *SARD1* expression in the absence of pathogens (Zhou et al., 2018).

SA can undergo different chemical alterations, like hydroxylation, glycosylation, methylation, and amino acid conjugation (Peng et al., 2021). During pathogen infection, most newly synthesized SA is converted to salicylic acid beta-glucoside (SAG) by UDP-glycosyltransferases *UGT74F1* and *UGT76B1* (Noutoshi et al., 2012). A minor portion of SA can be methylated to produce methyl salicylate (MeSA) by carboxyl methyltransferase *BSMT1* (*BENZOIC ACID/SA CARBOXYL METHYLTRANSFERASE 1*) (Attaran et al., 2009; Chen et al., 2003; Liu et al., 2010).

NPR1 protein has been identified as the receptor for SA and largely regulates SA

downstream signaling (Pieterse et al., 2012; Wu et al., 2012). *NPR1* was discovered using map-based approach and found to encode a protein with ankyrin repeats (Cao et al., 1997). Uninfected plants exhibit *NPR1* in oligomeric complexes in the cytosol, while pathogen infection or SA treatment triggers *NPR1* complex dissociation into monomers (Lindermayr et al., 2005; Spoel et al., 2003; Tada et al., 2008). *NPR3* and *NPR4*, act as adaptors for cullin3 E3 ligase, facilitating the regulation of *NPR1* optimal levels during plant defenses (Ding et al., 2018; Fu et al., 2012). In systemic acquired resistance (SAR) tests with *Pseudomonas syringae pv. maculicola ES4326 (Psm ES4326)*, the *npr3 npr4* double mutant showed a notable decrease in *Psm ES4326* growth even without SAR induction (Fu et al., 2012). However, after SAR induction by local inoculation of avirulent *Psm ES4326/avrRpt2*, there was no additional reduction in virulent *Psm ES4326* growth in systemic tissue observed in the *npr3 npr4* double mutant (Fu et al., 2012), indicating compromised SAR (Fu et al., 2012). Nuclear *NPR1* is essential for SA-mediated defense gene expression, while cytosolic *NPR1* is crucial for mediating the crosstalk between SA and JA (Spoel et al., 2003). Additionally, SA inhibits JA accumulation by repressing *CATALASE2* (*CAT2*), which promotes JA biosynthesis by enhancing JA biosynthetic enzymes *ACX2* and *ACX3* (*ACYL-COA OXIDASES 2* and *3)* (Yuan et al., 2017b).

2.6. Jasmonic acid and interactions with SA

JA signaling pathways typically respond to necrotrophic pathogens, insects, herbivores, and injury (Yang et al., 2015a). JA synthesis begins with linolenic acid (18:3) oxygenation in chloroplasts via enzymes like *LIPOXYGENASES* (*LOX*), *ALLENE OXIDE SYNTHASES* (*AOS*), and *ALLENE OXIDE CYCLASES* (*AOC*), yielding 12-oxo phytodienoic acid (OPDA) (Wasternack & Song, 2017). OPDA, produced in chloroplasts, is transferred to peroxisomes where it is reduced by OXOPHYTODIENOATE-*REDUCTASE* 3 (*OPR3*) and oxidized by *ACYL-COA OXIDASE 1* (*ACX1*), leading to JA biosynthesis (Wasternack & Song, 2017). *JASMONATE RESISTANT 1* (*JAR1*) catalyzes the conjugation of JA with isoleucine in the cytosol to form JA-Ile (JA-isoleucine), which is the most active form of JA (Kombrink, 2012; Staswick & Tiryaki, 2004). Some members of the *CYTOCHROME P450 94* family (*CYP94B1, CYP94B3, CYP94C1*) in the ER, hydroxylate JA-Ile to produce 12-OH-JA-Ile, and *CYP94C1* can further convert it to 12-COOH-JA-Ile (Caarls et al., 2017; Heitz et al., 2012; Koo et al., 2014). 12-OH-JA-Ile activates *COI1* (*CORONATINE INSENSITIVE 1*)-dependent JA signaling (Jimenez-Aleman et al., 2019; Poudel et al., 2019). The F-box protein *COI1* mediates JA signaling by promoting the ubiquitylation and degradation of JAZ repressor proteins in a hormone-dependent manner (Sheard et al., 2010). The JA signaling pathway has two branches: the *MYC*-branch and the *ERF*-branch (Wu & Ye, 2020).

MYC2 is a key regulator in many JA-mediated pathways for defense and development in *A. thaliana* (Luo et al., 2023). In resting cells, *JAZ* proteins physically bind and inhibit *MYC2* and related *MYC* transcription factors (Fernández-Calvo et al., 2011; Song et al., 2017). JAZ proteins interact with *NOVEL INTERACTOR OF JAZ* (*NINJA*) to recruit the transcriptional co-repressor TOPLESS (Pauwels et al., 2010). JAZ proteins also competitively block the interaction between *MYC* proteins and the

MED25 subunit of the transcriptional mediator complex (Çevik et al., 2012; Zhang et al., 2015). Upon hormone perception, the binding of JA-Ile and *COI1*, promotes the assembly of the *COI1*-JAZs complex, leading to the ubiquitination and subsequent degradation of JAZ proteins by the 26S proteasome (Chini et al., 2007; Sheard et al., 2010; Thines et al., 2007). *MYC* (*bHLH*) TFs positively regulate the synthesis of proteins like *VEGETATIVE STORAGE PROTEIN* 2 (*VSP2*), mainly triggering defensive responses against wounding and insect herbivores attacks (Boter et al., 2004; Schweizer et al., 2013).

The *ERF* branch of the JA pathway boosts resistance to necrotrophic pathogens (Pieterse et al., 2012). The *ORA59* (*OCTADECANOID-RESPONSIVE ARABIDOPSIS AP2/ERF 59*) / *ERF1* pathway induces *PDF1.2* expression, counteracting the *MYC2*-mediated pathway (Kazan & Manners, 2013). The synergistic interaction between JA and ET mainly occurs in response to necrotrophic pathogens (Pieterse et al., 2012). JAZ proteins inhibit *EIN3*-mediated expression of *ORA59* and *ERF1*(Zhu et al., 2011). *EIN3* and *EIL1*, central TFs in ET signaling, bind to *JAZ1*, *JAZ3*, and *JAZ9*, suppressing *EIN3*/*EIL1* activity (Zhu et al., 2011).

Low JA and SA concentrations synergistically upregulate the expression of *PDF1*.2 and *PR-1* genes in *A. thaliana*, while higher concentrations lead to antagonistic effects (Mur et al., 2006; Pieterse et al., 2012). Indeed, JA inhibits SA accumulation, and SA negatively regulates the expression of JA-responsive genes (Peng et al., 2021).

WRKY70 likely plays a crucial role in negative feedback regulation of SA-mediated defense responses (Ding et al., 2018; Wang et al., 2006). Overexpressing *WRKY70* reduces expression of the JA-responsive gene *PDF1.2* and compromises resistance to the necrotrophic pathogen *Alternaria brassicicola*, while loss of *WRKY70* function increases *PDF1.2* expression and enhances resistance to *Alternaria brassicicola* (Li et al., 2006; Li et al., 2004). The *edr1* mutant exhibits increased SA signaling, leading to reduced expression of JA-regulated *PDF1.2* and related defensins (Hiruma et al., 2011). *EDR1* (*ENHANCED DISEASE RESISTANCE 1*), a protein kinase like *MAPKKKs*, is also crucial for *A. thaliana* pre-invasive nonhost resistance against *Colletotrichum* species (Frye et al., 2001; Hiruma et al., 2011).

The formation of the *COI1-JAZ* receptor-substrate complex can be promoted by either JA-Ile or coronatine (COR) (Katsir et al., 2008; Yan et al., 2009). COR, a toxin secreted from various *P. syringae* strains, imitates JA-Ile and facilitates bacterial entry by inducing the reopening of stomata (Melotto et al., 2006). In the COR-insensitive *coi1* mutant (Feys et al., 1994), there is an increase in SA levels, resulting in heightened resistance against *Pst DC3000* (Kloek et al., 2001). COR promotes the expression of *NAC* TFs, which suppress the expression of *ICS1* while inducing the expression of *BSMT1*, ultimately resulting in reduced SA (Zheng et al., 2012). COR-induced JA signaling upregulates three *NAC* transcription factors, *ANAC019*, *ANAC055*, and *ANAC072*, which are direct targets of *MYC2* (Zheng et al., 2012). The *myc2* mutant exhibits increased SA biosynthesis and responses, suggesting that *MYC2* acts as a negative regulator of the SA pathway (Laurie-Berry et al., 2006; Nickstadt et al., 2004).

2.7 Reactive Oxygen Species (ROS) and plant defense

ROS is a term encompassing oxygen derivatives more reactive than O_2 itself (Zhou et al., 2014). ROS are universally generated as bioproducts during cellular metabolism in all living organisms (de Almeida et al., 2022; Sies et al., 2022). ROS can be classified into two categories based on their molecular structure: free radicals and non-free radicals. Free radicals, such as superoxide anions ($O_2•^-$), and hydroxyl radicals (HO•), contain unpaired electrons (de Almeida et al., 2022; Radi, 2018). On the other hand, non-free radicals with oxidizing properties include hydrogen peroxide (H_2O_2), singlet oxygen($^1O_2$), peroxynitrite ($ONOO^-$), and hypochlorous acid (HOCl) (de Almeida et al., 2022; Epe, 1991).

H_2O_2 exhibits relative stability owing to the neutral charge, enabling unhindered passage through the cell membrane via aquaporins for effortless entry and exit (Bienert & Chaumont, 2014; Dynowski et al., 2008). The half-life of H_2O_2 spans a mere 1 millisecond, whereas $O_2•^-$ exhibits an even briefer half-life of only 1 microsecond (Bienert et al., 2006; Reth, 2002). In plants, the primary forms of ROS include H_2O_2, $O_2•^-$, $^1O_2$, and HO• (Waszczak et al., 2018).

As per the ROS generation site within a plant, it can be categorized into two main compartments: apoplast and intracellular. In *A. thaliana*, the generation of ROS in the apoplastic region primarily relies on NADPH oxidases, cell wall *PEROXIDASES* (*PRXs*), and amine oxidases (Qi et al., 2017; Torres et al., 2006). The plasma membrane NADPH Oxidase enzyme is most likely involved in promoting superoxide production in plants (Sagi & Fluhr, 2001).

The role of cell wall peroxidases as producers of ROS was first demonstrated pharmacologically in cotton cotyledons (Martinez et al., 1998). Following this, class III *PEROXIDASE PRX33* and *PRX34* were identified in *A. thaliana*, characterized by their sensitivity to azide but insensitivity to DPI (Bindschedler et al., 2006). These peroxidases, encoded by loci *At3g49110* and *At3g49120* respectively, serve as sources of extracellular oxidative bursts when challenged with avirulent strains of *Pseudomonas syringae* (Bindschedler et al., 2006). In *A. thaliana* cell suspensions treated with various PAMP elicitors, peroxidases, mainly *PRX33* and *PRX34*, accounted for over 50% of the produced H_2O_2, with the remainder attributed to NADPH oxidases and intracellular sources (O'Brien et al., 2012). *COPPER AMINE OXIDASES* (*CuAOs*) and FAD-dependent *POLYAMINE OXIDASES* (*PAOs*), comprising 10 and 5 genes in *A. thaliana* respectively, catalyze the oxidation of amines to produce H_2O_2 (Smirnoff & Arnaud, 2019).

Chloroplast, peroxisomes, and mitochondria are the primary sites where intracellular ROS are predominantly produced (Smirnoff & Arnaud, 2019). In PSII, the excitation energy from triplet chlorophyll can be transferred to state triplet oxygen ($^3O_2$), resulting in the formation of highly reactive $^1O_2$ (Durrant et al., 1990; Taylor et al., 2009). Additionally, at PSI, oxygen undergoes one-electron reduction, producing the superoxide anion (Mehler, 1951; Taylor et al., 2009). A membrane-bound *COPPER/ZINC SUPEROXIDE DISMUTASE* (*Cu/ZnSOD*) located near PSI converts superoxide radicals into H_2O_2 (Miller et al., 2010). Furthermore, in the presence of

metal ions like Fe^{2+}, the superoxide radical further transforms into the more harmful HO• via H_2O_2 in the Fenton reaction (Das & Roychoudhury, 2014; Demidchik, 2015; Singh, 2022).

Peroxisomes have been reported to generate various ROS, including H_2O_2, O_2•$^-$and $^1O_2$ (Del Río & López-Huertas, 2016; Mor et al., 2014). In mitochondria, ubiquinone oxidoreductase complex I reduces O_2 to O_2•$^-$ (Das & Roychoudhury, 2014; Pryde & Hirst, 2011). Mitochondria Complex III promotes the production of superoxide anion by leaking electrons to O_2 from the unstable ubisemiquinone semi-radical (Singh, 2022). Superoxide anion is converted to H_2O_2 by *Mn-SOD* or *APX* (*ASCORBATE PEROXIDASE*) in mitochondria (Sharma et al., 2012).

Increased $^1O_2$ production in *A. thaliana* mutants leads to photooxidative stress, causing significant lipid peroxidation and programmed cell death, and $^1O_2$ is the primary ROS responsible for PSII activity loss (Czarnocka & Karpiński, 2018; Triantaphylides et al., 2008). The OH• is the most reactive and toxic ROS known (Das & Roychoudhury, 2014). Due to the lack of an existing enzymatic system to scavenge this radical, excessive buildup of OH• leads to cellular death (Czarnocka & Karpiński, 2018; Das & Roychoudhury, 2014). It can damage various cellular components through lipid peroxidation (LPO), protein damage, DNA single-strand breakage, and membrane destruction (Czarnocka & Karpiński, 2018; Das & Roychoudhury, 2014; Hiramoto et al., 1996; Pinto et al., 2003). Generation and scavenging of ROS in plants can be seen in figure 2.

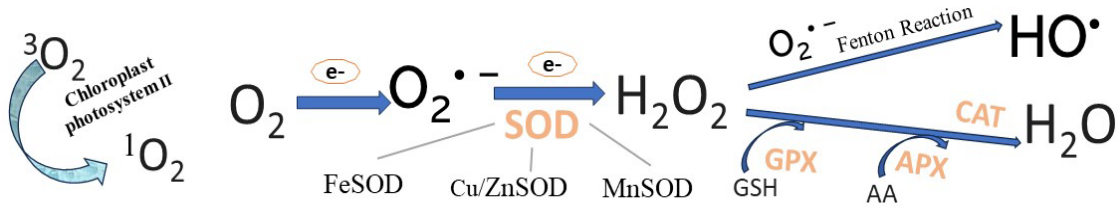

Figure 2 Generation and scavenging of ROS in plants. Ascorbic acid (AA), reduced glutathione (GSH), *SUPEROXIDE DISMUTASE* (*SOD*), *CATALASE* (*CAT*), *ASCORBATE PEROXIDASE (APX*), *GSH PEROXIDASE* (*GPX*).

In redox signaling, low levels of H_2O_2 cause the oxidation of cysteine (Cys) residues, resulting in the formation of the reversible sulfenic form (R–SOH) (Akter et al., 2015; Czarnocka & Karpiński, 2018; Jacques et al., 2013). The sulfenic acid acts as a redox sensor in various physiological pathways, impacting the activities of crucial signaling proteins and TFs that regulate gene expression (Akter et al., 2015; Poole & Nelson, 2008; Reddie & Carroll, 2008). Highly reactive sulfenic acids can form disulfide bonds with nearby thiols, mixed disulfide bonds via S-glutathionylation, or sulfenylamide with the adjacent residue's backbone nitrogen (Akter et al., 2015). These disulfides exhibit reversibility since they can undergo reduction facilitated by thioredoxins (Trx) or glutaredoxins (Grx) (Akter et al., 2015; Messens & Collet, 2013; Meyer et al., 2012). A total of 44 Trx/Trx-like and 50 Grx/Grx-like proteins exist in *A. thaliana* (Akter et al., 2015; Meyer et al., 2012). However, under high H_2O_2 levels, the sulfenic acid can be overoxidized to irreversible sulfenic ($R\text{-}SO_2H$) and sulfonic acids ($R\text{-}SO_3H$)

(Czarnocka & Karpiński, 2018). Typically, overoxidation is irreversible and results in protein degradation via the proteasome or through autophagy (Akter et al., 2015; Czarnocka & Karpiński, 2018; Kehm et al., 2021). Additionally, high concentrations of H_2O_2 can also trigger PCD (programmed cell death) (Elena-Real et al., 2021).

ROS plays a double-edged role in plant cell. Typically, low levels of ROS are essential for the advancement of various fundamental biological processes, but elevated ROS levels pose a considerable threat (Huang et al., 2019). When ROS levels surpass the capacity of cellular defense mechanisms, the cell enters a state known as "oxidative stress" (Sharma et al., 2012). Plants have both enzymatic and non-enzymatic mechanisms for scavenging ROS (Singh, 2022).

Enzymatic systems mainly consist of *SUPEROXIDE DISMUTASE* (*SOD*), *CATALASE* (*CAT*), *ASCORBATE PEROXIDASE* (*APX*), and *glutathione* (*GSH*) *PEROXIDASE* (*GPX*) (Apel & Hirt, 2004). *SOD* converts $O_2^{\bullet -}$ into O_2 and H_2O_2, which reduces the likelihood of OH• formation (Gill & Tuteja, 2010b; Liochev & Fridovich, 2007; Scandalios, 1993). There are three *FeSOD* forms (*FSD1, FSD2*, and *FSD3*), three *Cu/ZnSOD* (*CSD1, CSD2, and CSD3*) and one *MnSOD* (*MSD1*), distinguished based on the presence of metal cofactors in their active sites (Gill & Tuteja, 2010b).

APX, *GPX*, and *CAT* are capable of detoxifying H_2O_2 (Apel & Hirt, 2004). *CAT* has a strong affinity for H_2O_2 and is unique among antioxidant enzymes as it doesn't necessitate a reducing equivalent (Das & Roychoudhury, 2014). Three *CAT* genes were discovered in *A. thaliana*, with *CAT1* and *CAT2* found in the cytosol and peroxisomes, and *CAT3* located in mitochondria (Chaturvedi et al., 2020; Ghosh & Majee, 2023). *APX* utilizes electron transfer from ascorbic acid (AA) to produce monodehydroascorbate (MDHA) and H_2O, thereby removing H_2O_2 (Celi et al., 2023). GPX detoxifies H_2O_2 to H_2O using GSH directly as a reducing agent (Gill et al., 2012). There are also enzymes that can indirectly play a role in scavenging, such as *DEHYDROASCORBATE REDUCTASE* (*DHAR*), *MONODEHYDROASCORBATE REDUCTASE* (*MDHAR*), and *GSH REDUCTASE* (GR) (Dvořák et al., 2021; Gill et al., 2013). *MDHAR* and *DHAR* assist in the production of AA, while *GR* generates GSH (Gill & Tuteja, 2010b).

In addition to AA and GSH mentioned above, non-enzymatic clearance mechanisms involve α-tocopherol (vitamin E), carotenoids, proline, and flavonoids (Das & Roychoudhury, 2014). α-Tocopherol belongs to the lipid-soluble antioxidant, and primarily scavenges OH• and $^1O_2$, thus protecting the chloroplast (Munné-Bosch, 2005; Singh, 2022). Flavonoids, as a group of water-soluble antioxidants, contribute to reducing $^1O_2$, similarly to the function of carotenoids, which belong to the family of lipophilic antioxidants (Agati et al., 2012; Ramel et al., 2012; Singh, 2022). Additionally, there is strong evidence indicating that anthocyanins scavenge H_2O_2 following mechanical injury in living organisms (Agati et al., 2012; Gould et al., 2002). Proposed roles of free proline include acting as osmoprotectant, protein stabilizer, metal chelator, inhibitor of lipid peroxidation, and scavenger of OH• and $^1O_2$ (Ashraf & Foolad, 2007; Gill & Tuteja, 2010b).

ROS generation is among the initial reactions, commencing shortly after treatment with

PAMPs, often within minutes in PTI, but also occurs during ETI, and the rate is considerably slower in comparison (Kadota et al., 2015; Wu et al., 2023). The efficiency of apoplastic ROS-scavenging mechanisms is lower compared to intracellular systems, resulting in high ROS accumulation in the apoplast, which is crucial for systemic signaling and pathogen defenses (Choudhury et al., 2017). ROS has critical roles in various aspects of plant biology, including growth and development (Swanson & Gilroy, 2010), stomatal closure (Qi et al., 2018b), maintenance of vegetative apical meristems (Kong et al., 2018; Tsukagoshi et al., 2010), stress responses (Mittler et al., 2022), epigenetic modifications (Locato et al., 2018; Wang et al., 2016), and hormone regulation (Xia et al., 2015).

2.8. Ca^{2+} signaling and plant defense

In typical plant environments like seawater, freshwater, and soils, the Ca^{2+} concentration ranges from 0.1 to 10 mM, while cytosolic Ca^{2+}levels typically remain around 100 nM in the resting state (Luan & Wang, 2021; Wang & Luan, 2024). Possibly to avoid toxicity, plants possess various calcium reservoirs, such as the apoplast, vacuole, nuclear envelope, ER, chloroplast, and mitochondria (Stael et al., 2012; Wang & Luan, 2024). The central vacuole is the main calcium storage in plants, with vacuolar Ca^{2+} concentrations ranging from 0.2 mM to 1–5 mM to 80 mM (Stael et al., 2012). Calcium (Ca^{2+}) acts as a universal second messenger in all eukaryotes, including plants (Kudla et al., 2018; Webb et al., 1996). When *A. thaliana* plants are cultivated in a low 0.1 mM Ca^{2+} medium, the flg22-induced cytosolic $Ca^{2+}$and ROS bursts are significantly diminished compared with those grown in standard 1.5 mM-Ca^{2+} medium (Tian et al., 2019). This indicates that external Ca^{2+} levels affect the plant response to PAMPs (Tian et al., 2019).

The cytoplasmic Ca^{2+} signals' stimulus-specific details can be conveyed through temporal-spatial characteristics like recurrence, size, and positioning (Berridge et al., 2003; Dodd et al., 2010; Kudla et al., 2018). The typical Ca^{2+} signaling process involves several sequential steps: a stimulus activates Ca^{2+}-permeable channels, generating specific Ca^{2+} signals (encoding); Ca^{2+} then binds to specific proteins (Ca^{2+} sensors), which regulate effector proteins and induce changes in cellular activities (decoding); finally, Ca^{2+} removal from the cytoplasm restores the resting state (Tian et al., 2020).

About the encoding, the joint action of Ca^{2+} influx through Ca^{2+} channels and energy dependent Ca^{2+} efflux via Ca^{2+} transporters result in the formation of Ca^{2+} signatures (Kudla et al., 2018). *A. thaliana* has five families of Ca^{2+}-permeable channels: *CYCLIC NUCLEOTIDE GATED CHANNEL* (*CNGC*, 20 members), *GLUTAMATE RECEPTOR* (*GLR*, 20 members), *TWO PORE CHANNEL* (*TPC*, one representative), *MECHANOSENSITIVE PROTEIN CHANNEL* (*MCA*, two members), and *HYPEROSMOLALITY-GATED CALCIUM-PERMEABLE CHANNEL* (*OSCA*, 15 members) (Edel et al., 2017; Kudla et al., 2018). The *A. thaliana* genome contains five distinct Ca^{2+} efflux mechanisms, including *AUTOINHIBITED Ca^{2+}-ATPases* (*ACAs*), *ER-type Ca^{2+}ATPases* (*ECAs*), *P1-type ATPases* (*P1-ATPases*), *MITOCHONDRIAL CALCIUM UNIPORTER COMPLEX* (*MCUC*), and *Ca^{2+} EXCHANGERS* (*CAXs*) (Edel et al., 2017). For decoding calcium signals, the *A. thaliana* genome encodes three prominent families: 34 *CDPKs*, 10 *CBLs* (*CALCINEURIN B-LIKE PROTEINS*) and 26

CBL-CIPKs (*CBL - INTERACTING PROTEIN KINASES*), and 7 *CaMs* (*CALMODULIN PROTEINS*) and 50 *CMLs* (*CaM-LIKE PROTEINS*) (Edel et al., 2017).

CNGC2 (*CYCLIC NUCLEOTIDE-GATED CHANNEL 2*) has been documented to play a role in Ca^{2+} influx following the recognition of PAMPs and DAMPs (Ma et al., 2012; Tian et al., 2019). The *cngc2* mutant shows reduced cytosolic Ca^{2+} elevations in response to LPS (lipopolysaccharide) and Pep3 (Ali et al., 2007; Ma et al., 2012). In *A. thaliana*, the plant elicitor peptides (Pep 1–6) serve as DAMPs (Yamaguchi & Huffaker, 2011). Pep receptors *PEPR1/2* (*PEPTIDES RECEPTOR 1* and *2*), which possess guanylyl cyclase activity, can produce cyclic GMP (guanosine monophosphate) to activate *CNGC2* (Ali et al., 2007; Ma et al., 2012).The kinases *BIK1* phosphorylates and activates the *CNGC2* and *CNGC4* and *OSCA1.3* channels upon PAMP perception (Thor et al., 2020; Tian et al., 2019).The Ca^{2+}-permeable channel *OSCA1.3* and *OSCA1.7* play the critical role in PTI- stomatal closure (Thor et al., 2020). A contrasting discovery is that the mutant *cngc20-4* induces Ca^{2+} influx, enhancing PTI responses and triggering ETI hypersensitive cell death (Zhao et al., 2021b). Moreover, *CNGC20* engages in self-association, establishes heteromeric complexes with *CNGC19*, and undergoes phosphorylation and stabilization by *BIK1*(Zhao et al., 2021b).

An earlier pharmacological investigation proposed that the Ca^{2+} influx triggered by the recognition of various PAMPs, such as flg22, elf18, and chitin, occurs through *iGluR* (*IONOTROPIC GLUTAMATE RECEPTOR*)-like channels (Kwaaitaal et al., 2011). The *glr3.3-1* and *glr3.3-2* mutants showed notably increased susceptibility to *Pst DC3000* infection compared to the wild-type, suggesting that *GLR3.3* (*GLUTAMATE RECEPTOR 3.3*) plays a role in innate immunity (Li et al., 2013). *GLRs* may also participate in JA signal transduction (Kang et al., 2006; Mousavi et al., 2013). *BAK1* is involved in *GLR3.3* and *GLR3.6* induced Ca^{2+} elevation during aphid feeding (Vincent et al., 2017). By analyzing the transcriptional landscape during PTI by flg22, elf18, pep1 (peptide 1), nlp20 (necrosis- and ethylene-inducing peptide 1 (nep1)-like protein 20), OGs (Oligogalacturonides) and others, it has been confirmed that some *GLRs* participate in the PTI responses (Bjornson et al., 2021). For example, the triple mutant *glr2.7 glr2.8 glr2.9* exhibited impaired Ca^{2+} responses to various elicitors (flg22, elf18 and pep1) and decreased resistance to *P. syringae* infection (Bjornson et al., 2021).

Vacuolar transporters *CAX1* (Ca^{2+} exchanger 1) and *CAX3* (Ca^{2+} exchangers 3) play a crucial role in helping plants manage external Ca^{2+} conditions, likely by sequestering excessive Ca^{2+} into the vacuolar lumen (Cheng et al., 2005; Conn et al., 2011). Plants utilize a Ca^{2+}*–CBL–CIPK–CAX* (Ca^{2+} - *Calcineurin B-like protein - INTERACTING PROTEIN KINASE - Ca^{2+} EXCHANGER*) cascade to link Ca^{2+} influx to vacuolar sequestration, thus preserving cytosolic Ca^{2+} level under normal circumstances (Wang et al., 2024). This pathway constitutes a Ca^{2+}-dependent feedback loop, or self-regulation, facilitating plant adjustment to the natural soil Ca^{2+} concentrations (Luan & Wang, 2021; Wang et al., 2024). Additionally, in PTI, the *FLS2–BAK1–BIK1/PBL1* module triggers the activation of *CAX1/3*, thereby modulating Ca^{2+} signals involved in immunity (Wang et al., 2024).

The PM-localized proteins *ACA8* (*AUTOINHIBITED Ca^{2+}-ATPase 8*) and *ACA10*

(*AUTOINHIBITED Ca^{2+}-ATPase 10*) interact with copine - like protein *BON1* (*BONZAI 1)*, contributing to the creation of vital cytosolic calcium for stomatal closure and affecting plant immunity (Yang et al., 2017). The PM-localized protein BON1 negatively influences the expression of immune receptor genes while positively affects stomatal closure and interacts with both *BAK1* and *BIR1* (*BAK1-INTERACTING RECEPTOR-LIKE KINASE 1*) (Wang, et al., 2011a). Stomatal closure induced by calcium and pathogens was found to be impaired in *aca10* and *bon1* (Yang et al., 2017). *ACA8* has been demonstrated to associate with *FLS2* to form a complex (Frei dit Frey et al., 2012). The *aca8 aca10* mutant exhibits reduced flg22-triggered calcium and ROS, along with modified transcriptional reprogramming (Frei dit Frey et al., 2012). Furthermore, *aca8 aca10* displays decreased stomatal aperture and transpiration under heat stress compared to the wild type, while it shows increased basal and peak levels of transient Ca^{2+} induced by flg22 (Li et al., 2023).Other *AUTOINHIBITED Ca^{2+}-ATPases* (*ACAs*), found in the ER like *ACA1/2/7*, and in vacuole membranes such as *ACA4/11*, might also play a role during PTI (Hilleary et al., 2020; Rahmati Ishka et al., 2021; Wang & Luan, 2024).

In *A. thaliana*, *CDPK4, CDPK5, CDPK6*, and *CDPK11* serve as activators of the ROS burst by PAMPs (Boudsocq et al., 2010). The mutants *cpk4, cpk5, cpk6,* and *cpk11* respond normally to *Pst DC3000,* while the double *cpk5 cpk6* and triple *cpk5 cpk6 cpk11* mutants display heightened susceptibility and decreased ROS production, suggesting redundancy among closely related *CDPKs* (Boudsocq et al., 2010). Prolonged activation of *CPK4/5/6/11* leads to the direct phosphorylation of a specific subset of *WRKY* TFs, like *WRKY8/28/48* (Gao et al., 2013). This collaborative action is vital for transcriptional reprogramming essential for the NLR (nucleotide-binding/leucine-rich-repeat receptor)-mediated limitation of pathogen proliferation (Gao et al., 2013). *CPK1/2/4/11* phosphorylate NADPH oxidases located at the PM to induce the production of ROS (Gao et al., 2013).

CDPK5 directly phosphorylates *CBP60g* in response to flg22, thereby enhancing its transcription factor activity (Sun et al., 2022). *CDPK5* overexpression leads to activation of *SARD1* and genes for SA biosynthesis, like *ICS1* and *EDS5*, markedly boosting SA and NHP (N-hydroxypipecolic acid) levels (Guerra et al., 2020). *CPK28* was shown to play a negative regulatory role in immune signaling (Wang al., 2018a). *CDPK28* activation phosphorylates U-BOX–type E3 ubiquitin ligases *PUB25* and *PUB26*, leading to *BIK1* degradation and subsequent attenuation of elicitor-induced Ca^{2+} influx and ROS production (Monaghan et al., 2015; Monaghan et al., 2014; Wang et al., 2018a).

3. Polyamines in plant defense

Polyamines (PAs) are low molecular weight polycationic amines (Chen & Shao, 2019). PAs are widely present in most organisms and play important roles in regulating plant growth, development, and responses to biotic or abiotic stress conditions (Gill & Tuteja, 2010a). PAs can generally be found in various forms: free soluble, non-covalently conjugated, or covalently conjugated (Pál et al., 2021). Covalently conjugated PAs can be categorized into two groups: perchloric acid-soluble and perchloric acid-insoluble

(Pál et al., 2021).

Free PAs primarily include putrescine (Put), spermidine (Spd), and spermine (Spm) in higher plants (Mustafavi et al., 2018). In *A. thaliana*, Spd is predominantly found in most organs with the highest content, particularly abundant in flowers where it exists in both free and conjugated forms (Tassoni et al., 2000). In lower plants such as algae and mosses, unusual PAs, norspermidine (NorSpd) and norspermine (NorSpm), structurally resemble their more common polyamine counterparts Spd and Spm respectively, except they possess one fewer methyl group in their carbon chain (Hamana & Matsuzaki, 1985; Michael, 2016).

The diamine cadaverine (Cad) has been reported in various plants including rice, oat, rye, wheat, barley, maize, and sorghum (Tomar et al., 2013). Cad content level is below detectable limits in *A. thaliana* (Liu et al., 2014; Strohm et al., 2015). Thermospermine (tSpm), a structural isomer of spermine, is essential for the proper development of plant vasculature, thereby facilitating stem elongation (Kakehi et al., 2008; Muñiz et al., 2008). T-Spm plays a role in vascular development by regulating *SUPPRESSOR-OF-ACL5 SAC51* family genes encoding *bHLH* TFs through uORF (upstream Open Reading Frame) -mediated mRNA translational regulation in *A. thaliana* (Cai et al., 2016; Y. Takahashi et al., 2018; Yamamoto & Takahashi, 2017).

3.1 Polyamine biosynthesis

Put is a four-carbon diamine that serves as precursor of Spd and Spm, which are seven-carbon triamine and ten-carbon tetraamine, respectively (Gerlin et al., 2021). In plants, Put biosynthesis occurs through three distinct pathways (Chen & Shao, 2019). *ARGININE DECARBOXYLASE* (*ADC*) converts arginine to agmatine, and agmatine is further converted to N-carbamoyl Put via *AGMATINE IMINOHYDROLASE* (*AIH*), followed by the hydrolysis of N-carbamoyl Put by *N-CARBAMOYLPUTRESCINE AMIDOHYDROLASE* (*CPA*) to yield Put (Alcázar et al., 2010). In this pathway, *ADC* serves as the rate-limiting step for Put biosynthesis in plants (Alcázar et al., 2005). There are two *ADC* genes *(ADC1* and *2*) in *Arabidopis* (Alcázar et al., 2010). Analysis of *adc* mutants revealed that *ADC2* contributes significantly more than *ADC1* to basal *ADC* activity and Put biosynthesis during stress conditions (Rossi et al., 2015). *ADC* activity can be inhibited by DL-α- difluoromethylarginine (DFMA), an irreversible competitive inhibitor, and by D-Arginine, a reversible inhibitor (González-Hernández et al., 2022). The double mutant *adc1 adc2* is embryo lethal, indicating the requirement of polyamines for cell viability (Kaoru Urano et al., 2005). In the *ODC* (*ORNITHINE DECARBOXYLASE*) route, ornithine is decarboxylated by *ODC* to produce Put (Chen & Shao, 2019). The *ODC* gene is absent in *A. thaliana* and other *Brassicaceae* family members (Hanfrey et al., 2001). In the third pathway, arginine is transformed into citrulline, which is followed by the decarboxylation catalyzed by citrulline decarboxylase to yield Put (Chen & Shao, 2019; de Oliveira et al., 2018). The citrulline pathway has only been identified in sesame (Chen & Shao, 2019; Crocomo & Basso, 1974).

Spd is produced from Put by adding an aminopropyl group catalyzed by *SPERMIDINE SYNTHASE* (*SPDS*) (Alcázar et al., 2010). Spd is vital for cell survival, possibly

because it serves as a substrate for the hypusination of eukaryotic translation initiation factor 5A (Takahashi & Kakehi, 2010). Spm is generated when *SPM SYNTHASE* (*SPMS*) transfers an aminopropyl group to Spd (Alcázar et al., 2010). While Spm is not crucial for *A. thaliana* survival, it does play a role in enhancing resistance to salt stress (Imai et al., 2004; Yamaguchi et al., 2006a). Plants also contain trace amounts of other PAs, such as tSpm produced by *THERMOSPERMINE SYNTHASE* (*TSPMS*) (Alcázar et al., 2010; Kakehi et al., 2008). *SPDS1, SPDS2*, and *SPMS* are found in the nucleus and cytosol, capable of forming homo and heterodimers (Tiburcio et al., 2014). Notably, heterodimers are exclusively located in the nucleus, indicating a nuclear-focused metabolic channeling from Put to Spm in *A. thaliana* (Tiburcio et al., 2014).

Methionine is converted to S-adenosylmethionine (SAM), which undergoes decarboxylation by *SAM DECARBOXYLASE* (*SAMDC*) to produce decarboxylated SAM, donnor of aminopropyl groups for polyamine biosynthesis (Alcázar et al., 2010). The *A. thaliana* genome carries four *SAMDC* (*SAMDC1-4*) two *SPDS* (*SPDS1* and *2*), and one single *SPMS* gene (Alcázar et al., 2010; K Urano et al., 2003).

3.2 Polyamine oxidation

Polyamines undergo oxidation by amine oxidases to produce ROS and other metabolites. There are two major classes of amine oxidases, namely *COPPER-CONTAINING AMINE OXIDASES* (*CuAO*s) and FAD-dependent *POLYAMINE OXIDASES* (*PAO*s) (Tavladoraki et al., 2016).

*CuAO*s preferentially oxidize diamines such as Put, primarily catalyzing their oxidation at primary amino groups, resulting in the production of 4-aminobutanal, H_2O_2, and ammonia (NH_3) (Alcázar et al., 2010; Tavladoraki et al., 2016). 4-aminobutanal cyclizes to form pyrroline, which is then converted to γ-aminobutyric acid (GABA) by pyrroline dehydrogenase (Alcázar et al., 2010). Subsequently, GABA is further converted to succinate, entering the Krebs cycle (Chen & Shao, 2019). *A. thaliana* possesses about ten identified *CuAO* genes, yet only five of them (*AtAO1 (At4g14940), AtCuAO1* (*At1g62810), AtCuAO2 (At1g31710), AtCuAO3 (At2g42490), and AtCuAO8 (At1g31690))* have been thoroughly characterized (Tavladoraki et al., 2016; Wang et al., 2019).

In situ hybridization reveals that *ATAO1* is expressed in lateral root cap cells, root vasculature, developing leaves, hypocotyls, and stigma/style tissue in *A. thaliana* (Møller & McPherson, 1998). Histochemical analysis indicates that the expression of *ATAO1* in developing tracheary elements precedes and coincides with lignification (Møller & McPherson, 1998). *ATAO1* expression is significantly induced by methyl jasmonate (MeJA) treatment, and H_2O_2 produced by *ATAO1* mediates MeJA-induced early protoxylem differentiation in *A. thaliana* roots (Ghuge et al., 2015).

AtCuAO1, similar to *ATAO1*, is an extracellular protein containing an N-terminal signal peptide, whereas *AtCuAO2* and *AtCuAO3* are located in peroxisomes (Planas-Portell et al., 2013; Wang et al., 2019). *AtCuAO1* transcripts are high in rosette leaves, peaking in stems and flowers (Planas-Portell et al., 2013). After 24 h of SA treatment, *CuAO1* expression is induced (Planas-Portell et al., 2013), whereas wounding or ACC (1-aminocyclopropane-1-carboxylate) treatment does not significantly affect *AtCuAO1*

expression (Planas-Portell et al., 2013). *cuao1-1* and *cuao1-2* mutants have been described to be ABA-insensitive (Wimalasekera et al., 2011a). In the two mutants, NO synthesis induced by PAs and ABA is compromised, while seed germination, seedling growth, and root growth sensitivity to ABA are reduced (Wimalasekera et al., 2011a). Additionally, In the two mutants the expression of stress-responsive genes *RD29A* (*RESPONSE-TO-DEHYDRATION 29A*) and *ADH1* (*ALCOHOL DEHYDROGENASE 1*) induced by ABA are also compromised (Wimalasekera et al., 2011a).

AtCuAO2 transcript levels are high in stems but low in other organs, with no observed increase during development (Planas-Portell et al., 2013). At about 8 h, *CuAO2* expression increases sharply in wounded and MeJA-treated seedlings (Planas-Portell et al., 2013). *AtCuAO3* transcripts are high in flowers, leaves and stems (Planas-Portell et al., 2013). At 24 hours, *AtCuAO3* expression increased with MeJA, and decreased with ABA or SA (Planas-Portell et al., 2013). *AtCuAO3* has the SKL (serine-lysine-leucine) tripeptide at its C-terminus, which targets the protein to the peroxisome matrix (Khan & Zolman, 2010; Planas-Portell et al., 2013). The *cuao3* mutant showed insensitivity to ABA in stomata closure, but responded to H_2O_2 or Ca^{2+}, indicating that *CuAO3* acts downstream of ABA stimulus (Qu et al., 2014).

AtCuAO1, AtCuAO2, and *AtCuAO3* enzymes oxidize Put and Spd, releasing H_2O_2 (Planas-Portell et al., 2013). In contrast, animal *CuAOs* preferentially oxidize Spd and Spm (Tavladoraki et al., 2012).

In monocotyledonous plants, *PAOs* facilitate the terminal degradation of PAs by oxidizing Spd and Spm (Gerlin et al., 2021; Planas-Portell et al., 2013). This process yields 4-aminobutanal and N-(3-aminopropyl)-4-aminobutanal, respectively, along with 1,3-diaminopropane (DAP) and H_2O_2 (Gerlin et al., 2021; Planas-Portell et al., 2013). In *A. thaliana*, *PAOs* oxidize Spd and Spm, leading to a pathway where Spm is converted back to Spd, Spd to Put, along with the production of 3-aminopropanal and H_2O_2 (Liu et al., 2019b; Planas-Portell et al., 2013). The *A. thaliana* genome contains five *PAOs*, named from *AtPAO1* to *AtPAO5* (Fincato et al., 2011). *AtPAO1* and *AtPAO5* are localized in the cytosol, while *AtPAO2, AtPAO3*, and *AtPAO4* are localized in peroxisomes, forming a distinct subfamily with similar gene structures and high sequence homology (Fincato et al., 2012; Kim et al., 2014).

AtPAO1 is subcellularly localized in the cytoplasm and prefers to utilize Spm, tSpm, and NorSpm as substrates (Tavladoraki et al., 2006). *AtPAO1* shows a preference for tSpm compared to Spm (Fincato et al., 2012). *AtPAO1* exhibits specific expression in the root transition region and anther tapetum (Fincato et al., 2012; Yu et al., 2019). *AtPAO2* and *AtPAO3* exhibit similar substrate preferences, with Spd being the most favorable substrate, although they also recognize Spm, tSpm and NorSpm (Takahashi et al., 2010). *AtPAO2* is expressed in the quiescent center, columella initials, and pollen, with higher expression observed in shoot meristem, root tip, leaf petiole, and anther during later growth stages (Fincato et al., 2012; Takahashi et al., 2010). *AtPAO3* shows constitutive expression, with highest levels in flower organs, and its promoter activity is detected in cotyledon, root tip, mature leaf boundary, and flower filaments, with expression also observed in columella, guard cells, and pollen (Fincato et al., 2012; Takahashi et al., 2010). Loss of *AtPAO3* function increased $O_2^{\bullet -}$ production via NADPH

oxidase, activating the mitochondrial alternative oxidase pathway (Andronis et al., 2014).

AtPAO4 primarily accepts Spm as a substrate and shows limited acceptance of tSpm (Takahashi et al., 2010). *AtPAO4* is highly expressed throughout young seedlings, including roots, and its expression remains ubiquitous in the mature stage, with lower levels observed in the stem (Takahashi et al., 2010). Two *pao4* loss-of-function mutants, *pao4-1* and *pao4-2*, exhibit a 10-fold increase in Spm accumulation and delayed senescence onset under dark conditions (Sequera-Mutiozabal et al., 2016). *AtPAO5* catalyzes the conversion of Spm and tSpm to Spd but does not catalyze the conversion to Put (Kim et al., 2014). It is highly likely that *AtPAO5* primarily metabolizes T-Spm in plants (Kim et al., 2014). The *pao5-1* and *pao5-2* mutants showed about 2-fold higher T-Spm levels but similar levels of Put, Spd, and Spm compared to wild-type plants (Kim et al., 2014). *AtPAO5* is widely expressed during development, particularly in roots, stems, leaves, and floral organs, playing a role in stem elongation and rosette leaf development (Fincato et al., 2012; Kim et al., 2014; Takahashi et al., 2010; Yu et al., 2019). The pathway of polyamine metabolism in *Arabidopsis* can be seen in Figure 3.

There is potential crosstalk between NO and PAs in plant development, and abiotic and biotic stress responses (Wimalasekera et al., 2011b). Applying exogenous Put, Spd, and Spm to *A. thaliana* seedlings induces NO production, suggesting NO as a potential mediator of polyamine actions (Wimalasekera et al., 2011). Put, Spd and Spm induced stomatal closure and elevated levels of NO and ROS in guard cells (Agurla et al., 2018). Mutants lacking functional *AtCuAO1* and *AtPAO2* exhibit deficiencies in PAs- and/or ABA-induced NO production (Wimalasekera et al., 2011ab, 2015). *CuAO8* is involved in arginine-dependent NO synthesis (Groß et al., 2017). The *cuao8* mutants showed reduced NO production in seedlings under 2,6-dichloroisonicotinic acid treatment and salt stress (Groß et al., 2017). The NO scavenger, cPTIO (2-4-carboxyphenyl-4,4,5,5-tetramethylimidazoline-1-oxyl-3-oxide), could abolish the function of PAs (Gong et al., 2014). A fluorimetric method showed that Spd and Spm significantly boosted NO release in *A. thaliana* seedlings, while arginine and put had minimal impact (Tun et al., 2006). Spm, the most potent polyamine, induced NO release without any noticeable delay (Tun et al., 2006). Spm and Spd promoted NO biosynthesis in the elongation region of *A. thaliana* root tips and primary leaves, notably in veins and trichomes (Tun et al., 2006).

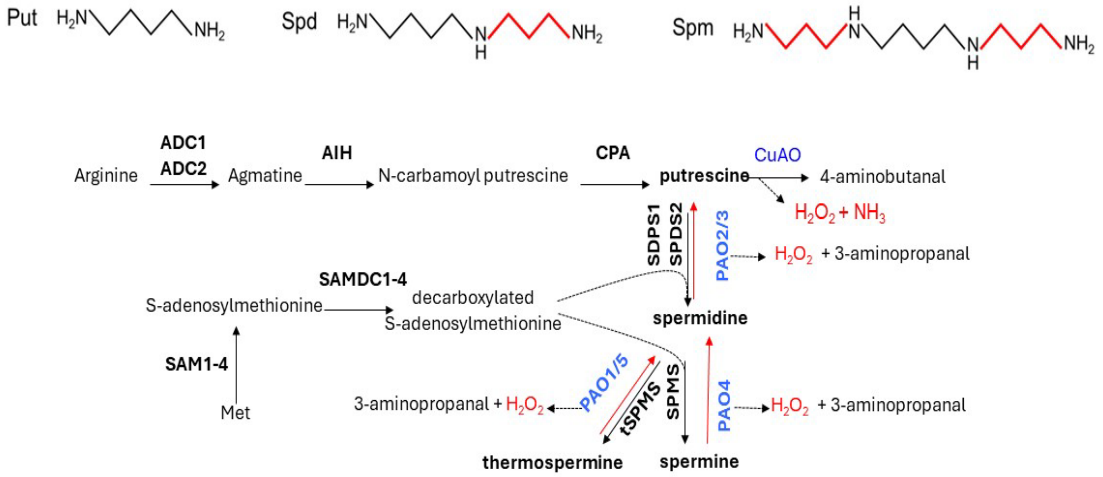

Figure 3 Polyamine metabolism in *Arabidopsis* (Alcázar et al. 2010). *ADC: ARGININE DECARBOXYLASE, AIH: AGMATINE IMINOHYDROLASE, CPA: CARBAMOYL PUTRESCINE AMIDOHYDROLASE, CuAO: COPPER-CONTAINING AMINE OXIDASE, PAO: POLYAMINE OXIDASE Put: putrescine, Spd: spermidine, Spm: spermine, SPDS: SPERMIDINE SYNTHASE , SPMS: SPM SYNTHASE, tSPMS: THERMOSPERMINE SYNTHASE.*

3.3. Polyamines and plant stress

3.3.1. Polyamines and abiotic stress

Put acts as a precursor for various alkaloids, including nornicotine, nicotine, retronecine, and hyoscine, offering significant adaptive benefits to plants synthesized from primary metabolites (Zeiss et al., 2021). Put serves as a precursor to nicotine, the signature alkaloid in *Nicotiana* species, acting as a defensive neurotoxin against herbivores (Xu et al., 2017). Put accumulates under certain conditions, such as low pH, heavy metals, K^+ deficiency, low Mg^{2+}, anoxia, cold, or osmotic stress (Cui et al., 2020). *ADC2* expression is induced by high osmolarity, drought, salinity, and wounding stress leading to Put accumulation in *A. thaliana* (Alcázar et al., 2010; Perez-Amador et al., 2002; Soyka & Heyer, 1999; Kaoru Urano et al., 2004).

Exogenous Put application or overexpression of *ADC* genes generally improves plant tolerance to abiotic stresses and enhances growth, photosynthesis, and antioxidant activity (González-Hernández et al., 2022). Under salt stress, exogenous Put application offers various advantages, such as enhanced growth in citrus rootstocks, enhanced activity of antioxidant enzymes in barley, optimized photosynthesis rate in rice, increased stomatal conductivity in wheat, protection of photosynthetic pigments in beans, and decreased lipid peroxidation in *Brassica juncea* (Ghalati et al., 2020).

Exogenous Spd or Spm application enhanced the resistance of wheat seedlings to the harmful effects of Cd (Cadmium) stress (Rady & Hemida, 2015). Spd exhibited the protective role when applied through seed soaking, and increased Cd-induced oxidative stress when pre-treated hydroponically in wheat (Tajti et al., 2018). The combination of Spd and Cd resulted in elevated Put, Cd, SA, and proline contents, while only hydroponically applied Spd influenced the expression of the phytochelatin synthase gene, reducing it under Cd stress (Tajti et al., 2018). Endogenous levels of Spd and Spm,

along with GSH, were boosted under Cd stress in silicon-treated wheat plants, enhancing tolerance against metal toxicity (Howladar et al., 2018).

Exogenous Spd and Spm shows potential to enhance salt tolerance by reducing oxidative damage and enhancing some enzyme activities (Baniasadi et al., 2018). Spm and Spd influence PSI activity in thylakoid membranes during photoinhibition (Yaakoubi et al., 2014). Pre-treating thylakoid membranes with Spm and Spd markedly attenuated the inhibition of O_2 uptake rates, P700 photooxidation, and O_2•⁻accumulation in light stress (Yaakoubi et al., 2014). The introduction of *SPDS* cDNA from *Cucurbita ficifolia* into *A. thaliana* resulted in transgenic plants with increased *SPDS* activity and Spd content in leaves, leading to enhanced tolerance to chilling, freezing, salinity, hyperosmosis, drought, and paraquat toxicity (Kasukabe et al., 2004). cDNA microarray analysis under chilling stress also showed increased transcription of several stress-responsive genes, including *DREB* (*DEHYDRATION RESPONSIVE ELEMENT BINDING*) and *RD29A* (*RESPONSE-TO-DEHYDRATION 29A*) (Kasukabe et al., 2004).

The *A. thaliana* double-knockout mutant *acl5 spms* shows heightened sensitivity to high salt and drought (Yamaguchi et al., 2007). The phenotype was alleviated by pretreatment with Spm, but not with Put or Spd, highlighting the drought hypersensitivity by Spm deficiency (Yamaguchi et al., 2007). Exogenously applied Spm exhibited potential protection during heat stress, with higher Spm contents correlating with increased thermotolerance in *A. thaliana* (Sagor et al., 2013).

3.3.2. Polyamines and biotic stress

Plant polyamines increase during defense and play an important role in biotic stress responses. Put enhances the plant defense response by increasing ROS production, callose deposition and expression of defense-related marker genes (Liu et al., 2019b, 2020b). *MPK3* and *MPK6* positively regulate Put biosynthesis by transcriptionally influencing *ADC1* and *ADC2* expression during pathogen defense in *A. thaliana* (Kim et al., 2013c). The *adc2* mutant exhibits higher susceptibility to *Pst DC3000* infection compared to the wild type, and this susceptibility has been linked to decreased expression of the *PR1* gene (Kim. et al., 2013c). *ADC1* expression in pepper *Capsicum annuum* induces elevated levels of PAs and GABA (gamma-aminobutyric acid), prompting bursts of NO and H_2O_2, ultimately eliciting plant defense and cell death responses (Kim et al., 2013a). Exogenous Put suppressed nematode development in tomato (Khajuria & Ohri, 2018). Spd enhanced resistance to rice blast by upregulating marker genes in the SA signaling pathway and phytoalexin biosynthesis (Moselhy et al., 2016). In addition, the Spm signaling pathway in *A. thaliana* is vital for limiting *cucumber mosaic virus (CMV*) infection-induced HR (Mitsuya et al., 2009). Transgenic *A. thaliana* plants overexpressing SPMS showed increased resistance to *Pseudomonas viridiflava*, while *spms* mutants with low spermine levels were more susceptible (Gonzalez et al., 2011). Spd and Spm also prime resistance against *Botrytis cinerea* (Janse van Rensburg et al., 2021).

Apoplastic PAs are also crucial in plant-pathogen interactions in tobacco, and their effects depend on the type of pathogen (necrotrophs or biotrophs) (Marina et al., 2008). Infection by the necrotrophic fungus *Sclerotinia sclerotiorum* increases *ADC*

expression and activity in tobacco tissues, leading to accumulation of Put and Spm in the leaf apoplast that correlates with increased tissue necrosis. This response contrasts with the enhanced disease resistance to the biotrophic pathogen *P. viridiflava* triggered by polyamine accumulation (Marina et al., 2008). The importance of the polyamine pathway in plant-pathogen interactions is illustrated by the effector Brg11, a *TALE* (transcription-activator-like effector) effector from *Ralstonia solanacearum*, that targets tomato ADC genes, inducing elevated PA levels that inhibit bacterial niche competitors of *Ralstonia solanacearum* (Wu et al., 2019). However, contrasting results have been documented that would require further validations. For example, *A. thaliana adc*-silenced lines have been reported to show heightened susceptibility to *Botrytis cinerea* but increased resistance to *P.syringae* infection (Chávez-Martínez et al., 2020). Standarization of pathoassay methodologies may help at a proper comparison between works.

PAs can interact with hormonal pathways in potential crosstalk for plant defense. An increase in Spd levels in the plant attenuates ET synthesis, leading to increased susceptibility of tomato to *Botrytis Cinerea* (Nambeesan et al., 2012). Quantitative RT-PCR and pharmacological tests demonstrated that both *AtPAO2* and *AtPAO4* transcripts were induced by ET (Hou et al., 2013). *PAO* generates H_2O_2 in *A. thaliana* guard cells, playing a crucial role in stomatal movement (Hou et al., 2013). Dehydration and high salinity increased the expression of *AtPAO2* and *AtPAO4* to varying extents, contributing to stomatal closure (Hou et al., 2013). ABA increases the expression of *SPMS* (Hanzawa et al., 2002). Additionally, it has been observed that *CuAO* and *PHOSPHOLIPASE D* (*PLD*) function independently in ABA-induced stomatal closure (Qu et al., 2014). NH_4^+ nutrition enhances resistance to *P. syringae* in tomato by increasing H_2O_2 accumulation, which activates SAA (systemic acquired acclimation) through ABA and Put (Fernández-Crespo et al., 2015; González-Hernández et al., 2022). In *Vicia faba* guard cells, *CuAO* is crucial for H_2O_2 production during ABA-induced stomatal closure by degrading Put, with calcium signaling playing a key role (An et al., 2008). COR or MeJA also can hamper PAs biosynthesis (Adio et al., 2011; Lou et al., 2016). SA is suggested to have a correlation with PAs under different stress conditions, including osmotic stress, and Cd exposure (Doneva et al., 2021; Szalai et al., 2017; Tajti et al., 2018). Defense signaling elicited by Put in *A. thaliana* relies partially on the accumulation of SA (Liu et al., 2019b, 2020b), although stimulation of Put biosynthesis during defense is largely SA-independent (Zhang et al., 2023)

Conjugated PAs also play a role in plant development and responses (Pál et al., 2021). PAs are frequently conjugated to cinnamic acids, such as *p*-coumaric, ferulic, and caffeic acids, forming conjugates referred to as hydroxycinnamic acid amides (HCAAs) (Walters, 2003). Aliphatic amine-containing HCAAs are water-soluble, while aromatic amine-containing HCAAs are not (Walters, 2003). HCAAs are potent antimicrobial molecules and can strengthen cell walls by forming bonds with polysaccharides and bridging dimers, creating complex crosslinkages (Walters, 2003; Zeiss et al., 2021). In *A. thaliana*, COR induces acetylation of Put catalyzed by *NATA1* (*N-ACETYL TRANSFERASE ACTIVITY 1*) to N-acetyl-Put, competing with *SPDS* for the shared substrate and thereby reducing Spd accumulation (Lou et al., 2016). Compared to wild-type, *nata1* mutants respond to *P. syringae* infection with decreased acetyl-Put levels,

increased nonacetylated PAs, higher PAs oxidase-mediated ROS production, and upregulated expression of pathogen defense genes (Adio et al., 2011; Lou et al., 2016). Under heat stress, inhibition of *HEAT SHOCK PROTEINS 90* (*HSP90s*) leads to the upregulation of *NATA1* expression in *A. thaliana* (Toumi et al., 2019). *HSP90s* promote PAs acetylation (acetylated Spd and Spm) and interact with *PAOs*, influencing PAs oxidation and H_2O_2 balance in *A. thaliana* (Toumi et al., 2019).

Enzymes involved in PA synthesis or metabolism are also associated with plant defense. Overexpressing the *SAMDC* in rice boosts polyamine levels (Spd and Spm) and improves tolerance to NaCl stress (Roy & Wu, 2002). Silencing the *SAMDC* gene reduces tomato resistance to *Cladosporium fulvum*, leading to small chlorotic spots on leaf margins and subsequent hyphal growth during HR (Zhao et al., 2018). Amine oxidases are associated with H_2O_2 production in defense mechanisms (Angelini et al., 2010; Cona et al., 2006). *P. syringae* infection increases the expression of *AtPAO1* and *AtPAO2* genes, and the *pao1-1 pao2-1* double mutant shows higher susceptibility to the pathogen (Jasso-Robles et al., 2020). The *PAO* mutants displayed changes in ROS levels (H_2O_2 and $O_2^{\bullet -}$) and activities of *RBOH*, *CAT*, and *SOD* enzymes in both infected and control plants (Jasso-Robles et al., 2020). Silencing *ACL5* in cotton which had low tSpm levels, resulted in a dwarf phenotype and decreased resistance to *Verticillium dahliae*(Mo et al., 2015).

PAs are also related to systemic acquired resistance (SAR), thereby enhancing plant immunity. SAR is a plant defense mechanism induced by an avirulent pathogen that triggers programmed cell death locally (Fu & Dong 2013). This process leads to SAR through the generation of mobile signals, accumulation of salicylic acid (SA), and secretion of antimicrobial *PR* proteins (Fu & Dong 2013). Put treatment induced local SA production and triggered local and systemic transcriptional reprogramming that intersected with SAR (Liu et al., 2020b). Spm primes defense response by inducing SAR and hypersensitive response (HR) in *A. thaliana* (Seifi et al., 2019). Furthermore, simultaneous coapplication of Spm and SA effectively suppresses *Botrytis cinerea* disease in tomato (Seifi et al., 2019).

Objectives

OBJECTIVES

Polyamines are small molecules that accumulate during plant defense. Most abundant polyamines in plants are the diamine putrescine (Put), triamine spermidine, and tetramines spermine (Spm), and its isomer thermospermine (tSpm). These molecules can be found as free forms, but also acetylated, or conjugated to hydroxycinnamic acids, proteins, or cell wall components. Despite the body of evidence pointing to their positive contribution to plant defense responses against pathogenic microorganisms, the modes of action of polyamines and detailed analyses on their contributions to the different layers of the plant immune system remained poorly investigated. In this context, the main objective of my PhD project was investigating the contribution of the polyamines (Put and Spm) to PAMP-triggered immunity, and SA/JA-mediated defenses in *Arabidopsis*. The Thesis is constituted by three chapters, which specific objectives are outlined below.

In **Chapter 1,** I explored how polyamines affect PTI transcriptional responses and early immune responses triggered by PAMPs, focusing on flg22-induced ROS burst and Ca^{2+} influxes, which represent key components of PTI. The specific objectives of this chapter were:

1. To investigate whether the polyamines Spm and Put affect early PTI responses such as PAMP (flg22)-elicited ROS production in *Arabidopsis*.

2. To explore the mechanisms underlying the Spm inhibitory effect on ROS production, including its independence on polyamine oxidation, NO signaling, and various defense components.

3. To investigate how Ca^{2+} influx dynamics induced by flg22 are affected by the polyamines Spm Put, and their combinations.

4. To analyze the differential transcriptional responses to flg22 induced by Put and Spm treatments, and their effects on disease resistance against *P. syringae*.

In **Chapter 2,** I examined the role of Spm in the defense respose against *P. syringae* and its impact on JA and SA signaling pathways. The specific objectives of this chapter were:

1. To explore the regulatory role of SA, COR and JA signaling to polyamine metabolism during the defense response to *P. syringae*.

2. To analyze the effect of Spm deficiency in the defense respose to *Pst DC3000*, with a particular focus on JA/SA signaling.

3. To determine the impact of Spm deficiency on lipid metabolism.

4. To determine the effect of Spm deficiency on endoplasmic reticulum (ER) stress signaling.

5. To analyze the contribution of Spm to disease resitance against the necrotrophic fungal pathogen *Botrytis cinerea*.

In **Chapter 3,** I conducted Genome-Wide Association Studies (GWAS) to identify the genetic determinisms underlying the natural variation of the Spm inhibitory effect on flg22-triggered ROS production, using 136 world-wide *Arabidopsis* accessions. The specific objectives of this chapter were:

1. To quantify the flg22-triggered ROS response in the presence of flg22 in 136 natural accessions of *Arabidopsis* from different populations.

2. To use the quantitative data obtained to perform GWAS mapping using already available genotyping information from these accessions.

3. To identify SNP associated with the variation of the trait and identify the candidate genes in linkage disequilibrium (LD).

4. To validate at least one candidate gene using loss-of-function mutants in *Arabidopsis*.

Results

Supervisor's report

Dr. Rubén Alcázar Hernández (Professor Agregat) at the **Departament de Biologia, Sanitat i Medi Ambient** of the **Facultat de Farmàcia i Ciències de l'Alimentació** (Universitat de Barcelona), Director of the PhD Thesis entitled **"The Contribution of the Polyamine Spermine to Plant Defense"** declares that:

The Thesis hereby presented is the result of the work performed by **Chi Zhang** under my supervision and guidance.

The contribution of the PhD candidate to different articles and chapters included in this Thesis is detailed below.

Chapter 1: Spermine inhibits PAMP-induced ROS and Ca^{2+} burst and reshapes the transcriptional landscape of PTI in Arabidopsis

Authors: **Chi Zhang***, Kostadin E. Atanasov, Rubén Alcázar

Journal of Experimental Botany (2023) 74: 427-442

Impact Factor: 6.9 (WOS)
Position: Plant Sciences 18 out of 239
Quartile: 1

Contribution of listed authors: **C.Z.** performed most of the experimental work with minor contributions of K.E.A. in RNA-seq; **C.Z.** and R.A. planned the experiments; **C.Z.** analyzed the data; **C.Z.** and R.A. wrote the paper; **C.Z.** and R.A. conceived the project

*This article is part of **Chi Zhang** PhD Thesis

Chapter 2: Spermine deficiency shifts the balance between jasmonic acid and salicylic acid-mediated defence responses in Arabidopsis.

Chi Zhang*, Kostadin E. Atanasov, Ester Murillo , Vicente Vives-Peris , Jiaqi Zhao, Cuiyun Deng, Aurelio Gómez-Cadenas , Rubén Alcázar

Plant, Cell & Environment (2023) 46: 3949-3970

Impact Factor: 7.3 (WOS)
Position: Plant Sciences 16 out of 239
Quartile: 1

Contribution of listed authors: **C.Z.** performed most of the experimental work with minor contributions from other authors in RNA-seq (K.E.A.), hormone quantitation (V.V.P. and A.G.C.) and *Botrytis cinerea* infections (E.M., J.Z., C.D.); **C.Z.** and R.A. planned the experiments; **C.Z.** analyzed the data; **C.Z.** and R.A. wrote the paper. **C.Z.** and R.A. conceived the project

*This article is part of **Chi Zhang** PhD Thesis

Chapter 3: Identification of genes underlying the natural variation of Spm+flg22 responses by GWAS mapping

Chi Zhang* and Rubén Alcázar

Publication status: Submission in preparation. This work is published as an attached chapter to this Thesis.

Contribution of listed authors: **C.Z.** performed all the experimental work. **C.Z.** and R.A planned the experiments. **C.Z.** analyzed the data and wrote the paper with R.A.; **C.Z.** and RA conceived the project

*This article is part of **Chi Zhang** PhD Thesis

Barcelona, 7 de Maig de 2024.

Rubén Alcázar Hernández

(Director i Tutor)

Chapter 1- Spermine inhibits PAMP-induced ROS and Ca^{2+} burst and reshapes the transcriptional landscape of PTI in *Arabidopsis*

Journal of Experimental Botany, Vol. 74, No. 1 pp. 427–442, 2023
https://doi.org/10.1093/jxb/erac411 Advance Access Publication 20 October 2022
This paper is available online free of all access charges (see https://academic.oup.com/jxb/pages/openaccess for further details)

RESEARCH PAPER

Spermine inhibits PAMP-induced ROS and Ca^{2+} burst and reshapes the transcriptional landscape of PAMP-triggered immunity in Arabidopsis

Chi Zhang, Kostadin E. Atanasov and Rubén Alcázar*

Department of Biology, Healthcare and Environment. Section of Plant Physiology, Faculty of Pharmacy and Food Sciences, Universitat de Barcelona, Av. Joan XXIII 27-31, 08028 Barcelona, Spain

* Correspondence: ralcazar@ub.edu

Received 21 June 2022; Editorial decision 7 October 2022; Accepted 18 October 2022

Editor: Wen-Ming Wang, Sichuan Agricultural University, China

Abstract

Polyamines are small polycationic amines whose levels increase during defense. Previous studies support the contribution of the polyamine spermine to defense responses. However, the potential contribution of spermine to pathogen-associated molecular pattern (PAMP)-triggered immunity (PTI) has not been completely established. Here, we compared the contribution of spermine and putrescine to early and late PTI responses in Arabidopsis. We found that putrescine and spermine have opposite effects on PAMP-elicited reactive oxygen species (ROS) production, with putrescine increasing and spermine lowering the flg22-stimulated ROS burst. Through genetic and pharmacological approaches, we found that the inhibitory effect of spermine on flg22-elicited ROS production is independent of polyamine oxidation, nitric oxide, and salicylic acid signaling but resembles chemical inhibition of RBOHD (RESPIRATORY BURST OXIDASE HOMOLOG D). Spermine can also suppress ROS elicited by FLS2-independent but RBOHD-dependent pathways, thus pointing to compromised RBOHD activity. Consistent with this, we found that spermine but not putrescine dampens flg22-stimulated cytosolic Ca^{2+} influx. Finally, we found that both polyamines differentially reshape transcriptional responses during PTI and disease resistance to *Pseudomonas syringae*. Overall, we provide evidence for the differential contributions of putrescine and spermine to PTI, with an impact on plant defense.

Keywords: Defense, NADPH oxidase, pathogen-associated molecular pattern, polyamines, reactive oxygen species, putrescine, spermine.

Introduction

The most abundant polyamines in plants are the diamine putrescine (Put), the triamine spermidine (Spd), and the tetramine spermine (Spm). The plant contents of polyamines are increased in response to stress. Polyamine levels are regulated through tight control of their biosynthesis, oxidation by polyamine oxidases (PAOs) or copper-containing amine oxidases (CuAOs), conjugation to hydroxycinnamic acids, acylation, and transport (Cona *et al.*, 2006; Alcázar *et al.*, 2010; Tiburcio *et al.*, 2014; Zeiss *et al.*, 2021). Increasing evidence supports the contribution of polyamines to biotic stress resistance, although their effects on defense signaling have not been completely established (Walters, 2003; Tiburcio *et al.*, 2014; Seifi and Shelp,

2019). We recently reported that Put is synthesized in response to systemic acquired resistance (SAR)-inducing bacteria and this polyamine triggers local salicylic acid (SA) accumulation and systemic responses contributing to SAR establishment and defense against *Pseudomonas syringae* (Liu *et al.*, 2020). Studies in Arabidopsis and tobacco indicate that Spm enhances resistance against cauliflower mosaic virus, *Pseudomonas viridiflaba*, *P. syringae*, *Hyaloperonospora arabidopsidis*, *Verticillium dahliae*, and *Botrytis cinerea*. In most cases, Spm responses were found to be dependent on polyamine oxidation (Marina *et al.*, 2008; Moschou *et al.*, 2009; Mitsuya *et al.*, 2009; Sagor *et al.*, 2012; Marco *et al.*, 2014; Mo *et al.*, 2015). Spm also activates the protein kinases SIPK (SA-induced protein kinase) and WIPK (wound-induced protein kinase) in tobacco (Takahashi *et al.*, 2003), as well as mitogen-activated protein kinases (Zhang and Klessig, 1997; Seo *et al.*, 2007), leading to the expression of a number of hypersensitive response marker genes in a reactive oxygen species (ROS)- and Ca^{2+}-dependent but SA-independent manner (Takahashi *et al.*, 2004). Overall, the data suggest that Spm contributes to defense through potentiation of the hypersensitive response. However, the potential contribution of Spm to other layers of defense, and pathogen-associated molecular pattern (PAMP)-triggered immunity (PTI) in particular, has not been fully established. *Pseudomonas syringae* produces the small molecule phevamine A, a modified form of Spd that suppresses the potentiating effect of this polyamine on the flagellin-stimulated ROS burst (O'Neill *et al.*, 2018). Therefore, polyamine analogs can be used by pathogens to subvert PTI responses, suggesting the participation of polyamines in the modulation of PTI.

Plants have two layers of pathogen recognition (Dodds and Rathjen, 2010). The first layer is initiated upon the perception of PAMPs by pattern recognition receptors, which leads to PTI. A second intracellular layer relies on nucleotide-binding domain and leucine-rich repeat-containing receptor (NLR) proteins, which directly or indirectly recognize virulence effectors and induce effector-triggered immunity. The Arabidopsis leucine-rich repeat receptor kinase FLS2 (FLAGELLIN SENSITIVE 2) recognizes bacterial flagellin (Gómez-Gómez *et al.*, 2000; Zipfel, 2014). Binding of the immunogenic flagellin peptide (flg22) initiates several downstream responses. One of the earliest signaling events after PAMP recognition is a rapid increase in cytosolic Ca^{2+} concentration ($[Ca^{2+}]_{cyt}$), ROS generation, and the activation of MAPKs and Ca^{2+}-dependent protein kinases (CPKs), ultimately leading to transcriptional and metabolic reprogramming (Boller and Felix, 2009; Segonzac and Zipfel, 2011). Ca^{2+} is a ubiquitous second messenger whose signal specificity is explained by the duration, amplitude, frequency, and spatial distribution of the Ca^{2+} burst. Specific Ca^{2+} signatures are decoded by Ca^{2+}-binding proteins that translate this information into changes in the phosphorylation status of proteins and transcriptional responses (Dodd *et al.*, 2010). ROS have been proposed to act as an antimicrobial agent, facilitate cell wall modifications, and act in local and systemic defense signaling (Lamb and Dixon, 1997; Suzuki *et al.*, 2011; Nathan and Cunningham-Bussel, 2013). ROS are generated by different enzymatic complexes, including Class III peroxidases, oxalate oxidases, lipoxygenases, quinone reductases, amine oxidases including CuAO and PAO, and NADPH oxidases (Cona *et al.*, 2006; Miller *et al.*, 2010). Polyamine oxidation is a source of ROS due to the release of hydrogen peroxide (H_2O_2) in the reactions catalyzed by CuAO and PAO. Arabidopsis CuAOs, which localize to the apoplast and peroxisomes, show high affinity for oxidizing Put and much lower affinity for Spd and Spm (Moschou *et al.*, 2012; Planas-Portell *et al.*, 2013). Arabidopsis PAOs, which are found in the cytosol and peroxisomes, use Spd and Spm as preferential substrates and catalyze back-conversion reactions that reverse the polyamine biosynthetic pathway (Alcázar *et al.*, 2010; Moschou *et al.*, 2012; Tiburcio *et al.*, 2014). ROS production during PTI is predominantly dependent on the NADPH oxidase RBOHD (RESPIRATORY BURST OXIDASE HOMOLOG D) (Nühse *et al.*, 2007; Zhang *et al.*, 2007). In general, RBOH proteins transfer electrons from cytosolic NADPH or NADH to apoplastic oxygen, producing superoxide anion (O_2^-), which can be converted to H_2O_2 by superoxide dismutases (Marino *et al.*, 2012; Suzuki *et al.*, 2012). RBOHs have Ca^{2+}-binding EF-hand motifs in their N-terminal region that bind Ca^{2+}. Indeed, Ca^{2+} binding is important for the regulation of RBOHD, since treatment with Ca^{2+} chelators and point mutations in EF-hand motifs compromise PAMP-triggered ROS production (Kadota *et al.*, 2004, 2014; Ogasawara *et al.*, 2008; Ranf *et al.*, 2011; Segonzac and Zipfel, 2011; Kimura *et al.*, 2012). ROS produced by RBOHD activity also induce Ca^{2+} influx, thus suggesting a positive feedback regulation that boosts ROS production (Ranf *et al.*, 2011). Other mechanisms of RBOHD regulation involve phosphorylation at different sites by the protein kinase BIK1 (BOTRYTIS-INDUCED KINASE1) and CPKs upon PAMP perception (Boudsocq *et al.*, 2010; Suzuki *et al.*, 2011; Marino *et al.*, 2012; Dubiella *et al.*, 2013; Li *et al.*, 2014; Kadota *et al.*, 2014). RBOHD phosphorylation by BIK1 is independent of calcium-based regulatory mechanisms, but Ca^{2+} is required for the ultimate PAMP-triggered RBOHD activation (Kadota *et al.*, 2014). In addition, RBOHs are also regulated by binding of small GTPases, 14-3-3 proteins, phosphatidic acid, and *S*-nitrosylation (Morel *et al.*, 2004; Elmayan *et al.*, 2007; Wong *et al.*, 2007; Zhang *et al.*, 2009; Yun *et al.*, 2011). The many regulatory mechanisms, as well as the broad range of functions of RBOH family members in stress and development, suggest their participation as molecular hubs mediating ROS signaling.

In this work, we investigated the effect of polyamines on the PAMP-elicited ROS burst, which is one of the earliest PTI responses. By focusing on flg22 elicitation of PTI, we found that Spm strongly inhibits flg22-mediated ROS production, whereas Put exhibited the opposite effect. Through genetic and pharmacological approaches, we provide evidence that the inhibitory effect of Spm on the flg22-triggered

ROS burst is independent of polyamine oxidation, nitric oxide (NO) signaling, and the defense components EDS1 (ENHANCED DISEASE SUSCEPTIBILITY 1), PAD4 (PHYTOALEXIN DEFICIENT 4), SA, and NPR1 (NON-EXPRESSER OF PR GENES 1), and cannot be ameliorated by Put treatment. Inhibition of ROS production by Spm is also observed in response to FLS2-independent but RBOHD-dependent ROS-inducing agents such as methyl viologen (MV). Spm mimics the effect of Ca^{2+} chelators and Ca^{2+} channel blockers that compromise RBOHD-dependent ROS production in response to flg22. In agreement with this, we found that Spm, but not Put, dampens the flg22-triggered Ca^{2+} influx required for RBOHD activation. These polyamines also differentially reshape the transcriptional responses to flg22 and PAMP-mediated disease resistance against *P. syringae*. Overall, we provide evidence for the differential contributions of Put and Spm to PTI signaling, with an impact on plant defense.

Materials and methods

Plant materials

Seeds of the different genotypes were directly sown on soil (40% peat moss, 50% vermiculite, and 10% perlite). Seeds were stratified in the dark at 4 °C for 2–3 days to stimulate germination. The different plant genotypes were grown at 20–22 °C under 12 h light/12 h dark photoperiod cycles. Genotypes used in this work were obtained from the Eurasian Arabidopsis Stock Center (https://arabidopsis.info/) or were previously described: *adc1-3*, *adc2-4*, and *spms* (Alcázar *et al.*, 2006; Cuevas *et al.*, 2008; Liu *et al.*, 2019), *eds1-2* (Feys *et al.*, 2005), *pad4-1* (Glazebrook *et al.*, 1997), *sid2-1* (Wildermuth *et al.*, 2001), *npr1-1* (Cao *et al.*, 1997), *fls2* (Heese *et al.*, 2007), *rbohd* N663633 (SALK_109396C), *rbohd* N670541 (SALK_035391C), *rbohf* N657584 (SALK_034674C), *rbohd/f* N9558 (CS9558), *atao1* N672056 (SALK_127609C), *cuao1* N608014 (SALK_108014), *cuao2* N677606 (SALK_012167C), *cuaoα1* N661128 (SALK_125537C), *cuaoα2* N677690 (SALK_037584C), *cuaoδ* N686526 (SALK_094630C), *cuaoε1* N670103 (SALK_124509C), *cuaoε2* N730426 (GK-422D03.08), *cuaoγ2* N2054517 (GK-051A08.10), *pao1* N658095 (SALK_013026C), *pao2* N660420 (SALK_049456C), *pao3* N668943 (SALK_121288C), *pao4* N653495 (SALK_133599C), and *pao5* N679676 (SALK_053110C). The *nia1 nia2 noa1-2* triple mutant described by Lozano-Juste and León (2010) was kindly provided by Prof. José León (Instituto de Biología Molecular y Celular de Plantas, Spain).

Flg22-elicited ROS measurements

The detection and quantitation of flg22-elicited ROS was performed by monitoring luminescence using a 96-well microplate luminometer (Luminoskan, Thermo Fisher Scientific). Leaf discs (0.5 cm diameter) from fully expanded leaves of 5-week-old plants were incubated for 24 h in 200 µl sterile water. The water was then replaced with a solution containing 10 µg ml^{-1} horseradish peroxidase (Merck), 100 µM of the luminol derivative L-012 (Wako Chemicals) and the different treatments. For pre-incubation assays, leaf discs were incubated with Put (100 µM) or Spm (100 µM) for 24 h before flg22 (1 µM) elicitation. A minimum of 12 replicates per genotype and treatment were used in each analysis. Photon counts (expressed as relative light units) were determined every 2 min in each replicate. Total photon counts were obtained by summing all photon counts over the time of analysis.

Determination of free polyamine concentrations

The concentrations of free Put, Spd, and Spm were determined by high-performance liquid chromatography separation of dansyl chloride-derived polyamines as described by Liu *et al.* (2020). Analyses were performed in three biological replicates per treatment, each including three technical replicates.

Pathogen infection assays

Pseudomonas syringae pv. *tomato* DC3000 (*Pst* DC3000) was inoculated into fully expanded leaves of 5-week-old plants by syringe infiltration using a bacterial suspension (OD_{600}=0.005) in 10 mM $MgCl_2$. The number of *Pst* DC3000 colony-forming units per cm^2 leaf area was determined at 72 h post-inoculation as described by Liu *et al.* (2020), using eight biological replicates per treatment and genotype.

Pharmacological treatments

Leaf discs (0.5 cm diameter) from fully expanded leaves of 5-week-old plants were incubated at room temperature for 24 h in 200 µl sterile water. The water was then replaced with a solution containing the different pharmacological treatments (as described below) and further incubated for 3 h at room temperature. After the incubation, flg22 was added to a final concentration of 1 µM and flg22-elicited ROS production was detected by monitoring luminescence as described above. The pharmacological treatments and concentrations used were as follows: 5 mM dimethylthiourea (DMTU), 5 mM 2-bromoethylamine hydrobromide (BEA), 20 µM diphenyleneiodonium chloride (DPI), 1 mM reduced L-glutathione (GSH), 100 µM 2-4-carboxyphenyl-4,4,5,5-tetramethylimidazoline-1-oxyl-3-oxide (cPTIO), 2 mM EGTA, 1 mM lanthanum chloride ($LaCl_3$), 50 µM or 300 µM cycloheximide (CHX), 20 µM latrunculin B (Lat B), and 2.5 µM brassinazole (BRZ).

DAB and trypan blue staining

3,3′-diaminobenzidine (DAB) staining was performed by incubation of leaves in 3,3′-diaminobenzidine tetrahydrochloride (1 mg ml^{-1}, pH 3.8) overnight followed by destaining in 100% ethanol for 3 h (Clarke, 2009). Trypan blue staining for cell death visualization was performed as previously described (Alcázar *et al.*, 2009).

Ca^{2+} measurements

A transgenic (Col-0) line expressing cytosolic apoaequorin was used for the quantitation of $[Ca^{2+}]_{cyt}$ (Knight *et al.*, 1991). Leaf discs from 5-week-old plants expressing apoaequorin were incubated in 10 µM coelenterazine for 24 h in the dark in 96-well plates. Afterwards, the liquid was replaced with 100 µl H_2O. Luminescence was recorded every 2 min during the different treatments, using a microplate luminometer (Luminoskan, Thermo Fisher Scientific). To calculate absolute cytoplasmic Ca^{2+} concentrations, the remaining aequorin present in each replicate was completely discharged by adding 100 µl $CaCl_2$ (2 M) in 20% ethanol (Fricker *et al.*, 1999) and photon counts were recorded for a further 20 min. The final $[Ca^{2+}]_{cyt}$ was calculated according to Rentel and Knight (2004).

RNA-seq gene expression analyses

Polyamines (Spm and Put), flg22, and mock (water) treatments were performed in three biological replicates by leaf infiltration of 5-week-old wild-type (Col-0) plants. Infiltrated leaves were collected at 24 h of treatment for total RNA extraction. Total RNA was extracted using TRIzol (Thermo Fisher Scientific) and further purified using a RNeasy kit (Qiagen)

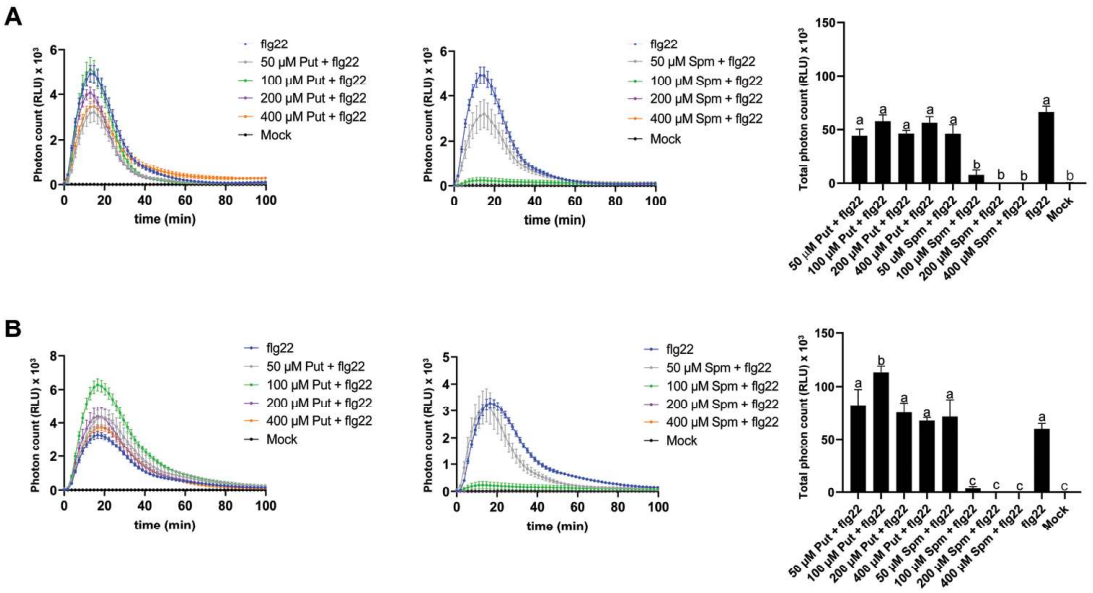

Fig. 1. Effect of Put and Spm on the flg22-elicited ROS burst. (A) Leaf discs from fully expanded leaves of 5-week-old wild-type (Col-0) plants were treated with flg22 (1 µM) and Put or Spm at the indicated concentrations (50–400 µM). (B) Leaf discs were pre-incubated with Put or Spm at the indicated concentrations 24 h before treatment with flg22 (1 µM) to elicit ROS. Values represent the mean ±SE from at least 12 replicates per treatment and are expressed in photon counts [relative light units (RLU)]. Different letters indicate values that are significantly different (P<0.05) according to Tukey's HSD test.

according to the manufacturer's instructions. Total RNA was quantified in a Qubit fluorometer (Thermo Fisher Scientific) and checked for purity and integrity in a Bioanalyzer-2100 device (Agilent Technologies). RNA samples were further processed by the Beijing Genomics Institute for library preparation and RNA sequencing using DNBSEQ. Libraries were prepared using the MGIEasy RNA Library Prep kit (MGI Tech) according to the manufacturer's instructions and each library was paired-end sequenced (2 × 100 bp) on DNBSEQ-G400 sequencers. Read mapping and expression analyses were performed using the CLC Genomics Workbench 21 version 21.0.5 (Qiagen). Only significant expression differences (fold change≥2; Bonferroni-corrected P-value≤0.05) were considered. Principal component analysis (PCA), hierarchical clustering analysis (HCA) and Gene Ontology (GO) analyses were performed using the CLC Genomics Workbench 21 version 21.0.5 (Qiagen) and the Gene Ontology resource (http://geneontology.org) using annotations from Araport11 (Cheng *et al.*, 2017; Carbon *et al.*, 2019). Pathway enrichment analyses were performed using PLANTCYC 15.0.1 (https://plantcyc.org/) (Hawkins *et al.*, 2021) and KEGG pathway analyses (https://www.genome.jp/kegg/) (Kanehisa and Goto, 2000).

qRT–PCR gene expression analyses

Total RNA was extracted using TRIzol reagent (Thermo Fisher Scientific). RNA (2 µg) was treated with DNAse I (Thermo Fisher Scientific) and first-strand cDNA was synthesized using Superscript IV reverse transcriptase (Thermo Fisher Scientific) and oligo(dT) according to the manufacturer's instructions. Quantitative real-time PCR using the SYBR Green I dye method was performed on a Roche LightCycler 480 II detector system with the following PCR conditions: 95 °C for 2 min, followed by 40 cycles of 95 °C for 15 s, 60 °C for 30 s, and 68 °C for 20 s. Standard curves were performed for quantification. Gene expression was normalized using *ACTIN2* (*At3g18780*) and *UBQ10* (*At4g05320*) as housekeeping genes. Primer sequences used for gene expression analyses were previously reported: *WRKY22*, *WRKY29*, *FRK1*, *NHL10*, and *ACTIN2* (Liu *et al.*, 2019), and *UBQ10* (Alcázar *et al.*, 2014). The qRT–PCR analyses were always performed on at least three biological replicates, each with three technical replicates.

Results

Effect of Put and Spm on the flg22-triggered ROS burst

To study the effect of different polyamines on PTI, we first analyzed the contribution of Put and Spm to the flg22-triggered ROS burst in Arabidopsis. ROS production was measured in wild-type plants treated with flg22 (1 µM) supplemented with different concentrations of Put and Spm (50, 100, 200, and 400 µM) or mock treated (Fig. 1). Co-treatments consisting of flg22 with Put produced no significant changes in the flg22-triggered ROS burst (Fig. 1A). However, pre-incubation with Put (100 µM) 24 h before flg22 elicitation triggered higher ROS production compared with mock pre-treatment (Fig. 1B). In contrast, concentrations of Spm of 100 µM and higher strongly inhibited flg22-triggered ROS production (Fig. 1A, 1B). Co-treatment consisting of flg22 with Put and Spm also led to inhibition of the ROS burst (Supplementary Fig. S1). The inhibitory effect of Spm on the flg22-triggered ROS

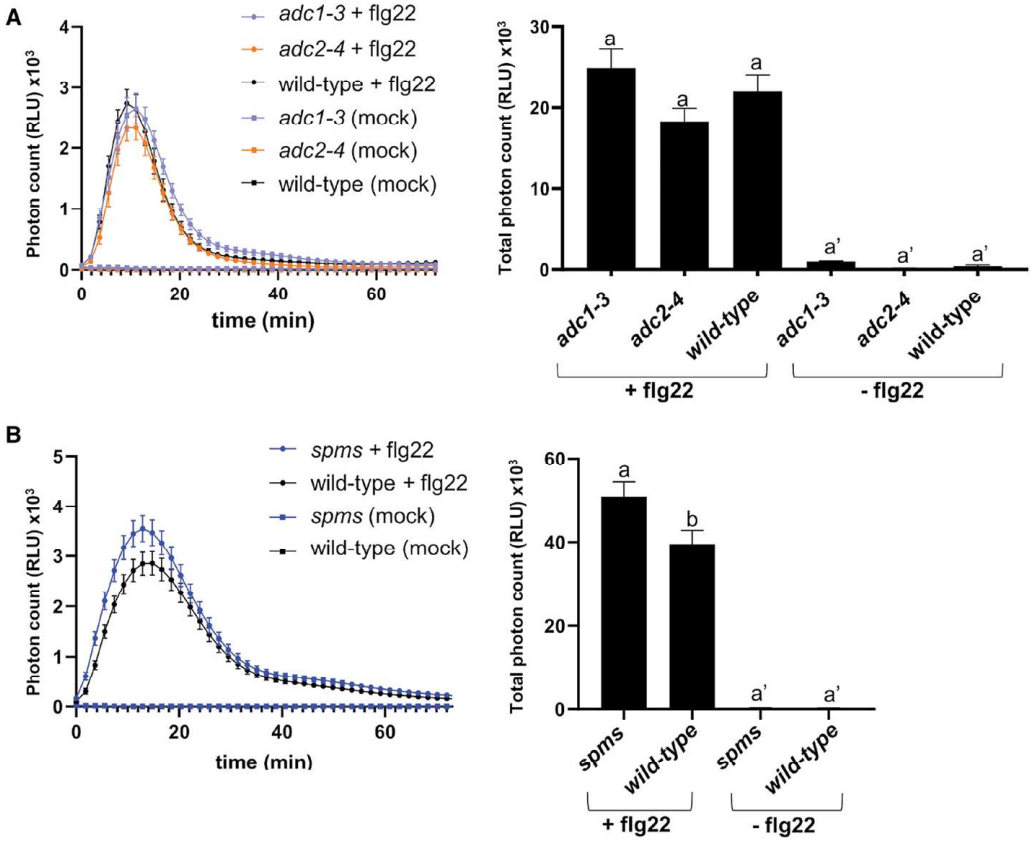

Fig. 2. Flg22-stimulated ROS burst in (A) *adc1-3*, *adc2-4*, and (B) *spms* mutants. Leaf discs from fully expanded leaves of 5-week-old wild-type (Col-0) plants and mutants were treated with flg22 (1 μM) or mock (water). Values represent the mean ±SE from at least 12 replicates per treatment and are expressed in photon counts [relative light units (RLU)]. Different letters indicate values that are significantly different ($P<0.05$) according to Tukey's HSD test.

burst was also evident in the SA-related defense mutants *eds1-2*, *pad4-1*, *sid2-1*, and *npr1-1* (Supplementary Fig. S2), pointing to an EDS1/PAD4, SA and NPR1-independent response.

Incubation with the individual polyamines (Put or Spm) at different concentrations resulted in much lower but sustained apoplastic ROS production, which showed a plateau between 4 h and 8 h of the 100 μM Put or 100 μM Spm treatments (Supplementary Fig. S3A). On the other hand, flg22 (1 μM) triggered a significant accumulation of Put and dampened Spm content at 24 h of treatment in wild-type plants (Supplementary Fig. S3B). The polyamine-triggered ROS production kinetics did not overlap with the flg22-elicited ROS production response. Interestingly, Spm-triggered ROS production was abrogated in *rbohd* but not *rbohf* mutants (Supplementary Fig. S4). The results indicated that the increase in apoplastic ROS stimulated by Spm is mainly derived from RBOHD activity. Since RBOHD is sensitive to redox perturbations (Torres *et al.*, 2005), the effect of Spm on the stimulation of RBOHD activity might be due to a Spm-triggered intracellular ROS imbalance.

Flg22-triggered ROS burst in adc1, adc2, *and* spms *mutants*

To further study the effect of Put and Spm on the flg22-triggered ROS burst, we used the *arginine decarboxylase 1* (*adc1-3*) and *arginine decarboxylase 2* (*adc2-4*) mutants compromised in Put biosynthesis, and the *spermine synthase* (*spms*) mutant deficient in Spm biosynthesis (Fig. 2). The *adc1-3* and *adc2-4* mutants showed similar flg22-triggered ROS production to that of the wild type (Fig. 2A). In contrast, flg22-triggered ROS levels were significantly higher in *spms* than in wild-type plants (Fig. 2B). The data were consistent with an inhibitory effect of Spm on the flg22-elicited ROS burst (Fig. 1). We

concluded that Put and Spm have opposite effects on flg22-triggered ROS production, with Put increasing and Spm lowering the amplitude of the ROS response.

Effect of Put and Spm on flg22-triggered Pst *DC3000 disease resistance*

Pre-treatment of wild-type plants with flg22 induces resistance to *Pst* DC3000 (Zipfel *et al.*, 2004). Given the opposite effects of Put and Spm on the flg22-triggered ROS burst, we determined the *Pst* DC3000 disease resistance phenotypes in wild-type plants and *eds1-2* mutant plants treated with flg22 (1 μM), Put (100 μM), Spm (100 μM), combinations (100 μM Put+1 μM flg22; 100 μM Spm+1 μM flg22), and mock treatment (Fig. 3). Wild-type plants pre-infiltrated with (Spm+flg22) supported higher bacterial growth than those pre-treated with flg22 or (Put+flg22) (Fig. 3A). These results were consistent with the observed inhibition of the flg22-triggered ROS burst by Spm, which could partly compromise flg22-elicited defenses (Figs 1, 2). In contrast, pre-treatment of wild-type plants with the individual polyamines (100 μM) did not lead to significant changes in *Pst* DC3000 disease resistance compared with mock treatment (Fig. 3A). The data indicated that Spm is not a non-specific suppressor of defense responses. No differences were observed in bacterial growth between the different treatments in the *eds1-2* mutant (Fig. 3B).

Although we did not detect increased disease resistance to *Pst* DC3000 after treatment with 100 μM Put, higher concentrations of Put (200–500 μM) caused lower bacterial growth in the wild type (Supplementary Fig. S5), which otherwise did not correlate with the amplitude of the flg22-triggered ROS burst (Fig. 1B). The *adc1-3* and *adc2-4* mutants were more susceptible to infection by *Pst* DC3000 than wild-type plants in both flg22-pre-infiltrated and mock-treated conditions (Fig. 3C). The data supported a positive contribution of Put to defense independent of FLS2 signaling. Infiltration of the *spms* mutant with *Pst* DC3000 led to similar bacterial growth to that

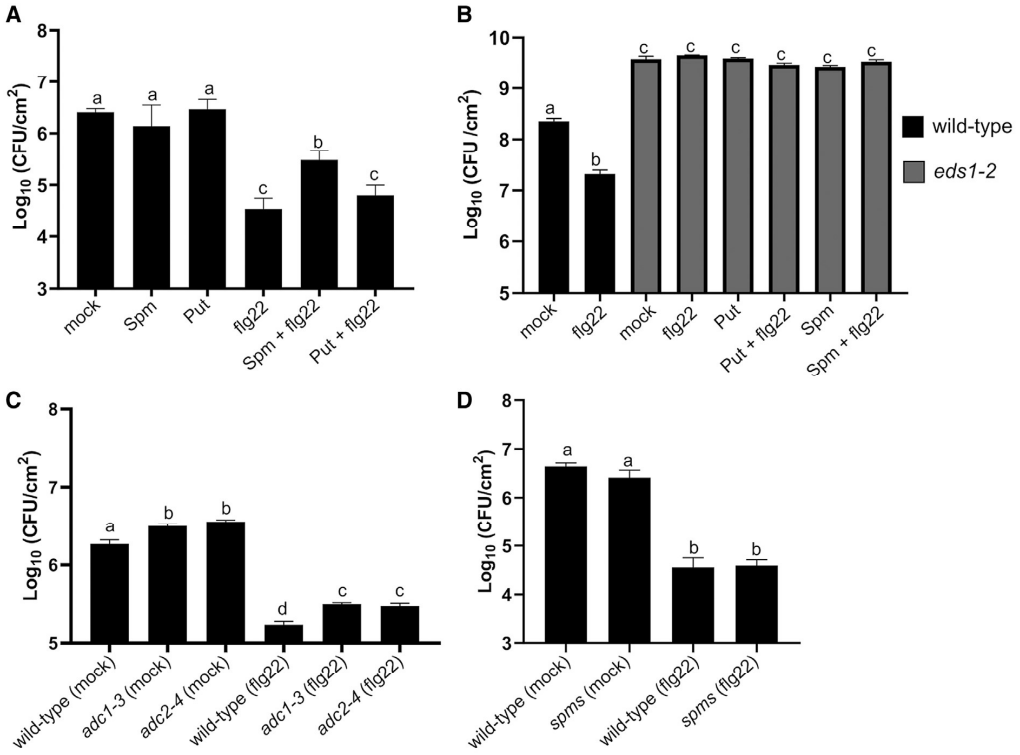

Fig. 3. Analysis of *Pst* DC3000 disease resistance in (A) wild-type plants and (B) *eds1-2* mutant plants pre-infiltrated with mock (10 mM $MgCl_2$), Put (100 μM), Spm (100 μM), flg22 (1 μM), or combinations (Spm+flg22, Put+flg22). (C, D) Disease resistance phenotypes to *Pst* DC3000 in (C) *adc1-3*, *adc2-4* and (D) *spms* mutants pre-infiltrated with flg22 (1 μM) or mock (10 mM $MgCl_2$). Pre-infiltrations were performed 24 h before *Pst* DC3000 inoculation. In all treatments, fully expanded leaves of 5-week-old Arabidopsis plants were infiltrated with *Pst* DC3000 ($OD_{600\ nm}$=0.005). Bacterial numbers were assessed at 72 h post-inoculation and expressed as colony-forming units (CFU) per cm^2 leaf area. Values are the mean ±SD from at least eight biological replicates. Different letters indicate values that are significantly different (P<0.05) according to Tukey's HSD test.

observed in the wild type. In addition, no significant differences in *Pst* DC3000 growth were observed between wild-type and *spms* plants pre-treated with flg22 (Fig. 3D). This indicated that the enhanced flg22-triggered ROS burst in *spms* (Fig. 2B) did not translate into higher disease resistance. Due to the striking inhibitory effect of Spm on the flg22-triggered ROS burst, we focused on this polyamine in further analyses.

Contribution of polyamine oxidation to the Spm-mediated inhibition of the flg22-triggered ROS burst

Many defense-related traits attributed to polyamines are associated with ROS production derived from polyamine oxidation. To determine whether polyamine oxidation by amine oxidases (CuAO and PAO) is necessary for the inhibitory effect of Spm on the flg22-triggered ROS burst, we used *cuao* (*atao1*, *cuao1*, *cuao2*, *cuaoα1*, *cuaoα2*, *cuaoδ*, *cuaoε1*, *cuaoε2*, *cuaoγ2*) and *pao* (*pao1–pao5*) loss-of-function mutants to study their ROS production in response to flg22 and (Spm+flg22). The different *cuao* and *pao* mutants did not show significant differences in flg22-triggered ROS levels compared with the wild type (Supplementary Fig. S6A). In addition, the different amine oxidase (CuAO and PAO) mutations or treatment with the amine oxidase inhibitor BEA did not rescue the inhibitory effect of Spm on the flg22-elicited ROS burst (Supplementary Figs S6B, S7). The data suggested that polyamine oxidation is dispensable for the inhibitory effect of Spm on the flg22-elicited ROS burst.

Spm inhibits RBOHD-dependent ROS production

The inhibition of the flg22-triggered ROS burst by Spm was mimicked by treatments with the NADPH oxidase inhibitor DPI, the ROS scavengers DMTU and GSH, the Ca^{2+} chelator EGTA, and the Ca^{2+} channel blocker $LaCl_3$ (Supplementary Fig. S7). To further study the inhibitory effect of Spm on the flg22-triggered ROS burst, we used a pharmacological approach with wild-type plants treated with the NO scavenger cPTIO, the protein synthesis inhibitor CHX, the actin depolymerization inhibitor Lat B, which strongly reduces flg22-induced FLS2 internalization (Robatzek *et al.*, 2006), and the brassinosteroid (BR) biosynthesis inhibitor BRZ (Supplementary Figs S7, S8). Brassinolides have also been shown to inhibit FLS2 signaling, including the flg22-elicited ROS burst in Arabidopsis (Albrecht *et al.*, 2012; Belkhadir *et al.*, 2012).

Treatments with cPTIO, Lat B, or BRZ did not rescue flg22-triggered ROS production in the presence of Spm (Supplementary Figs S7, S8A). In addition, the inhibitory effect of Spm on the flg22-elicited ROS burst was not compromised in the NO-deficient *nia1 nia2 noa1-2* triple mutant (Supplementary Fig. S8B). Therefore, the inhibitory effect of Spm on the flg22-triggered ROS burst is not mediated by NO, and is not due to FLS2 internalization or *de novo* BR biosynthesis (Albrecht *et al.*, 2012; Belkhadir *et al.*, 2012). Treatment with CHX did not compromise the inhibition of the flg22-triggered ROS burst by Spm, which indicated that this effect does not require *de novo* protein biosynthesis. Interestingly, CHX treatment produced very high amounts of ROS, which were absent in (CHX+Spm) treatments (Supplementary Figs S7, S8C). CHX-triggered ROS production was also compromised in *rbohd* but not *fls2*, which supported the dependence of CHX-triggered ROS production on RBOHD independent of FLS2 (Supplementary Fig S8C, D). The data suggested that Spm inhibits flg22-triggered ROS production through inhibition of RBOHD activity and/or ROS scavenging capacity.

Analysis of the ROS scavenging and cell death trigger capacity of Spm

To investigate the potential ROS-scavenging capacity of Spm in plants, we performed DAB staining in wild-type and *rbohd* leaves infiltrated with Spm (100 μM), the ROS producer MV (100 μM), Spm (100 μM)+MV (100 μM), or mock treated (Fig. 4). Infiltration with MV led to uniform DAB precipitates in wild-type and *rbohd* leaves, indicative of high H_2O_2 production independent of RBOHD. In contrast, infiltration with Spm (100 μM) did not lead to evident DAB staining and resembled the mock treatment. Co-infiltration of MV+Spm only partly alleviated the presence of DAB precipitates, which otherwise were still evident in wild-type and *rbohd* leaves (Fig. 4). MV, Spm, or MV+Spm did not induce cell death in any of the genotypes tested, as revealed by trypan blue staining (Supplementary Fig. S9). The data indicated that Spm (100 μM) only partly scavenges ROS production in Arabidopsis leaves and, at this concentration, is not a cell death trigger.

Effect of Spm on flg22-induced Ca^{2+} influx

PAMPs induce a rapid and transient increase of $[Ca^{2+}]_{cyt}$ by the influx of Ca^{2+} from the extracellular environment or internal stores (McAinsh and Pittman, 2009). This Ca^{2+} burst operates upstream of many PAMP-elicited responses and is necessary for RBOHD activity (Boller and Felix, 2009; Segonzac and Zipfel, 2011; Ranf *et al.*, 2011). We used the apoaquorein bioluminescent Ca^{2+} sensor to measure the steady-state levels and dynamics of $[Ca^{2+}]_{cyt}$ in response to flg22, Spm, Put, and combinations thereof in the wild-type background (Fig. 5). Flg22 treatment triggered a rapid Ca^{2+} influx, which was significantly inhibited by co-treatment with Spm (Fig. 5A). The inhibitory effect of Spm on the flg22-triggered $[Ca^{2+}]_{cyt}$ influx was more evident in plants pre-incubated with Spm before the flg22 challenge (Fig. 5B). Spm also triggered significant increases in $[Ca^{2+}]_{cyt}$ (Fig. 5A) that were attenuated by flg22 pre-treatment (Fig. 5B).

Put also triggered $[Ca^{2+}]_{cyt}$ elevation, although the amplitude of the Ca^{2+} signal was much lower than with Spm (Fig. 5C). Flg22-triggered increases in $[Ca^{2+}]_{cyt}$ were not significantly affected by co-treatments or pre-treatments with Put (Fig 5C, D). We concluded that Put and Spm trigger different

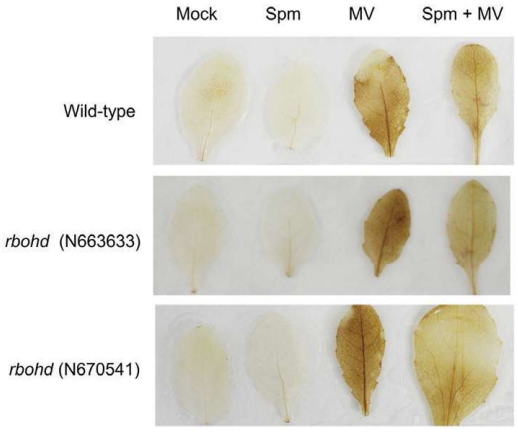

Fig. 4. 3,3′-diaminobenzidine staining of wild-type and *rbohd* mutants infiltrated with Spm (100 µM), methyl viologen (MV) (100 µM), or both (100 µM Spm+100 µM MV). Staining was performed at 24 h of treatment.

Ca^{2+} signals that may contribute to polyamine specificity. Furthermore, we showed that Spm compromises the Ca^{2+} influx elicited by flg22 that is necessary for RBOHD activation, thus providing a plausible explanation for the inhibitory effect of Spm on flg22-triggered ROS production beyond its ROS-scavenging capacity.

Effect of Spm and Put on flg22-elicited transcriptional responses

To further investigate the differential effect of Put and Spm on the modulation of flg22-triggered responses, we determined global changes in expression at 24 h of Put (100 µM), Spm (100 µM), flg22 (1 µM), Spm (100 µM)+flg22 (1 µM), Put (100 µM)+flg22 (1 µM), and mock treatments in wild-type plants. The RNA-seq data were used for PCA and HCA (Supplementary Fig. S10; Supplementary Tables S1.1–S1.5, S2.1–S2.19, S3.1–S3.19). The principal component 1 (PC1) of the PCA explained 32% of total variance and mainly

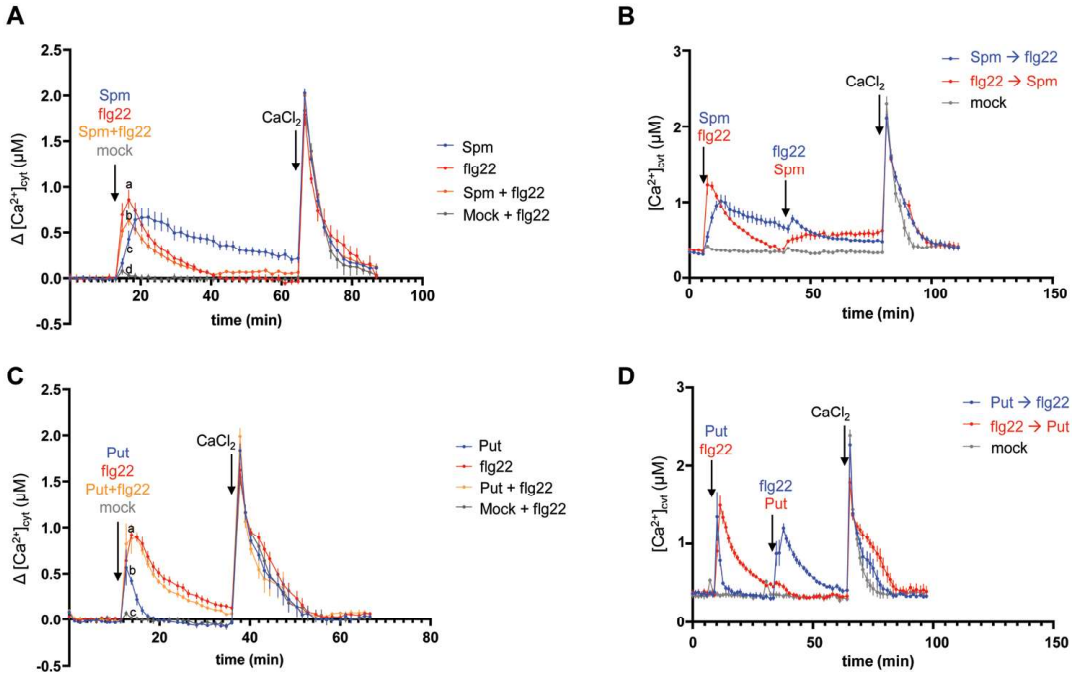

Fig. 5. Flg22, Put, and Spm-induced Ca^{2+} signatures. Leaf discs of an apoaequorin-expressing line (Knight *et al.*, 1991) were (A) treated with 1 µM flg22, 100 µM Spm, 100 µM Spm+1 µM flg22, or mock treated (water); (B) pre-incubated with 100 µM Spm or 1 µM flg22 at the indicated time before flg22 (1 µM) or Spm (100 µM) elicitation, respectively; (C) treated with 1 µM flg22, 100 µM Put, 100 µM Put+1 µM flg22, or mock treated (water); or (D) pre-incubated with 100 µM Put or 1 µM flg22 at the indicated time before flg22 (1 µM) or Put (100 µM) elicitation, respectively. Data represent $\Delta[Ca^{2+}]_{cyt}$ after normalization to steady-state $[Ca^{2+}]_{cyt}$ prior to polyamine or flg22 elicitation, or absolute $[Ca^{2+}]_{cyt}$ (µM). Values were obtained from at least six replicates per treatment. Each point represents the mean ±SE. Different letters indicate values that are significantly different ($P<0.05$) according to Tukey's HSD test. This experiment was repeated twice with similar results.

differentiated between flg22-treated and flg22-untreated samples (Supplementary Fig. S10A). Flg22 treatment also discriminated between the two major clades of the HCA analysis (Supplementary Fig. S10B). The principal component 2 (PC2) (16.1% of total variance) revealed the differences in expression due to the polyamine treatments (Supplementary Fig. S10A), which also grouped into separate subclades of the HCA analysis (Supplementary Fig. S10B).

A total of 554 and 368 genes were significantly deregulated (fold-change≥2.0 and Bonferroni-corrected *P*-value≤0.05) after 100 μM Put or 100 μM Spm treatments, respectively (Supplementary Fig. S11; Supplementary Tables S1.1, S1.2). Among the 396 genes deregulated only by Put (Supplementary Table S1.3), we found a significant enrichment in up-regulated genes related to translation, and down-regulated genes related to stress (Supplementary Fig. S11). A low correlation was found between Put and Spm treatments in the set of Put-only deregulated genes (r^2=0.4149) (Supplementary Fig. S11). On the other hand, in the set of 210 genes deregulated only by Spm (Supplementary Table S1.4), up-regulated genes were enriched in hormone, lipid and cytokinin responses, while those down-regulated included GO terms related to the regulation of transcription factor activity, senescence, and biotic responses (Supplementary Fig. S11). Spm-only-deregulated genes also showed a low correlation with Put treatment (r^2=0.6305) (Supplementary Fig. S11). The data were consistent with a differential regulation of gene expression by these two polyamines at 24 h of treatment. Indeed, only 158 genes were commonly deregulated by Put and Spm (Supplementary Fig. S11; Supplementary Table S1.5). Overexpressed genes within this gene expression sector were mainly related to cell wall biogenesis and cell wall organization (Supplementary Fig. S11). Overall, Put showed a transcriptional effect on ribosome biogenesis that was not evident in the Spm treatment at 24 h of treatment. The polyamines also showed contrasting effects on the expression of genes involved in primary metabolism and transcription factor families. However, both polyamines enhanced the expression of genes encoding enzymes that modify the composition and assembly of the cell wall (Supplementary Fig. S11).

Comparative gene expression analysis of wild-type plants treated with (Spm+flg22) and flg22

Compared with the mock treatment, flg22 triggered the deregulation of 1415 genes (Fig. 6A; Supplementary Table S2.1). Most flg22-responsive genes were related to defense but also included genes involved in ribosome biogenesis (Supplementary Tables S2.1, S2.2). Out of the 1415 flg22-responsive genes, 462 (33%) were not significantly deregulated by flg22 in the presence of Spm (Fig. 6A; Supplementary Fig. S12A; Table S2.3). This set of flg22-only genes was enriched in ribosomal proteins (55 genes) and GO terms related to translation (Supplementary Fig. S13; Supplementary Tables S2.3, S2.4). The flg22-only sector also included genes involved in phenylpropanoid biosynthesis (up-regulated), and down-regulated genes related to carbon starvation, biosynthesis of amino acids, glucosinolates, trehalose and fatty acid metabolism, among others (Supplementary Fig. S13; Supplementary Table S2.5). The data suggested that Spm dampens the expression of a subsector of flg22-responsive genes involved in ribosomal biogenesis and stress metabolism adaptation.

Treatment of wild-type plants with (Spm+flg22) triggered the deregulation of 1534 genes (Fig. 6A; Supplementary Table S2.6), of which only 868 (Supplementary Fig. S12B; Supplementary Table S2.8) and 63 (Supplementary Table S2.17) were common with the flg22 and Spm treatments, respectively. The flg22 and (Spm+flg22) common genes were enriched in GO categories related to SAR, defense, SA and jasmonic acid responses, phenylpropanoid metabolism (all up-regulated), plant hormone biosynthesis and starch degradation (down-regulated), among other biological functions (Fig. 6A; Supplementary Fig. S14; Supplementary Tables S2.9, S2.10). The most abundant molecular functions included enzymes (246 genes), transporters (60 genes), transcription factors (55 genes), and ribosomal proteins and rRNA processing enzymes (47 genes) (Supplementary Fig. S14; Supplementary Table S2.8). The suppressive effect of Spm on the flg22-elicited ROS burst was consistent with the lower up-regulation of the flg22-inducible genes *WRKY22*, *WRKY29*, *FRK1*, and *NHL10* in wild-type plants treated with (Spm+flg22) compared with flg22, determined by qRT–PCR (Fig. 6B).

The (Spm+flg22)-only sector included 543 genes whose biological functions were related to defense responses to bacteria, ROS responses, protein phosphorylation, flavonoid biosynthesis (all up-regulated), and transcription regulation (down-regulated), among others (Fig. 6A, Supplementary Figs S12C, S15; Supplementary Tables S2.11–S2.13). This set of (Spm+flg22)-only genes was used to determine correlation coefficients between flg22 and (Spm+flg22) treatments. We found that both treatments were correlated (r^2=0.9036), despite the difference in the number of genes assigned to each sector (Supplementary Fig. S12E). This is probably due to the threshold criteria used to identify differentially expressed genes (fold change≥2 and Bonferroni-corrected *P*-value≤0.05), which overestimated the differences between treatments (Supplementary Fig. S12B; Supplementary Table S2.8). The correlation between the flg22 and (Spm+flg22) treatments in genes within the flg22-only sector was lower (r^2=0.8056) (Supplementary Fig. S12E).

Genes exclusively deregulated by Spm were significantly enriched in GO terms related to cell wall biogenesis (up-regulated) (Fig. 6A; Supplementary Figs S12D, S16; Supplementary Tables S2.14, S2.15), which suggested that polyamines could contribute to cell wall reinforcement and modifications during plant defense. In this case, no strong correlations were detected between the Spm and (Spm+flg22) treatments (r^2=0.5353) (Supplementary Fig. S12E). We concluded that Spm dampens the up-regulation of flg22-responsive genes, genes encoding

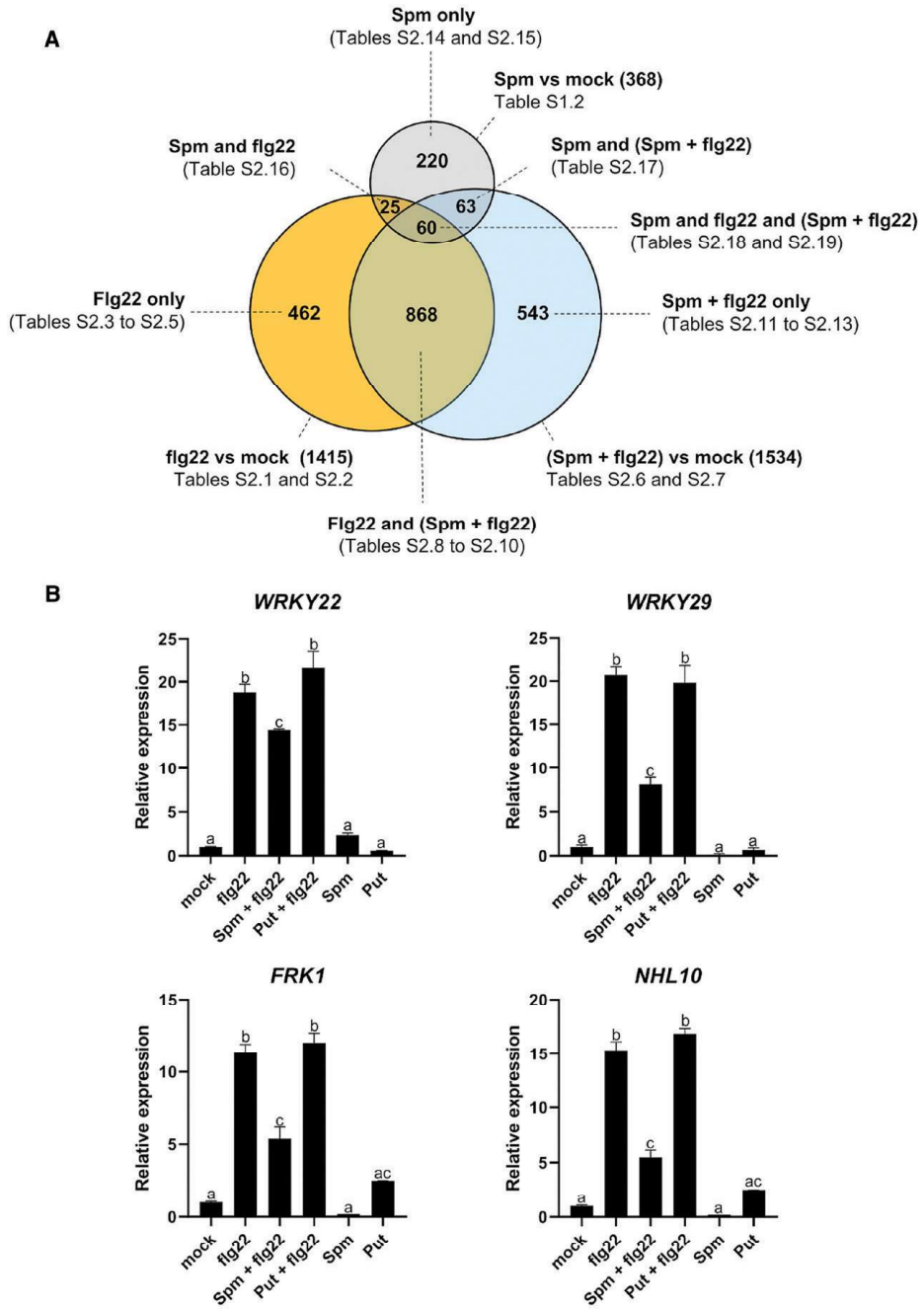

Fig. 6. Comparative gene expression analysis of wild-type plants treated with flg22 and Spm+flg22. (A) Venn diagram of genes differentially expressed (fold change≥2; Bonferroni-corrected *P*-value≤0.05) in response to flg22 (1 μM), Spm (100 μM), and Spm (100 μM)+flg22 (1 μM). Genes and GO enrichment analyses within each category are listed in Supplementary Tables S2.1–S2.19. (B) qRT–PCR gene expression analyses of the flg22-inducible genes *WRKY22*, *WRKY29*, *FRK1*, and *NHL10* in wild-type plants at 24 h of treatment with flg22 (1 μM), Spm (100 μM), Put (100 μM), Spm (100 μM)+flg22 (1 μM) or Put (100 μM)+flg22 (1 μM). Values represent the mean ±SD. Different letters indicate values that are significantly different (*P*<0.05) according to Tukey's HSD test.

ribosomal proteins, and genes related to metabolism adaptation during flg22-elicited defenses.

Comparative gene expression analysis of wild-type plants treated with (Put+flg22) and flg22

In the Put treatment, out of the 1415 flg22-responsive genes, 259 (18.3%) were not significantly deregulated by flg22 in the presence of Put (flg22-only in Fig. 7 and Supplementary Fig. S17A; Supplementary Table S3.1). However, the flg22 and (Put+flg22) treatments were highly correlated (r^2=0.9439) (Supplementary Fig. S17E), which suggested that the significance threshold also overestimated the differences between the treatments. Flg22-only genes were also enriched in ribosomal proteins (30 genes) (Fig. 7; Supplementary Fig. S18; Supplementary Tables S3.1, S3.2). However, these genes represented almost half of the ribosomal genes detected within the same sector in the comparison with (Spm+flg22) treatment (55 genes) (Fig. 6A; Supplementary Table S2.3). The 'Put and flg22' (91 genes) and 'Put, flg22, and (Put+flg22)' (163 genes) gene expression sectors were also enriched in GO terms related to translation (Supplementary Tables S3.15–S3.18). This was consistent with the effect of Put on the up-regulation of genes encoding ribosomal proteins and rRNA processing enzymes (Supplementary Fig. S11; Supplementary Table S1.1). Flg22-only up-regulated genes also included enzymes (59) enriched in the phenylpropanoid pathway that were also up-regulated in the common flg22 and (Put+flg22) gene expression sectors (Supplementary Figs S18, S19; Supplementary Tables S3.1–S3.3, S3.6–S3.8).

Treatment of wild-type plants with (Put+flg22) triggered the deregulation of 1395 genes (Fig. 7; Supplementary Table S3.4), of which 902 (Supplementary Fig. S17B; Supplementary Table S3.6) and 30 (Supplementary Table S3.19) were common with the flg22 and Put treatments, respectively. The flg22 and (Put+flg22) common gene expression sector was enriched in GO terms related to SAR, SA signaling, defense, lignin metabolism, ribosome biogenesis, phenylpropanoid metabolism (all up-regulated) and starch catabolism (down-regulated), among other biological functions (Supplementary Fig. S19; Supplementary Tables S3.6–S3.8). The most abundant molecular functions included enzymes (252 genes), transporters (67 genes), transcription factors (53 genes), and others, including 26 ribosomal proteins (Supplementary Fig. S19; Supplementary Table S3.6). In contrast to Spm, the treatment of wild-type plants with (Put+flg22) did not trigger significant changes in the expression of the flg22-inducible genes *WRKY22*, *WRKY29*, *FRK1*, and *NHL10* compared with flg22 treatment alone, as determined by qRT–PCR (Fig. 6B). The data were consistent with the specific effect of Spm on the inhibition of flg22-elicited responses.

The (Put+flg22)-only sector included 300 genes mainly related to defense responses to bacteria (up-regulated), response to oxygen-containing compounds, and response to lipids (down-regulated) (Supplementary Figs S17C, S20;

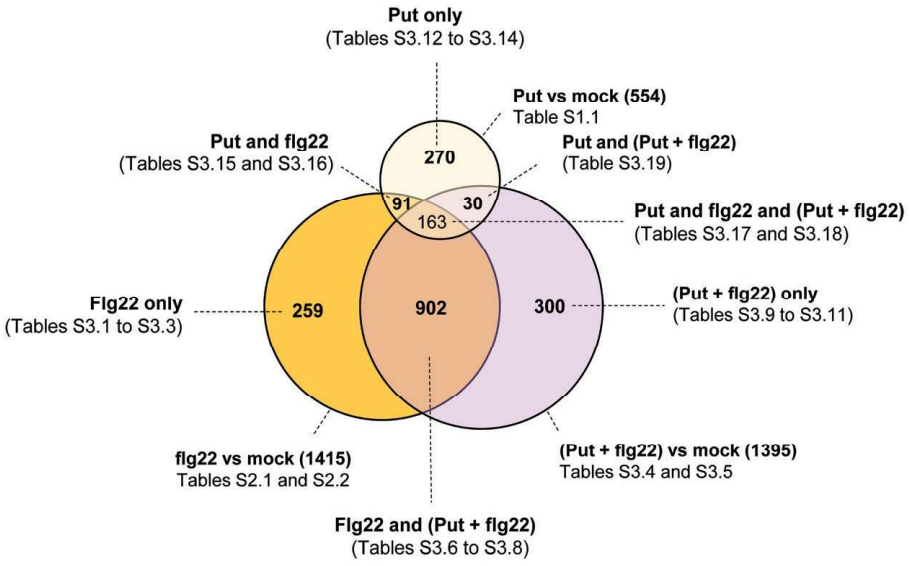

Fig. 7. Comparative gene expression analysis of wild-type plants treated with flg22 and Put+flg22. Venn diagram of genes differentially expressed (fold change≥2; Bonferroni corrected *P*-value≤0.05) in response to flg22 (1 μM), Put (100 μM), and Put (100 μM)+flg22 (1 μM). Genes and GO enrichment analyses within each category are listed in Supplementary Tables S3.1–S3.19.

Supplementary Tables S3.9–S3.11). The expression of genes within this sector was also correlated with flg22 treatment (r^2=0.8757), which accounted for quantitative rather than qualitative differences between the sectors (Supplementary Fig. S17E). As in the case of Spm, genes up-regulated only by Put were mostly enriched in cell wall biogenesis functions and showed a low correlation with the other treatments (Fig. 7; Supplementary Figs S17D, S17E, S21; Supplementary Tables S3.12–S3.14).

Collectively, the data indicated that Spm, but not Put, dampens the up-regulation of flg22-inducible genes. In addition, Spm and, less markedly, Put compromise flg22-induced transcriptional up-regulation of genes encoding ribosomal proteins, and both trigger the up-regulation of cell wall biogenesis and modification enzymes that are not deregulated by flg22, thus reshaping the PAMP-induced transcriptional responses.

Discussion

Spm and its precursors Put and Spd show opposite effects on the stimulation of flg22-elicited ROS production and defense elicitation. While Spm inhibits the flg22-triggered ROS burst (Fig 1A, B), Put (Fig. 1B) and Spd (Supplementary Fig. S22) (O'Neill *et al.*, 2018) potentiate ROS production. Importantly, the inhibitory effect of Spm does not require its oxidation (Supplementary Fig. S6B), is independent of NO signaling (Supplementary Figs S7, S8B), and cannot be compensated for by Put (Supplementary Fig. S1). Put and Spm also show opposite accumulation patterns during PTI. Whereas the Put concentration is increased at 24 h of flg22 elicitation in the wild type, the Spm concentration is decreased (Supplementary Fig. S3B) (Liu *et al.*, 2019). Upon flg22 binding, FLS2 forms a complex with BAK1 (BRI1-ASSOCIATED KINASE1), an LRR-receptor kinase that also serves as co-receptor of BRI1 (BRASSINOSTEROID INSENSITIVE1), which is involved in BR signaling (Zipfel, 2014). BR has also been shown to inhibit FLS2 signaling, including the flg22-elicited ROS burst in Arabidopsis, downstream or independently of the FLS2–BAK1 complex or through competition for BAK1 recruitment by FLS2 and the BR receptor BRI1 (Albrecht *et al.*, 2012; Belkhadir *et al.*, 2012). However, treatment with the BR biosynthesis inhibitor BRZ did not rescue the inhibitory effect of Spm on flg22-triggered ROS production (Supplementary Fig. S8A). In addition, compromised internalization of FLS2 caused by treatment with Lat B did not rescue Spm-triggered ROS inhibition (Supplementary Fig. S7). In addition to the flg22-triggered ROS burst, Spm also inhibited CHX-induced ROS production, which was RBOHD-dependent but FLS2-independent (Supplementary Fig S8C, D). The data suggested that Spm inhibition of flg22-elicited ROS was not due to impaired FLS2 signaling. Rather, Spm mimicked the inhibitory effect of the NADPH oxidase inhibitor DPI, the Ca^{2+} chelator EGTA, and the Ca^{2+} channel blocker $LaCl_3$ on flg22-triggered ROS production (Supplementary Fig. S7). Flg22-elicited ROS is mainly produced by RBOHD, whose activation requires Ca^{2+} binding to its N-terminal EF-hand motifs (Kadota *et al.*, 2004, 2014; Ogasawara *et al.*, 2008; Segonzac and Zipfel, 2011; Ranf *et al.*, 2011; Kimura *et al.*, 2012). Flg22 treatment triggered a rapid $[Ca^{2+}]_{cyt}$ increase that was significantly dampened by Spm but not by Put (Fig. 5). The suppressive effect of Spm on the flg22-triggered Ca^{2+} influx might compromise RBOHD-triggered ROS production, thus being a plausible explanation for the inhibitory effect of Spm on flg22-elicited ROS production.

On the other hand, Spm and Put also triggered the elevation of $[Ca^{2+}]_{cyt}$, but the Ca^{2+} signature lasted longer in the treatments with Spm (Fig. 5). The different Ca^{2+} signatures triggered by Put and Spm might contribute to signal specificity, as noted in our RNA-seq analyses (Supplementary Fig. S11).

Rocha *et al.* (2020) reported that Spm was necessary for mucilage production during appressoria morphogenesis in the blast fungus *Magnaporthe oryzae*, by buffering oxidative stress in the endoplasmic reticulum lumen and preventing the unfolded protein response. The antioxidant properties of Spm in plants have been documented (Drolet *et al.*, 1986) and involve the conversion of the polyamine into different adducts, including Spm dialdehyde, in the presence of hydroxyl radicals (Ha *et al.*, 1998). However, the potential ROS scavenging capacity of Spm does not fully explain the inhibitory effect of Spm on flg22-elicited ROS production. We found that Spm (100 μM) shows only partial antioxidant capacity in Arabidopsis leaves infiltrated with MV, a ROS-inducing agent that transfers electrons from photosystem I to molecular oxygen (Fig. 4). In addition, Spm and also its precursor Spd act as ROS scavengers through seemingly similar mechanisms (Khan *et al.*, 1992). However, these two polyamines show opposite effects on flg22-triggered ROS stimulation (Fig. 1; Supplementary Fig. S22) (O'Neill *et al.*, 2018). Furthermore, we found that thermospermine (100 μM), an isomer of Spm, does not inhibit flg22-triggered ROS production (Supplementary Fig. S22). These data indicate that the effect of Spm on flg22-elicited ROS burst inhibition is highly specific.

Polyamines are known to affect ion transport across membranes through intricate mechanisms that are also dependent on polyamine charge (Pottosin and Shabala, 2014). Spm can induce membrane depolarization or hyperpolarization, depending on the concentration at which it is supplied. At low concentration (100 μM), Spm causes weak membrane hyperpolarization and transient efflux of H^+ but not Ca^{2+}. In contrast, Spm at higher concentration (1 mM) causes membrane depolarization in a ROS-independent manner (Pottosin *et al.*, 2014). In contrast to Spm, other polyamines trigger membrane depolarization at any given concentration (Pottosin *et al.*, 2014). ROS derived from polyamine oxidation can also activate a variety of non-selective Ca^{2+}-permeable channels leading to increases in $[Ca^{2+}]_{cyt}$. Externally supplied polyamines can also trigger NO generation and intracellular Ca^{2+} release through a pathway involving cGMP and cADPR (Pottosin and Shabala,

2014). In addition, polyamines can stimulate Ca^{2+} efflux by the activation of plasma membrane Ca^{2+}-ATPase activity (Pottosin *et al.*, 2014). The plasma membrane Ca^{2+}-ATPases ACA8 (ARABIDOPSIS-AUTOINHIBITED Ca^{2+}-ATPase 8) and ACA10 have been found in complex with FLS2, and the double *aca8 aca10* mutant has been reported to show a decreased flg22-induced Ca^{2+} and ROS burst (Frei dit Frey *et al.*, 2012). However, the identity of the Ca^{2+} channels and detailed mechanisms that mediate the differential Ca^{2+} signature triggered by Put and Spm remain largely unknown.

To further investigate the effect of Spm and Put on PTI, we performed global gene expression analyses in the wild type at 24 h of treatment with flg22, Spm, Put, and combinations (Spm+flg22 and Put+flg22). Despite the inhibitory effect of Spm on the flg22-triggered ROS burst, transcriptional responses to flg22 and *Pst* DC3000 disease resistance were only partly compromised by the polyamine (Figs 3A, 6). Both Put and Spm triggered the up-regulation of genes related to cell wall biogenesis. However, the polyamines exhibited differences in the transcriptional responses of genes related to primary metabolism, transcription factors, and protein synthesis and degradation at 24 h (Supplementary Fig. S11). In a previous study (Liu *et al.*, 2020), we found that polyamines exhibited similar early transcriptional responses at 1 h of treatment. Therefore, there are differences between the early and late transcriptional responses to polyamines. Such differences have also been documented in response to different PAMPs, such as flg22 or oligogalacturonides (Denoux *et al.*, 2008). The flg22, (Spm+flg22), and (Put+flg22) treatments also revealed that polyamines differentially reshape the transcriptional responses to PAMPs. In particular, Spm but not Put compromised the up-regulation of flg22-responsive genes (Fig. 6B). On the other hand, Spm and less markedly Put dampened the flg22-elicited expression of ribosome biogenesis genes (Supplementary Figs S13, S18). Bach-Pages *et al.* (2020, Preprint) found that the RNA-binding activity of eukaryotic initiation factors, elongation factors, and ribosomal proteins was inhibited in response to flg22. The overexpression of genes encoding ribosomal proteins caused by flg22 might be a compensatory mechanism to the PAMP-triggered inhibition of translation. In contrast, the polyamines Spd and Spm, and less markedly Put, are known to stimulate translation elongation and thus protein biosynthesis, which might compensate for the inhibitory effect of flg22 on translation (Igarashi and Kashiwagi, 2015; Dever and Ivanov, 2018).

Collectively, we conclude that polyamines differentially modulate PTI responses including Ca^{2+} signals and ROS production, ultimately leading to changes in global transcriptional responses with an impact on plant defense against *P. syringae*.

Supplementary data

The following supplementary data are available at *JXB* online.

Fig. S1. Effect of the Put and Spm co-treatment on flg22-elicited ROS burst.

Fig. S2. Effect of Spm on flg22-elicited ROS burst in *eds1-2*, *pad4-1*, *sid2-1*, *npr1-1*, and *fls2* mutants.

Fig. S3. ROS produced by Put and Spm treatments, and free polyamine concentrations in response to flg22.

Fig. S4. Effect of Spm on flg22-elicited ROS burst in *rbohd*, *rbohf*, and double *rbohd/f* mutants.

Fig. S5. Analysis of *Pst* DC3000 disease resistance phenotypes in wild-type plants locally pre-treated with different concentrations of Put.

Fig. S6. Flg22-elicited ROS and effect of Spm on flg22-elicited ROS production in *cuao* and *pao* mutants.

Fig. S7. Pharmacological studies on Spm inhibition of flg22-triggered ROS burst.

Fig. S8. Effect of BRZ, NO, and CHX treatments on Spm inhibition of flg22-triggered ROS burst.

Fig. S9. Trypan blue staining of wild-type and *rbohd* leaves infiltrated with Spm, MV, or both.

Fig. S10. PCA and HCA of RNA-seq gene expression data obtained from wild-type plants treated with Put, Spm, flg22, Put+flg22, Spm+flg22, or mock for 24 h.

Fig. S11. Venn diagram, GO, and expression correlation analyses of genes significantly deregulated in response to Put and Spm at 24 h of treatment in the wild type.

Fig. S12. Mean expression values and correlation analyses of wild-type plants treated with flg22, Spm, and (Spm+flg22).

Fig. S13. Molecular function categorization and metabolic pathway enrichment analysis of genes deregulated by only flg22 compared with Spm and (Spm+flg22) treatments in the wild type.

Fig. S14. Molecular function categorization and metabolic pathway enrichment analysis of genes commonly deregulated in flg22 and (Spm+flg22) treatments in the wild type.

Fig. S15. Molecular function categorization and metabolic pathway enrichment analysis of genes differentially expressed in only (Spm+flg22) compared with flg22 and Spm treatments.

Fig. S16. Molecular function categorization and metabolic pathway enrichment analysis of genes differentially expressed in only Spm compared with flg22 and (Spm+flg22) treatments.

Fig. S17. Mean expression values and correlation analyses of wild-type plants treated with flg22, Put, and (Put+flg22).

Fig. S18. Molecular function categorization and metabolic pathway enrichment analysis of genes deregulated by only flg22 compared with Put and (Put+flg22) treatments.

Fig. S19. Molecular function categorization and metabolic pathway enrichment analysis of genes commonly deregulated in flg22 and (Put+flg22) treatments in the wild type.

Fig. S20. Molecular function categorization and metabolic pathway enrichment analysis of genes deregulated in only (Put+flg22) compared with flg22 and Put treatments.

Fig. S21. Molecular function categorization and metabolic pathway enrichment analysis of genes only deregulated by Put compared to flg22 and (Put+flg22) treatments.

Fig. S22. Effect of thermospermine and Spd on flg22-elicited ROS burst in the wild type.

Table S1.1. List of 554 differentially expressed genes at 24 h of Put treatment.
Table S1.2. List of 368 differentially expressed genes at 24 h of Spm treatment.
Table S1.3. List of 396 genes deregulated only by Put.
Table S1.4. List of 210 genes deregulated only by Spm.
Table S1.5. List of 158 common genes differentially expressed in Spm and Put treatments.
Table S2.1. List of 1415 differentially expressed genes at 24 h of flg22 treatment.
Table S2.2. GO analysis of genes deregulated in Table S2.1.
Table S2.3. List of 462 flg22-only genes that show significant expression differences at 24 h of flg22 treatment.
Table S2.4. GO analysis of genes deregulated in Table S2.3.
Table S2.5. Pathway enrichment analysis of genes deregulated in Table S2.3.
Table S2.6. List of 1534 differentially expressed genes at 24 h of (Spm+flg22) treatment.
Table S2.7. GO analysis of genes deregulated in Table S2.6.
Table S2.8. List of 868 common genes differentially expressed in flg22 and (Spm+flg22) treatments.
Table S2.9. GO analysis of genes deregulated in Table S2.8.
Table S2.10. Pathway enrichment analysis of genes deregulated in Table S2.8.
Table S2.11. List of 543 (Spm+flg22)-only genes that show significant differences in expression at 24 h of (Spm+flg22) treatment.
Table S2.12. GO analysis of genes deregulated in Table S2.11.
Table S2.13. Pathway enrichment analysis of genes deregulated in Table S2.11.
Table S2.14. List of 220 (Spm-only) genes that show significant differences in expression at 24 h of Spm treatment.
Table S2.15. GO analysis of genes deregulated in Table S2.14.
Table S2.16. List of 25 common genes differentially expressed in flg22 and Spm treatments.
Table S2.17. List of 63 common genes differentially expressed in Spm and (Spm+flg22) treatments.
Table S2.18. List of 60 common genes differentially expressed in Spm, flg22, and (Spm+flg22) treatments.
Table S2.19. GO analysis of genes deregulated in Table S2.18.
Table S3.1. List of 259 flg22-only genes that show significant expression differences at 24 h of flg22 treatment.
Table S3.2. GO analysis of genes deregulated in Table S3.1.
Table S3.3. Pathway enrichment analysis of genes deregulated in Table S3.1.
Table S3.4. List of 1395 differentially expressed genes at 24 h of (Put+flg22) treatment.
Table S3.5. GO analysis of genes deregulated in Table S3.4.
Table S3.6. List of 902 common genes differentially expressed in flg22 and (Put+flg22) treatments.
Table S3.7. GO analysis of genes deregulated in Table S3.6.
Table S3.8. Pathway enrichment analysis of genes deregulated in Table S3.6.
Table S3.9. List of 300 (Put+flg22)-only genes that show significant differences in expression at 24 h of (Put+flg22) treatment.
Table S3.10. GO analysis of genes deregulated in Table S3.9.
Table S3.11. Pathway enrichment analysis of genes deregulated in Table S3.9.
Table S3.12. List of 270 (Put-only) genes that show significant differences in expression at 24 h of Put treatment.
Table S3.13. GO analysis of genes deregulated in Table S3.12.
Table S3.14. Pathway enrichment analysis of genes deregulated in Table S3.12.
Table S3.15. List of 91 common genes differentially expressed in Put and flg22 treatments.
Table S3.16. GO analysis of genes deregulated in Table S3.15.
Table S3.17. List of 163 common genes differentially expressed in Put, flg22, and (Put+flg22) treatments.
Table S3.18. GO analysis of genes deregulated in Table S3.17.
Table S3.19. List of 30 common genes differentially expressed in Put and (Put+flg22) treatments.

Author contributions

CZ, KEA, and RA planned the experiments; CZ and KEA performed most of the experimental work; CZ and RA analyzed the data; RA conceived the project and wrote the article with contributions from CZ and KEA.

Conflict of interest

No conflict of interest declared.

Funding

This work was financially supported by grants BFU2017-87742-R and PID2021-126896OB-I00 funded by the Ministerio de Ciencia e Innovación MCIN/Agencia Estatal de Investigación AEI/10.13039/501100011033 (Spain) and by the 'European Regional Development Fund (ERDF) a way of making Europe'. CZ is supported by a doctoral fellowship from the China Scholarship Council (CSC).

Data availability

RNA-seq data have been deposited to ArrayExpress (https://www.ebi.ac.uk/arrayexpress/) under accession number E-MTAB-11820. All other data supporting the findings of this study are available within the paper and within its supplementary materials published online.

References

Albrecht C, Boutrot F, Segonzac C, Schwessinger B, Gimenez-Ibanez S, Chinchilla D, Rathjen JP, de Vries SC, Zipfel C. 2012. Brassinosteroids inhibit pathogen-associated molecular pattern-triggered immune signaling independent of the receptor kinase BAK1. Proceedings of the National Academy of Sciences, USA **109**, 303–308.

Alcázar R, Altabella T, Marco F, Bortolotti C, Reymond M, Koncz C, Carrasco P, Tiburcio AF. 2010. Polyamines: molecules with regulatory functions in plant abiotic stress tolerance. Planta **231**, 1237–1249.

Alcázar R, Cuevas JC, Patron M, Altabella T, Tiburcio AF. 2006. Abscisic acid modulates polyamine metabolism under water stress in *Arabidopsis thaliana*. Physiologia Plantarum **128**, 448–455.

Alcázar R, García AV, Parker JE, Reymond M. 2009. Incremental steps toward incompatibility revealed by Arabidopsis epistatic interactions modulating salicylic acid pathway activation. Proceedings of the National Academy of Sciences, USA **106**, 334–339.

Alcázar R, von Reth M, Bautor J, Chae E, Weigel D, Koornneef M, Parker JE. 2014. Analysis of a plant complex Resistance gene locus underlying immune-related hybrid incompatibility and its occurrence in nature. PLoS Genetics **10**, e1004848.

Bach-Pages M, Chen H, Sanguankiattichai N, Soldan R, Kaschani F, Kaiser M, Mohammed S, Van Der Hoorn RAL, Castello A, Preston GM. 2020. Proteome-wide profiling of RNA-binding protein responses to flg22 reveals novel components of plant immunity. bioRxiv doi: 10.1101/2020.09.16.299701. [Preprint]

Belkhadir Y, Jaillais Y, Epple P, Balsemão-Pires E, Dangl JL, Chory J. 2012. Brassinosteroids modulate the efficiency of plant immune responses to microbe-associated molecular patterns. Proceedings of the National Academy of Sciences, USA **109**, 297–302.

Boller T, Felix G. 2009. A renaissance of elicitors: perception of microbe-associated molecular patterns and danger signals by pattern-recognition receptors. Annual Review of Plant Biology **60**, 379–406.

Boudsocq M, Willmann MR, McCormack M, Lee H, Shan L, He P, Bush J, Cheng S-H, Sheen J. 2010. Differential innate immune signalling via Ca^{2+} sensor protein kinases. Nature **464**, 418–422.

Cao H, Glazebrook J, Clarke JD, Volko S, Dong X. 1997. The Arabidopsis *NPR1* gene that controls systemic acquired resistance encodes a novel protein containing ankyrin repeats. Cell **88**, 57–63.

Carbon S, Douglass E, Dunn N, *et al*. 2019. The Gene Ontology resource: 20 years and still GOing strong. Nucleic Acids Research **47**, D330–D338.

Cheng CY, Krishnakumar V, Chan AP, Thibaud-Nissen F, Schobel S, Town CD. 2017. Araport11: a complete reannotation of the *Arabidopsis thaliana* reference genome. The Plant Journal **89**, 789–804.

Clarke JD. 2009. Phenotypic analysis of *Arabidopsis* mutants: Diaminobenzidine stain for hydrogen peroxide. Cold Spring Harbor Protocols **2009**, pdb.prot4981.

Cona A, Rea G, Angelini R, Federico R, Tavladoraki P. 2006. Functions of amine oxidases in plant development and defence. Trends in Plant Science **11**, 80–88.

Cuevas JC, López-Cobollo R, Alcázar R, Zarza X, Koncz C, Altabella T, Salinas J, Tiburcio AF, Ferrando A. 2008. Putrescine is involved in Arabidopsis freezing tolerance and cold acclimation by regulating abscisic acid levels in response to low temperature. Plant Physiology **148**, 1094–1105.

Denoux C, Galletti R, Mammarella N, Gopalan S, Werck D, De Lorenzo G, Ferrari S, Ausubel FM, Dewdney J. 2008. Activation of defense response pathways by OGs and Flg22 elicitors in *Arabidopsis* seedlings. Molecular Plant **1**, 423–445.

Dever TE, Ivanov IP. 2018. Roles of polyamines in translation. Journal of Biological Chemistry **293**, 18719–18729.

Dodd AN, Kudla J, Sanders D. 2010. The language of calcium signaling. Annual Review of Plant Biology **61**, 593–620.

Dodds PN, Rathjen JP. 2010. Plant immunity: towards an integrated view of plant-pathogen interactions. Nature Reviews Genetics **11**, 539–548.

Drolet G, Dumbroff EB, Legge RL, Thompson JE. 1986. Radical scavenging properties of polyamines. Phytochemistry **25**, 367–371.

Dubiella U, Seybold H, Durian G, Komander E, Lassig R, Witte CP, Schulze WX, Romeis T. 2013. Calcium-dependent protein kinase/NADPH oxidase activation circuit is required for rapid defense signal propagation. Proceedings of the National Academy of Sciences, USA **110**, 8744–8749.

Elmayan T, Fromentin J, Riondet C, Alcaraz G, Blein JP, Simon-Plas F. 2007. Regulation of reactive oxygen species production by a 14-3-3 protein in elicited tobacco cells. Plant, Cell and Environment **30**, 722–732.

Feys BJ, Wiermer M, Bhat RA, Moisan LJ, Medina-Escobar N, Neu C, Cabral A, Parker JE. 2005. *Arabidopsis* SENESCENCE-ASSOCIATED GENE101 stabilizes and signals within an ENHANCED DISEASE SUSCEPTIBILITY1 complex in plant innate immunity. The Plant Cell **17**, 2601–2613.

Frei dit Frey N, Mbengue M, Kwaaitaal M, *et al*. 2012. Plasma membrane calcium ATPases are important components of receptor-mediated signaling in plant immune responses and development. Plant Physiology **159**, 798–809.

Fricker MD, Plieth C, Knight H, Blancaflor E, Knight MR, White NS, Gilroy S. 1999. Fluorescence and luminescence techniques to probe ion activities in living plant cells. In: Mason WT, ed. Fluorescent and luminescent probes for biological activity. London, Academic Press, 569–596.

Glazebrook J, Zook M, Mert F, Kagan I, Rogers EE, Crute IR, Holub EB, Hammerschmidt R, Ausubel FM. 1997. Phytoalexin-deficient mutants of Arabidopsis reveal that *PAD4* encodes a regulatory factor and that four *PAD* genes contribute to downy mildew resistance. Genetics **146**, 381–392.

Gómez-Gómez L, Boller T, Klessig D, *et al*. 2000. FLS2: an LRR receptor-like kinase involved in the perception of the bacterial elicitor flagellin in *Arabidopsis*. Molecular Cell **5**, 1003–1011.

Ha HC, Sirisoma NS, Kuppusamy P, Zweier JL, Woster PM, Casero RA. 1998. The natural polyamine spermine functions directly as a free radical scavenger. Proceedings of the National Academy of Sciences, USA **95**, 11140–11145.

Hawkins C, Ginzburg D, Zhao K, *et al*. 2021. Plant Metabolic Network 15: a resource of genome-wide metabolism databases for 126 plants and algae. Journal of Integrative Plant Biology **63**, 1888–1905.

Heese A, Hann DR, Gimenez-Ibanez S, Jones AM, He K, Li J, Schroeder JI, Peck SC, Rathjen JP. 2007. The receptor-like kinase SERK3/BAK1 is a central regulator of innate immunity in plants. Proceedings of the National Academy of Sciences, USA **104**, 12217–12222.

Igarashi K, Kashiwagi K. 2015. Modulation of protein synthesis by polyamines. IUBMB Life **67**, 160–169.

Kadota Y, Goh T, Tomatsu H, Tamauchi R, Higashi K, Muto S, Kuchitsu K. 2004. Cryptogein-induced initial events in tobacco BY-2 cells: pharmacological characterization of molecular relationship among cytosolic Ca^{2+} transients, anion efflux and production of reactive oxygen species. Plant and Cell Physiology **45**, 160–170.

Kadota Y, Sklenar J, Derbyshire P, *et al*. 2014. Direct regulation of the NADPH oxidase RBOHD by the PRR-associated kinase BIK1 during plant immunity. Molecular Cell **54**, 43–55.

Kanehisa M, Goto S. 2000. KEGG: Kyoto Encyclopedia of Genes and Genomes. Nucleic Acids Research **28**, 27–30.

Khan AU, Di Mascio P, Medeiros MHG, Wilson T. 1992. Spermine and spermidine protection of plasmid DNA against single-strand breaks induced by singlet oxygen. Proceedings of the National Academy of Sciences, USA **89**, 11428–11430.

Kimura S, Kaya H, Kawarazaki T, Hiraoka G, Senzaki E, Michikawa M, Kuchitsu K. 2012. Protein phosphorylation is a prerequisite for the Ca^{2+}-dependent activation of *Arabidopsis* NADPH oxidases and may function as a trigger for the positive feedback regulation of Ca^{2+} and reactive oxygen species. Biochimica et Biophysica Acta - Molecular Cell Research **1823**, 398–405.

Knight MR, Campbell AK, Smith SM, Trewavas AJ. 1991. Transgenic plant aequorin reports the effects of touch and cold-shock and elicitors on cytoplasmic calcium. Nature **352**, 524–526.

Lamb C, Dixon RA. 1997. The oxidative burst in plant disease resistance. Annual Review of Plant Physiology and Plant Molecular Biology **48**, 251–275.

Li L, Li M, Yu L, *et al*. 2014. The FLS2-associated kinase BIK1 directly phosphorylates the NADPH oxidase RbohD to control plant immunity. Cell Host and Microbe **15**, 329–338.

Liu C, Atanasov KE, Arafaty N, Murillo E, Tiburcio AF, Zeier J, Alcázar R. 2020. Putrescine elicits ROS-dependent activation of the salicylic acid pathway in *Arabidopsis thaliana*. Plant, Cell and Environment **43**, 2755–2768.

Liu C, Atanasov KE, Tiburcio AF, Alcázar R. 2019. The polyamine putrescine contributes to H_2O_2 and *RbohD/F*-dependent positive feedback loop in *Arabidopsis* PAMP-triggered immunity. Frontiers in Plant Science **10**, 894.

Lozano-Juste J, León J. 2010. Enhanced abscisic acid-mediated responses in *nia1nia2noa1-2* triple mutant impaired in NIA/NR- and AtNOA1-dependent nitric oxide biosynthesis in Arabidopsis. Plant Physiology **152**, 891–903.

Marco F, Busó E, Carrasco P. 2014. Overexpression of *SAMDC1* gene in *Arabidopsis thaliana* increases expression of defense-related genes as well as resistance to *Pseudomonas syringae* and *Hyaloperonospora arabidopsidis*. Frontiers in Plant Science **5**, 1–9.

Marina M, Maiale SJ, Rossi FR, Romero MF, Rivas EI, Gárriz A, Ruiz OA, Pieckenstain FL. 2008. Apoplastic polyamine oxidation plays different roles in local responses of tobacco to infection by the necrotrophic fungus *Sclerotinia sclerotiorum* and the biotrophic bacterium *Pseudomonas viridiflava*. Plant Physiology **147**, 2164–2178.

Marino D, Dunand C, Puppo A, Pauly N. 2012. A burst of plant NADPH oxidases. Trends in Plant Science **17**, 9–15.

McAinsh MR, Pittman JK. 2009. Shaping the calcium signature. New Phytologist **181**, 275–294.

Miller G, Suzuki N, Ciftci-Yilmaz S, Mittler R. 2010. Reactive oxygen species homeostasis and signalling during drought and salinity stresses. Plant, Cell and Environment **33**, 453–467.

Mitsuya Y, Takahashi Y, Berberich T, Miyazaki A, Matsumura H, Takahashi H, Terauchi R, Kusano T. 2009. Spermine signaling plays a significant role in the defense response of *Arabidopsis thaliana* to cucumber mosaic virus. Journal of Plant Physiology **166**, 626–643.

Mo H, Wang X, Zhang Y, Zhang G, Zhang J, Ma Z. 2015. Cotton polyamine oxidase is required for spermine and camalexin signalling in the defence response to *Verticillium dahliae*. The Plant Journal **83**, 962–975.

Morel J, Fromentin J, Blein JP, Simon-Plas F, Elmayan T. 2004. Rac regulation of NtrbohD, the oxidase responsible for the oxidative burst in elicited tobacco cell. The Plant Journal **37**, 282–293.

Moschou PN, Sarris PF, Skandalis N, Andriopoulou AH, Paschalidis KA, Panopoulos NJ, Roubelakis-Angelakis KA. 2009. Engineered polyamine catabolism preinduces tolerance of tobacco to bacteria and oomycetes. Plant Physiology **149**, 1970–1981.

Moschou PN, Wu J, Cona A, Tavladoraki P, Angelini R, Roubelakis-Angelakis KA. 2012. The polyamines and their catabolic products are significant players in the turnover of nitrogenous molecules in plants. Journal of Experimental Botany **63**, 5003–5015.

Nathan C, Cunningham-Bussel A. 2013. Beyond oxidative stress: An immunologist's guide to reactive oxygen species. Nature Reviews Immunology **13**, 349–361.

Nühse TS, Bottrill AR, Jones AME, Peck SC. 2007. Quantitative phosphoproteomic analysis of plasma membrane proteins reveals regulatory mechanisms of plant innate immune responses. The Plant Journal **51**, 931–940.

O'Neill EM, Mucyn TS, Patteson JB, Finkel OM, Chung EH, Baccile JA, Massolo E, Schroeder FC, Dangl JL, Li B. 2018. Phevamine A, a small molecule that suppresses plant immune responses. Proceedings of the National Academy of Sciences, USA **115**, E9514–E9522.

Ogasawara Y, Kaya H, Hiraoka G, *et al*. 2008. Synergistic activation of the *Arabidopsis* NADPH oxidase AtrbohD by Ca^{2+} and phosphorylation. Journal of Biological Chemistry **283**, 8885–8892.

Planas-Portell J, Gallart M, Tiburcio AF, Altabella T. 2013. Copper-containing amine oxidases contribute to terminal polyamine oxidation in peroxisomes and apoplast of *Arabidopsis thaliana*. BMC Plant Biology **13**, 109.

Pottosin I, Shabala S. 2014. Polyamines control of cation transport across plant membranes: implications for ion homeostasis and abiotic stress signaling. Frontiers in Plant Science **5**, 154.

Pottosin I, Velarde-Buendía AM, Bose J, Fuglsang AT, Shabala S. 2014. Polyamines cause plasma membrane depolarization, activate Ca^{2+}-, and modulate H^{+}-ATPase pump activity in pea roots. Journal of Experimental Botany **65**, 2463–2472.

Ranf S, Eschen-Lippold L, Pecher P, Lee J, Scheel D. 2011. Interplay between calcium signalling and early signalling elements during defence responses to microbe- or damage-associated molecular patterns. The Plant Journal **68**, 100–113.

Rentel MC, Knight MR. 2004. Oxidative stress-induced calcium signaling in Arabidopsis. Plant Physiology **135**, 1471–1479.

Robatzek S, Chinchilla D, Boller T. 2006. Ligand-induced endocytosis of the pattern recognition receptor FLS2 in *Arabidopsis*. Genes and Development **20**, 537–542.

Rocha RO, Elowsky C, Pham NTT, Wilson RA. 2020. Spermine-mediated tight sealing of the *Magnaporthe oryzae* appressorial pore–rice leaf surface interface. Nature Microbiology **5**, 1472–1480.

Sagor GHM, Takahashi H, Niitsu M, Takahashi Y, Berberich T, Kusano T. 2012. Exogenous thermospermine has an activity to induce a subset of the defense genes and restrict cucumber mosaic virus multiplication in *Arabidopsis thaliana*. Plant Cell Reports **31**, 1227–1232.

Segonzac C, Zipfel C. 2011. Activation of plant pattern-recognition receptors by bacteria. Current Opinion in Microbiology **14**, 54–61.

Seifi HS, Shelp BJ. 2019. Spermine differentially refines plant defense responses against biotic and abiotic stresses. Frontiers in Plant Science **10**, 117.

Seo S, Katou S, Seto H, Gomi K, Ohashi Y. 2007. The mitogen-activated protein kinases WIPK and SIPK regulate the levels of jasmonic and salicylic acids in wounded tobacco plants. The Plant Journal **49**, 899–909.

Suzuki N, Koussevitzky S, Mittler R, Miller G. 2012. ROS and redox signalling in the response of plants to abiotic stress. Plant, Cell and Environment **35**, 259–270.

Suzuki N, Miller G, Morales J, Shulaev V, Torres MA, Mittler R. 2011. Respiratory burst oxidases: the engines of ROS signaling. Current Opinion in Plant Biology **14**, 691–699.

Takahashi Y, Berberich T, Miyazaki A, Seo S, Ohashi Y, Kusano T. 2003. Spermine signalling in tobacco: activation of mitogen-activated protein kinases by spermine is mediated through mitochondrial dysfunction. The Plant Journal **36**, 820–829.

Takahashi Y, Uehara Y, Berberich T, Ito A, Saitoh H, Miyazaki A, Terauchi R, Kusano T. 2004. A subset of hypersensitive response marker genes, including *HSR203J*, is the downstream target of a spermine signal transduction pathway in tobacco. The Plant Journal **40**, 586–595.

Tiburcio AF, Altabella T, Bitrián M, Alcázar R. 2014. The roles of polyamines during the lifespan of plants: from development to stress. Planta **240**, 1–18.

Torres MA, Jones JDG, Dangl JL. 2005. Pathogen-induced, NADPH oxidase–derived reactive oxygen intermediates suppress spread of cell death in *Arabidopsis thaliana*. Nature Genetics **37**, 1130–1134.

Walters DR. 2003. Polyamines and plant disease. Phytochemistry **64**, 97–107.

Wildermuth MC, Dewdney J, Wu G, Ausubel FM. 2001. Isochorismate synthase is required to synthesize salicylic acid for plant defence. Nature **414**, 562–565.

Wong HL, Pinontoan R, Hayashi K, *et al*. 2007. Regulation of rice NADPH oxidase by binding of Rac GTPase to its N-terminal extension. The Plant Cell **19**, 4022–4034.

Yun BW, Feechan A, Yin M, *et al*. 2011. *S*-nitrosylation of NADPH oxidase regulates cell death in plant immunity. Nature **478**, 264–268.

Zeiss DR, Piater LA, Dubery IA. 2021. Hydroxycinnamate amides: intriguing conjugates of plant protective metabolites. Trends in Plant Science **26**, 184–195.

Zhang J, Shao F, Li Y, *et al*. 2007. A *Pseudomonas syringae* effector inactivates MAPKs to suppress PAMP-induced immunity in plants. Cell Host and Microbe **1**, 175–185.

Zhang S, Klessig DF. 1997. Salicylic acid activates a 48-kD MAP kinase in tobacco. The Plant Cell **9**, 809–824.

Zhang Y, Zhu H, Zhang Q, Li M, Yan M, Wang R, Wang L, Welti R, Zhang W, Wang X. 2009. Phospholipase Dα1 and phosphatidic acid regulate NADPH oxidase activity and production of reactive oxygen species in ABA-mediated stomatal closure in *Arabidopsis*. The Plant Cell **21**, 2357–2377.

Zipfel C. 2014. Plant pattern-recognition receptors. Trends in Immunology **35**, 345–351.

Zipfel C, Robatzek S, Navarro L, Oakeley EJ, Jones JD, Felix G, Boller T. 2004. Bacterial disease resistance in *Arabidopsis* through flagellin perception. Nature **428**, 764–767.

Chapter 2 - Spermine deficiency shifts the balance between jasmonic acid and salicylic acid-mediated defence responses in *Arabidopsis*.

Received: 3 May 2023 | Revised: 18 August 2023 | Accepted: 21 August 2023

DOI: 10.1111/pce.14706

ORIGINAL ARTICLE

Plant, Cell & Environment WILEY

Spermine deficiency shifts the balance between jasmonic acid and salicylic acid-mediated defence responses in *Arabidopsis*

Chi Zhang[1] | Kostadin E. Atanasov[1] | Ester Murillo[1] | Vicente Vives-Peris[2] | Jiaqi Zhao[1] | Cuiyun Deng[3] | Aurelio Gómez-Cadenas[2] | Rubén Alcázar[1]

[1]Department of Biology, Healthcare and Environment, Section of Plant Physiology, Faculty of Pharmacy and Food Sciences, Universitat de Barcelona, Barcelona, Spain

[2]Departamento de Biología, Bioquímica y Ciencias Naturales, Universitat Jaume I, Castelló de la Plana, Spain

[3]Plant Synthetic Biology and Metabolic Engineering Program, Centre for Research in Agricultural Genomics (CRAG), CSIC-IRTA-UAB-UB, Cerdanyola, Barcelona, Spain

Correspondence
Rubén Alcázar, Department of Biology, Healthcare and Environment, Section of Plant Physiology, Faculty of Pharmacy and Food Sciences, Universitat de Barcelona, Av. Joan XXIII 27-31, 08028 Barcelona, Spain.
Email: ralcazar@ub.edu

Funding information
Ministerio de Ciencia e Innovación MCIN/ Agencia Estatal de Investigación AEI/ 10.13039/501100011033 (Spain)

Abstract

Polyamines are small aliphatic polycations present in all living organisms. In plants, the most abundant polyamines are putrescine (Put), spermidine (Spd) and spermine (Spm). Polyamine levels change in response to different pathogens, including *Pseudomonas syringae* pv. *tomato* DC3000 (*Pst* DC3000). However, the regulation of polyamine metabolism and their specific contributions to defence are not fully understood. Here we report that stimulation of Put biosynthesis by *Pst* DC3000 is dependent on coronatine (COR) perception and jasmonic acid (JA) signalling, independently of salicylic acid (SA). Conversely, lack of Spm in *spermine synthase* (*spms*) mutant stimulated galactolipids and JA biosynthesis, and JA signalling under basal conditions and during *Pst* DC3000 infection, whereas compromised SA-pathway activation and defence outputs through SA–JA antagonism. The dampening of SA responses correlated with COR and *Pst* DC3000-inducible deregulation of *ANAC019* expression and its key SA-metabolism gene targets. Spm deficiency also led to enhanced disease resistance to the necrotrophic fungal pathogen *Botrytis cinerea* and stimulated endoplasmic reticulum (ER) stress signalling in response to *Pst* DC3000. Overall, our findings provide evidence for the integration of polyamine metabolism in JA- and SA-mediated defence responses, as well as the participation of Spm in buffering ER stress during defence.

KEYWORDS
Botrytis cinerea, coronatine, ER stress, galactolipids, JA, polyamines, *Pseudomonas syringae*, SA

1 | INTRODUCTION

Polyamines are aliphatic polycations of small molecular weight present in all living organisms. In plants, the major polyamines are putrescine (Put), spermidine (Spd) and spermine (Spm) (Figure 1a). Changes in polyamine metabolism are part of the metabolic reprogramming that takes place during the defence response of plants (Gerlin et al., 2021; Tiburcio et al., 2014). Exogenously supplied Put triggers the formation of callose deposits and the expression of PAMP (pathogen associated molecular pattern)-triggered immunity (PTI) marker genes, which are reliant on hydrogen peroxide (H_2O_2) production and NADPH oxidase function (Liu et al., 2019). Moreover, Put stimulates salicylic acid (SA) accumulation in local leaves and triggers local and systemic transcriptional reprogramming that

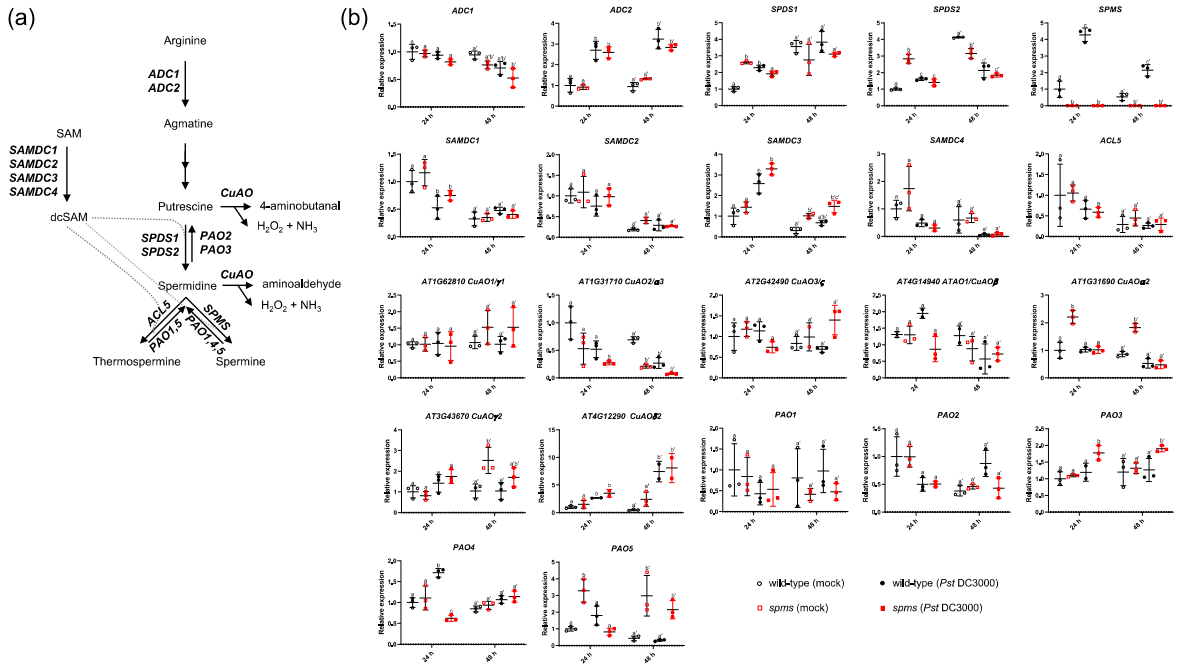

FIGURE 1 (a) Polyamine biosynthesis and oxidation in *Arabidopsis*. (b) Transcriptional changes of polyamine metabolism genes in response to *Pst* DC3000. Expression analyses of polyamine biosynthesis and oxidation genes in wild-type and *spermine synthase* (*spms*) plants at 24 and 48 h of *Pst* DC3000 and mock (10 mM $MgCl_2$) inoculation. Expression values are relative to wild-type (mock) treatment and represent the mean ± SD from three biological replicates per point of analysis. Different letters indicate significant differences ($p < 0.05$) according to two-way analysis of variance followed by Tukey's posthoc test. *ACL5* (*ACAULIS5*), thermospermine synthase; ADC, arginine decarboxylase; CuAO, copper-containing amine oxidase; dcSAM, decarboxylated SAM; PAO, polyamine oxidase; SAM, S-adenosylmethionine; SAMDC, S-adenosylmethionine decarboxylase; SPDS, spermidine synthase; SPMS, spermine synthase.

partially overlap with the systemic acquired resistance (SAR) response (Liu et al., 2020a). The transcriptional changes elicited by Put are partially compromised in *eds1-2*, *sid2-1* and *npr1-1* mutants, thus highlighting the importance of the SA-pathway in Put responses (Liu et al., 2020a).

The oxidation of Spm via polyamine oxidase (PAO) activity stimulates the activation of mitogen-activated protein kinases (MAPKs) (Seo et al., 2007; Zhang et al., 1997) and plays a crucial role in conditioning resistance to different pathogenic microorganisms such as *Pseudomonas syringae*, *Pseudomonas viridiflaba*, *Hyaloperonospora arabidopsidis*, *Verticillium dahlia*, *Botrytis cinerea* and cucumber mosaic virus (Gonzalez et al., 2011; Lou et al., 2016; Marco et al., 2014; Marina et al., 2008; Mitsuya et al., 2009; Mo et al., 2015; Moschou et al., 2009; Sagor et al., 2012). In tobacco, Spm induces the activation of protein kinases SA-induced protein kinase and wound-induced protein kinase, as well as MAPKs (Seo et al., 2007; Takahashi et al., 2003; Zhang et al., 1997). This activation leads to the expression of several hypersensitive response marker genes in a reactive oxygen species (ROS) and Ca^{2+}-dependent manner, independently of SA (Takahashi et al., 2004). Spm also inhibits PAMP-elicited RESPIRATORY BURST OXIDASE HOMOLOGUE D ROS production in a SA-independent manner, thus reshaping PTI responses (Zhang et al., 2023). Although there has been a substantial body of research conducted on the contribution of polyamines to defence, the precise mechanisms involved in this process are not yet fully understood. Specifically, the interaction between polyamines, SA and jasmonic acid (JA) pathways during defence deserved further investigation.

SA is an important plant defence hormone that provides immunity against biotrophic and semibiotrophic pathogens (Peng et al., 2021). In *Arabidopsis*, SA production during pathogen defence is primarily derived from the isochorismate synthase (ICS) pathway (Wildermuth et al., 2001). Mutations in *ICS1*, which are found in SA-deficient 2 (*sid2*) mutants, compromise SA accumulation (Garcion et al., 2008). SA biosynthesis also requires AvrPphB Susceptible 3 (PBS3), which catalyses the conjugation of isochorismate to glutamate, and ENHANCED DISEASE SUSCEPTIBILITY 5 (EDS5), which transports isochorismate to the cytosol (Nawrath et al., 2002; Serrano et al., 2013). *ICS1*, *PBS3*, and *EDS5* expression are strongly induced during the defence response and their transcription is coordinately regulated by the master regulators of plant immune responses SAR-DEFICIENT 1 (SARD1) and CALMODULIN-BINDING PROTEIN 60-LIKE g (CBP60g) (Sun et al., 2015; Wang et al., 2011; Zhang et al., 2010). Overexpression of *SARD1* is sufficient to activate *ICS1* expression, which points to a

regulation of SARD1 activity at transcriptional level (Zhang et al., 2010). ENHANCED DISEASE SUSCEPTIBILITY 1 (EDS1) and PHYTOALEXIN DEFICIENT 4 (PAD4) are also required for SA synthesis during effector-triggered immunity and basal defences (Dongus & Parker, 2021; Feys et al., 2001; Zhou et al., 1998).

SA is subject to multiple chemical modifications, including methylation and glycosylation. SALICYLIC ACID/BENZOIC ACID CARBOXYL METHYLTRANSFERASE (BSMT1) catalyses the production of the volatile methyl SA (Attaran et al., 2009). In addition, SALICYLIC ACID GLUCOSYLTRANSFERASE 1 (SAGT1) converts SA to its glucose ester (Dean & Delaney, 2008), thereby modulating the dynamics of SA homoeostasis and defence outputs (Zhang et al., 2010). SA is also a well-established signalling molecule for SAR. It is essential for the activation of genes involved in N-hydroxypipecolic acid biosynthesis, including *AGD2-LIKE DEFENCE RESPONSE PROTEIN 1* (*ALD1*), *SAR-DEFICIENT 4*, and *FLAVIN-DEPENDENT MONOOXYGENASE 1* (*FMO1*) (Liu et al., 2020b; Sun et al., 2020).

Although the promotion of disease resistance against biotrophic pathogens is attributed to SA, immunity against necrotrophic pathogens is associated with JA (Glazebrook, 2005). Jasmonates (JAs) are a type of lipid-derived signalling compound that are synthesized from α-linolenic acid (α-LeA) released from galactolipids (Ishiguro et al., 2001). α-LeA is a substrate of plastidial 13-Lipoxygenases (LOX2, LOX3, LOX4 and LOX6), which catalyse the synthesis of 13-hydroperoxy derivatives (Andreou & Feussner, 2009; Wasternack & Song, 2017). In turn, the 13-hydroperoxy derivatives are substrates of allene oxide synthase (AOS), a cytochrome P450 enzyme of the CYP74 family. The unstable allylic epoxides formed by AOS are converted into 12-oxophytodienoic acid (OPDA) by allene oxide cyclase (AOC), being the last reaction of the JA biosynthesis pathway in the chloroplast. Subsequently, the downstream steps in the biosynthesis of JA take place in the peroxisomes. OPDA is a substrate of OPDA reductase (OPR3) and this is followed by shortening of the carboxyl side chain by the fatty acid β-oxidation machinery (Hu et al., 2012; Wasternack & Song, 2017).

JA is conjugated to amino acids, such as isoleucine, and JA-Ile represents the major active jasmonate. JA is perceived by the JA receptor F-box protein CORONATINE INSENSITIVE1 (COI1) that forms a Skp-Cullin-F-box E3 ubiquitin ligase complex SCF (COI1) (Sheard et al., 2010; Wasternack & Feussner, 2018). JASMONATE ZIM DOMAIN (JAZ) proteins act as transcriptional repressors and function as co-receptors of JA perception (Chini et al., 2007; Sheard et al., 2010; Thines et al., 2007). When JA-Ile binds to COI1, it leads to the degradation of JAZ proteins through the 26S proteasome. This degradation removes the inhibitory effect of JAZ on the transcription factor MYC2 and its homologues, thus promoting the expression of genes that are responsive to JA signalling (Hou & Tsuda, 2022; Li et al., 2021).

Notably, SA and JA exhibit mutually antagonistic effects (Glazebrook, 2005). JA inhibits SA accumulation, as evidenced by the high levels of SA in JA-insensitive *coi1* and *myc2* mutants (Kloek et al., 2001; Nickstadt et al., 2004). The bacterial phytotoxin coronatine (COR), which is produced by various strains of *P. syringae* and exhibits structural similarity to JA-Ile (Mittal & Davis, 1995), facilitates bacterial growth and disease symptom development by stimulating the reopening of stomata and inhibiting SA accumulation (Brooks et al., 2005; Cui et al., 2005; Melotto et al., 2006; Mittal & Davis, 1995; Zheng et al., 2012). The *Arabidopsis ANAC019*, *ANAC055*, and *ANAC072*, which are homologous to NAC (NAM-ATAF1,2-CUC2) transcription factors, have been identified as key mediators of the COR-induced effects. Specifically, they contribute to *MYC2*-dependent inhibition of the SA pathway by suppressing *ICS1* and activating *BSMT1* expression, resulting in an overall reduction of SA (Zheng et al., 2012).

In this work, we investigated the involvement of the polyamine Spm in the defence response to *P. syringae* in *Arabidopsis*. We provide evidence that COR and JA signalling are important regulators of polyamine metabolism during the defence response to *P. syringae*. By performing RNA sequencing (RNA-seq) gene expression analyses in Spm-deficient mutant (*spms*) challenged with *Pst* DC3000, we find that Spm deficiency modifies the balance between JA and SA, and triggers endoplasmic reticulum (ER) stress responses. Through an untargeted lipidomics analysis, we demonstrate that Spm-deficient plants contain higher levels of monogalactosyldiacylglycerol (MGDG) and stimulate JA biosynthesis through expression regulation not involving increased peroxisomal β-oxidation. Spm deficiency dampens SA-mediated defences in correlation with the transcriptional upregulation of *ANAC019* and *BSMT1* expression, and *ICS1* down-regulation. In contrast, Spm deficiency is found to enhance disease resistance to *B. cinerea* infection. Finally, Spm is shown to be critical for the mitigation of ER stress during the defence response to *P. syringae*. Overall, this work sheds new light on the integration of polyamines in the defence responses mediated by JA and SA, and in buffering ER stress signalling.

2 | MATERIALS AND METHODS

2.1 | Plant materials and growth conditions

Seeds of the different genotypes were directly sown on soil (40% peat moss, 50% vermiculite and 10% perlite). Seeds were stratified in the dark at 4°C for 2–3 days to stimulate germination. The different plant genotypes were grown at 20°C–22°C under 12 h light/12 h dark photoperiod cycles at 100–125 µmol photons $m^{-2} s^{-1}$ of light intensity and 60%–70% relative humidity. The genotypes used in this work were in the Col-0 background: *spms* (Zhang et al., 2023), *eds1-2* (Feys et al., 2005), *sid2-1* (Wildermuth et al., 2001), *npr1-1* (Cao et al., 1997), *coi1-1* (Feys et al., 1994), *myc2* (Chini et al., 2007), *adc1* and *adc2* (Cuevas et al., 2008). For in vitro growth, seeds were sterilized in 30% sodium hypochlorite supplemented with 0.5% Triton X-100 (Merck) for 10 min, followed by three washes with sterile distilled H_2O. Seeds were sown on half-strength Murashige and Skoog (MS) medium (0.5× MS salts supplemented with vitamins [Duchefa Biochemie], 1% sucrose, 0.6% plant agar and 0.05% MES adjusted to pH 5.7 with 1 M KOH). To synchronize germination,

seeds were stratified in the dark at 4°C for 2–3 days. The seeds were kindly provided by Professor Jane Parker (*eds1-2*, *sid2-1*), Professor Xinnian Dong (*npr1-1*), Dr. Andrea Chini (*coi1-1*) or obtained from the Nottingham *Arabidopsis* Stock Centre (www.arabidopsis.info).

2.2 | Leaf infiltration and sampling

Infiltration of leaves with *Pst* DC3000 (OD_{600} = 0.001), *Pst* DC3000 Δ*cor* (OD_{600} = 0.001) (Ma et al., 1991) or mock (10 mM $MgCl_2$) was conducted on 5-week-old *Arabidopsis* plants using a 1 mL needleless syringe. The infiltration was performed on fully expanded rosette leaves using three leaves per plant, which represented one biological replicate. A minimum of three biological replicates were used in every analysis. Leaves at the same developmental stage were always chosen for infiltration of the different genotypes. At the indicated time points, only the infiltrated leaves were collected for the determination of polyamine levels, expression analyses (RNA-seq and quantitative reverse-transcription polymerase chain reaction [qRT-PCR]) and measurement of hormone levels (SA, JA, JA-Ile and OPDA). For the untargeted proteomics and lipidomics analyses, rosette leaves from untreated 5-week-old *spms* and wild-type plants were directly harvested using three leaves per plant as single biological replicate (n = 4 untargeted proteomics; n = 5 untargeted lipidomics). Leaves at the same developmental stage were always chosen for the analyses. The *Pst* DC3000 Δ*cor* strain was kindly provided by Professor Jane Parker.

2.3 | qRT-PCR gene expression analyses

Total RNA was extracted using TRIzol reagent (Thermo Fisher). Two micrograms of RNA were treated with DNAse I (Thermo Fisher) and first-strand complementary DNA (cDNA) synthesized using Superscript IV reverse transcriptase (Thermo Fisher) and oligo(dT) according to manufacturer's instructions. Quantitative real-time PCR using SYBR Green I dye method was performed on Roche LightCycler 480 II detector system following the PCR conditions: 95°C 2 min, 40 cycles (95°C, 15 s; 60°C, 30 s; 68°C, 20 s). To ensure comparable PCR efficiencies between the primer pairs used, standard curves were generated by performing serial dilutions of wild-type cDNA. The relative quantification was then determined using the $\Delta\Delta C_T$ method (Livak & Schmittgen, 2001). Gene expression was normalized using *ACTIN2* (*At3g18780*) and *UBQ10* (*At4g05320*) as housekeeping genes. Primer sequences used for gene expression analyses are listed in Table S1. qRT-PCR analyses were always performed on at least three biological replicates.

2.4 | Determination of polyamine levels

The levels of free Put, Spd and Spm were determined by high-performance liquid chromatography (HPLC) separation of dansyl derivatives, as described in (Zhang et al., 2023). Analyses were performed in four biological replicates per point of analysis.

2.5 | RNA-seq gene expression analyses

Pst DC3000 (OD_{600} = 0.001) and mock (10 mM $MgCl_2$) inoculation treatments were performed in three biological replicates using three different plants per genotype and treatment. Infiltration was performed as described above. Only infiltrated leaves were collected at 24 h of treatment for total RNA extraction. Total RNA was extracted using *TriZol* (Thermo Fisher) and further purified using RNeasy kit (Qiagen) according to manufacturer's instructions. Total RNA was quantified in Qubit fluorometer (Thermo Fisher) and checked for purity and integrity in a *Bioanalyzer-2100* device (Agilent Technologies). RNA samples were further processed at the Beijing Genomics Institute (BGI) for library preparation and RNA-seq using DNBSEQ. Libraries were prepared using the MGIEasy RNA Library Prep kit (MGI Tech) according to manufacturer's instructions and each library was paired-end sequenced (2 × 100 bp) on DNBSEQ-G400 sequencers. Read mapping and expression analyses were performed using the *CLC Genomics Workbench 21 version 21.0.5* (Qiagen). Only significant expression differences (fold-change ≥ 2; Bonferroni corrected $p \leq 0.05$) were considered. Gene Ontology (GO) analyses were performed using GO resource (http://geneontology.org) and PANTHER classification system (http://www.pantherdb.org/) with annotations from Araport11 (Carbon et al., 2019; Cheng et al., 2017; Mi et al., 2019). A binomial test was used to identify over-represented GO terms in the sample gene set compared with the reference genome set, using a significance threshold of $p < 0.05$ (Mi et al., 2013; Rivals et al., 2007).

2.6 | Proteomics analysis

Protein content of the samples in 7 M Urea buffer were determined using PIERCE™ 660 Protein Assay Kit (Thermo Scientific) following the product's specifications. Twenty micrograms of proteins from each sample were digested as follows: samples were reduced with 200 mM dithiothreitol (DTT) in 50 mM NH_4HCO_3 for 90 min at 32°C. The samples were then alkylated using 300 mM iodoacetamide in 50 mM NH_4HCO_3 and incubated in the dark for 30 min at room temperature. Another round of 200 mM DTT was added to do the quenching, and an appropriate amount of 50 mM NH_4HCO_3 was added to dilute the urea to a final concentration of 1 M. Digestion was done in two steps: an initial digestion with 1:20 (w/w) trypsin 0.1 μg μL^{-1} (sequence grade-modified trypsin, Promega) for 2 h at 32°C followed by a digestion with 1:20 (w/w) trypsin 0.1 μg μL^{-1} for 16 h at 32°C. Finally, the resulting peptide mixtures were acidified with formic acid (FA) and concentrated in a SpeedVac vacuum system (Eppendorf). Peptides were cleaned up with C18 tips (P200 top tip, PolyLC Inc.). Briefly, peptides were loaded on the tip columns (previously washed with 70% acetonitrile [ACN] in 0.1% FA and

equilibrated with 0.1% FA) by centrifugation at 350*g* for 2 min. Columns were washed twice with 100 µL 0.1% FA by centrifugation (350*g* for 2 min) and then peptides eluted in 2 × 80 µL of 50% ACN and 0.1% FA by centrifugation (350*g* for 2 min and 900*g* for 1 min). The peptides were dried-down in Speed Vacuum (Eppendorf) and delivered to IRB (Institute for Research in Biomedicine) Mass Spectrometry and Proteomics Core Facility to perform LC–tandem mass spectrometry (MS/MS) analysis. Raw data obtained in the MS analyses were processed with MaxQuant software (v_1.6.6.0). The spectra were searched using its built-in Andromeda search engine, against the SwissProt *Arabidopsis thaliana* database (v_220419) including contaminants. The following parameters were used: fixed modifications: carbamidomethylation of cysteins (C); variable modifications: methionine (M) oxidation and deamidation of asparagine and glutamine (NQ); enzyme: trypsin; maximum allowed missed cleavage: 2; match between runs and alignment time window were set to 0.7 and 20 min, respectively. Other nonspecified parameters were left as default. For label-free quantification, minimum ratio count was set to 1 and both razor and unique peptides were used for quantification. False discovery rate was set to 1% for both protein and peptide spectrum match levels. Label-free quantitative data were processed using Perseus open software (v. 1.6.15.0). Perseus was used to obtain the curated protein data set, which was built by removing from the list of identified proteins, those proteins identified as contaminants, proteins identified only by site, and proteins identified from the redundant and reversed databases. In addition, data were base 2 log transformed, and missing values were excluded unless three valid values were present in at least one group. Finally, imputation was done using normal distribution method. To test for differentially accumulated proteins, Student's *T* test was applied to the curated proteins and absolute fold-change values calculated.

2.7 | *Pst* DC3000 disease resistance assays

P. syringae pv. *tomato* DC3000 (*Pst* DC3000) was inoculated in 5-week-old plants by spray inoculation using a bacterial suspension (OD_{600} = 0.1) in 10 mM $MgCl_2$ and 0.04% Silwet L-77. *Pst* DC3000 colony forming units cm^{-2} were determined at 24, 48 and 72 h postinoculation as described (Liu et al., 2020a; Zhang et al., 2023).

2.8 | *B. cinerea* disease resistance assays

Spores of *B. cinerea* (CECT2100 obtained from the Spanish Collection of Type Cultures at Universidad de Valencia) cultivated in Potato Dextrose Agar medium were collected, washed with sterile water, counted and diluted to 4×10^6 spores mL^{-1} in inoculation buffer (Gamborg's B5 medium [Duchefa Biochemie] with 2% sucrose). The spores were incubated 2 h at room temperature and gentle agitation before inoculation on 5-week-old plant leaves, by placing 10 µL droplets of the spore suspension. Inoculated plants were covered with a transparent plastic dome to maintain high humidity and returned to the growth chamber. Leaves were photographed at 72 h postinoculation. Images were used to determine the lesion area using ImageJ (https://imagej.nih.gov).

Quantitative PCR (qPCR)-based quantification of fungal growth was determined by quantification of fungal and plant DNA (Gachon & Saindrenan, 2004). Five-week-old plants were spray-inoculated with a suspension of 5×10^5 spores mL^{-1} in inoculation buffer (Gamborg's B5 medium [Duchefa Biochemie] with 2% sucrose). Leaf samples were taken at 24 and 48 h of inoculation and the fungal and plant DNA was extracted using DNeasy Plant Minikit (Qiagen) according to manufacturer's instructions (Gachon & Saindrenan, 2004). The analysis was performed in six independent biological replicates, each containing three leaves from three different plants. The *B. cinerea β-tubulin* and *Arabidopsis Actin2* genes were used for real-time PCR analyses using specific primers listed in Supporting Information: Table S1.

2.9 | Quantification of SA, JA, JA-Ile and OPDA

Phytohormone analysis was performed as described in (Šimura et al., 2018) with some modifications. Briefly, around 20 mg of dry material were extracted in 1 mL ACN:water 1:1 (v:v) solution using a ball mill equipment (MillMix 20, Domel) at 17 rps for 10 min, adding a mixture containing 25 ng of ^{13}C-SA and dihydrojasmonic acid, as internal standards. After this, samples were sonicated for 5 min (Elma S30, Elma) and centrifuged for 10 min at 4000*g* and 4°C. The supernatant was filtered through solid-phase extraction (SPE) columns (Oasis HLV 30 mg 1 cc, Waters), taking the obtained eluent in new tubes and adding 0.5 mL 30% ACN to the SPE columns, which was also recovered with the previous eluent. Finally, the obtained samples were injected in an ultra-performance LC-MS (UPLC-MS) system (Xevo TQ-S, Waters). The chromatographic separation was achieved using a reverse phase C18 column (Luna Omega C18 50 × 2.1 mm, 1.8 µm particle size, Phenomenex) and a gradient of ultrapure deionized water and ACN, both supplemented with 0.1% FA at a flow rate of 0.3 mL min^{-1}. The phytohormones were detected with a triple quadrupole mass spectrometer coupled through a Z-spray electrospray ion source, configured in MRM mode. Finally, hormone levels were quantified in the samples through the interpolation of the obtained response in a standard curve, and the data was processed with the Masslynx v4.2 software.

2.10 | Stomatal assays

Leaf peels were obtained using clear adhesive tape from the abaxial side of mature leaves from 5-week-old wild-type plants. The leaf peels were immediately placed in contact with 20 mL of buffer solution (25 mM MES, 10 mM KCl, pH 6.15) or *Pst* DC3000 bacteria resuspended in buffer solution (OD_{600} = 0.001) (Zeng & He, 2010). The leaf peels were incubated in the different solutions for 1 and 4 h before being mounted on glass slides and directly observed under a light microscope. A minimum of 30 images from at least 10

independent leaf peels per treatment were randomly taken and stomata recorded for each sample treatment. Stomatal apertures were measured from images using ImageJ (https://imagej.nih.gov).

2.11 | Acyl CoA oxidase assays

Acyl-CoA oxidase activity assays were performed according to previously described methods (Adham et al., 2005; Gerhardt, 1987; Hryb & Hogg, 1979). Seeds of *spms* and wild-type plants were sterilized in 30% sodium hypochlorite supplemented with 0.5% Triton X-100 (Merck) for 10 min, followed by three washes with sterile distilled H_2O. Seeds were sown on growth media containing 1/2 MS salts supplemented with vitamins (Duchefa Biochemie), 0.5% sucrose, 0.6% plant agar (Duchefa Biochemie) and 0.05% MES adjusted to pH 5.7 with 1 M KOH. To synchronize germination, plates were stratified in the dark at 4°C during 2–3 days. Plates were incubated under 16 h light/8 h dark cycles at 20°C–22°C and 100–125 µmol photons m^{-2} s^{-1} of light intensity for 3 days. At 3 days after germination, around 100 mg of tissue was harvested per biological replicate, weighted and frozen immediately in liquid nitrogen. The tissue was ground to a powder using a mortar and pestle. The ground tissue was added 1 mL of cold extraction buffer (50 mM potassium phosphate buffer pH 7.6, 50 µM FAD, 100 µg mL^{-1} bovine serum albumin [BSA], 0.025% Triton X-100) supplemented with 10 µL of protease inhibitor cocktail (P9599, Merck). Extracts were centrifuged at 12 000*g* and 4°C for 15 min. For each replicate, 100 µL of enzyme supernatant was combined with 100 µL of reaction buffer (0.8 mM fatty acyl-CoA substrate, 50 mM potassium phosphate buffer pH 7.6, 50 µM FAD, 100 µg mL^{-1} BSA, 0.025% Triton X-100, 110 U horseradish peroxidase, 50 mM *p*-hydroxybenzoic acid and 2 mM 4-aminoantipyrine). Reactions were monitored spectrophotometrically at 500 nm to detect H_2O_2 production as an indirect measure of acyl-CoA oxidase activity. A H_2O_2 standard curve was used to determine H_2O_2 concentrations in the extracts and calculate reaction rates (mmol H_2O_2 g^{-1} min^{-1}). All chemicals were purchased from Merck.

2.12 | Root growth assays

Seeds of the different genotypes were sterilized in 30% sodium hypochlorite supplemented with 0.5% Triton X-100 (Merck) for 10 min, followed by three washes with sterile distilled H_2O. Seeds were sown, stratified, and germinated on 50 mL vertical plates containing 1/2 MS salts supplemented with vitamins (Duchefa Biochemie), 1% sucrose, 0.8% plant agar (Duchefa Biochemie) and 0.05% MES pH 5.7. The media was supplemented with methyl jasmonate (100 µM MeJA, Merck), COR (1 µM COR, Merck), tunicamycin (1 µg mL^{-1} TM, Merck), 2,4-dichlorophenoxybutyric acid (0.2 µg mL^{-1} 2,4-DB, Merck), 2,4-dichlorophenoxyacetic acid (0.05 µg mL^{-1} 2,4-D, Merck) or mock (0.1% dimethyl sulfoxide [DMSO] in water), as required. After 12 days of growth at 16 h light/8 h dark cycles, 20°C–22°C and 100–125 µmol photons m^{-2} s^{-1} of light intensity, pictures were taken and the primary root length of the seedlings measured using ImageJ (https://imagej.nih.gov).

2.13 | Untargeted lipidomics analyses

One hundred milligrams of leaves from 5-week-old *spms* and wild-type plants were used for an untargeted lipidomics analysis using five biological replicates. The analyses were performed at the BGI. The different samples were spiked with internal standards 15:0-18:1(d7)PC, 18:1-d7 Lyso PE, 15:0-18:1(d7)PS (Avanti Polar Lipids) and extracted in methyl tert-butyl ether/methanol (MeOH) (3:1 v/v) precooled at −20°C. Tissue lysis was performed in a tissue grinder device (50 Hz, 5 min), followed by bath ultrasonication for 15 min and precipitation at −20°C for 2 h. Afterwards, 0.5 mL of (H_2O/MeOH 3:1 v/v) was added to each sample and vortexed for 1 min. Samples were centrifuged at 24 000*g* for 10 min and 0.6 mL of the supernatant taken and dried. Before LC-MS analysis, the extracts were reconstituted in 400 µL isopropanol containing 10 mM ammonium acetate. For quality control, 50 µL of supernatant from each sample were mixed. The UPLC-MS analysis was performed on a Waters UPC I-Class Plus (Waters) tandom Q Exactive high resolution mass spectrometer (Thermo Fisher Scientific) for separation and detection of lipids. Chromatographic separation was performed on CSH C18 Column (1.7 µm 2.1 × 100 mm, Waters). At positive ion mode with mobile phase A consisting of 60% ACN in water + 10 mM ammonium formate + 0.1% FA and mobile phase B consisting of 90% isopropanol + 10% ACN + 10 mM ammonium formate + 0.1% FA. At negative ion mode, with mobile phase A consisting of 60% ACN in water + 10 mM ammonium formate and mobile phase B consisting 90% isopropanol + 10% ACN + 10 mM ammonium formate. The column temperature was maintained at 55°C. The gradient conditions were as follows: 40% ~ 43% B over 0 ~ 2 min, 43% ~ 50% B over 2 ~ 2.1 min, 50% ~ 54% B over 2.1 ~ 7 min, 54% ~70% B over 7 ~ 7.1 min, 70% ~ 99% B over 7.1 ~ 13 min, 99% ~ 40% B over 13 ~ 13.1 min, held constant at 99% ~ 40% B over 13.1 ~ 15 min and washed with 40% B over 13.1–15 min. The flow rate was 0.4 mL min^{-1} and the injection volume was 5 µL. Q Exactive (Thermo Fisher Scientific) was used for primary and secondary MS data acquisition. The full scan range was 70–1050 *m/z* with a resolution of 70 000 and the automatic gain control (AGC) target for MS acquisitions was set to 3e6 with a maximum ion injection time of 100 ms. Top three precursors were selected for subsequent MSMS fragmentation with a maximum ion injection time of 50 ms and resolution of 17 500, the AGC was 1e5. The stepped normalized collision energy was set to 15, 30 and 45 eV. Electrospray ionization parameters were setting as follows: Sheath gas flow rate was 40, Aux gas flow rate was 10, positive-ion mode Spray voltage (|KV|) was 3.80, negative-ion mode Spray voltage (|KV|) was 3.20, Capillary temperature was 320°C, and Aux gas heater temperature was 350°C. Lipid identification was performed on Lipidsearch v.4.1 (Thermo Fisher Scientific). Data preprocessing included (i) removing metabolites with >50% missing values in QC samples and more than 80% missing values in experimental samples. (ii) Filling in missing values

with k-nearest neighbour algorithm. (iii) Normalizing the data to obtain relative peak areas by probabilistic quotient normalization (Di Guida et al., 2016). (iv) Using quality control-based robust locally estimated scatterplot smoothing signal correction to correct Batch effect (Dunn et al., 2011). (v) Removing metabolites with a coefficient of variation >30% on their Relative peak area in QC samples. Values for each identified lipid were expressed as relative content (mol%).

2.14 | ER stress, COR and ABA treatments

Wild-type and *spms* seedlings were grown in half-strength MS medium and 1% sucrose under 16 h light/8 h dark cycles at 20°C–22°C and 100–125 µmol photons m^{-2} s^{-1} of light intensity for 10 days. The seedlings were transferred to liquid MS medium supplemented with 1 µg mL^{-1} TM, 100 µM Brefeldin A (BFA), 100 µM DTT or mock (0.1% DMSO) for 6–24 h. Samples were collected for qRT-PCR gene expression analyses and/or polyamine levels determination. For COR and ABA treatments, 10-day-old seedlings grown on half-strength MS medium were transferred to the same media containing 1 µM COR or 5 µM ABA. Samples were harvested at 24 h of treatment for qRT-PCR gene expression analyses.

3 | RESULTS

3.1 | Polyamine responses to *Pst* DC3000 and their dependence on COR, SA and JA signalling

To study the modulation of polyamine metabolism and the role of Spm during the defence response to *Pst* DC3000, we first determined the changes in expression of all polyamine biosynthesis and oxidation genes in both wild-type and *spms* plants at 24 and 48 h of bacterial and mock inoculation (Figure 1b). Inoculation with *Pst* DC3000 consistently increased the expression of *ARGININE DECARBOXYLASE 2* (*ADC2*), *SPERMINE SYNTHASE* (*SPMS*), *S-ADENOSYLMETHIONINE DECARBOXYLASE 3* (*SAMDC3*), and *COPPER-CONTAINING AMINE OXIDASE δ2* (*CuAOδ2*). The expression levels in the wild-type and *spms* mutant were comparable for all genes, except for *SPMS*, which expression was undetectable in the mutant (Figure 1b). Interestingly, inoculation with the COR-deficient strain *Pst* DC3000 Δ*cor* (Ma et al., 1991) compromised the transcriptional activation of *ADC2* at both 24 and 48 h, and that of *SPMS*, *SAMDC3* and *CuAOδ2* at 24 h (Figure 2a). Consistent with the *ADC2* expression, *Pst* DC3000 Δ*cor* inoculation also led to lower increases in Put compared with *Pst* DC3000 treatment (Figure 2b). The data indicated that COR triggers

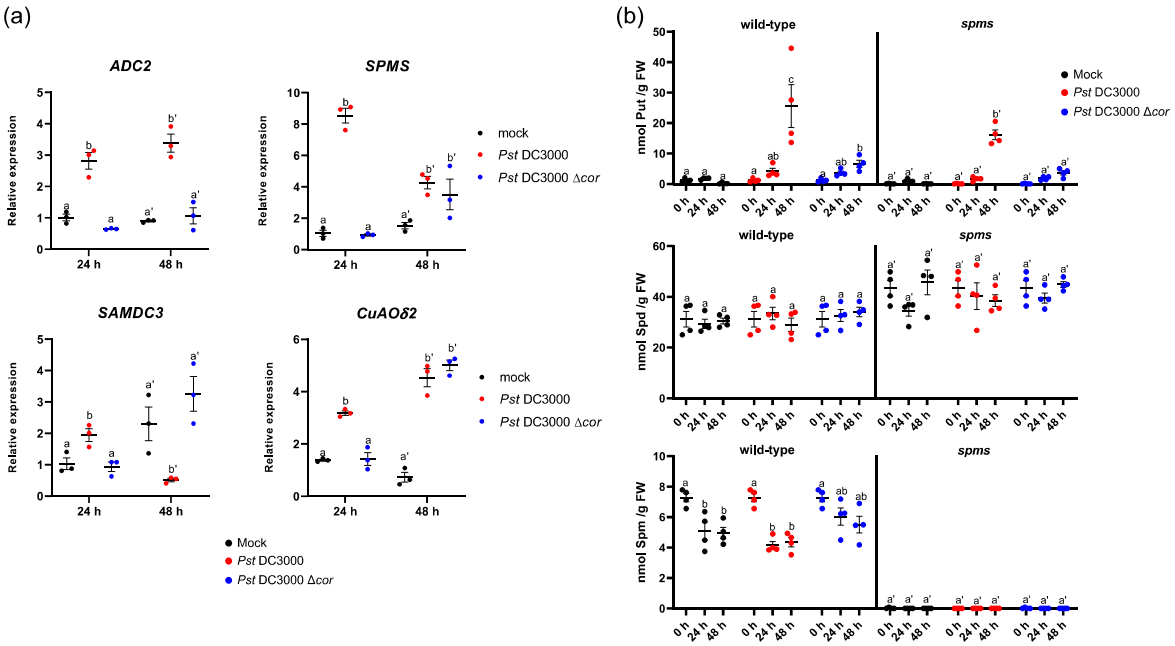

FIGURE 2 Effect of coronatine (COR) on the elicitation of polyamine metabolism. (a) Expression analyses of polyamine biosynthesis genes *ADC2* (*ARGININE DECARBOXYLASE 2*), *SPMS* (*SPERMINE SYNTHASE*), *SAMDC3* (*S-ADENOSYLMETHIONINE DECARBOXYLASE 3*) and polyamine oxidation CuAOδ2 (*COPPER AMINE OXIDASE δ2*) in response to *Pst* DC3000 (OD_{600} = 0.001), COR-deficient *Pst* DC3000 Δ*cor* (OD_{600} = 0.001) and mock (10 mM $MgCl_2$) infiltration, determined in wild-type plants at 24 and 48 h of treatment. Expression values are relative to the wild-type (mock) treatment and represent the mean ± SD from three biological replicates per point of analysis. (b) Concentrations of putrescine (Put), spermidine (Spd) and spermine (Spm) at 0, 24, and 48 h of *Pst* DC3000, *Pst* DC3000 Δ*cor* and mock (10 mM $MgCl_2$) inoculation. Values represent the mean ± SD from four biological replicates per point of analysis. Different letters indicate significant differences ($p < 0.05$) according to two-way analysis of variance followed by Tukey's posthoc test. [Color figure can be viewed at wileyonlinelibrary.com]

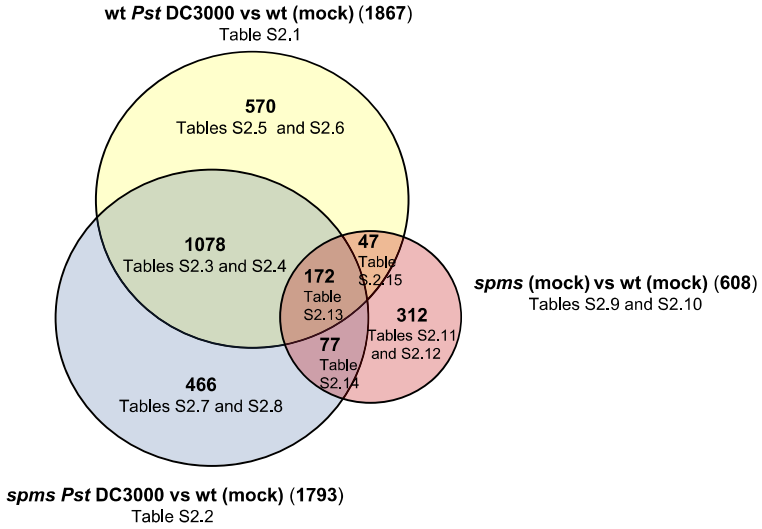

FIGURE 3 RNA sequencing analyses of *spms* and wild-type (wt) plants infiltrated with *Pst* DC3000 (OD_{600} = 0.001) or mock (10 mM $MgCl_2$). Venn diagram of differentially expressed genes (fold change ≥ 2; Bonferroni corrected *p*-value < 0.05) in *spms* and wt plants at 24 h of treatment. A detailed list of genes and Gene Ontology terms is found in Supporting Information: Tables S2.1–S2.18. [Color figure can be viewed at wileyonlinelibrary.com]

important changes in polyamine metabolism during the defence response to *Pst* DC3000, thus pointing to polyamine metabolism as potential target to modify defence responses.

To investigate the involvement of JA and SA pathways in the regulation of polyamine metabolism, we performed a detailed analysis of *ADC2*, *SPMS*, *SAMDC3*, and *CuAOδ2* expression (Supporting Information: Figure S1) and measured polyamine levels (Supporting Information: Figure S2) in response to *Pst* DC3000 in *coi1-1*, *myc2*, *sid2-1*, *eds1-2*, *npr1-1* and wild-type plants. The *coi1-1* and *myc2* mutants showed compromised upregulation of *ADC2*, *SPMS* and *SAMDC3* expression in response to *Pst* DC3000, providing evidence for the involvement of the JA pathway in the regulation of polyamine metabolism. Conversely, *CuAOδ2* expression was not consistently affected by *coi1-1* or *myc2* mutations. The upregulation of *SPMS* and *SAMDC3* expression was also dampened by the *sid2-1*, *eds1-2* and *npr1-1* mutations, whereas higher *ADC2* expression was observed in *npr1-1* at 48 h of *Pst* DC3000 inoculation (Supporting Information: Figure S1). After 48 h of *Pst* DC3000 treatment, Put accumulation in *coi1-1* and *myc2* mutants was significantly lower than in the wild type, in correlation with *ADC2* expression. In contrast, Put levels in *sid2-1*, *eds1-2*, *npr1-1* and *spms* mutants were almost twofold higher than the wild-type (Supporting Information: Figure S2). Remarkably, *adc2* but not *adc1* mutants exhibited compromised accumulation of Put in response to *Pst* DC3000 inoculation, providing evidence that ADC2 is the major contributor to Put biosynthesis in response to *Pst* DC3000 and that the polyamine originates from the plant rather than the bacteria (Supporting Information: Figure S3).

Collectively, these results indicated that functional COI1 and MYC2 are required for *ADC2* responsiveness to *Pst* DC3000 and Put accumulation, this being a SA-independent response. On the other hand, both COI1/MYC2 and EDS1/SA/NPR1 signalling modules are required for the full activation of *SPMS* and *SAMDC3* expression in response to *Pst* DC3000. *CuAOδ2* responses were attenuated in *sid2-1*, *eds1-2* and *npr1-1* mutants. The high Put levels found in the susceptible genotypes *sid2-1*, *eds1-2*, *npr1-1* and *spms* inoculated with *Pst* DC3000, suggested a correlation between Put levels and the progression of bacteria growth. Alternatively, it may result from the potentiation of JA responses in SA pathway (Spoel et al., 2003) or *spms* mutants (this work). Taken together, these findings indicated that both JA and SA play crucial roles in modulating polyamine metabolism in response to *Pst* DC3000, with a major contribution of COR and JA-signalling to the modulation of Put levels.

3.2 | RNA-seq expression analyses shed light on the role of Spm in modulating SA, JA and ER stress in response to *Pst* DC3000

To investigate in deeper detail the contribution of Spm to the defence response to Pst DC3000, we performed RNA-seq gene expression analyses in *spms* and wild-type plants at 24 h of *Pst* DC3000 and mock inoculation (Figure 3 and Supporting Information: S4A and Tables S2.1–S2.18). Significant alterations in gene expression were observed following *Pst* DC3000 treatment, with 1867 and 1793 genes being differentially expressed in the wild type and *spms*, respectively (fold change ≥ 2; Bonferroni corrected *p*-value < 0.05; Supporting Information: Tables S2.1 and S2.2). Treatment with *Pst* DC3000 resulted in the differential expression of 1078 common genes in both genotypes (Supporting Information: Table S2.3), which represented 58% and 60% of the total genes exhibiting significant expression changes in the wild type and *spms*, respectively (Figure 3). As expected, upregulated genes within the common expression sector were related to defence responses to bacterium, SA responses, SAR, ROS signalling, oxidative stress, as well as other GO terms (Supporting Information: Table S2.4). Despite

the overlap, noticeable differences in gene expression were observed between the genotypes in important genes related to SA metabolism and SAR establishment: *ICS1*, *EDS5*, *PBS3*, *SARD1*, *FMO1*, and *ALD1*; and ER stress signalling *BINDING PROTEIN 3* (*BIP3*), *PROTEIN DISULFIDE ISOMERASE-LIKE 1-1* (*PDIL1-1*) and *PDIL1-2* (Figure 4a and Supporting Information: Table S2.3).

Pst DC3000 treatment also elicited the differential expression of 570 genes specifically in wild-type plants ('wild-type *Pst* DC3000 only'; Supporting Information: Table S2.5). The expression of genes within this sector showed moderate correlation between wild-type and *spms* mutant ($r^2 = 0.77$) (Supporting Information: Figure S4B), which suggested a genotype-specific response. The 'wild-type *Pst* DC3000 only' sector was enriched in genes related to JA responses, lipid metabolism and wounding (Figure 3 and Supporting Information: Tables S2.5 and S2.6). The data suggested that JA transcriptional activation was compromised in *spms* at 24 h of *Pst* DC3000 treatment. Other 466 genes were deregulated only in the *spms* mutant in response to *Pst* DC3000 ('*spms Pst* DC3000 only'; Figure 3 and Supporting Information: Table S2.7). The expression of genes in this sector was also moderately correlated ($r^2 = 0.70$) between the genotypes (Supporting Information: Figure S4B). The '*spms Pst* DC3000 only' sector was enriched in genes associated with ER stress signalling (Supporting Information: Table S2.8).

Under basal conditions, without any type of treatment, the *spms* mutant already showed 91 differentially expressed genes, of which only five were upregulated compared with the wild type. Among these, the most upregulated gene in *spms* was *DELTA 9 ACYL-LIPID DESATURASE 1* (*ADS1*), which is involved in fatty acid desaturation (Supporting Information: Table S3.1 and Figure S5). This further suggested a potential impact of Spm deficiency on lipid metabolism. Downregulated genes in *spms* were enriched in GO terms related to defence and SA responses (Supporting Information: Tables S3.1–S3.3). They included key genes in SA biosynthesis and signalling: *SARD1*, *CBP60g*, *PBS3*, *WRKY46* and *PATHOGENESIS-RELATED GENE 1* (*PR1*) (Supporting Information: Figure S5). The data further suggested a role for Spm in regulating SA responses. Overall, RNA-seq analyses indicated that the deficiency of Spm leads to altered transcriptional activation of both JA and SA pathways, as well as expression changes compatible with ER stress in response to *Pst* DC3000.

3.3 | Spm deficiency compromises SA-mediated defence responses to *Pst* DC3000

We further investigated the impact of Spm deficiency on SA-mediated immune signalling in response to *Pst* DC3000 by examining the expression of SA metabolism and signalling genes by qRT-PCR in both *spms* and wild type plants at 24 and 48 h postbacterial and mock inoculation (Figure 4b). Consistent with the RNA-seq data, the expression levels of important SA biosynthesis and signalling genes (*ICS1*, *EDS5*, *PBS3*, *PAD4*, *CBP60g*, *SARD1*), and SA-inducible *PR1* were significantly lower in *spms* relative to the wild type at 24 h of *Pst* DC3000 inoculation (Figure 4b). In addition, *spms* exhibited delayed transcriptional activation of SAR-related genes *ALD1* and *FMO1* (Figure 4b). In agreement with the expression data, *spms* accumulated lower SA than the wild-type under basal conditions (0 h) and at 48 h of *Pst* DC3000 treatment (Figure 4c). The results indicated that Spm deficiency dampened SA-mediated immune responses to *Pst* DC3000. The decrease in SA responses correlated with a significant increase in *Pst* DC3000 growth in *spms* compared with the wild type at 72 h of *Pst* DC3000 spray inoculation (Figure 4d).

3.4 | Spm deficiency elicits JA biosynthesis and signalling

To further analyse the contribution of Spm to the transcriptional activation of the JA pathway in response to *Pst* DC3000, we performed qRT-PCR gene expression analyses of JA metabolism genes in both the wild type and *spms* at 24 and 48 h of *Pst* DC3000 and mock inoculation (Figure 5). Compared with the wild type, the *spms* mutant showed delayed transcriptional activation, but eventually equal or stronger expression of JA biosynthesis genes *LOX2*, *LOX3*, *AOC1*, *OPR3*, *OPC-8:0 COA LIGASE1* (*OPLC1*) and jasmonoyl-isoleucine-12-hydroxylase *CYTOCHROME P450 FAMILY 94 SUB-FAMILY B POLYPEPTIDE 3* (*CYP94B3*) in response to *Pst* DC3000. A similar response was observed for JA signalling genes *MYC2*, *JAZ1*, *JAZ9* and *JAZ10* (Figure 6). At 48 h after *Pst* DC3000 inoculation, *spms* also exhibited significantly higher expression of JA-marker genes *VEGETATIVE STORAGE PROTEIN 1* and *2* (*VSP1* and *VSP2*), which are related to the MYC2-branch of JA signalling (Lorenzo et al., 2004) (Figure 6). The data suggested the occurrence of a delayed but stronger transcriptional activation of the JA-MYC2 pathway in *spms*. To further study the effect of Spm deficiency on JA biosynthesis, we determined the concentrations of JA, JA-Ile and OPDA in *spms* and wild-type plants at 0, 24, and 48 h of *Pst* DC3000 and mock inoculation. As shown in Figure 7, JA and JA-Ile levels were higher in *spms* than in the wild type already under basal conditions (0 h) and in response to the different treatments. The levels of the JA precursor, OPDA, were also higher in *spms* than in the wild type upon *Pst* DC3000 inoculation. The data indicated that JA biosynthesis was stimulated in *spms*. In agreement with this, the *spms* mutant exhibited higher sensitivity to MeJA and COR treatments in root growth inhibition assays (Supporting Information: Figure S6).

3.5 | Analysis of the *spms* proteome

Owing to the elevated levels of JA in *spms* under basal conditions, we conducted a proteomics analysis to identify proteins that accumulated differentially between *spms* and wild type plants in the absence of pathogen infection. Of the 1612 proteins quantified in both genotypes, 59 showed 1.3-fold or higher differences in abundance between *spms* and the wild type (Supporting Information: Figure S7A and Table S4.1). Among proteins significantly more abundant in *spms* than in the wild type, we found an enrichment in biological processes

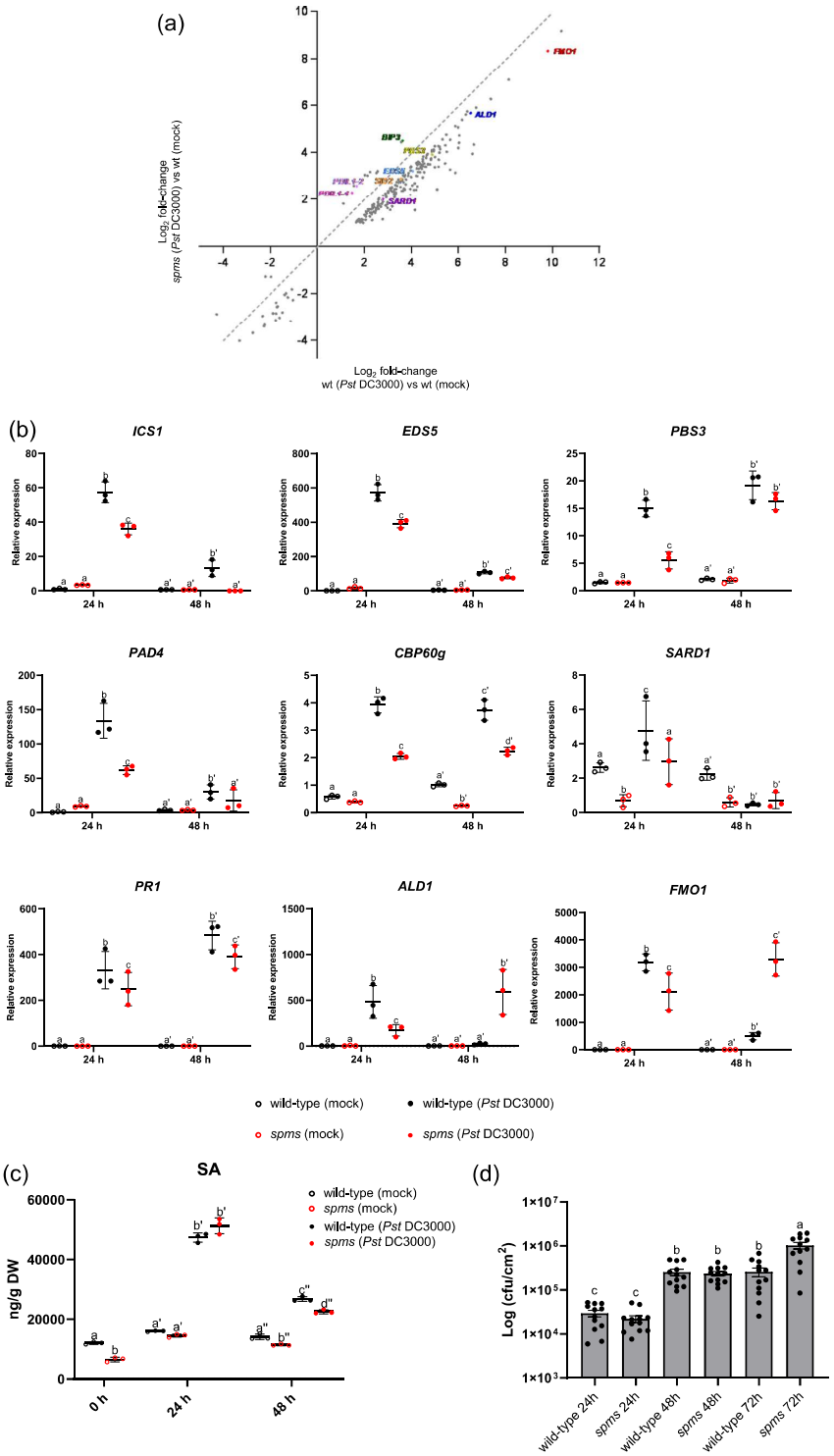

FIGURE 4 (See caption on next page).

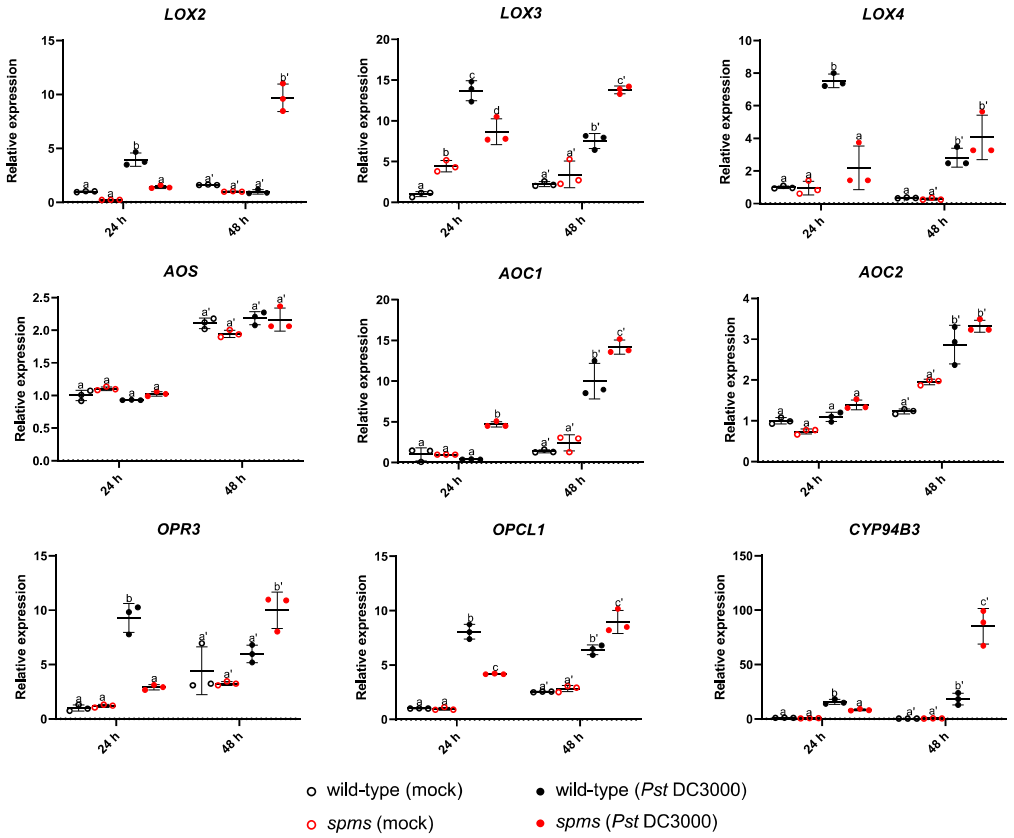

FIGURE 5 Expression analyses of jasmonic acid biosynthesis genes in wild type and *spermine synthase* (*spms*) plants at 24 and 48 h of *Pst* DC3000 (OD_{600} = 0.001) and mock (10 mM $MgCl_2$) infiltration. Values represent the mean ± SD from three biological replicates per point of analysis. Different letters indicate significant differences ($p < 0.05$) according to two-way analysis of variance followed by Tukey's posthoc test. AOC, allene oxide cyclase; AOS, allene oxide synthase; CYP94B3, jasmonoyl-isoleucine-12-hydroxylase; LOX, Lipoxygenase; OPCL1, OPC-8:CoA ligase 1; OPR3, OPDA reductase 3. [Color figure can be viewed at wileyonlinelibrary.com]

related to serine and oxoacid metabolism (Supporting Information: Table S4.2). Spm deficiency also led to increased abundance of JA-inducible KAT5 (3-KETO-ACYL-COENZYME A THIOLASE 5) (fold-change *spms*/wt = 1.39; $p = 0.010$) that encodes one of the three KAT enzymes catalysing the last step of β-oxidation (Castillo et al., 2004; Goepfert & Poirier, 2007; Wasternack & Feussner, 2018) and of the ER stress sensor protein FK506- AND RAPAMYCIN-BINDING PROTEIN 15 KD-2 (FKBP15-2) (Fan et al., 2018) (fold-change *spms*/wt = 5.13; $p = 0.03$). Lesser but still statistically significant differences in protein abundance were detected in AOC2 (fold-change *spms*/wt = 1.2; $p = 0.0016$) and the ER stress marker PDIL1-1 (fold-change *spms*/wt = 1.2; $p = 0.006$) (Supporting Information: Table S4.1). In contrast, *spms* accumulated lower levels of proteins associated with photosynthesis and water transport relative to the wild type (Supporting Information: Table S4.2). No correlation was detected between protein abundance and gene expression under

FIGURE 4 Effect of spermine (Spm) deficiency on salicylic acid (SA) metabolism. (a) Expression correlation of commonly deregulated genes in wild-type and *spermine synthase* (*spms*) mutant in response to *Pst* DC3000. Genes related to SA-mediated defences and endoplasmic reticulum (ER) stress are indicated. (b) Quantitative reverse-transcription polymerase chain reaction (qRT-PCR) gene expression analyses of SA metabolism and signalling, and systemic acquired resistance (SAR) establishment in wild-type and *spms* in response to *Pst* DC3000 (OD_{600} = 0.001) and mock (10 mM $MgCl_2$) infiltration, at 24 and 48 h of treatment. Expression values are relative to wild-type (mock) treatment and represent the mean ± SD from three biological replicates per point of analysis. (c) Quantification of SA levels in wild-type and *spms* in response to *Pst* DC3000 (OD_{600} = 0.001) and mock (10 mM $MgCl_2$) infiltration at 0, 24 and 48 h of treatment. (d) Disease resistance phenotypes to *Pst* DC3000 in wild-type and *spms* mutant at 24, 48 and 72 h of spray inoculation (OD_{600} = 0.1). Different letters indicate significant differences ($p < 0.05$) according to two-way analysis of variance followed by Tukey's posthoc test. [Color figure can be viewed at wileyonlinelibrary.com]

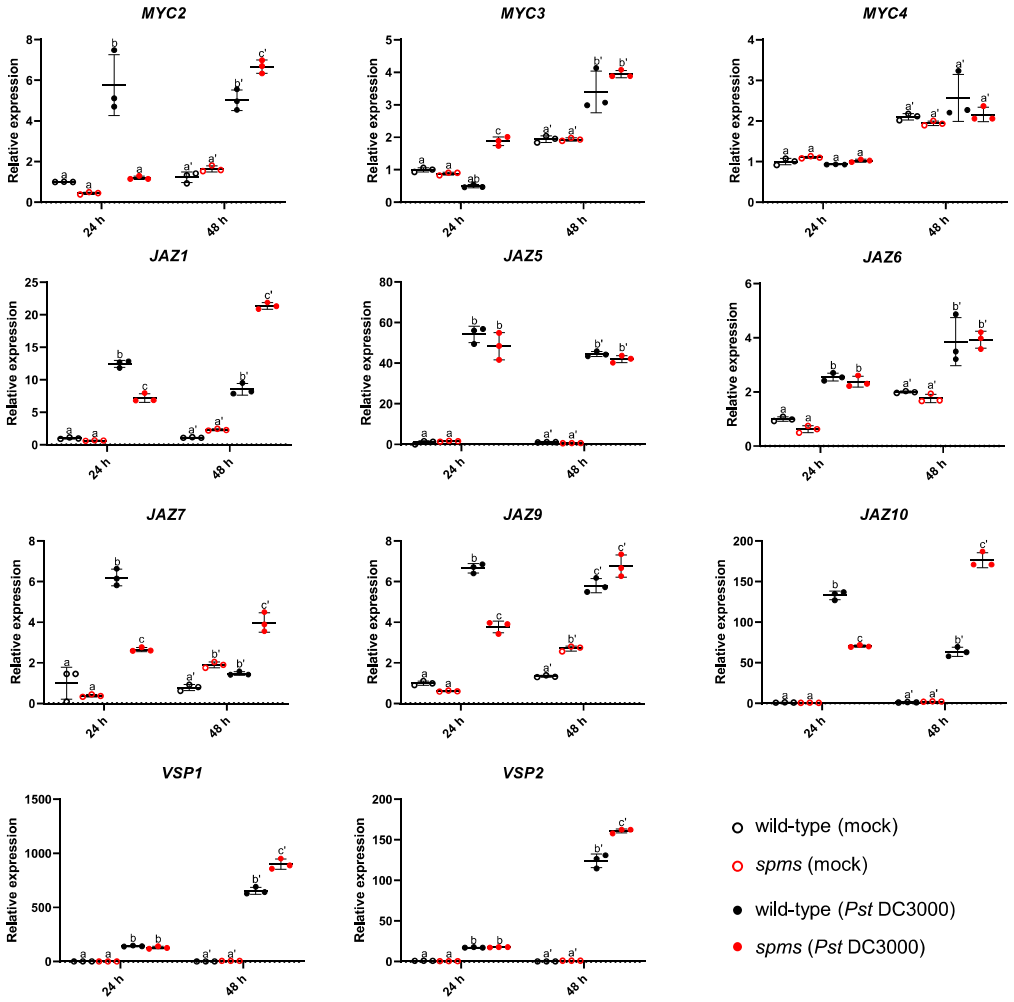

FIGURE 6 Expression analyses of jasmonic acid signalling genes in wild type and *spermine synthase* (*spms*) plants at 24 and 48 h of *Pst* DC3000 (OD_{600} = 0.001) and mock (10 mM $MgCl_2$) infiltration. Values represent the mean ± SD from three biological replicates per point of analysis. Different letters indicate significant differences ($p < 0.05$) according to two-way analysis of variance followed by Tukey's posthoc test. [Color figure can be viewed at wileyonlinelibrary.com]

basal conditions, which suggested a potential effect of polyamines on posttranscriptional regulation, translational control and/or protein degradation (Supporting Information: Figure S7B). Overall, the proteomics data pointed to the implication of Spm in the regulation of JA biosynthesis, ER stress signalling, amino acid and oxoacid metabolism, photosynthesis and water transport.

3.6 | JA-SA crosstalk in *spms*

We hypothesized that the constitutively high levels of JA in *spms* could reduce SA responses through crosstalk modulation. The bacterial phytotoxin COR mimics JA-Ile and activates the JA signalling pathway to boost bacterial virulence by suppressing SA-defences mediated by *ANAC019*, *ANAC055*, and *ANAC072*, thus providing a mechanism by which JA counteracts SA responses (Zheng et al., 2012). The expression of *ANAC019*, *ANAC055* and *ANAC072* is upregulated in response to COR, abscisic acid (ABA) and *P. syringae* treatments (Zheng et al., 2012). We then analysed *ANAC019*, *ANAC055* and *ANAC072* responsiveness in *spms* and wild-type plants challenged with these elicitors (Figure 8a). The expression of *ANAC019* was significantly higher in *spms* than in the wild-type under basal conditions and in response to COR, but not ABA. Conversely, no differences in *ANAC055* or *ANAC072* expression were detected in response to COR or ABA. In agreement with *ANAC019* expression, transcripts of the target genes *ICS1* and *BSMT1* exhibited significant differences between the genotypes in response to COR, but not in response to ABA (Figure 8a). *ICS1* expression in *spms* was lower than in the wild type under basal conditions and after COR treatment.

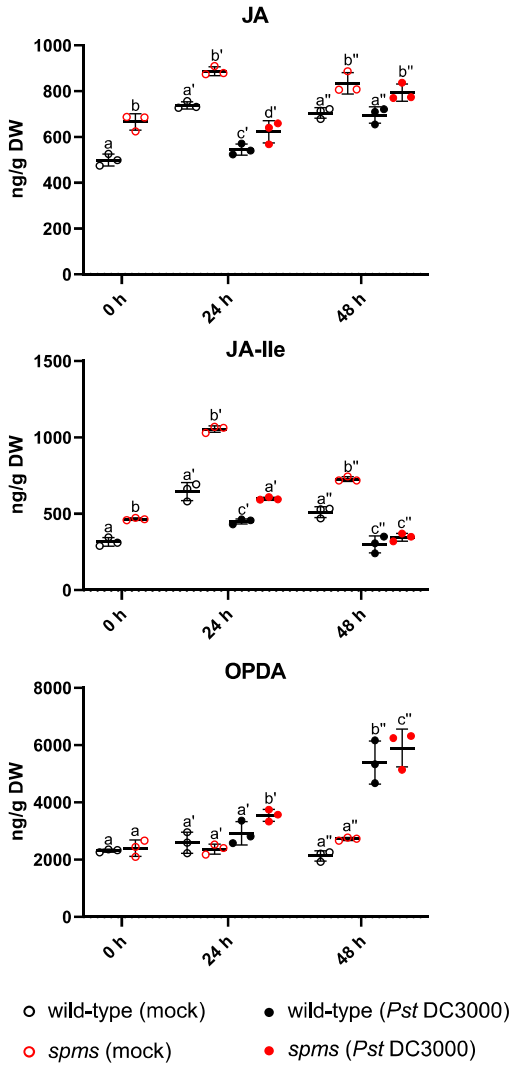

FIGURE 7 Quantification of jasmonic acid (JA), JA-isoleucine (JA-Ile) and 12-oxophytodienoic acid (OPDA) in wild-type and *spermine synthase* (*spms*) plants under basal conditions (0 h) and at 24 and 48 h of *Pst* DC3000 (OD_{600} = 0.001) and mock (10 mM $MgCl_2$) infiltration. Values represent the mean ± SD from three biological replicates per point of analysis. Different letters indicate significant differences ($p < 0.05$) according to two-way analysis of variance followed by Tukey's posthoc test.

In contrast, the expression of *BSMT1* resulted significantly higher in *spms* than in wild type plants after COR treatment. The increased expression of *VSP2* in *spms*, following COR treatment, provided further evidence for the stimulation of the JA pathway in the *spms* mutant. No significant differences in *SAGT1* expression were detected between the genotypes in response to COR or ABA (Figure 8a).

We further analysed the expression of *BSMT1*, *SAGT1* and *ANAC019* in response to *Pst* DC3000 and mock in both wild type and *spms* mutant plants, at 24 and 48 h of treatment (Figure 8b). These expression analyses revealed a substantial elevation of *ANAC019* and *BSMT1* transcripts in *spms*, as compared with wild type plants, upon exposure to *Pst* DC3000. Our findings indicated that lack of Spm causes a more pronounced deregulation of *ICS1* and *BSMT1* in correlation with *ANAC019* expression, in response to COR and *Pst* DC3000, resulting in decreased SA accumulation (Figures 4 and 8a,b).

3.7 | Stomata responses to *Pst* DC3000 are not affected by Spm deficiency

ANAC019, *ANAC055* and *ANAC072* are required for COR-triggered reopening of closed stomata to facilitate bacterial entry (Melotto et al., 2006). Based on the stronger JA and COR responses, as well as the differential modulation of *ANAC019* expression, we investigated whether Spm deficiency affected stomata responses to *Pst* DC3000 (Figure 8c). Stomata aperture was measured in *spms* and wild type leaf peels following 1 and 4 h incubation with *Pst* DC3000 and mock. The application of *Pst* DC3000 induced stomata closure at 1 h and reopening at 4 h in both *spms* and wild type leaf peels, with no significant variation between the two genotypes (Figure 8c). The results indicated that Spm deficiency does not affect stomata responses to bacteria.

3.8 | Effect of Spm deficiency on Acyl-CoA oxidase activity

In animal cells, Spd has been documented to stimulate mitochondrial β-oxidation of long-chain fatty acids by allosteric binding to hydroxyacyl-CoA dehydrogenase subunits α and β, which constitute the mitochondrial trifunctional protein complex. Interestingly, this Spd-mediated effect was found to be competitively inhibited by Spm (Al-Habsi et al., 2022). In plants, β-oxidation is involved in the latter steps of JA biosynthesis. Owing to the high levels of JA found in the *spms* mutant already under basal conditions, we determined whether Spm deficiency could lead to increased peroxisomal β-oxidation. To this aim, we determined acyl-CoA oxidase enzyme activities using different chain length fatty acyl-CoA substrates in extracts from 3-day-old light-grown *spms* and wild type seedlings. Our findings indicated that the acyl-CoA oxidase activity using *n*-hexanoyl-CoA (C6:0), lauroyl-CoA (C12:0) and stearoyl-CoA (C18:0) as substrates was similar between *spms* and wild type (Figure 9). Consistent with this, we found no differences on root growth phenotypes between *spms* and wild type seedlings grown in the presence of 2,4-DB or 2,4-D, which are used to identify genotypes affected in peroxisomal β-oxidation (Supporting Information: Figure S8) (Hayashi et al., 1998). The data indicated that the stimulation of JA biosynthesis in Spm-deficient plants was not due to increased β-oxidation. Rather, it correlated with higher MGDG levels and increased expression of genes involved in early steps of the JA biosynthesis pathway occurring in the chloroplast (Figure 5).

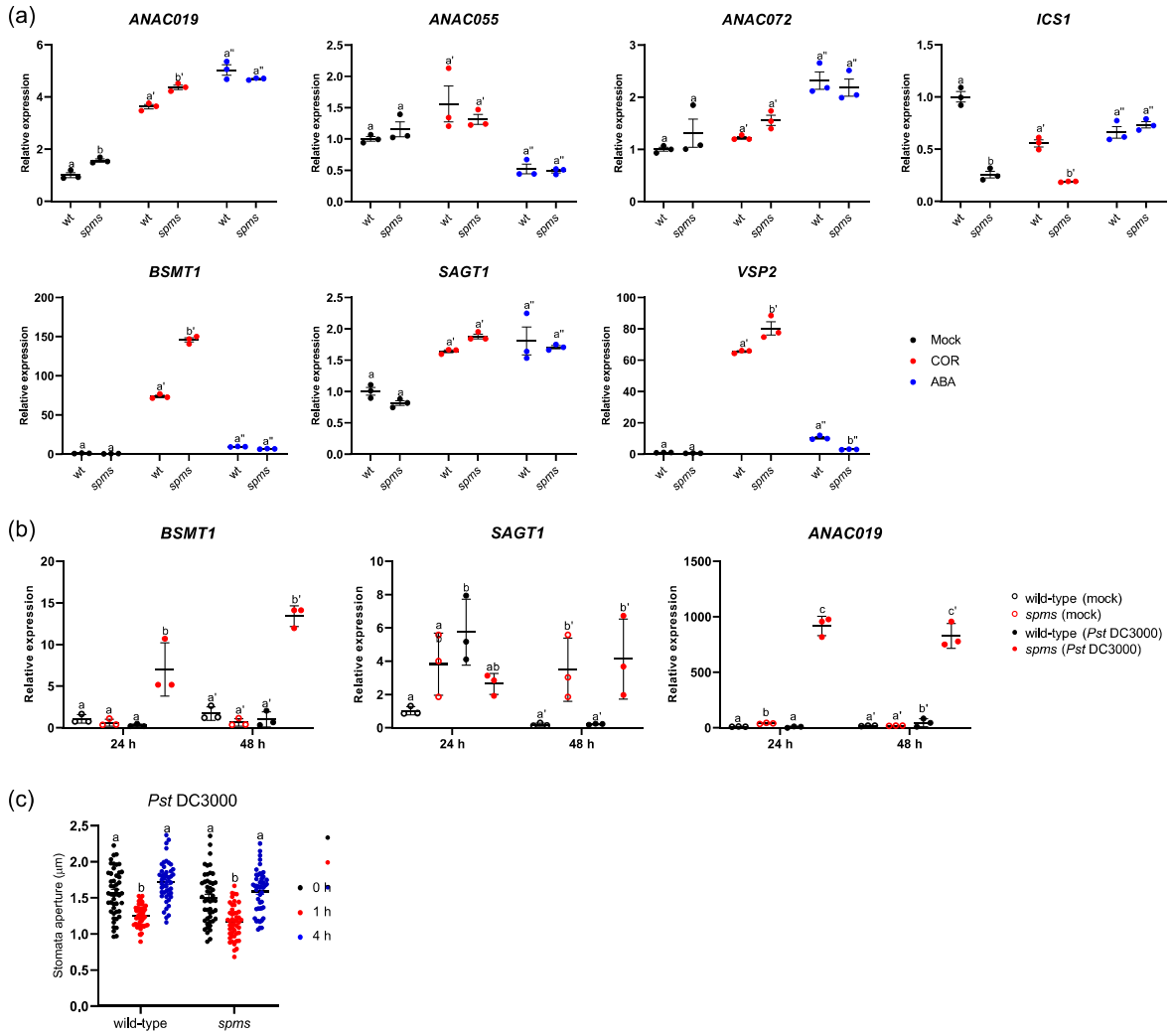

FIGURE 8 (a) Quantitative reverse-transcription polymerase chain reaction (qRT-PCR) expression analyses of *ANAC019*, *ANAC055* and *ANAC072*, SA metabolism genes (*ICS1*, *BSMT1* and *SAGT1*), and JA-responsive *VSP2* in wild type and *spermine synthase* (*spms*) treated with 1 μM coronatine (COR), 5 μM abscisic acid (ABA) or water (mock). Samples were harvested at 24 h of treatment. (b) qRT-PCR expression analyses of *BSMT1*, *SAGT1* and *ANAC019* in wild type and *spms* at 24 and 48 h of *Pst* DC3000 and mock (10 mM $MgCl_2$) inoculation. Expression values are relative to the wild-type (mock) treatment and represent the mean ± SD from three biological replicates per point of analysis. (c) Measurement of stomata aperture in leaf peels of wild-type and *spms* at 0, 1 and 4 h of *Pst* DC3000 treatment. [Color figure can be viewed at wileyonlinelibrary.com]

3.9 | Untargeted lipidomics analysis of *spms*

To further investigate the relationship between Spm deficiency and lipid metabolism, an untargeted lipidomics analysis was performed to identify differentially accumulating lipids between the *spms* mutant and wild-type plants under basal conditions. A total of 193 lipids could be identified (Supporting Information: Table S5), which were assigned to various lipid classes, including glycerophospholipids (representing 69% in the wild-type), sphingolipids (13%), galactolipids (9.5%), sterol lipids (6.7%), prenol lipids (1.4%) and glycerolipids (0.21%) (Figure 10a). Most lipid classes showed similar levels between the *spms* mutant and wild-type, except for galactolipids, most predominant lipids in thylakoid membranes of chloroplasts, which exhibited significant accumulation in *spms* (12.9%) (Figure 10a). Detailed examination of galactolipid subclasses revealed a significant increase in the levels of MGDG (18:3, 16:3), MGDG (18:3, 16:2), and monogalactosylmonoacylglycerol (MGMG) (16:3) in the *spms* mutant compared with the wild type (Figure 10b).

α-LeA (C18:3) derived from MGDG serves as the principal substrate for JA biosynthesis (Li & Yu, 2018; Lin et al., 2016). In the

digalactosyldiacylglycerol synthase 1 (*dgd1*) mutant, characterized by increased MGDG to digalactosyldiacylglycerol (DGDG) ratio due to impaired MGDG to DGDG conversion, there is a notable elevation in JA production even under basal conditions (Lin et al., 2016). This observation suggests that the augmented availability of MGDG in *spms*, as compared with wild-type plants, may contribute to the enhanced biosynthesis of JA. Collectively, these findings substantiate the specific impact of Spm deficiency on galactolipid metabolism, leading to the accumulation of MGDG and MGMG containing unsaturated C16 fatty acids and a greater pool of α-LeA (C18:3) that can be used as precursor for JA biosynthesis.

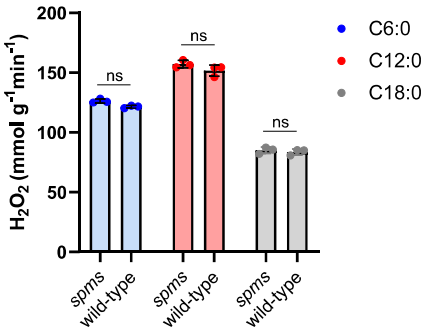

FIGURE 9 Measurement of Acyl-CoA oxidase activity. Acyl-CoA oxidase activity assays in 3-day-old wild-type and *spermine synthase* (*spms*) seedlings using *n*-hexanoyl-CoA (C6:0), lauroyl-CoA (C12:0) and stearoyl-CoA (C18:0) as substrates. Values represent the mean ± SD from three biological replicates. Ns, not significant according to Student's *t* test. [Color figure can be viewed at wileyonlinelibrary.com]

3.10 | Spm deficiency enhances disease resistance to *B. cinerea*

As the *spms* mutant already displayed higher JA levels than the wild type under basal conditions, we aimed to investigate the disease resistance phenotypes to the necrotrophic fungal pathogen *B. cinerea*. To accomplish this, we measured the lesion size induced by droplet inoculation of *B. cinerea* on leaves of both *spms* and wild-type plants (Ferrari et al., 2003), and determined fungal growth by real-time quantification at 24 and 48 h of spray inoculation (Gachon & Saindrenan, 2004). Compared with *spms*, the wild type exhibited larger lesion formation (Figure 11a) and higher fungal growth determined by qPCR quantification of *B. cinerea* and Arabidopsis DNA using specific primers for *β-tubuline* and *Actin2*, respectively (Figure 11b). The data indicated that Spm deficiency triggers greater resistance to *B. cinerea* infection compared with wild-type plants. Quantification of polyamine levels in wild-type plants inoculated with *B. cinerea* revealed a significant raise in Put and decline in Spm levels after 48 h of treatment (Figure 11c). Overall, the data indicated that *B. cinerea* infection leads to a decrease in Spm levels, and the absence of Spm results in increased resistance to the pathogen.

3.11 | Spm alleviates ER stress during *Pst* DC3000 infection

In addition to the effect of Spm deficiency on JA and SA-mediated defence responses to *Pst* DC3000, RNA-seq data also pointed to a potential contribution of Spm in mitigating ER stress (Figure 3). The ER is an important organelle that performs various functions, including the proper folding and processing of proteins. Accumulation of unfolded or misfolded proteins triggers a stress response within

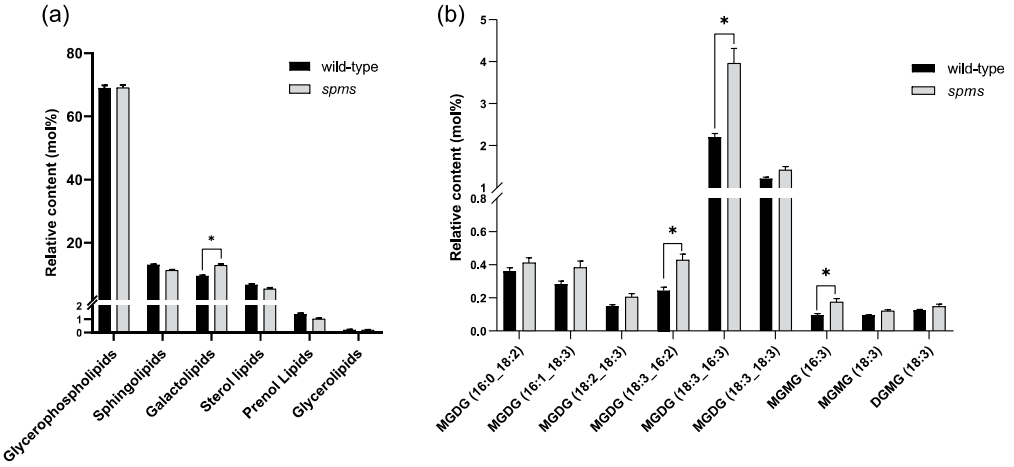

FIGURE 10 (a) Relative content of main lipid classes and (b) major galactolipids subclasses identified by ultra-performance-mass spectrometry untargeted lipidomics analysis in 5-week-old *spermine synthase* (*spms*) and wild-type plants under basal conditions. Asterisks indicate significant differences according to Student's *t* test (*$p < 0.05$, **$p < 0.01$).

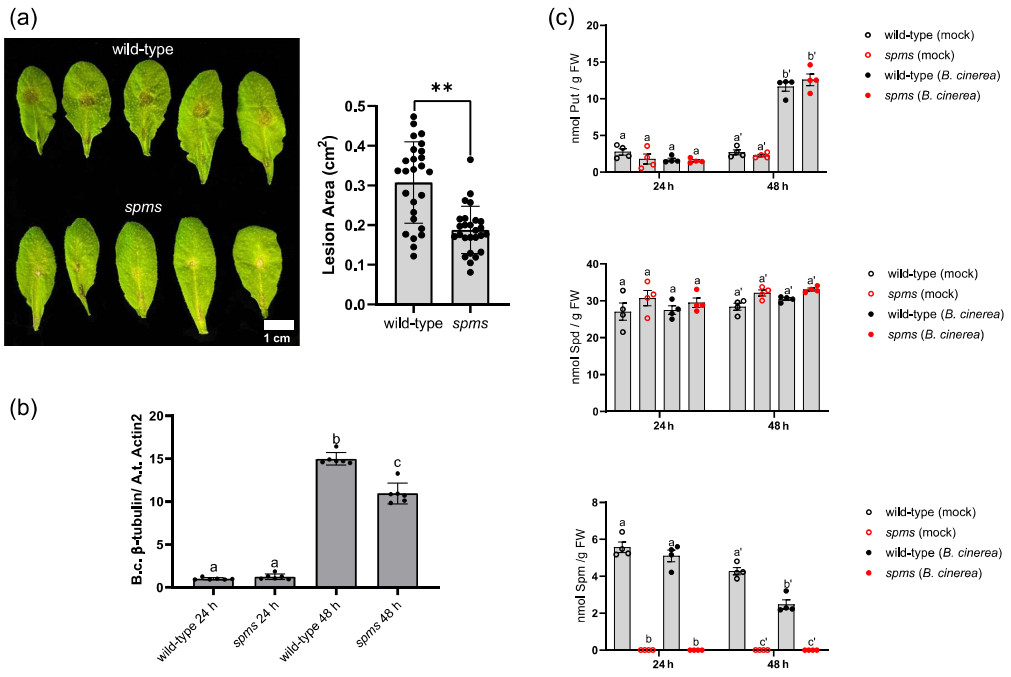

FIGURE 11 (a) Disease resistance phenotypes to *B. cinerea* infection in 5-week-old *spermine synthase* (*spms*) and wild-type plants determined by measurement of lesion size induced by droplet inoculation (4×10^6 spores mL^{-1}) at 72 h of treatment. (b) Real-time quantification of the relative abundance of *B. cinerea* (*B.c.*) and *A. thaliana* (*A.t.*) DNA at 24 h and 48 h of spray inoculation (5×10^5 spores mL^{-1}), using specific primers for *β-tubuline* (*B.c.*) and *Actin2* (*A.t.*). (c) Concentrations of free putrescine (Put), spermidine (Spd) and spermine (Spm) at 24 and 48 h of *B. cinerea* (5×10^5 spores mL^{-1}) and mock (Gamborg's B5 medium with 2% sucrose) spray inoculation in the wild type. Different letters indicate significant differences ($p < 0.05$) according to two-way analysis of variance followed by Tukey's posthoc test. [Color figure can be viewed at wileyonlinelibrary.com]

the ER, which is known as the unfolded protein response (UPR) (Pastor-Cantizano et al., 2020; Yu et al., 2022). To further investigate the potential contribution of Spm to ER stress avoidance, we determined the expression of known ER stress responsive genes in *spms* and wild-type plants at 24 and 48 h of bacteria and mock inoculation (Figure 12a). In response to *Pst* DC3000, the biomarkers for UPR activation *BIP3*, *PDIL1-1* and spliced-*bZIP60* (*sbZIP60*) were more strongly induced in *spms* than in the wild-type. Furthermore, treatment with the ER stress-trigger TM that inhibits N-linked glycosylation of proteins also led to stronger upregulation of these genes in *spms* compared with the wild-type (Figure 12b). However, treatment of wild-type seedlings with TM did not elicit significant changes in polyamine levels compared with the mock treatment (Figure 12c). Root growth inhibition assays were consistent with the gene expression data and indicated that the *spms* mutant was more sensitive to TM than the wild type (Figure 12d). The data indicated that Spm is required to alleviate ER stress during *Pst* DC3000 infection. When treated with various compounds that induce ER stress, such as BFA, which disrupts the structure and function of the Golgi apparatus, or DTT, which interferes with disulfide bonds and proper protein folding, the biosynthesis of Put was stimulated (Supporting Information: Figure S9). These findings suggest that polyamine metabolism responds to specific ER-stress-inducing agents, potentially due to variations in their underlying mechanisms.

4 | DISCUSSION

In this work, we report that Spm deficiency shifts the balance between JA and SA responses, by stimulating JA biosynthesis and dampening SA responses. This leads to enhanced disease resistance to the necrotrophic fungal pathogen *B. cinerea* and susceptibility to spray inoculated *Pst* DC3000. SARD1 and CBP60g are members of the CBP60 family of plant-specific transcription factors that play a direct role in regulating SA metabolism during defence. Transcription of key genes involved in SA biosynthesis *ICS1*, *EDS5* and *PBS3* is coordinately regulated by SARD1 and CBP60g (Sun et al., 2015; Wang et al., 2009, 2011; Zhang et al., 2010). Through RNA-seq and further qRT-PCR expression analyses, we found that transcripts of *SARD1* and *CBP60g*, as well as *ICS1*, *EDS5*, *PBS3* and other SA and SAR-related genes were more strongly upregulated in wild type than Spm-deficient (*spms*) plants in response to *Pst* DC3000 (Figure 4a,b). Consistent with this, SA accumulated significantly less in *spms* than in wild-type plants at 48 h of *Pst* DC3000 treatment (Figure 4c). The

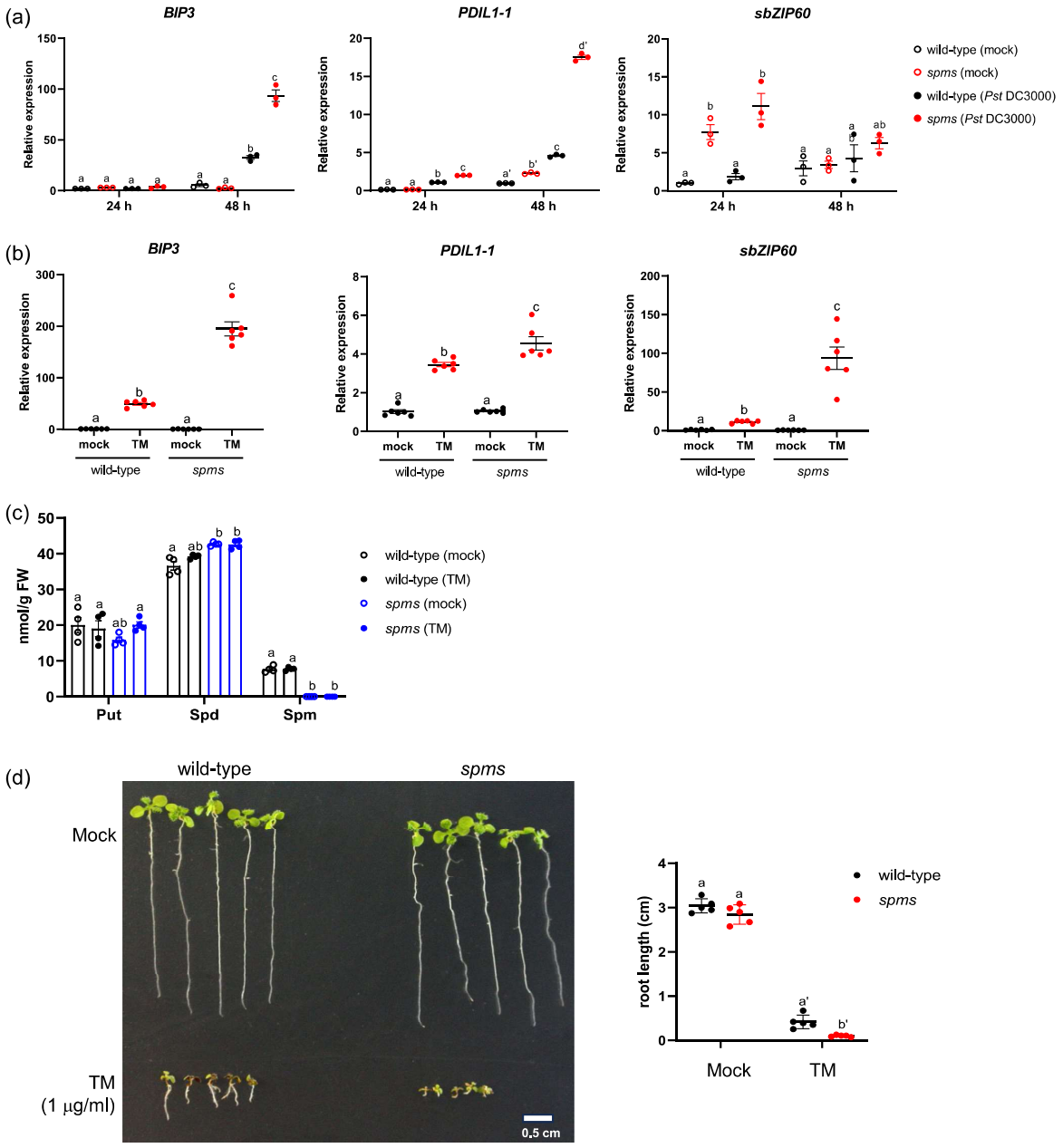

FIGURE 12 Effect of Spm deficiency on ER stress. Quantitative reverse-transcription polymerase chain reaction (qRT-PCR) expression analyses of *BIP3*, *PDIL1-1* and spliced-*bZIP60* (*sbZIP60*) in *spms* and wild-type plants at (a) 24 and 48 h of *Pst* DC3000 (OD_{600} = 0.001) and mock (10 mM $MgCl_2$) infiltration and (b) at 6 h of tunicamycin (1 µg mL^{-1}, TM) and mock treatment. Expression values are relative to the wild-type (mock) treatment and represent the mean ± SD from three to six biological replicates per point of analysis. (c) Polyamine levels in *spms* and wild-type seedlings at 24 h of 1 µg mL^{-1} TM treatment. (d) Root growth phenotypes of *spms* and wild-type seedlings grown in the presence of TM or mock. Values represent the mean ± SD from the indicated biological replicates per point of analysis. Different letters indicate significant differences ($p < 0.05$) according to two-way analysis of variance followed by Tukey's posthoc test. [Color figure can be viewed at wileyonlinelibrary.com]

data indicated that Spm deficiency compromises SA biosynthesis and the defence response to *Pst* DC3000.

Interestingly, when *Pst* DC3000 was directly infiltrated into the intercellular leaf space, there were no significant differences in the growth rate of *Pst* DC3000 between the *spms* mutant and the wild type (Zhang et al., 2023). The distinct disease resistance in response to spray or leaf infiltration has also been documented in the *fls2* mutant (Zipfel et al., 2004) and likely reflects differences in the capacity of the bacteria to reach the intercellular leaf space of the host tissue and propagate under more natural conditions (Melotto et al., 2006).

Spm-deficient plants contained higher levels of JA, JA-Ile and OPDA under basal conditions and during the defence response to *Pst* DC3000 (Figure 7). They also showed enhanced JA/COR responses (Supporting Information: Figure S6) in correlation with increased *LOX2*, *LOX3*, *AOC1*, *OPR3*, *OPCL1*, *MYC2*, *JAZ1*, *JAZ10*, *VSP1* and *VSP2* expression at 48 h of *Pst* DC3000 inoculation, and AOC2 protein abundance already under basal conditions (Figures 5 and 6, and Supporting Information: Table S4.1). It has been reported that the coordinated action of *ANAC019*, *ANAC055* and *ANAC072* mediates JA responses and COR-induced suppression of SA accumulation. The latter is achieved by repressing *ICS1* and activating *BSMT1* expression, leading to a shift in SA metabolism dynamics that contributes to JA-SA antagonism and bacterial virulence (Bu et al., 2008; Zheng et al., 2012). The stimulation of JA biosynthesis and signalling in *spms* might contribute to the dampening of SA responses through JA-SA antagonism (Hou & Tsuda, 2022). In agreement with this, the expression of *ANAC019* and its target genes *ICS1* and *BSMT1* were more strongly deregulated in *spms* than in the wild-type in response to *Pst* DC3000 and COR (Figure 8a,b).

By employing shotgun lipidomics, we observed a significant increase in the levels of MGDG (18:3, 16:3), MGDG (18:3, 16:2) and MGMG (16:3) in Spm-deficient compared with wild-type plants (Figure 10b). As MGDG serves as a primary precursor for JA biosynthesis (Li & Yu, 2018; Lin et al., 2016), the elevated levels of MGDG levels could enhance the availability of α-LeA (C18:3), used as substrate of plastidial 13-LOX. The *spms* mutant also showed enhanced disease resistance to *B. cinerea* compared with wild-type plants. Our results are consistent with previous reports that suggest polyamines may facilitate the growth of certain necrotrophic pathogens through additional potential interactions with the ethylene pathway and ROS production (Marina et al., 2008; Nambeesan et al., 2012; Rea et al., 2002).

Chromatin immunoprecipitation sequencing identified the promoters of *ADC1*, *ADC2* and *SAMDC1* as potential targets of SARD1, suggesting a coordination of polyamine and SA pathways (Sun et al., 2015). However, we found that Put accumulation triggered by *Pst* DC3000 was not compromised but stimulated in *eds1*, *sid2-1* and *npr1-1* mutants, thus being an SA-independent response (Figure S2). In contrast, Put increases triggered by *Pst* DC3000 were significantly reduced in *coi1-1* and *myc2* mutants (Supporting Information: Figure S2), indicating an important contribution of JA signalling in modulating Put metabolism in *Arabidopsis*. The modulation of polyamine metabolism by JA has been observed in various species. In *Hyosciamus muticus*, MeJA treatment triggers an increase in the levels of Put, as well as Spd and Spm to a lesser extent (Biondi et al., 2000). In *Zea mays*, the expression and activity of the PAO enzyme, ZmPAO, are induced by wounding and MeJA treatment, resulting in higher levels of ROS, lignin, and suberin deposition that are required for wound healing (Angelini et al., 2008). In *Nicotiana attenuata*, the biosynthesis of polyamines conjugated to phenolic compounds (phenolamides) is triggered by herbivore attack and is associated with increased JA and LOX3 activity (Onkokesung et al., 2012). Similarly, in tomato, MYC1 and MYC2 play a role in the JA-mediated activation of phenolamide biosynthesis (Swinnen et al., 2022). In *Arabidopsis*, *N-acetyltransferase 1* (*NATA1*), which acetylates Put, is upregulated in response to COR, leading to a reduction in free Put levels and enhanced disease susceptibility to *Pst* DC3000 (Lou et al., 2016). Taken together, these findings indicate that JA and the bacterial phytotoxin COR can reshape polyamine metabolism in different plant species.

In addition to an impact on JA-SA balance, we found that Spm deficiency enhanced ER stress in response to *Pst* DC3000. The ER is an essential organelle for phospholipid synthesis, Ca^{2+} storage and the synthesis and folding of proteins. During cellular stress, the protein folding capacity of the ER can be compromised, leading to the accumulation of misfolded or unfolded proteins in the ER lumen. This triggers a cellular response, known as the UPR, to restore net protein folding capacity by increased ER chaperone production, upregulation of lipid synthesis and repression of translation (Pastor-Cantizano et al., 2020; Yu et al., 2022). We found increased expression of UPR biomarkers *BIP3*, *sbZIP60* and *PDIL1-1* in *spms* mutant relative to the wild type during *Pst* DC3000 infection, and in response to TM treatment (Figure 12a,b). In agreement with a potential effect of Spm buffering ER stress, *spms* was more sensitive to TM than the wild type (Figure 12d). Even though the treatment with TM did not result in any significant changes in polyamine contents relative to the mock treatment (Figure 12c), other ER-stress-inducing compounds such as BFA and DTT triggered changes in polyamine homoeostasis. This is likely attributed to their different underlying mechanisms in triggering ER stress (Supporting Information: Figure S9). Deregulation of Spm homoeostasis by *SPMS* overexpression also triggers transcriptional responses compatible with ER stress in *Arabidopsis*, such as upregulation of UPR biomarker genes *bZIP17*, *bZIP28* and *BIP3*. This response, which was dependent on Ca^{2+} signalling, suggested an effect of Spm on Ca^{2+} homoeostasis in the ER (Sagor et al., 2015; Zhang et al., 2023). The involvement of Spm in buffering ER stress responses has also been reported in *Magnaporthe oryzae*, the blast fungus responsible for rice blast disease. In this case, Spm plays a crucial role in pathogenicity by ensuring a secure seal of the appressorium on the host leaf surface by facilitating the production of mucilage, which is rich in glycoproteins. In this context, Spm acts as ROS scavenger, buffering NADPH oxidase-1-generated oxidative stress in the ER lumen and preventing ER stress and mucilage production (Rocha et al., 2020). Collectively, an imbalance in Spm levels during stress conditions could disrupt Ca^{2+} and ROS homoeostasis in the ER, potentially leading to ER stress and UPR activation.

In summary, our study provides evidence that Spm deficiency potentiates JA biosynthesis influencing SA dynamics, *Pst* DC3000

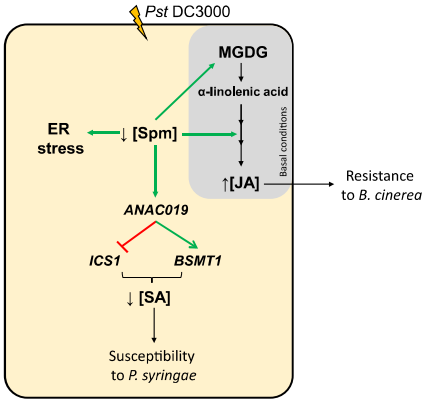

FIGURE 13 Mechanistic model for the influence of spermine (Spm) on the modulation of salicylic acid (SA) and jasmonic acid (JA) defence responses. Spm deficiency results in increased levels of monogalactosyldiacylglycerol (MGDG) and increased expression of JA biosynthesis genes that correlate with elevated levels of JA under basal conditions and in response to *Pst* DC3000. Spm deficiency enhances *ANAC019* expression in response to *Pst* DC3000, leading to a more robust deregulation of SA-metabolism genes *ICS1* and *BSMT1*, and reduced SA content. This way, Spm deficiency shifts the balance between JA and SA, which associates with enhanced susceptibility to *Pst* DC3000 and disease resistance to *B. cinerea*. Spm deficiency also triggers endoplasmic reticulum (ER) stress signalling in response to *Pst* DC3000, which indicates the importance of this polyamine in alleviating ER stress during defence. [Color figure can be viewed at wileyonlinelibrary.com]

and *B. cinerea* disease resistance, and exacerbating ER stress in response to the bacteria (Figure 13).

ACKNOWLEDGEMENTS

This work was financially supported by the grants: PID2021-126896OB-I00 funded by Ministerio de Ciencia e Innovación MCIN/Agencia Estatal de Investigación AEI/10.13039/501100011033 (Spain) and by the "European Regional Development Fund (ERDF) a way of making Europe"; PDC2021-121267-I00 funded by Ministerio de Ciencia e Innovación MCIN/Agencia Estatal de Investigación AEI/10.13039/501100011033 (Spain) and European Union Next GenerationEU/PRTR. A.G-C. acknowledges support from Generalitat Valenciana (CIAICO/2021/063). C.Z., J.Z. and C.D. acknowledge support from the CSC (China Scholarship Council) for funding their doctoral fellowship. E.M. is holder of the grant PRE2018-083289 funded by MCIN/AEI/10.13039/501100011033 and by "European Social Fund Investing in your future".

CONFLICT OF INTEREST STATEMENT

The authors declare no conflict of interest.

DATA AVAILABILITY STATEMENT

All data supporting the findings of this study are available within the paper and within its Supporting Information published online. The RNA-seq data have been deposited to ArrayExpress (https://www.ebi.ac.uk/arrayexpress/) under the accession identifier E-MTAB-13086. The mass spectrometry proteomics data have been deposited to the ProteomeXchange Consortium via the PRIDE (https://www.ebi.ac.uk/pride/) partner repository with the data set identifier PXD041901.

ORCID

Aurelio Gómez-Cadenas http://orcid.org/0000-0002-4598-2664
Rubén Alcázar http://orcid.org/0000-0002-3567-7586

REFERENCES

Adham, A.R., Zolman, B.K., Millius, A. & Bartel, B. (2005) Mutations in *Arabidopsis* acyl-CoA oxidase genes reveal distinct and overlapping roles in β-oxidation. *The Plant Journal*, 41, 859–874.

Al-Habsi, M., Chamoto, K., Matsumoto, K., Nomura, N., Zhang, B., Sugiura, Y. et al. (2022) Spermidine activates mitochondrial trifunctional protein and improves antitumor immunity in mice. *Science*, 378, eabj3510.

Andreou, A. & Feussner, I. (2009) Lipoxygenases–structure and reaction mechanism. *Phytochemistry*, 70, 1504–1510.

Angelini, R., Tisi, A., Rea, G., Chen, M.M., Botta, M., Federico, R. et al. (2008) Involvement of polyamine oxidase in wound healing. *Plant Physiology*, 146, 162–177.

Attaran, E., Zeier, T.E., Griebel, T. & Zeier, J. (2009) Methyl salicylate production and jasmonate signaling are not essential for systemic acquired resistance in *Arabidopsis*. *The Plant Cell*, 21, 954–971.

Biondi, S., Fornalé, S., Oksman-Caldentey, K.M., Eeva, M., Agostani, S. & Bagni, N. (2000) Jasmonates induce over-accumulation of methylputrescine and conjugated polyamines in *Hyoscyamus muticus* L. root cultures. *Plant Cell Reports*, 19, 691–697.

Brooks, D.M., Bender, C.L. & Kunkel, B.N. (2005) The *Pseudomonas syringae* phytotoxin coronatine promotes virulence by overcoming salicylic acid-dependent defences in *Arabidopsis thaliana*. *Molecular Plant Pathology*, 6, 629–639.

Bu, Q., Jiang, H., Li, C.-B., Zhai, Q., Zhang, J., Wu, X. et al. (2008) Role of the *Arabidopsis thaliana* NAC transcription factors ANAC019 and ANAC055 in regulating jasmonic acid-signaled defense responses. *Cell Research*, 18, 756–767.

Cao, H., Glazebrook, J., Clarke, J.D., Volko, S. & Dong, X. (1997) The *Arabidopsis NPR1* gene that controls systemic acquired resistance encodes a novel protein containing ankyrin repeats. *Cell*, 88, 57–63.

Carbon, S., Douglass, E., Dunn, N., Good, B., Harris, N.L., Lewis, S.E. et al. (2019) The Gene Ontology resource: 20 years and still GOing strong. *Nucleic Acids Research*, 47, D330–D338.

Castillo, M.C., Martínez, C., Buchala, A., Métraux, J.-P. & León, J. (2004) Gene-specific involvement of β-oxidation in wound-activated responses in *Arabidopsis*. *Plant Physiology*, 135, 85–94.

Cheng, C.Y., Krishnakumar, V., Chan, A.P., Thibaud-Nissen, F., Schobel, S. & Town, C.D. (2017) Araport11: a complete reannotation of the *Arabidopsis thaliana* reference genome. *The Plant Journal*, 89, 789–804.

Chini, A., Fonseca, S., Fernández, G., Adie, B., Chico, J.M., Lorenzo, O. et al. (2007) The JAZ family of repressors is the missing link in jasmonate signalling. *Nature*, 448, 666–671.

Cuevas, J.C., López-Cobollo, R., Alcázar, R., Zarza, X., Koncz, C., Altabella, T. et al. (2008) Putrescine is involved in *Arabidopsis* freezing tolerance and cold acclimation by regulating abscisic acid levels in response to low temperature. *Plant Physiology*, 148, 1094–1105.

Cui, J., Bahrami, A.K., Pringle, E.G., Hernandez-Guzman, G., Bender, C.L., Pierce, N.E. et al. (2005) *Pseudomonas syringae* manipulates systemic plant defenses against pathogens and herbivores. *Proceedings of the National Academy of Sciences*, 102, 1791–1796.

Dean, J.V. & Delaney, S.P. (2008) Metabolism of salicylic acid in wild-type, *ugt74f1* and *ugt74f2* glucosyltransferase mutants of *Arabidopsis thaliana*. *Physiologia Plantarum*, 132, 417–425.

Dongus, J.A. & Parker, J.E. (2021) EDS1 signalling: at the nexus of intracellular and surface receptor immunity. *Current Opinion in Plant Biology*, 62, 102039.

Dunn, W.B., Broadhurst, D., Begley, P., Zelena, E., Francis-McIntyre, S., Anderson, N. et al. (2011) Human Serum Metabolome (HUSERMET) Consortium. Procedures for large-scale metabolic profiling of serum and plasma using gas chromatography and liquid chromatography coupled to mass spectrometry. *Nature Protocols*, 6, 1060–1083.

Fan, G., Yang, Y., Li, T., Lu, W., Du, Y., Qiang, X. et al. (2018) A *Phytophthora capsici* RXLR effector targets and inhibits a plant PPIase to suppress endoplasmic reticulum-mediated immunity. *Molecular Plant*, 11, 1067–1083.

Ferrari, S., Plotnikova, J.M., De Lorenzo, G. & Ausubel, F.M. (2003) Arabidopsis local resistance to *Botrytis cinerea* involves salicylic acid and camalexin and requires EDS4 and PAD2, but not SID2, EDS5 or PAD4. *The Plant Journal*, 35, 193–205.

Feys, B.J., Moisan, L.J., Newman, M.A. & Parker, J.E. (2001) Direct interaction between the *Arabidopsis* disease resistance signaling proteins, EDS1 and PAD4. *The EMBO Journal*, 20, 5400–5411.

Feys, B.J., Wiermer, M., Bhat, R.A., Moisan, L.J., Medina-Escobar, N., Neu, C. et al. (2005) *Arabidopsis* SENESCENCE-ASSOCIATED GENE101 stabilizes and signals within an ENHANCED DISEASE SUSCEPTIBILITY1 complex in plant innate immunity. *The Plant Cell*, 17, 2601–2613.

Feys, B.J.F., Benedetti, C.E., Penfold, C.N. & Turner, J.G. (1994) Arabidopsis mutants selected for resistance to the phytotoxin coronatine are male sterile, insensitive to methyl jasmonate, and resistant to a bacterial pathogen. *The Plant Cell*, 6, 751–759.

Gachon, C. & Saindrenan, P. (2004) Real-time PCR monitoring of fungal development in *Arabidopsis thaliana* infected by *Alternaria brassicicola* and *Botrytis cinerea*. *Plant Physiology and Biochemistry*, 42, 367–371.

Garcion, C., Lohmann, A., Lamodière, E., Catinot, J., Buchala, A., Doermann, P. et al. (2008) Characterization and biological function of the *ISOCHORISMATE SYNTHASE2* gene of *Arabidopsis*. *Plant Physiology*, 147, 1279–1287.

Gerhardt, B. (1987) Peroxisomes and fatty acid degradation, *Methods in Enzymology. Plant Cell Membranes*. Academic Press, pp. 516–525.

Gerlin, L., Baroukh, C. & Genin, S. (2021) Polyamines: double agents in disease and plant immunity. *Trends in Plant Science*, 26, 1061–1071.

Glazebrook, J. (2005) Contrasting mechanisms of defense against biotrophic and necrotrophic pathogens. *Annual Review of Phytopathology*, 43, 205–227.

Goepfert, S. & Poirier, Y. (2007) β-Oxidation in fatty acid degradation and beyond. *Current Opinion in Plant Biology*, 10, 245–251.

Gonzalez, M.E., Marco, F., Minguet, E.G., Carrasco-Sorli, P., Blázquez, M.A. & Carbonell, J. et al. (2011) Perturbation of spermine synthase gene expression and transcript profiling provide new insights on the role of the tetraamine spermine in *Arabidopsis* defense against *Pseudomonas viridiflava*. *Plant Physiology*, 156, 2266–2277.

Di Guida, R., Engel, J., Allwood, J.W., Weber, R.J.M., Jones, M.R., Sommer, U. et al. (2016) Non-targeted UHPLC-MS metabolomic data processing methods: a comparative investigation of normalisation, missing value imputation, transformation and scaling. *Metabolomics*, 12, 93.

Hayashi, M., Toriyama, K., Kondo, M., Nishimura, M., Hayashi, M., Toriyama, K. et al. (1998) 2,4-Dichlorophenoxybutyric acid-resistant mutants of *Arabidopsis* have defects in glyoxysomal fatty acid b-oxidation. *The Plant Cell*, 10, 183–195.

Hou, S. & Tsuda, K. (2022) Salicylic acid and jasmonic acid crosstalk in plant immunity. *Essays in Biochemistry*, 66, 647–656.

Hryb, D.J. & Hogg, J.F. (1979) Chain length specificities of peroxisomal and mitochondrial β-oxidation in rat liver. *Biochemical and Biophysical Research Communications*, 87, 1200–1206.

Hu, J., Baker, A., Bartel, B., Linka, N., Mullen, R.T., Reumann, S. et al. (2012) Plant peroxisomes: biogenesis and function. *The Plant Cell*, 24, 2279–2303.

Ishiguro, S., Kawai-Oda, A., Ueda, J., Nishida, I. & Okada, K. (2001) The DEFECTIVE IN ANTHER DEHISCENCE1 gene encodes a novel phospholipase A1 catalyzing the initial step of jasmonic acid biosynthesis, which synchronizes pollen maturation, anther dehiscence, and flower opening in *Arabidopsis*. *The Plant Cell*, 13, 2191–2209.

Kloek, A.P., Verbsky, M.L., Sharma, S.B., Schoelz, J.E., Vogel, J., Klessig, D.F. et al. (2001) Resistance to *Pseudomonas syringae* conferred by an *Arabidopsis thaliana* coronatine-insensitive (coi1) mutation occurs through two distinct mechanisms: disease resistance in an *A. thaliana* COI1 mutant. *The Plant Journal*, 26, 509–522.

Li, H. & Yu, C.-W. (2018) Chloroplast galactolipids: the link between photosynthesis, chloroplast shape, jasmonates, phosphate starvation and freezing tolerance. *Plant and Cell Physiology*, 59, 1128–1134.

Li, M., Yu, G., Cao, C. & Liu, P. (2021) Metabolism, signaling, and transport of jasmonates. *Plant Communications*, 2, 100231.

Lin, Y.-T., Chen, L.-J., Herrfurth, C., Feussner, I. & Li, H. (2016) Reduced biosynthesis of digalactosyldiacylglycerol, a major chloroplast membrane lipid, leads to oxylipin overproduction and phloem cap lignification in *Arabidopsis*. *The Plant Cell*, 28, 219–232.

Liu, C., Atanasov, K.E., Arafaty, N., Murillo, E., Tiburcio, A.F., Zeier, J. et al. (2020a) Putrescine elicits ROS-dependent activation of the salicylic acid pathway in *Arabidopsis thaliana*. *Plant, Cell and Environment*, 43, 2755–2768.

Liu, C., Atanasov, K.E., Tiburcio, A.F. & Alcázar, R. (2019) The polyamine putrescine contributes to H2O2 and RbohD/F-dependent positive feedback loop in *Arabidopsis* PAMP-triggered immunity. *Frontiers in Plant Science*, 10, 894.

Liu, Y., Sun, T., Sun, Y., Zhang, Y., Radojičić, A., Ding, Y. et al. (2020b) Diverse roles of the salicylic acid receptors NPR1 and NPR3/NPR4 in plant immunity. *The Plant Cell*, 32, 4002–4016.

Livak, K.J. & Schmittgen, T.D. (2001) Analysis of relative gene expression data using real-time quantitative PCR and the $2^{-\Delta\Delta CT}$ method. *Methods*, 25, 402–408.

Lorenzo, O., Chico, J.M., Saénchez-Serrano, J.J. & Solano, R. (2004) JASMONATE-INSENSITIVE1 encodes a MYC transcription factor essential to discriminate between different jasmonate-regulated defense responses in *Arabidopsis*. *The Plant Cell*, 16, 1938–1950.

Lou, Y.-R., Bor, M., Yan, J., Preuss, A.S. & Jander, G. (2016) Arabidopsis NATA1 acetylates putrescine and decreases defense-related hydrogen peroxide accumulation. *Plant Physiology*, 171, 1443–1455.

Ma, S.-W., Morris, V. L. & Cuppels, D.A. (1991) Characterization of a DNA region required for production of the phytotoxin coronatine by *Pseudomonas syringae* pv. *tomato*. *Molecular Plant-Microbe Interactions*, 4, 69–74.

Marco, F., BusÃ³, E. & Carrasco, P. (2014) Overexpression of *SAMDC1* gene in *Arabidopsis thaliana* increases expression of defense-related genes as well as resistance to *Pseudomonas syringae* and *Hyaloperonospora arabidopsidis*. *Frontiers in Plant Science*, 5, 115.

Marina, M., Maiale, S.J., Rossi, F., Romero, F., Rivas, E.I., Gárriz, A. et al. (2008) Apoplastic polyamine oxidation plays different roles in local responses of tobacco to infection by the necrotrophic fungus *Sclerotinia sclerotiorum* and the biotrophic bacterium *Pseudomonas viridiflava*. *Plant Physiology*, 147, 2164–2178.

Melotto, M., Underwood, W., Koczan, J., Nomura, K. & He, S.Y. (2006) Plant stomata function in innate immunity against bacterial invasion. *Cell*, 126, 969–980.

Mi, H., Muruganujan, A., Casagrande, J.T. & Thomas, P.D. (2013) Large-scale gene function analysis with the PANTHER classification system. *Nature Protocols*, 8, 1551–1566.

Mi, H., Muruganujan, A., Ebert, D., Huang, X. & Thomas, P.D. (2019) PANTHER version 14: more genomes, a new PANTHER GO-slim and improvements in enrichment analysis tools. *Nucleic Acids Research*, 47, D419–D426.

Mitsuya, Y., Takahashi, Y., Berberich, T., Miyazaki, A., Matsumura, H., Takahashi, H. et al. (2009) Spermine signaling plays a significant role in the defense response of *Arabidopsis thaliana* to cucumber mosaic virus. *Journal of Plant Physiology*, 166, 626–643.

Mittal, S. (1995) Role of the phytotoxin coronatine in the infection of *Arabidopsis thaliana* by *Pseudomonas syringae* pv. *tomato*. *Molecular Plant-Microbe Interactions*, 8, 165–171.

Mo, H., Wang, X., Zhang, Y., Yang, J. & Ma, Z. (2015) Cotton ACAULIS5 is involved in stem elongation and the plant defense response to *Verticillium dahliae* through thermospermine alteration. *Plant Cell Reports*, 34, 1975–1985.

Moschou, P.N., Sarris, P.F., Skandalis, N., Andriopoulou, A.H., Paschalidis, K.A., Panopoulos, N.J. et al. (2009) Engineered polyamine catabolism preinduces tolerance of tobacco to bacteria and oomycetes. *Plant Physiology*, 149, 1970–1981.

Nambeesan, S., AbuQamar, S., Laluk, K., Mattoo, A.K., Mickelbart, M.V., Ferruzzi, M.G. et al. (2012) Polyamines attenuate ethylene-mediated defense responses to abrogate resistance to *Botrytis cinerea* in tomato. *Plant Physiology*, 158, 1034–1045.

Nawrath, C., Heck, S., Parinthawong, N. & Métraux, J.-P. (2002) EDS5, an essential component of salicylic acid–dependent signaling for disease resistance in *Arabidopsis*, is a member of the MATE transporter family. *The Plant Cell*, 14, 275–286.

Nickstadt, A., Thomma, B.P.H.J., Feussner, I., Kangasjarvi, J., Zeier, J., Loeffler, C. et al. (2004) The jasmonate-insensitive mutant *jin1* shows increased resistance to biotrophic as well as necrotrophic pathogens. *Molecular Plant Pathology*, 5, 425–434.

Onkokesung, N., Gaquerel, E., Kotkar, H., Kaur, H., Baldwin, I.T. & Galis, I. (2012) MYB8 controls inducible phenolamide levels by activating three novel Hydroxycinnamoyl-Coenzyme A:Polyamine transferases in *Nicotiana attenuata*. *Plant Physiology*, 158, 389–407.

Pastor-Cantizano, N., Ko, D.K., Angelos, E., Pu, Y. & Brandizzi, F. (2020) Functional diversification of ER stress responses in *Arabidopsis*. *Trends in Biochemical Sciences*, 45, 123–136.

Peng, Y., Yang, J., Li, X. & Zhang, Y. (2021) Salicylic acid: biosynthesis and signaling. *Annual Review of Plant Biology*, 72, 761–791.

Rea, G., Metoui, O., Infantino, A., Federico, R. & Angelini, R. (2002) Copper amine oxidase expression in defense responses to wounding and *Ascochyta rabiei* invasion. *Plant Physiology*, 128, 865–875.

Rivals, I., Personnaz, L., Taing, L. & Potier, M.-C. (2007) Enrichment or depletion of a GO category within a class of genes: which test? *Bioinformatics*, 23, 401–407.

Rocha, R.O., Elowsky, C., Pham, N.T.T. & Wilson, R.A. (2020) Spermine-mediated tight sealing of the *Magnaporthe oryzae* appressorial pore-rice leaf surface interface. *Nature Microbiology*, 5, 1472–1480.

Sagor, G.H.M., Chawla, P., Kim, D.W., Berberich, T., Kojima, S., Niitsu, M. et al. (2015) The polyamine spermine induces the unfolded protein response via the MAPK cascade in *Arabidopsis*. *Frontiers in Plant Science*, 6, 687.

Sagor, G.H.M., Takahashi, H., Niitsu, M., Takahashi, Y., Berberich, T. & Kusano, T. (2012) Exogenous thermospermine has an activity to induce a subset of the defense genes and restrict cucumber mosaic virus multiplication in *Arabidopsis thaliana*. *Plant Cell Reports*, 31, 1227–1232.

Seo, S., Katou, S., Seto, H., Gomi, K. & Ohashi, Y. (2007) The mitogen-activated protein kinases WIPK and SIPK regulate the levels of jasmonic and salicylic acids in wounded tobacco plants. *The Plant Journal*, 49, 899–909.

Serrano, M., Wang, B., Aryal, B., Garcion, C., Abou-Mansour, E., Heck, S. et al. (2013) Export of salicylic acid from the chloroplast requires the multidrug and toxin extrusion-like transporter EDS5. *Plant Physiology*, 162, 1815–1821.

Sheard, L.B., Tan, X., Mao, H., Withers, J., Ben-Nissan, G., Hinds, T.R. et al. (2010) Jasmonate perception by inositol-phosphate-potentiated COI1–JAZ co-receptor. *Nature*, 468, 400–405.

Spoel, S.H., Koornneef, A., Claessens, S.M.C., Korzelius, J.P., Van Pelt, J.A., Mueller, M.J. et al. (2003) NPR1 modulates cross-talk between salicylate- and jasmonate-dependent defense pathways through a novel function in the cytosol. *The Plant Cell*, 15, 760–770.

Sun, T., Huang, J., Xu, Y., Verma, V., Jing, B., Sun, Y. et al. (2020) Redundant CAMTA transcription factors negatively regulate the biosynthesis of salicylic acid and N-hydroxypipecolic acid by modulating the expression of SARD1 and CBP60g. *Molecular Plant*, 13, 144–156.

Sun, T., Zhang, Y., Li, Y., Zhang, Q., Ding, Y. & Zhang, Y. (2015) ChIP-seq reveals broad roles of SARD1 and CBP60g in regulating plant immunity. *Nature Communications*, 6, 10159.

Swinnen, G., De Meyer, M., Pollier, J., Molina-Hidalgo, F.J., Ceulemans, E., Venegas-Molina, J. et al. (2022) The basic helix–loop–helix transcription factors MYC1 and MYC2 have a dual role in the regulation of constitutive and stress-inducible specialized metabolism in tomato. *New Phytologist*, 236, 911–928.

Takahashi, Y., Berberich, T., Miyazaki, A., Seo, S., Ohashi, Y. & Kusano, T. (2003) Spermine signalling in tobacco: activation of mitogen-activated protein kinases by spermine is mediated through mitochondrial dysfunction. *The Plant Journal*, 36, 820–829.

Takahashi, Y., Uehara, Y., Berberich, T., Ito, A., Saitoh, H., Miyazaki, A. et al. (2004) A subset of hypersensitive response marker genes, including HSR203J, is the downstream target of a spermine signal transduction pathway in tobacco. *The Plant Journal*, 40, 586–595.

Thines, B., Katsir, L., Melotto, M., Niu, Y., Mandaokar, A., Liu, G. et al. (2007) JAZ repressor proteins are targets of the SCFCOI1 complex during jasmonate signalling. *Nature*, 448, 661–665.

Tiburcio, A.F., Altabella, T., Bitrián, M. & Alcázar, R. (2014) The roles of polyamines during the lifespan of plants: from development to stress. *Planta*, 240, 1–18.

Wang, L., Tsuda, K., Sato, M., Cohen, J.D., Katagiri, F. & Glazebrook, J. (2009) *Arabidopsis* CaM binding protein CBP60g contributes to MAMP-induced SA accumulation and is involved in disease resistance against *Pseudomonas syringae*. *PLoS Pathogens*, 5, e1000301.

Wang, L., Tsuda, K., Truman, W., Sato, M., Nguyen, L.V., Katagiri, F. et al. (2011) CBP60g and SARD1 play partially redundant critical roles in salicylic acid signaling. *The Plant Journal*, 67, 1029–1041.

Wasternack, C. & Feussner, I. (2018) The oxylipin pathways: biochemistry and function. *Annual Review of Plant Biology*, 69, 363–386.

Wasternack, C. & Song, S. (2017) Jasmonates: biosynthesis, metabolism, and signaling by proteins activating and repressing transcription. *Journal of Experimental Botany*, 68, 1303–1321.

Wildermuth, M.C., Dewdney, J., Wu, G. & Ausubel, F.M. (2001) Isochorismate synthase is required to synthesize salicylic acid for plant defence. *Nature*, 414, 562–565.

Yu, C.-Y., Cho, Y., Sharma, O. & Kanehara, K. (2022) What's unique? The unfolded protein response in plants. *Journal of Experimental Botany*, 73, 1268–1276.

Zeng, W. & He, S.Y. (2010) A prominent role of the flagellin receptor FLAGELLIN-SENSING2 in mediating stomatal response to *Pseudomonas syringae* pv *tomato* DC3000 in *Arabidopsis*. *Plant Physiology*, 153, 1188–1198.

Zhang, C., Atanasov, K.E. & Alcázar, R. (2023) Spermine inhibits PAMP-induced ROS and Ca2+ burst and reshapes the transcriptional landscape of PAMP-triggered immunity in *Arabidopsis*. *Journal of Experimental Botany*, 74, 427–442.

Zhang, S., Klessig, D.F., Zhang, S. & Klessig, D.F. (1997) Salicylic acid activates a 48-kD MAP kinase in tobacco. *The Plant Cell*, 9, 809–824.

Zhang, Y., Xu, S., Ding, P., Wang, D., Cheng, Y.T., He, J. et al. (2010) Control of salicylic acid synthesis and systemic acquired resistance

by two members of a plant-specific family of transcription factors. *Proceedings of the National Academy of Sciences*, 107, 18220–18225.
Zheng, X.Y., Spivey, N.W., Zeng, W., Liu, P.-P., Fu, Z.Q., Klessig, D.F. et al. (2012) Coronatine promotes *Pseudomonas syringae* virulence in plants by activating a signaling cascade that inhibits salicylic acid accumulation. *Cell Host & Microbe*, 11, 587–596.
Zhou, N., Tootle, T.L., Tsui, F., Klessig, D.F. & Glazebrook, J. (1998) PAD4 functions upstream from salicylic acid to control defense responses in *Arabidopsis*. *The Plant Cell*, 10, 1021–1030.
Zipfel, C., Robatzek, S., Navarro, L., Oakeley, E.J., Jones, J.D.G., Felix, G. et al. (2004) Bacterial disease resistance in *Arabidopsis* through flagellin perception. *Nature*, 428, 764–767.
Šimura, J., Antoniadi, I., Široká, J., Tarkowská, D., Strnad, M., Ljung, K. et al. (2018) Plant hormonomics: multiple phytohormone profiling by targeted metabolomics. *Plant Physiology*, 177, 476–489.

SUPPORTING INFORMATION

Additional supporting information can be found online in the Supporting Information section at the end of this article.

How to cite this article: Zhang, C., Atanasov, K.E., Murillo, E., Vives-Peris, V., Zhao, J., Deng, C. et al. (2023) Spermine deficiency shifts the balance between jasmonic acid and salicylic acid-mediated defence responses in *Arabidopsis*. *Plant, Cell & Environment*, 46, 3949–3970. https://doi.org/10.1111/pce.14706

Chapter 3 - Identification of genes underlying the natural variation of Spm+flg22 responses by GWAS mapping

Chapter 3. Identification of genes underlying the natural variation of Spm+flg22 responses by GWAS mapping

Polyamines (PAs) are small aliphatic amines present in all organisms. In plants, the three main PAs are putrescine (Put), spermidine (Spd), and spermine (Spm). PAs play important roles in plant growth and development, as well as in biotic and abiotic stress responses. Previous studies have shown that Spm inhibits flg22-triggered ROS in *Arabidopsis*. This study utilized Genome-wide association studies (GWAS) to identify the genetic determinisms underlying the natural variation of flg22+Spm ROS responses using 136 *Arabidopsis* accessions collected from worldwide.

Introduction

*Arabidopsis*is is capable of self-pollination, maintaining its nearly complete homozygous genome across generations (Tang et al., 2007). The average outcrossing rate ranges from 0.3% to 2.5% (Abbott & Gomes, 1989; Pico et al., 2008). Nordborg et al. examined the polymorphism pattern in a sizable sample of individuals, employing loci with sufficient density to gain insight into the genome-wide haplotype structure of the species, and endorsed the usefulness of *Arabidopsis* as a model for evolutionary functional genomics (Nordborg et al., 2005). The rapid development of genomics has accelerated the establishment of new connections between molecular biology, ecology, and evolutionary theory. GWAS enables the association between SNPs and quantitative phenotypes using naturally occurring polymorphisms in wild populations of *Arabidopsis*. Atwell et al. first conducted a GWAS analysis of 107 phenotypes in *Arabidopsis* accessions, identifying a significant concordance with already known genes and functions. This suggested that GWAS was also applicable for population genetic analyses of complex traits controlled by multiple genes in *Arabidopsis* (Atwell et al., 2010). Baxter et al. selected a set of 360 accessions based on the genotypes of 5,810 worldwide accessions genotyped with 149 SNPs from a previous study, after minimizing redundancy and close family relatedness (Baxter et al., 2010; Platt et al., 2010). More recently, and thanks to the 1001 genomes sequencing initiative, the number of accessions available for GWAS mapping has increased significantly, and online platforms have been developed to analyze the data (https://gwas.gmi.oeaw.ac.at/).

Given the inhibitory effect of Spm on flg22-triggered ROS burst (see Chapter 1), we aimed to use GWAS mapping to identify genes associated with the natural variation of this inhibitory effect. We utilized GWAS to screen 136 *Arabidopsis* accessions and identified several candidate genes, from which one was validated.

Results and discussion

Variation of flg22+Spm responses

The 136 accessions used in this work were randomly chosen in order to obtain a population with low population structure. The collection sites of these accessions are shown in Figure 1. Using these accessions, we quantified the total sum of RLU upon elicitation with flg22 (1 μM) in the presence of Spm (100 μM). In every 96-well plate,

the Col-0 accession treated with flg22 was included for signal normalization. We observed a significant variation in the flg22-elicited ROS burst generation in the presence of Spm that did not follow any evident geographical pattern. (Figure 2).

Figure 1 Geographical distribution of the main populations contained in the 136 *Arabidopsis* accessions used in this study. The data is detailed in ANNEX III Table S1.

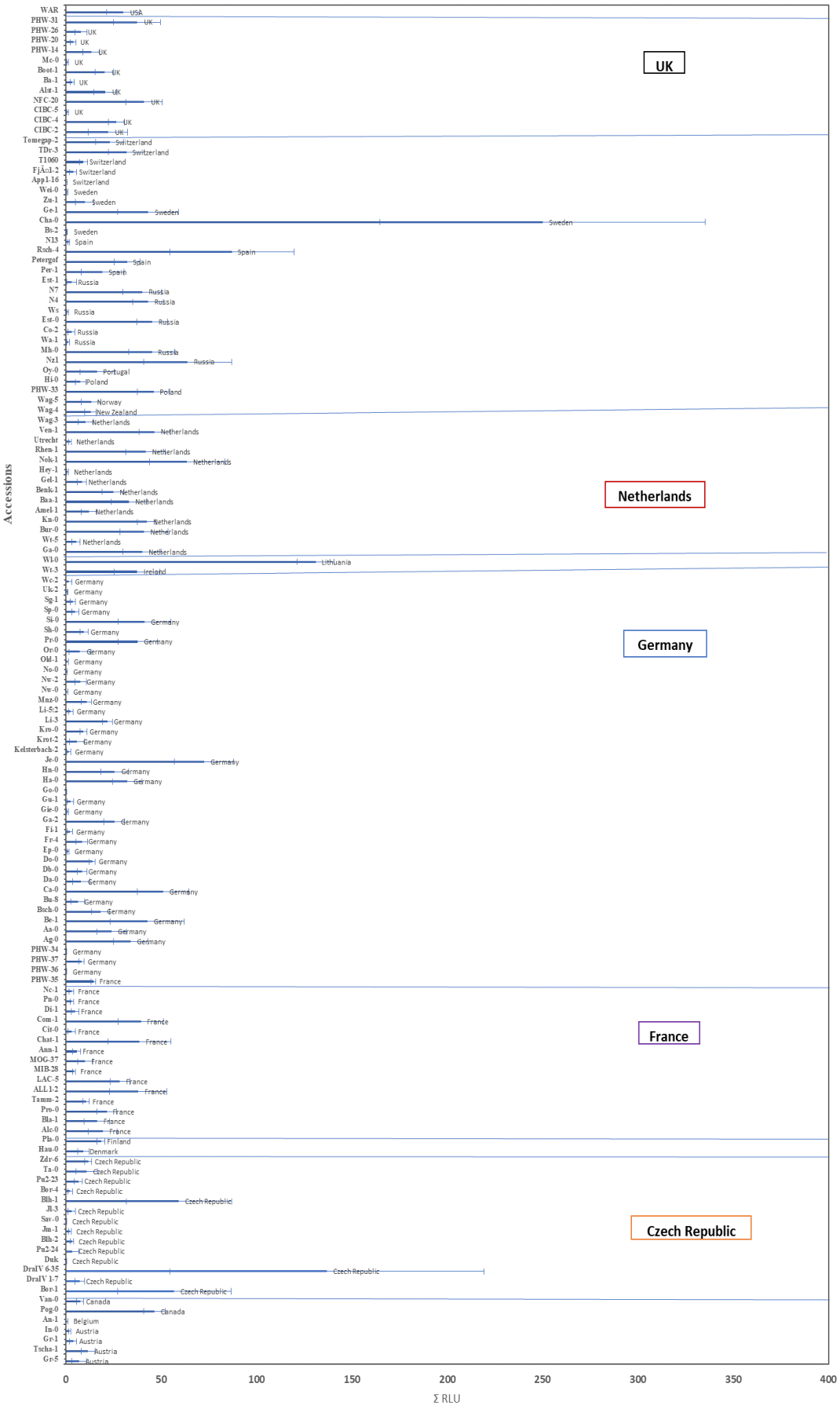

Figure 2 Quantitation of the mean sum of relative light units (Mean_SumRLU, ΣRLU) within one hour

of treatment with (flg22 + Spm) in 136 *Arabidopsis* accessions distributed by country. The data is based on ANNEX III Table S1. Values represent the mean ± standard error (SE) from six biological replicates.

GWAS analysis was conducted using the quantitative data collected (mean sum of relative light units within one hour of treatment with flg22 + Spm) in the 136 *Arabidopsis* accessions. For this, we utilized an online platform https://gwas.gmi.oeaw.ac.at/#/home (Seren, 2018) and performed GWAS mapping using an accelerated mixed model (AMM). Figure 3 presents the Manhattan and Q-Q plots depicting the GWAS results. A QQ plot compares the observed distribution of p-values (observed on the y-axis) against the expected distribution under the null hypothesis (expected on the x-axis). The p-values are sorted from smallest to largest and plotted against the quantiles of the uniform distribution (i.e., the expected values). If the observed p-values follow the null distribution closely, the points on the QQ plot will fall approximately along the diagonal line (y = x). Deviations from this diagonal line indicate departures from the null hypothesis. Based on the shape of the QQ-plot, we concluded that there were likely genuine associations between the genetic variants and the trait.

A Manhattan plot was constructed to illustrate the associations identified across the genome (Figure 3). A total of three SNPs were found to be significantly associated with the variation of the trait, based on the Benjamini-Hochberg test which is a less conservative method than the Bonferroni correction. Two other SNP were close to the significant threshold. Annotations for the candidate genes were obtained from the 1001 Genomes https://aragwas.1001genomes.org/ and TAIR www.*arabidopsis*.org. The candidate genes are listed in Table 1. Based on the GWAS score, we selected the potentially associated candidate gene *AT2G29930* that codes for an F-box/RNI-like superfamily (LRR-repeat) protein, for further investigation. To note that the SNP associated with this gene was not in linkage disequilibrium with other genes, as LD decayed sharply with distance (not shown). In addition, the MAF (minor allele frequency) value was low (0.158) indicating the presence of low frequent alleles that may cause the association. In these circumstances, the statistical power to detect associations is significantly reduced. To further validate the association, we utilized a loss-of function mutant line for *AT2G29930*, SALK_066142C (N654696).

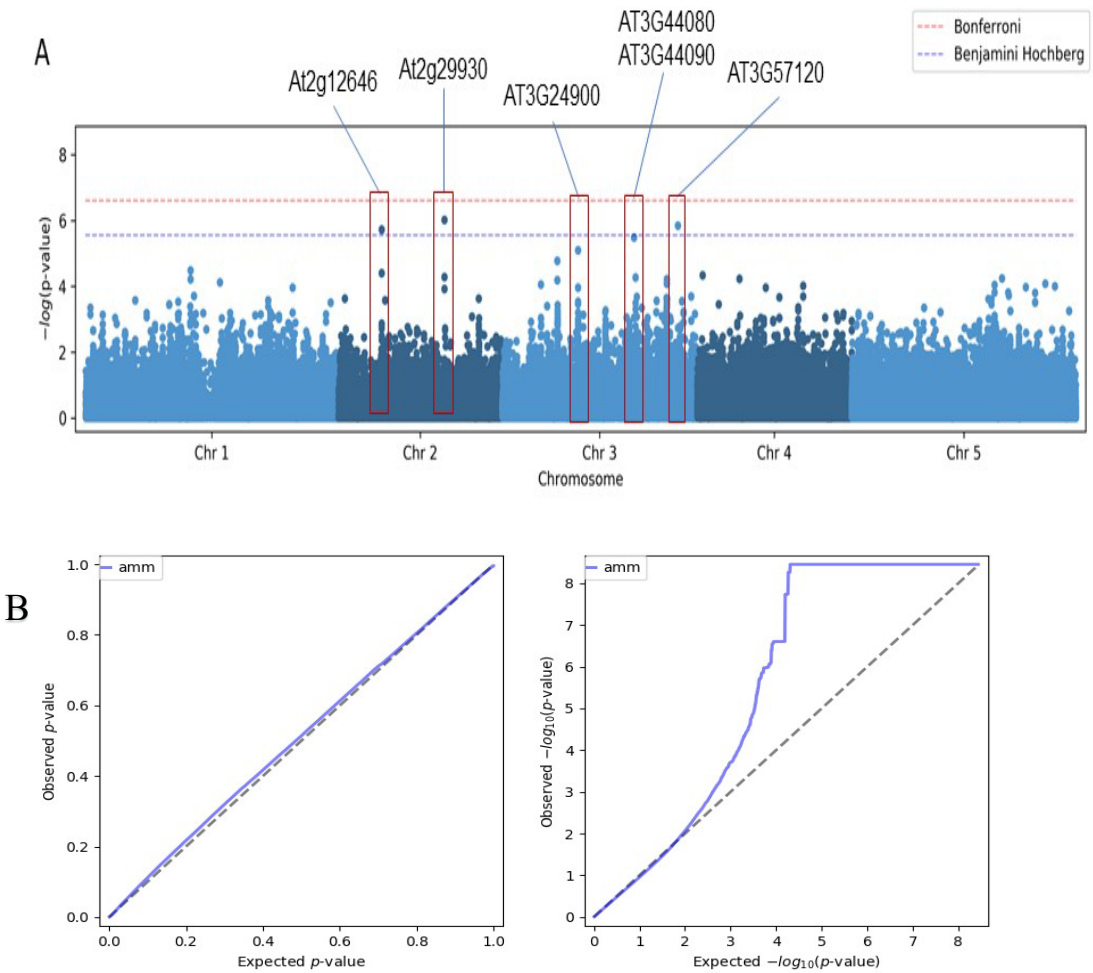

Figure 3 A. GWAS mapping profiles using the accelerated mixed model (AMM) of flg22+Spm ROS burst responses in 136 *Arabidopsis* accessions. The Manhattan plot indicates the significant SNP and potential candidate genes. B. QQ plots obtained from GWAS mapping.

Table1 Candidate genes obtained from the GWAS mapping based on SNP position and linkage disequilibrium (LD)

Chromosome	SNP location	Score	MAF	Candidate Gene	Annotation
2	5172900	5.73	0.203	*AT2G12646*	Plant AT-rich sequence and zinc-binding transcription factor (PLATZ) family protein which plays central role in mediating RGF1 signalling. Controls root meristem size through ROS signalling.
2	12757781	6.03	0.158	*AT2G29930*	F-box/RNI-like superfamily protein

3	9101246	5.10	0.241	*AT3G24900*	Receptor like protein 39
3	15836568	5.50	0.256	*AT3G44080*	F-box family protein
				AT3G44090	F-box family protein
3	21140514	5.86	0.143	*AT3G57120*	Protein kinase superfamily protein;

Phylogenetic analysis of *AT2G29930* gene

The sequence of the *AT2G29930* gene from 50 *Arabidopsis* accessions was obtained from the 1001 genomes project website and used to build a phylogenetic tree (Figure 5). We did not find a simple pattern of genotype-phenotype associations with the data of mean sum of relative light units (Mean_SumRLU) within 1h of treatment with (flg22 + Spm). In every major clade, accessions with high and low values were present. The data is in agreement with the occurrence of low-frequency (rare) alleles contributing to the variation of the trait, as anticipated by the low MAF value. Therefore, we could not identify conserved allele(s) clearly associated with the trait variation.

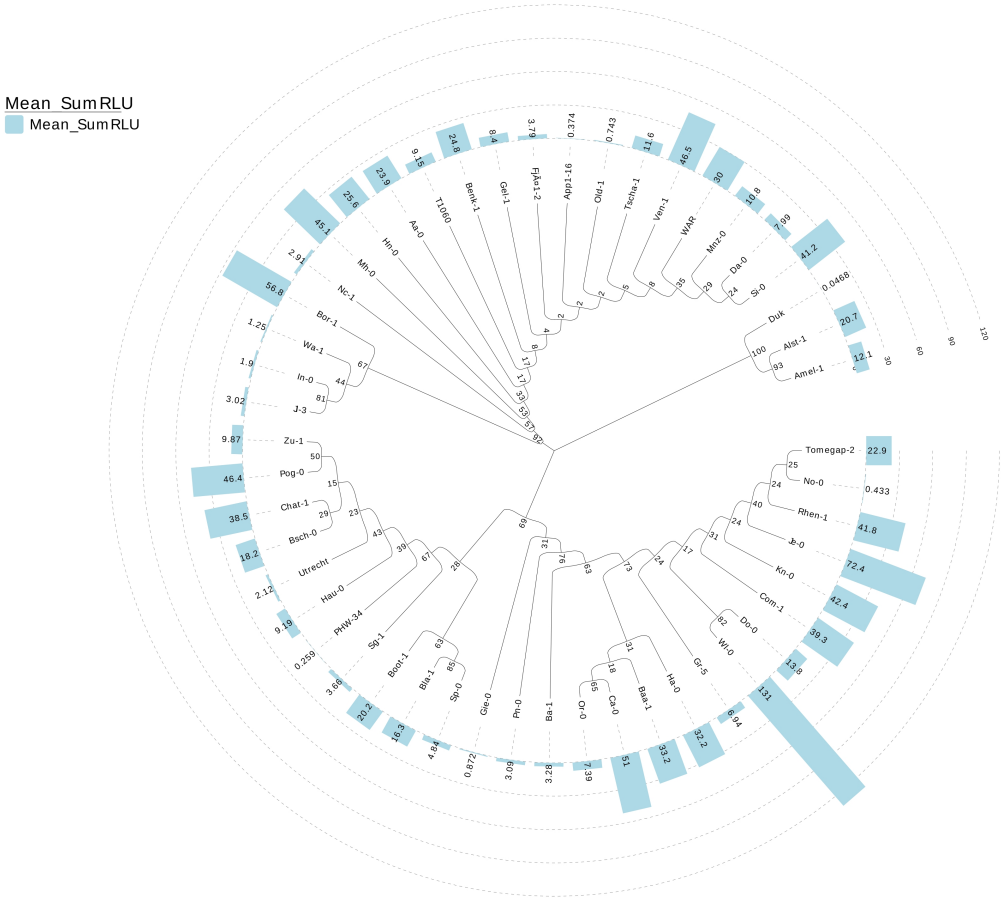

Figure 4 Phylogenetic trees of *AT2G29930* derived from 50 accessions and the blue histogram of the outer ring represents its corresponding the mean sum of relative light units (Mean_SumRLU) within one

hour of treatment with (flg22 + Spm) detailed in ANNEX III Table S1. Bootstrap values for different nodes are indicated (as percentages of 500 replicates).

Spm inhibition of flg22-induced ROS in N654696 mutant

To validate the GWAS association with the gene *AT2G29930*, we used the loss-of-function mutant N654696. In this mutant, we tested the inhibitory effect of different concentrations of Spm on flg22-induced ROS and found that the mutant N654696 was more sensitive to low concentrations of Spm, showing stronger ROS inhibition compared to the wild-type (Figure 5). There was little difference between the mutant N654696 and wild-type in ROS induced solely by flg22 (Figure 5D), thus indicating that the association was not due to flg22 but Spm responsiveness. Under treatment with 100 µM Spm, ROS induced by flg22 was almost completely inhibited (Figure 5C). But under treatment with 25 µM and 50 µM Spm, the mutant N654696 exhibited a stronger inhibition of ROS induced by flg22 compared to the wild-type (Figures 5A and 5B).

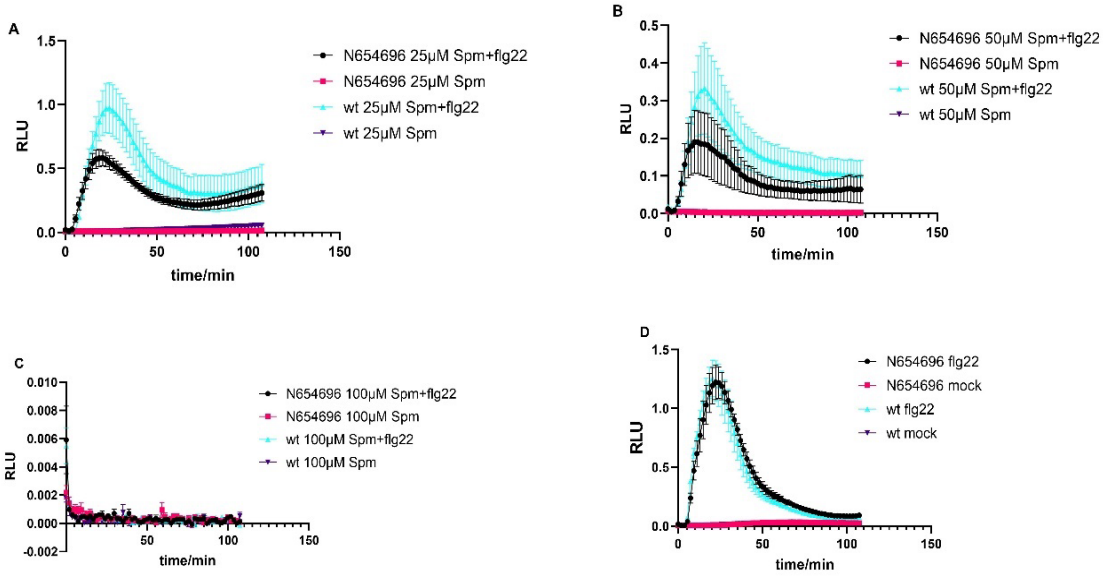

Figure 5 The inhibitory effect of different concentrations of Spm on flg22-induced ROS burst. A. 25 µM Spm B. 50 µM Spm C. 100 µM Spm and D. no Spm. Values are presented as the mean ± standard error (SE) from six replicates per treatment, measured in photon counts [expressed as relative light units (RLU)].

Quantitation of polyamine levels

We hypothesized that the elevated sensitivity to Spm of the N654696 mutant could be due to an elevation of the basal Spm levels. We then quantified the levels of free polyamines in this mutant and in the wild-type (Figure 6). The results evidenced the absence of significant differences in the levels of free Put, Spd or Spm between N654696 and the wild-type. We suggested that other mechanisms than the modulation of polyamine homeostasis might be involved in this exacerbated response to Spm.

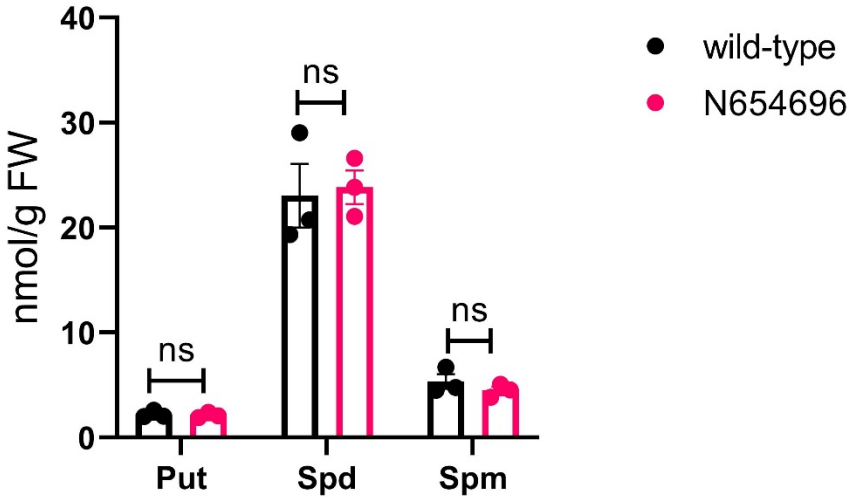

Figure 6 Polyamine levels in mutant N654696 and wild type. Values represent the mean ± standard error (SE) from three biological replicates. Ns, not significant according to Student's t test.

Overall, we provide evidence for the occurrence of natural variation in the inhibitory effect of Spm on flg22-triggered ROS burst. We further provide a number of candidate genes underlying such variation, for which one gene was further validated using a loss-of-function mutant, and confirmed that the association was not linked to flg22 but Spm responses. Despite the function of the identified F-box protein is not known, most F-box proteins (FBP) in plants are integral components of SCF (Skp1-Cul (Cullin) -FBP) complexes, which are the predominant type of E3 ubiquitin ligases (Malik et al., 2020). The FBP provides specificity through its motif at the C-terminal domain, enables the SCF complex to selectively recruit targeted proteins for degradation via the ubiquitin/26S proteasome pathway (UPP) in a process known as proteolysis (Abd-Hamid et al., 2020; Malik et al., 2020). Based on the characteristics of F-BOX proteins, they are more likely to form complexes with other specific proteins. Interestingly, the expression of SKP1-LIKE3 (*AT2G25700*), which is the putative E3 ubiquitin ligase SCF complex subunit SKP1 (Risseeuw et al., 2003) correlates with *AT2G29930*. However, the specific substrates of the F-box/RNI-like protein *AT2G29930* are unknown.

A number of FBP are known to participate in defense responses. For example, in *Arabidopsis*, the FBP *CONSTITUTIVE EXPRESSER OF PR GENES1* (*CPR1*) negatively regulates the NLR (nucleotide-binding/leucine-rich-repeat receptor) protein *SNC1* (*SUPPRESSOR OF NPR1-1, CONSTITUTIVE 1*) (Gou et al., 2012). *CPR1* is induced similarly to the negative defense regulator BON1 (BONZAI1) after infection by both virulent and avirulent pathogens (Gou et al., 2012). *SON1* (*SUPPRESSOR OF NIM1-1*), another FBP in *Arabidopsis*, acts as a negative regulator in defense responses independently of salicylic acid (SA) and SAR (Kim & Delaney, 2002). In tobacco, the FBP *Avr9/Cf-9–INDUCED F-BOX1 (ACIF1*) mediates the hypersensitive response (HR) and its silencing impairs HR triggered by various effectors, like Avr9 and Avr4 (van den Burg et al., 2008). ACIF1 influences N gene-mediated responses to *TMV*

(*tobacco mosaic virus*) infection, including lesion formation and the accumulation of SA (van den Burg et al., 2008). However, it remains to be investigated which are the substrates of the F-box/RNI-like protein *AT2G29930* and how this integrates with Spm responsiveness.

Materials and Methods

Plant materials

Seeds from 136 *Arabidopsis* accessions were sown directly on soil containing 40% peat moss, 50% vermiculite, and 10% perlite. Details about the accessions are provided in the Annex III. Seeds were subjected to cold stratification in darkness at 4°C for 2–3 days to induce germination. Plants were cultivated under 12-hour light/12-hour dark cycles at a temperature range of 20–22°C.

ROS measurements

The experimental procedure for ROS measurement is similar to the method described in Chapter 1(Zhang et al., 2023). Leaf discs (0.5 cm diameter) from 5-week-old plants were soaked in 200 µl sterile water for 24 h. Leaf discs were pre-incubated with Spm for 24 h before elicitation with flg22 (1 µM). Six replicates were used in each analysis. Horseradish peroxidase (Merck) and L-012 (Wako Chemicals) were used to detect luminescence as reported in Chapter 1. The sum of relative light units (Mean_SumRLU) within 1h of treatment with (flg22 + Spm) was used as quantitative data for GWAS mapping.

GWAS studies

GWAS was conducted using the GWAPP web interface at https://gwas.gmi.oeaw.ac.at/#/home (Seren, 2018). The overall process of data analysis is similar to that described by (López-Ruiz et al., 2022). GWAS was performed using the accelerated mixed-mode (AMM) method. Manhattan plots were generated after filtering for a minor allele frequency (MAF) ≥ 0.05 (Horton et al., 2012; López-Ruiz et al., 2022). GWAS results were plotted using the genomic location of each SNP and its association significance represented by [−log10(p-Value)] (López-Ruiz et al., 2022). The statistical significance of SNP associations was assessed using the Benjamini–Hochberg–Yekutieli method to correct for multiple testing, with a false discovery rate (FDR) threshold set at 5% (Benjamini & Yekutieli, 2001; López-Ruiz et al., 2022).

Phylogenetic Tree

The candidate DNA sequences were downloaded from the 1001 Genomes project (www.1001genomes.org). The phylogenetic Tree was constructed using the Neighbor-Joining method in MEGA 11. Bootstrap values for different nodes are derived from 500 replicates. To enhance visualization, the tree was optimized using the online tool Evolview (https://evolgenius.info/evolview-v2/), and the phylogenetic tree was annotated with the corresponding average sum RLU (Relative Light Units) values within 1 hour, as detailed in the supplementary data ANNEX III.

Polyamines Levels

The concentrations of free Put, Spd, and Spm were assessed using high-performance liquid chromatography (HPLC) after dansyl derivatization, following the procedures outlined in Chapter 1 and 2. Each analysis was conducted with three biological replicates.

References

Abbott, R. J., & Gomes, M. F. (1989). Population genetic structure and outcrossing rate of *Arabidopsis thaliana (L.) Heynh. Heredity, 62*, 411-418.

Abd-Hamid, N. A., et al. (2020). Diverse and dynamic roles of F-box proteins in plant biology. *Planta, 251*, 1-31.

Atwell, S., et al. (2010). Genome-wide association study of 107 phenotypes in *Arabidopsis thaliana* inbred lines. *Nature, 465*, 627-631.

Baxter, I., et al. (2010). A coastal cline in sodium accumulation in *Arabidopsis thaliana* is driven by natural variation of the sodium transporter *AtHKT1*; 1. *PLoS Genetics, 6* , e1001193.

Benjamini, Y., & Yekutieli, D. (2001). The control of the false discovery rate in multiple testing under dependency. *Annals of Statistics*, 1165-1188.

Gou, M., et al. (2012). The F-box protein *CPR1/CPR30* negatively regulates R protein *SNC1* accumulation. *The Plant Journal, 69*, 411-420.

Horton, M. W., et al. (2012). Genome-wide patterns of genetic variation in worldwide *Arabidopsis thaliana* accessions from the RegMap panel. *Nature genetics, 44*, 212-216.

Kim, H. S., & Delaney, T. P. (2002). *Arabidopsis SON1* is an F-box protein that regulates a novel induced defense response independent of both salicylic acid and systemic acquired resistance. *The Plant Cell, 14*, 1469-1482.

López-Ruiz, B. A., et al. (2022). Combined approach of GWAS and phylogenetic analyses to identify new candidate genes that participate in *Arabidopsis Thaliana* primary root development using cellular measurements and primary root length. *Plants, 11*, 3162.

Malik, A., et al. (2020). Classification and computational analysis of *Arabidopsis* thaliana sperm cell-specific F-box protein gene *3p.AtFBP113*. *Frontiers in Genetics, 11*, 609668.

Nordborg, M., et al. (2005). The pattern of polymorphism in *Arabidopsis thaliana*. *PLoS Biology, 3*, e196.

Pico, F. X., et al. (2008). Natural genetic variation of *Arabidopsis thaliana* is geographically structured in the Iberian Peninsula. *Genetics, 180*, 1009-1021.

Platt, A., et al. (2010). The scale of population structure in *Arabidopsis thaliana*. *PLoS Genetics, 6*, e1000843.

Risseeuw, E. P., et al. (2003). Protein interaction analysis of SCF ubiquitin E3 ligase subunits from *Arabidopsis*. *The Plant Journal, 34*, 753-767.

Seren, Ü. (2018). GWA-Portal: Genome-wide association studies made easy. *Root Development: Methods Protocols*, 303-319.

Tang, C., et al. (2007). The evolution of selfing in *Arabidopsis thaliana*. *Science, 317*, 1070-1072.

van den Burg, H. A., et al. (2008). The F-box protein *ACRE189/ACIF1* regulates cell death and defense responses activated during pathogen recognition in tobacco and tomato. *The Plant Cell, 20*, 697-719.

Zhang, et al. (2023). Spermine inhibits PAMP-induced ROS and Ca^{2+} burst and

reshapes the transcriptional landscape of PAMP-triggered immunity in *Arabidopsis*. *Journal of Experimental Botany, 74*, 427-442.

General Discussion

In line with present estimations, there is an anticipated need to increase food production by twofold by the year 2050 to fulfill the growing global demand (Tilman et al., 2011). This undertaking is further complicated by the escalating impacts of climate change, including heightened temperatures, frost, floods, and droughts (Tilman et al., 2011; Velásquez et al., 2018). A more detailed examination of the intricate relationships between plants and pathogens is anticipated to offer valuable insights for the advancement of agricultural technology. Extensive research on plant innate immunity signaling, coupled with gene editing technologies, will significantly enhance crop breeding for disease resistance (Shan et al., 2013).

Polyamines can be applied exogenously to better adapt to stressful environments. For example, in pistachio (*Pistacia vera* L.) seedlings, exogenous application of free polyamines (especially Spm and Spd) enhances salt stress tolerance (Kamiab et al., 2014). In terms of drought, pretreatment with exogenous Spd or Spm enhanced the activities of *ADC*, *ODC*, and *SAMDC* (Yin et al., 2014). Additionally, Spd or Spm pretreatment effectively prevented drought-induced oxidative damage in *Chinese dwarf cherry* (Yin et al., 2014). Perhaps in the future, we can use gene silencing technology and utilize the physiological advantages of polyamines during defense to obtain improved crop varieties.

In regard to the mechanisms of action for polyamines during plant immunity, we still have many unknowns that need to be explored. For instance, while *Arabidopsis CuAO* family comprises 10 genes, only five of them have been minimally characterized (Wang et al., 2019). Their biological specificities remain to be explored. In addition, little is known about polyamine signaling, although important insights have been recently achieved (Liu et al., 2019b; Zhang et al., 2022, 2023). Further investigations into polyamine oxidation and conjugation, the subcellular localization of polyamines and their signaling pathways may provide important clues for genetic crop improvement.

Our research findings shed light on the contrasting effects of polyamines, particularly Put and Spm, on several aspects of the defense response.

In Chapter 1 we report that co-treatment with flg22 and Put do not significantly alter the ROS burst triggered by flg22, while pre-incubation with Put leads to higher ROS production compared to the mock treatment. Conversely, Spm at concentrations of 100 μM and higher strongly inhibits ROS production triggered by flg22. These results suggest that Put enhances the amplitude of the ROS response, while Spm suppresses it, indicating opposing roles for these polyamines in modulating plant defense. The findings in Figure 2 further support this notion by demonstrating that mutants deficient in Put biosynthesis (*adc1-3 and adc2-4*) exhibited similar ROS production triggered by flg22 compared to wild-type plants, whereas the *spms* mutant, deficient in Spm biosynthesis, displayed significantly higher ROS levels. Insights were provided into the functional implications of the differential regulation of ROS production by Put and Spm on plant disease resistance. Wild-type plants pre-infiltrated with Spm and flg22 supported higher bacterial growth compared to those pre-treated with flg22 alone or with Put and flg22. In contrast, pre-treatment with individual polyamines did not significantly alter disease resistance compared to mock treatment (Figure 3). These

results suggest that Spm-mediated suppression of the ROS burst triggered by flg22 compromises flg22-elicited defenses, leading to increased susceptibility to pathogen infection.

Overall, our findings firstly demonstrate that Put and Spm have opposing effects on the ROS burst triggered by flg22 and subsequent disease resistance in *Arabidopsis*. While Put enhances ROS production and contributes to plant defense, Spm suppresses ROS dynamics, thereby attenuating defense responses and compromising resistance to pathogen infection. We utilized this characteristic to conduct a genome-wide association study (GWAS) on 136 *Arabidopsis* ecotypes, resulting in the identification of several candidate genes associated with this trait (Chapter 3).

In addition to ROS in Chapter 1, we investigated changes in cytosolic Ca^{2+} induced by PAMPs. Using a bioluminescent Ca^{2+} sensor, we analyzed the dynamics of cytosolic Ca^{2+} in response to flg22, Spm, Put, and their combinations. Flg22 elicits a robust Ca^{2+} influx, which is inhibited by Spm co-treatment (Figure 5A). Spm alone also increases cytosolic Ca^{2+} levels, but this effect was counteracted by pre-treatment with flg22 (Figure 5A, B). Put triggered a lower elevation of cytosolic Ca^{2+}, with minimal impact on flg22-induced Ca^{2+} influx (Figure 5C, D). These results suggest that Put and Spm induce distinct Ca^{2+} signals, which may cause different effects on *RBOHD* function. In addition, these specific Ca^{2+} signals by polyamines may be essential for signaling, not only during defense, but also in response to abiotic stress, plant growth and development.

In Chapter 2, we investigated the modulation of polyamine metabolism and the role of Spm during the defense response to *Pst DC3000*. Inoculation with *Pst DC3000* consistently upregulated several genes involved in polyamine metabolism, such as *ADC2*, *SPMS*, *SAMDC3*, and *CuAOδ2* (Figure 1). Interestingly, the COR-deficient strain *Pst DC3000 Δcor* was not successful in the transcriptional activation of most polyamine metabolism genes, suggesting that COR plays a crucial role in modulating polyamine metabolism during the defense response to *Pst DC3000* (Figure 2a). The COR toxin, produced by various strains of *P. syringae*, shares structural similarities with JA-Ile (Mittal & Davis, 1995). SA and JA are key hormones in plant immunity and research indicates that their signaling pathways interact (SA-JA crosstalk) to coordinate plant defenses against pathogens (Betsuyaku et al., 2018; Hou & Tsuda, 2022).

We found that Spm deficiency compromises SA-mediated defense responses to *Pst DC3000*. The expression levels of key SA biosynthesis and signaling genes, as well as SA-inducible *PR1* (*PATHOGENESIS-RELATED GENE 1*), were significantly lower in *spms* compared to the wild-type at 24 h of *Pst DC3000* inoculation. Additionally, *spms* exhibited delayed transcriptional activation of SAR (systemic acquired resistance)-related genes (Figure 4b). Correspondingly, *spms* accumulated lower SA levels than the wild-type, indicating that Spm deficiency dampened SA-mediated immune responses to *Pst DC3000* (Figure 4c). Consequently, *Pst DC3000* growth was significantly higher in *spms* compared to the wild type at 72 h post *Pst DC3000* spray inoculation (Figure 4d). Additionally, we found that Spm deficiency elicits JA biosynthesis and signaling. Compared to the wild type, *spms* showed delayed transcriptional activation but eventually equal or stronger expression of JA biosynthesis genes and JA signaling genes

in response to *Pst DC3000* (Figure 6). Additionally, *spms* exhibited significantly higher expression of JA-marker genes related to the *MYC2*-branch of JA signaling at *Pst DC3000* inoculation (Figure 6). Consistently, JA, JA-Ile, and OPDA levels were higher in *spms* than in the wild type under basal conditions and in response to different treatments, indicating stimulated JA biosynthesis in *spms* (Figure 7).

Subsequently, we conducted research to investigate whether Spm is involved in the crosstalk between SA and JA. We hypothesized that the sustained elevation of JA levels in *spms* might diminish SA responses by modulating crosstalk between the two signaling pathways. We analyzed the responsiveness of SA-related genes in *spms,* and wild-type plants challenged with COR and ABA, known modulators of JA-SA crosstalk (Figure 8a). The expression of *ANAC019*, a gene involved in JA-mediated suppression of SA defenses (Li et al., 2019), was significantly higher in *spms* than in the wild-type under basal conditions and in response to COR but not ABA. Additionally, differences in the expression of *ICS1* and *BSMT1*, genes targeted by *ANAC019*, were observed between the genotypes in response to COR. These findings suggest that the increased JA levels in *spms* may modulate SA responses through JA-SA crosstalk (Figure 8). These analyses revealed a significant increase in *ANAC019* and *BSMT1* transcripts in *spms* compared to wild-type plants upon exposure to *Pst DC3000*. In summary, these findings suggest that the absence of Spm leads to a more pronounced deregulation of *ICS1* and *BSMT1*, correlated with *ANAC019* expression, in response to COR and *Pst DC3000*, resulting in decreased SA accumulation (Figures 4 and 8a, b). We also investigated the role of Spm in the response to infection by the necrotrophic fungal pathogen *Botrytis cinerea*. Spm deficiency enhanced disease resistance to *Botrytis cinerea* (Figure 11).

Combining the results from Chapters 1 and 2, we can observe a significant role for Spm in plant-pathogen interactions. Therefore, we aimed to identify genes associated with Spm sensitivity through a GWAS analysis, aiming to provide additional information about the Spm signaling pathway in plant disease resistance processes (Chapter 3).

We first quantified ROS production in the elicitation with flg22+Spm in 136 accessions of *Arabidopsis* for GWAS analysis and identified several candidate genes, as shown in Figure 1 and Table 1. Subsequent research in this chapter focused solely on the top-scoring gene, *AT2G29930*. However, if time permits in future studies, we may conduct in-depth analyses of other candidate genes, which could yield more comprehensive results regarding Spm sensitivity.

The *AT2G29930* belongs to an F-BOX protein family. F-BOX proteins in plants are associated with various hormonal regulations and play roles in plant immunity processes (Abd-Hamid et al., 2020). As outlined in Chapter 2, Spm is linked to plant hormones such as SA and JA. This F-box protein may be a candidate link between polyamines and JA/SA signaling. Future studies on plant-pathogen interactions may explore the connection between this gene and Spm along with plant hormones, potentially elucidating further insights into plant defense mechanisms.

Conclusions

This Thesis primarily discusses the role of Spm in plant-pathogen interactions. The Chapter 1 demonstrates Spm's inhibitory effect on flg22-induced ROS during early PTI responses. The Chapter 2 illustrates Spm's interaction with plant hormones SA and JA in disease resistance. The Chapter 3 aims to identify candidate genes sensitive to Spm, providing further insights into Spm's signaling pathways in plant defense.

The main conclusions are as follows:

Chapter 1

1. While Spermine (Spm) inhibits flagellin22 (flg22)-induced *RBOHD*-dependent ROS production, Putrescine (Put) shows a stimulatory effect, thus indicating the specificity of the responses to different polyamines during PAMP-triggered immunity (PTI).

2. Spm's inhibitory effect on flg22-induced ROS production is independent of polyamine oxidation and NO signaling, but resembles chemical inhibition of *RBOHD*.

3. Put and Spm trigger cytosolic calcium influx, albeit at different amplitudes and durations. Like this, Spm but not Put dampens flg22-triggered Ca^{2+} influx required for *RBOHD* activation, indicating a specific regulatory effect of Spm in modulating *RBOHD* activity.

4. Put and Spm differentially modulate the global transcriptional responses to flg22, with Spm, but not Put, dampening the up-regulation of flg22-inducible genes.

5. These results demonstrate that polyamines can differentially reshape PTI responses in plants.

Chapter 2

1. Inoculation with the bacterial pathogen *Pseudomonas syringae* pv. *tomato DC3000* (*Pst* DC3000) triggers changes in polyamine metabolism, with coronatine (COR) playing a significant role in modulating polyamine metabolism during the defense response.

2. Spm deficiency alters transcriptional responses related to salicylic acid (SA) and jasmonic acid (JA) biosynthesis and signaling; and endoplasmic reticulum (ER) stress signaling in response to *Pst DC3000*, influencing defense outputs.

3. Spm deficiency compromises SA-mediated immune responses to *Pst DC3000*, leading to lower SA levels and decreased disease resistance. On the contrary, Spm deficiency elicits enhanced JA biosynthesis and signaling, resulting in higher JA levels and stronger transcriptional activation of the JA-*MYC2* pathway.

4. The results indicate that polyamines can shift the balance between JA and SA responses, with Spm deficiency favoring JA over SA responses, thus stimulating disease resistance to *B. cinerea*.

Chapter 3

1. We detected quantitative variation for the inhibitory effect of Spm on flg22-triggered ROS burst in natural accessions, highlighting the occurrence of natural variation in this response.

2. Through GWAS analysis, we identified the F-box/RNI-like superfamily protein *AT2G29930* as candidate gene potentially modulating Spm responses. By utilizing of a loss-of-function mutant, we confirmed the genetic association of *AT2G29930* with Spm responses.

3. The *at2g29930* loss-of-funcion mutant does not show differences in basal Spm levels, suggesting that factors other than polyamine homeostasis may be involved in the mutant's elevated Spm sensitivity.

References

Abbott, R. J., & Gomes, M. F. (1989). Population genetic structure and outcrossing rate *of Arabidopsis thaliana (L.) Heynh. Heredity, 62, 411-418.*

Abd-Hamid, N. A., et al. (2020). Diverse and dynamic roles of F-box proteins in plant biology. *Planta, 251*, 1-31.

Acharya, B. R., et al. (2007). Overexpression of *CRK13*, an *Arabidopsis* cysteine-rich receptor-like kinase, results in enhanced resistance to *Pseudomonas syringae*. *The Plant Journal, 50*, 488-499.

Adio, A. M., et al. (2011). Biosynthesis and defensive function of N^{δ}-acetylornithine, a jasmonate-induced *Arabidopsis* metabolite. *The Plant Cell, 23*, 3303-3318.

Agati, G., et al. (2012). Flavonoids as antioxidants in plants: location and functional significance. *Plant Science, 196*, 67-76.

Agurla, S., et al. (2018). Polyamines increase nitric oxide and reactive oxygen species in guard cells of *Arabidopsis thaliana* during stomatal closure. *Protoplasma, 255*, 153-162.

Aklilu, E. (2021). Review on forward and reverse genetics in plant breeding. *All Life, 14*, 127-135.

Akter, S., et al. (2015). Cysteines under ROS attack in plants: a proteomics view. *Journal of Experimental Botany, 66*, 2935-2944.

Al-Shehbaz, I. A., & O'Kane, S. L., Jr. (2002). Taxonomy and phylogeny of *Arabidopsis* (Brassicaceae). *Arabidopsis Book, 1*, e0001.

Albert, I., et al. (2015). An *RLP23–SOBIR1–BAK1* complex mediates NLP-triggered immunity. *Nature Plants, 1*, 1-9.

Alcázar, R., et al. (2010). Polyamines: molecules with regulatory functions in plant abiotic stress tolerance. *Planta, 231*, 1237-1249.

Alcázar, R., et al. (2005). Overexpression of *ADC2* in *Arabidopsis* induces dwarfism and late-flowering through GA deficiency. *The Plant Journal, 43*, 425-436.

Ali, R., et al. (2007). Death don't have no mercy and neither does calcium: *Arabidopsis CYCLIC NUCLEOTIDE GATED CHANNEL 2* and innate immunity. *The Plant Cell, 19*(3), 1081-1095.

Alonso, J. M., et al. (2003). Genome-wide insertional mutagenesis of *Arabidopsis thaliana*. *Science, 301*, 653-657.

Amsbury, S., et al. (2018). Emerging models on the regulation of intercellular transport by plasmodesmata-associated callose. *Journal of Experimental Botany, 69* 105-115.

An, Z., et al. (2008). Hydrogen peroxide generated by copper amine oxidase is involved in abscisic acid-induced stomatal closure in *Vicia faba*. *Journal of Experimental Botany, 59*, 815-825.

Andronis, E. A., et al. (2014). Peroxisomal polyamine oxidase and NADPH-oxidase cross-talk for ROS homeostasis which affects respiration rate in *Arabidopsis thaliana*. *Frontiers in Plant Science, 5*, 81929.

Angelini, R., et al. (2010). Plant amine oxidases “on the move”: an update. *Plant Physiology Biochemistry, 48*, 560-564.

Apel, K., & Hirt, H. (2004). Reactive oxygen species: metabolism, oxidative stress, and signal transduction. *Annual Review of Plant Biology, 55*, 373-399.

Asai, T., et al. (2002). MAP kinase signalling cascade in *Arabidopsis* innate immunity. *Nature, 415*, 977-983.

Ashraf, M., & Foolad, M. R. (2007). Roles of glycine betaine and proline in improving plant abiotic stress resistance. *Environmental Experimental Botany, 59*, 206-216.

Attaran, E., et al. (2009). Methyl salicylate production and jasmonate signaling are not essential for systemic acquired resistance in *Arabidopsis*. *The Plant Cell, 21*,

954-971.
Baniasadi, F., et al. (2018). Physiological and growth responses of *Calendula officinalis* L. plants to the interaction effects of polyamines and salt stress. *Scientia Horticulturae, 234*, 312-317.
Barragan, C. A., et al. (2019). *RPW8*/HR repeats control NLR activation in *Arabidopsis thaliana*. *PLoS Genetics, 15*, e1008313.
Bartels, S., et al. (2013). The family of Peps and their precursors in *Arabidopsis*: differential expression and localization but similar induction of pattern-triggered immune responses. *Journal of Experimental Botany, 64*, 5309-5321.
Bentham, A. R., et al. (2018). Uncoiling CNLs: Structure/function approaches to understanding CC domain function in plant NLRs. *Plant Cell Physiol, 59*, 2398-2408.
Berridge, M. J., et al. (2003). Calcium signalling: dynamics, homeostasis and remodelling. *Nature Reviews Molecular Cell Biology, 4*, 517-529.
Bethke, G., et al. (2012). Activation of the *Arabidopsis thaliana* mitogen-activated protein kinase *MPK11* by the flagellin-derived elicitor peptide, flg22. *Molecular Plant-Microbe Interactions, 25*, 471-480.
Bethke, G., et al. (2009). Flg22 regulates the release of an ethylene response factor substrate from MAP kinase 6 in *Arabidopsis thaliana* via ethylene signaling. *Proceedings of the National Academy of Sciences, 106*, 8067-8072.
Betsuyaku, S., et al. (2018). Salicylic acid and jasmonic acid pathways are activated in spatially different domains around the infection site during effector-triggered immunity in *Arabidopsis thaliana*. *Plant Cell Physiology, 59*, 8-16.
Beutler B. (2002). *TLR4* as the mammalian endotoxin sensor. *Current topics in microbiology and immunology*, *270*, 109–120.
Bi, G., et al. (2021). The *ZAR1* resistosome is a calcium-permeable channel triggering plant immune signaling. *Cell, 184*, 3528-3541.
Bian, Z., et al. (2020). NAC transcription factors as positive or negative regulators during ongoing battle between pathogens and our food crops. *International Journal of Molecular Sciences, 22*, 81.
Bienert, G. P., & Chaumont, F. (2014). Aquaporin-facilitated transmembrane diffusion of hydrogen peroxide. *Biochimica et Biophysica Acta-General Subjects, 1840*, 1596-1604.
Bienert, G. P., et al. (2006). Membrane transport of hydrogen peroxide. *Biochimica et Biophysica Acta -Biomembranes, 1758*, 994-1003.
Bigeard, J., et al. (2015). Signaling mechanisms in pattern-triggered immunity (PTI). *Molecular Plant, 8*, 521-539.
Bindschedler, L. V., et al. (2006). Peroxidase-dependent apoplastic oxidative burst in *Arabidopsis* required for pathogen resistance. *The Plant Journal, 47*, 851-863.
Bjornson, M., et al. (2021). The transcriptional landscape of *Arabidopsis thaliana* pattern-triggered immunity. *Nature Plants, 7*, 579-586.
Boter, M., et al. (2004). Conserved *MYC* transcription factors play a key role in jasmonate signaling both in tomato and *Arabidopsis*. *Genes Development, 18*, 1577-1591.
Boudsocq, M., et al. (2010). Differential innate immune signalling via Ca^{2+} sensor protein kinases. *Nature, 464*, 418-422.
Boutrot, F., et al. (2010). Direct transcriptional control of the *Arabidopsis* immune receptor *FLS2* by the ethylene-dependent transcription factors *EIN3* and *EIL1*. *Proceedings of the National Academy of Sciences, 107*, 14502-14507.
Bredow, M., & Monaghan, J. (2019). Regulation of plant immune signaling by calcium-

dependent protein kinases. *Molecular Plant-Microbe Interactions, 32*, 6-19.
Brutus, A., et al. (2010). A domain swap approach reveals a role of the plant wall-associated kinase 1 (*WAK1*) as a receptor of oligogalacturonides. *Proceedings of the National Academy of Sciences, 107*, 9452-9457.
Caarls, L., et al. (2017). *Arabidopsis JASMONATE-INDUCED OXYGENASES* down-regulate plant immunity by hydroxylation and inactivation of the hormone jasmonic acid. *Proceedings of the National Academy of Sciences, 114*, 6388-6393.
Cai, Q., et al. (2016). The *SAC51* family plays a central role in thermospermine responses in *Arabidopsis*. *Plant Cell Physiology, 57*, 1583-1592.
Cao, H., et al. (1997). The *Arabidopsis NPR1* gene that controls systemic acquired resistance encodes a novel protein containing ankyrin repeats. *Cell, 88*, 57-63.
Cao, Y., et al. (2014). The kinase *LYK5* is a major chitin receptor in *Arabidopsis* and forms a chitin-induced complex with related kinase *CERK1*. *eLife, 3*, e03766.
Catinot, J., et al. (2015). *ETHYLENE RESPONSE FACTOR 96* positively regulates A rabidopsis resistance to necrotrophic pathogens by direct binding to GCC elements of jasmonate–and ethylene-responsive defence genes. *Plant, Cell & Environment, 38*, 2721-2734.
Celi, G. E. A., et al. (2023). Physiological and biochemical roles of ascorbic acid on mitigation of abiotic stresses in plants. *Plant Physiology Biochemistry*, 107970.
Çevik, V., et al. (2012). MEDIATOR25 acts as an integrative hub for the regulation of jasmonate-responsive gene expression in *Arabidopsis*. *Plant Physiology, 160*, 541-555.
Chang, C., et al. (1988). Restriction fragment length polymorphism linkage map for *Arabidopsis thaliana*. *Proceedings of the National Academy of Sciences, 85*, 6856-6860.
Chang, C., & Meyerowitz, E. M. (1986). Molecular cloning and DNA sequence of the *Arabidopsis thaliana* alcohol dehydrogenase gene. *Proceedings of the National Academy of Sciences, 83*, 1408-1412.
Chapman, J. M., et al. (2019). *RBOH*-dependent ROS synthesis and ROS scavenging by plant specialized metabolites to modulate plant development and stress responses. *Chemical Research in Toxicology, 32*, 370-396.
Chaturvedi, R., et al. (2020). Heavy metal-induced toxicity responses in plants: an overview from physicochemical to molecular level. *Cellular Molecular Phytotoxicity of Heavy Metals*, 69-88.
Chávez-Martínez, A. I., et al. (2020). *Arabidopsis* adc-silenced line exhibits differential defense responses to Botrytis cinerea and *Pseudomonas syringae* infection. *Plant Physiology Biochemistry, 156*, 494-503.
Chen, F., et al. (2003). An *Arabidopsis thaliana* gene for methylsalicylate biosynthesis, identified by a biochemical genomics approach, has a role in defense. *The Plant Journal, 36*, 577-588.
Chen, Y. C., et al. (2018). N-hydroxy-pipecolic acid is a mobile metabolite that induces systemic disease resistance in *Arabidopsis*. *Proceedings of the National Academy of Sciences, 115*, E4920-E4929.
Chen, H., et al. (2022). MSD2, an apoplastic *Mn-SOD*, contributes to root skotomorphogenic growth by modulating ROS distribution in *Arabidopsis*. *Plant Science, 317*, 111192.
Chen, H., et al. (2009). *ETHYLENE INSENSITIVE 3* and *ETHYLENE INSENSITIVE 3-LIKE 1* repress *SALICYLIC ACID INDUCTION DEFICIENT 2* expression to negatively regulate plant innate immunity in *Arabidopsis*. *The Plant Cell, 21*,

2527-2540.
Cheng, N. H., et al. (2005). Functional association of *Arabidopsis CAX1* and *CAX3* is required for normal growth and ion homeostasis. *Plant Physiology, 138*, 2048-2060.
Cheng, A. S., et al. (2006). Combinatorial analysis of transcription factor partners reveals recruitment of c-*MYC* to estrogen receptor-α responsive promoters. *Molecular Cell, 21*, 393-404.
Cheng, C. Y., et al. (2017). Araport11: a complete reannotation of the *Arabidopsis thaliana* reference genome. *The Plant Journal, 89*, 789-804.
Chinchilla, D., et al. (2007). A flagellin-induced complex of the receptor *FLS2* and *BAK1* initiates plant defence. *Nature, 448*, 497-500.
Chinchilla, D., et al. (2006). The *Arabidopsis* receptor kinase *FLS2* binds flg22 and determines the specificity of flagellin perception. *The Plant Cell, 18*, 465-476.
Chini, A., et al. (2007). The *JAZ* family of repressors is the missing link in jasmonate signalling. *Nature, 448*, 666-671.
Choudhury, F. K., et al. (2017). Reactive oxygen species, abiotic stress and stress combination. *The Plant Journal, 90*, 856-867.
Coll, N. S., et al. (2011). Programmed cell death in the plant immune system. *Cell Death & Differentiation, 18*, 1247-1256.
Cona, A., et al. (2006). Functions of amine oxidases in plant development and defence. *Trends in Plant Science, 11*, 80-88.
Conn, S. J., et al. (2011). Cell-specific vacuolar calcium storage mediated by *CAX1* regulates apoplastic calcium concentration, gas exchange, and plant productivity in *Arabidopsis*. *The Plant Cell, 23*, 240-257.
Crocomo, O., & Basso, L. (1974). Accumulation of putrescine and related amino acids in potassium deficient Sesamum. *Phytochemistry, 13*, 2659-2665.
Cui, J., et al. (2020). What is the role of putrescine accumulated under potassium deficiency? *Plant, cel l& environment, 43*, 1331-1347.
Cui, H., et al. (2015). Effector-triggered immunity: from pathogen perception to robust defense. *Annual review of plant biology, 66*, 487-511.
Czarnocka, W., & Karpiński, S. (2018). Friend or foe? Reactive oxygen species production, scavenging and signaling in plant response to environmental stresses. *Free Radical Biology Medicine, 122*, 4-20.
D'Auria, J. C. (2006). Acyltransferases in plants: a good time to be BAHD. *Current Opinion in Plant Biology*, *9*, 331-340.
Dangl, J. L., & Jones, J. D. G. (2001). Plant pathogens and integrated defence responses to infection. *Nature, 411*(6839), 826-833.
Das, K., & Roychoudhury, A. (2014). Reactive oxygen species (ROS) and response of antioxidants as ROS-scavengers during environmental stress in plants. *Frontiers in Environmental Science, 2*, 53.
Daudi, A., et al. (2012). The apoplastic oxidative burst peroxidase in *Arabidopsis* is a major component of pattern-triggered immunity. *The Plant Cell, 24*, 275-287.
de Almeida, A. J. P. O., et al. (2022). ROS: Basic concepts, sources, cellular signaling, and its implications in aging pathways. *Oxidative Medicine Cellular Longevity, 2022*.
de Oliveira, L. F., et al. (2018). Polyamine-and amino acid-related metabolism: the roles of arginine and ornithine are associated with the embryogenic potential. *Plant Cell Physiology, 59*, 1084-1098.
Del Río, L. A., & López-Huertas, E. (2016). ROS generation in peroxisomes and its role in cell signaling. *Plant Cell Physiology, 57*, 1364-1376.

Demidchik, V. (2015). Mechanisms of oxidative stress in plants: from classical chemistry to cell biology. *Environmental Experimental Botany, 109*, 212-228.

Desikan, R., et al. (2006). Ethylene-induced stomatal closure in *Arabidopsis* occurs via *AtrbohF*-mediated hydrogen peroxide synthesis. *The Pant Journal, 47*, 907-916.

Dietrich, P., et al. (2020). Plant cyclic nucleotide-gated channels: new insights on their functions and regulation. Plant Physiology, 184, 27-38.

Ding, Y., et al. (2018). Opposite roles of salicylic acid receptors *NPR1* and *NPR3*/*NPR4* in transcriptional regulation of plant immunity. *Cell, 173*, 1454-1467. e1415.

Ding, L., et al. (2011). Resistance to hemi-biotrophic F. graminearum infection is associated with coordinated and ordered expression of diverse defense signaling pathways. *PloS One, 6*, e19008.

Djamei, A., et al. (2007). Trojan horse strategy in *Agrobacterium* transformation: abusing *MAPK* defense signaling. *Science, 318*, 453-456.

Dodd, A. N., et al. (2010). The language of calcium signaling. *Annual review of plant biology, 61*, 593-620.

Dodds, P. N., & Rathjen, J. P. (2010). Plant immunity: towards an integrated view of plant–pathogen interactions. *Nature Reviews Genetics, 11*, 539-548.

Doneva, D., et al. (2021). The effects of putrescine pre-treatment on osmotic stress responses in drought-tolerant and drought-sensitive wheat seedlings. *Physiologia Plantarum, 171*, 200-216.

Drerup, M. M., et al. (2013). The calcineurin B-like calcium sensors *CBL1* and *CBL9* together with their interacting protein kinase *CIPK26* regulate the *Arabidopsis* NADPH oxidase *RBOHF*. *Molecular Plant, 6*, 559-569.

Dubiella, U., et al. (2013). Calcium-dependent protein kinase/NADPH oxidase activation circuit is required for rapid defense signal propagation. *Proceedings of the National Academy of Sciences, 110*, 8744-8749.

Duggan, C., et al. (2021). Dynamic localization of a helper NLR at the plant–pathogen interface underpins pathogen recognition. *Proceedings of the National Academy of Sciences, 118*, e2104997118.

Durrant, J., et al. (1990). Characterisation of triplet states in isolated Photosystem II reaction centres: oxygen quenching as a mechanism for photodamage. *Biochimica et Biophysica Acta -Bioenergetics, 1017*, 167-175.

Dvořák, P., et al. (2021). Signaling toward reactive oxygen species-scavenging enzymes in plants. *Frontiers in Plant Science, 11*, 618835.

Dynowski, M., et al. (2008). Plant plasma membrane water channels conduct the signalling molecule H2O2. *Biochemical Journal, 414*, 53-61.

Eckardt, N. A. (2000). Sequencing the Rice Genome. *The Plant Cell, 12*, 2011-2017.

Edel, K. H., et al. (2017). The evolution of calcium-based signalling in plants. *Current Biology, 27*, R667-R679.

Elena-Real, C. A., et al. (2021). Proposed mechanism for regulation of H_2O_2-induced programmed cell death in plants by binding of cytochrome c to 14-3-3 proteins. *The Plant Journal, 106*, 74-85.

Ellinger, D., & Voigt, C. A. (2014). Callose biosynthesis in *Arabidopsis* with a focus on pathogen response: what we have learned within the last decade. *Annals of Botany, 114*, 1349-1358.

Engelsdorf, T., et al. (2018). The plant cell wall integrity maintenance and immune signaling systems cooperate to control stress responses in *Arabidopsis thaliana*. *Science signaling, 11*, eaao3070.

Feehan, J. M., et al. (2020). Plant NLRs get by with a little help from their friends. *Current Opinion in Plant Biology, 56*, 99-108.

Felix, G., et al. (1999). Plants have a sensitive perception system for the most conserved domain of bacterial flagellin. *The Plant Journal, 18*, 265-276.

Feng, F., et al. (2012). A Xanthomonas uridine 5′-monophosphate transferase inhibits plant immune kinases. *Nature, 485*, 114-118.

Fernández-Calvo, P., et al. (2011). The *Arabidopsis bHLH* transcription factors *MYC3* and *MYC4* are targets of *JAZ* repressors and act additively with *MYC2* in the activation of jasmonate responses. *The Plant Cell, 23*, 701-715.

Fernández-Crespo, E., et al. (2015). NH4+ protects tomato plants against *Pseudomonas syringae* by activation of systemic acquired acclimation. *Journal of Experimental Botany, 66*, 6777-6790.

Feys, B. J., et al. (1994). *Arabidopsis* mutants selected for resistance to the phytotoxin coronatine are male sterile, insensitive to methyl jasmonate, and resistant to a bacterial pathogen. *The Plant Cell, 6*, 751-759.

Fincato, P., et al. (2012). The members of *Arabidopsis thaliana PAO* gene family exhibit distinct tissue-and organ-specific expression pattern during seedling growth and flower development. *Amino acids, 42*, 831-841.

Fincato, P., et al. (2011). Functional diversity inside the *Arabidopsis* polyamine oxidase gene family. *Journal of Experimental Botany, 62*, 1155-1168.

Fishman, M. R., & Shirasu, K. (2021). How to resist parasitic plants: pre- and post-attachment strategies. *Current Opinion in Plant Biology, 62*, 102004.

Fletcher, J. C., et al. (1999). Signaling of cell fate decisions by *CLAVATA3* in *Arabidopsis* shoot meristems. *Science, 283*, 1911-1914.

Fletcher, J. C., & Meyerowitz, E. M. (2000). Cell signaling within the shoot meristem. *Current Opinion in Plant Biology, 3*, 23-30.

Frei dit Frey, N., et al. (2012). Plasma membrane calcium ATPases are important components of receptor-mediated signaling in plant immune responses and development. *Plant Physiology, 159*, 798-809.

Fridman, V. A., et al. (2023). Cultivation of *Arabidopsis thaliana* in a laboratory environment. *Russian Journal of Plant Physiology, 70*, 90.

Frye, C. A., et al. (2001). Negative regulation of defense responses in plants by a conserved *MAPKK* kinase. *Proceedings of the National Academy of Sciences, 98*, 373-378.

Fu, Z. Q., & Dong, X. (2013). Systemic acquired resistance: turning local infection into global defense. *Annual review of plant biology*, 64, 839-863.

Fu, Z. Q., et al. (2012). *NPR3* and *NPR4* are receptors for the immune signal salicylic acid in plants. *Nature, 486*, 228-232.

Gandhi, A., & Oelmüller, R. (2023). Emerging roles of receptor-like protein kinases in plant response to abiotic stresses. *International Journal of Molecular Sciences*, *24*, 14762.

Gao, X., et al. (2013). Bifurcation of *Arabidopsis* NLR immune signaling via Ca^{2+}-dependent protein kinases. *PLoS Pathogens, 9*, e1003127.

Gao, M., et al. (2008). *MEKK1, MKK1/MKK2* and *MPK4* function together in a mitogen-activated protein kinase cascade to regulate innate immunity in plants. *Cell research, 18*, 1190-1198.

Garcion, C., et al. (2008). Characterization and biological function of the *ISOCHORISMATE SYNTHASE2* gene of *Arabidopsis*. *Plant Physiology, 147*, 1279-1287.

Ge, D., et al. (2022). Knowing me, knowing you: Self and non-self recognition in plant immunity. *Essays in Biochemistry, 66*, 447-458.

Geiger, D., et al. (2011). Stomatal closure by fast abscisic acid signaling is mediated

by the guard cell anion channel *SLAH3* and the receptor *RCAR1*. *Science signaling, 4*, ra32.

Geiger, D., et al. (2010). Guard cell anion channel *SLAC1* is regulated by *CDPK* protein kinases with distinct Ca^{2+} affinities. *Proceedings of the National Academy of Sciences, 107*, 8023-8028.

Gerlin, L., et al. (2021). Polyamines: double agents in disease and plant immunity. *Trends in Plant Science, 26*, 1061-1071.

Ghalati, R. E., et al. (2020). Effect of putrescine on biochemical and physiological characteristics of guava *(Psidium guajava L.)* seedlings under salt stress. *Scientia Horticulturae, 261*, 108961.

Ghosh, S., & Majee, M. (2023). Protein l-isoAspartyl Methyltransferase (PIMT) and antioxidants in plants. *Vitamins and Hormones, 121*, 413–432.

Ghuge, S. A., et al. (2015). The MeJA-inducible copper amine oxidase *AtAO1* is expressed in xylem tissue and guard cells. *Plant Signaling Behavior, 10*, e1073872.

Gill, S. S., et al. (2013). Glutathione and glutathione reductase: a boon in disguise for plant abiotic stress defense operations. *Plant Physiology Biochemistry, 70*, 204-212.

Gill, S. S., et al. (2012). Generation and scavenging of reactive oxygen species in plants under stress. *Improving Crop Resistance to Abiotic Stress*, 49-70.

Gill, S. S., & Tuteja, N. (2010a). Polyamines and abiotic stress tolerance in plants. *Plant Signaling Behavior, 5*, 26-33.

Gill, S. S., & Tuteja, N. (2010b). Reactive oxygen species and antioxidant machinery in abiotic stress tolerance in crop plants. *Plant Physiology Biochemistry, 48*, 909-930.

Gómez-Gómez, L., et al. (2001). Both the extracellular leucine-rich repeat domain and the kinase activity of *FLS2* are required for flagellin binding and signaling in *Arabidopsis*. *The Plant Cell, 13*, 1155-1163.

Gómez-Gómez, L., & Boller, T. (2000). *FLS2*: an LRR receptor-like kinase involved in the perception of the bacterial elicitor flagellin in *Arabidopsis*. *Molecular Cell, 5*, 1003-1011.

Gómez-Gómez, L., et al. (1999). A single locus determines sensitivity to bacterial flagellin in *Arabidopsis thaliana*. *The Plant Journal, 18*, 277-284.

Gong, B., et al. (2014). Sodic alkaline stress mitigation by interaction of nitric oxide and polyamines involves antioxidants and physiological strategies in *Solanum lycopersicum*. *Free Radical Biology Medicine, 71*, 36-48.

González-Hernández, A. I., et al. (2022). Putrescine: A key metabolite involved in plant development, tolerance and resistance responses to stress. *International Journal of Molecular Sciences, 23*, 2971.

Gonzalez, M. E., et al. (2011). Perturbation of spermine synthase gene expression and transcript profiling provide new insights on the role of the tetraamine spermine in *Arabidopsis* defense against Pseudomonas viridiflava. *Plant Physiology, 156*, 2266-2277.

Gould, K., et al. (2002). Do anthocyanins function as antioxidants in leaves? Imaging of H_2O_2 in red and green leaves after mechanical injury. *Plant, Cell & Environment, 25*, 1261-1269.

Greene, E. A., et al. (2003). Spectrum of chemically induced mutations from a large-scale reverse-genetic screen in *Arabidopsis*. *Genetics, 164*, 731-740.

Groß, F., et al. (2017). Copper amine oxidase 8 regulates arginine-dependent nitric oxide production in *Arabidopsis thaliana*. *Journal of experimental botany, 68*,

2149-2162.
Guerra, T., et al. (2020). Calcium-dependent protein kinase 5 links calcium signaling with N-hydroxy-l-pipecolic acid-and *SARD1*-dependent immune memory in systemic acquired resistance. *New Phytologist, 225*, 310-325.
Guttman, D. S., et al. (2014). Microbial genome-enabled insights into plant–microorganism interactions. *Nature Reviews Genetics, 15*, 797-813.
Guzel Deger, A., et al. (2015). Guard cell *SLAC1*-type anion channels mediate flagellin-induced stomatal closure. *New Phytologist, 208*, 162-173.
Hamana, K., & Matsuzaki, S. (1985). Distinct difference in the polyamine compositions of Bryophyta and Pteridophyta. *The Journal of Biochemistry, 97*, 1595-1601.
Hanfrey, C., et al. (2001). *Arabidopsis* polyamine biosynthesis: absence of ornithine decarboxylase and the mechanism of arginine decarboxylase activity. *The Plant Journal, 27*, 551-560.
Hanzawa, Y., et al. (2002). Characterization of the spermidine synthase-related gene family in *Arabidopsis thaliana*. *FEBS Letters, 527*, 176-180.
Hartmann, M., et al. (2018). Flavin monooxygenase-generated N-hydroxypipecolic acid is a critical element of plant systemic immunity. *Cell, 173*, 456-469. e416.
Heitz, T., et al. (2012). Cytochromes P450 *CYP94C1* and *CYP94B3* catalyze two successive oxidation steps of plant hormone jasmonoyl-isoleucine for catabolic turnover. *Journal of Biological Chemistry, 287*, 6296-6306.
Hilleary, R., et al. (2020). Tonoplast-localized Ca^{2+} pumps regulate Ca^{2+} signals during pattern-triggered immunity in *Arabidopsis thaliana*. *Proceedings of the National Academy of Sciences, 117*, 18849-18857.
Hiramoto, K., et al. (1996). Effect of plant phenolics on the formation of the spin-adduct of hydroxyl radical and the DNA strand breaking by hydroxyl radical. *Biological Pharmaceutical Bulletin, 19*, 558-563.
Hiruma, K., et al. (2011). *Arabidopsis ENHANCED DISEASE RESISTANCE 1* is required for pathogen-induced expression of plant defensins in nonhost resistance, and acts through interference of *MYC2*-mediated repressor function. *The Plant Journal, 67*, 980-992.
Hou, S.,& Tsuda, K. (2022). Salicylic acid and jasmonic acid crosstalk in plant immunity. *Essays in Biochemistry, 66*, 647-656.
Hou, Z. H., et al. (2013). Regulatory function of polyamine oxidase-generated hydrogen peroxide in ethylene-induced stomatal closure in *Arabidopsis thaliana*. *Journal of Integrative Agriculture, 12*(2), 251-262.
Howladar, S. M., et al. (2018). Silicon and its application method effects on modulation of cadmium stress responses in *Triticum aestivum (L.)* through improving the antioxidative defense system and polyamine gene expression. *Ecotoxicology Environmental Safety, 159*, 143-152.
Hsu, P. K., et al. (2021). Signaling mechanisms in abscisic acid-mediated stomatal closure. *The Plant Journal, 105*, 307-321.
Huang, H., et al. (2019). Mechanisms of ros regulation of plant development and stress responses. *Frontiers in Plant Science, 10*. 800.
Huang, X., & Han, B. (2014). Natural variations and genome-wide association studies in crop plants. *Annual review of plant biology, 65*, 531-551.
Huaping, H., et al. (2017). *Chitin elicitor receptor kinase 1* (*CERK1*) is required for the non-host defense response of *Arabidopsis* to Fusarium oxysporum f. Sp. cubense. *European Journal of Plant Pathology, 147*, 571-578.
Hummel, I., et al. (2004). Differential gene expression of arginine decarboxylase *ADC1* and *ADC2* in *Arabidopsis thaliana*: characterization of transcriptional

regulation during seed germination and seedling development. *New Phytologist, 163*, 519-531.

Imai, A., et al. (2004). Spermine is not essential for survival of *Arabidopsis*. *FEBS Letters, 556*, 148-152.

International Rice Genome Sequencing Project. (2005). The map-based sequence of the rice genome. *Nature, 436*, 793-800.

Jabs, T., et al. (1997). Elicitor-stimulated ion fluxes and O_2^- from the oxidative burst are essential components in triggering defense gene activation and phytoalexin synthesis in parsley. *Proceedings of the National Academy of Sciences, 94*, 4800-4805.

Jacob, F., et al. (2018). A dominant-interfering *camta3* mutation compromises primary transcriptional outputs mediated by both cell surface and intracellular immune receptors in *Arabidopsis thaliana*. *New Phytologist, 217*, 1667-1680.

Jacob, P., et al. (2021). Plant "helper" immune receptors are Ca^{2+}-permeable nonselective cation channels. *Science, 373*, 420-425.

Jacobs, A. K., et al. (2003). An *Arabidopsis* callose synthase, GSL5, is required for wound and papillary callose formation. *The Plant Cell, 15*, 2503-2513.

Jacques, S., et al. (2013). Plant proteins under oxidative attack. *Proteomics, 13*(6), 932-940.

Janeway, C. A., Jr. (1989). Approaching the asymptote? Evolution and revolution in immunology. *Cold Spring Harbor Laboratory Press, 54 Pt 1*, 1-13.

Janse van Rensburg, H. C., et al. (2021). Spermine and spermidine priming against Botrytis cinerea modulates ROS dynamics and metabolism in *Arabidopsis*. *Biomolecules, 11*, 223.

Jasso-Robles, F. I., et al. (2020). Decrease of Arabidopsis *PAO* activity entails increased *RBOH* activity, ROS content and altered responses to *Pseudomonas*. *Plant Science, 292*, 110372.

Jegla, T., et al. (2018). Evolution and structural characteristics of plant voltage-gated K^+ channels. *The Plant Cell*, 30, 2898-2909.

Jeworutzki, E., et al. (2010). Early signaling through the *Arabidopsis* pattern recognition receptors *FLS2* and *EFR* involves Ca^{2+}-associated opening of plasma membrane anion channels. *The Plant Journal, 62*, 367-378.

Jiang, X., et al. (2020). Phosphorylation of the *CAMTA3* transcription factor triggers its destabilization and nuclear export. *Plant Physiology, 184*, 1056-1071.

Jimenez-Aleman, G. H., et al. (2019). Omega hydroxylated JA-Ile is an endogenous bioactive jasmonate that signals through the canonical jasmonate signaling pathway. *Biochimica et Biophysica Acta -Molecular Cell Biology of Lipids, 1864*, 158520.

Jones, J. D., & Dangl, J. L. (2006). The plant immune system. *Nature, 444*, 323-329.

Kadota, Y., et al. (2015). Regulation of the NADPH oxidase *RBOHD* during plant immunity. *Plant Cell Physiology, 56*, 1472-1480.

Kadota, Y., et al. (2014). Direct regulation of the NADPH oxidase *RBOHD* by the PRR-associated kinase *BIK1* during plant immunity. *Molecular Cell, 54*, 43-55.

Kakehi, J. I., et al. (2008). Thermospermine is required for stem elongation in *Arabidopsis thaliana*. *Plant Cell Physiology, 49*, 1342-1349.

Kamiab, F., et al. (2014). Exogenous application of free polyamines enhance salt tolerance of pistachio (Pistacia vera L.) seedlings. *Plant Growth Regulation, 72*, 257-268.

Kang, S., et al. (2006). Overexpression in *Arabidopsis* of a plasma membrane-targeting glutamate receptor from small radish increases glutamate-mediated Ca^{2+} influx

and delays fungal infection. *Molecules Cells, 21*. 418–427.

Kasukabe, Y., et al. (2004). Overexpression of spermidine synthase enhances tolerance to multiple environmental stresses and up-regulates the expression of various stress-regulated genes in transgenic *Arabidopsis thaliana*. *Plant Cell Physiology, 45*, 712-722.

Kaszler, N., et al. (2021). Polyamine metabolism is involved in the direct regeneration of shoots from *Arabidopsis* lateral root primordia. *Plants, 10*, 305.

Katsir, L., et al. (2008). COI1 is a critical component of a receptor for jasmonate and the bacterial virulence factor coronatine. *Proceedings of the National Academy of Sciences, 105*(19), 7100-7105.

Kazan, K., & Manners, J. M. (2013). *MYC2*: the master in action. *Molecular Plant, 6*, 686-703.

Kehm, R., et al. (2021). Protein oxidation-formation mechanisms, detection and relevance as biomarkers in human diseases. *Redox Biology, 42*, 101901.

Keller, T., et al. (1998). A plant homolog of the neutrophil NADPH oxidase gp91 phox subunit gene encodes a plasma membrane protein with Ca^{2+} binding motifs. *The Plant Cell, 10*, 255-266.

Kemen, E., & Jones, J. D. (2012). Obligate biotroph parasitism: can we link genomes to lifestyles? *Trends in Plant Science, 17*, 448-457.

Khajuria, A., & Ohri, P. (2018). Exogenously applied putrescine improves the physiological responses of tomato plant during nematode pathogenesis. *Scientia Horticulturae, 230*, 35-42.

Khan, B. R., & Zolman, B. K. (2010). *pex5* Mutants that differentially disrupt PTS1 and PTS2 peroxisomal matrix protein import in *Arabidopsis*. *Plant Physiology, 154*, 1602-1615.

Kim, N. H., et al. (2013a). Pepper arginine decarboxylase is required for polyamine and γ-aminobutyric acid signaling in cell death and defense response. *Plant Physiology, 162*, 2067-2083.

Kim, D. W., et al. (2014). Polyamine oxidase5 regulates *Arabidopsis* growth through thermospermine oxidase activity. *Plant Physiology, 165*, 1575-1590.

Kim, Y., et al. (2013b). Roles of *CAMTA* transcription factors and salicylic acid in configuring the low-temperature transcriptome and freezing tolerance of A rabidopsis. *The Plant Journal, 75*, 364-376.

Kim., S. H., et al. (2013c). Putrescine regulating by stress-responsive *MAPK* cascade contributes to bacterial pathogen defense in *Arabidopsis*. *Biochemical Biophysical Research Communications, 437*, 502-508.

Kimura, S., et al. (2012). Protein phosphorylation is a prerequisite for the Ca^{2+}-dependent activation of *Arabidopsis* NADPH oxidases and may function as a trigger for the positive feedback regulation of Ca^{2+} and reactive oxygen species. *Biochimica et Biophysica Acta -Molecular Cell Research, 1823*, 398-405.

Klessig, D. F., et al. (2018). Systemic acquired resistance and salicylic acid: past, present, and future. *Molecular Plant-Microbe Interactions, 31*, 871-888.

Kloek, A. P., et al. (2001). Resistance to *Pseudomonas syringae* conferred by an *Arabidopsis thaliana* coronatine-insensitive (coi1) mutation occurs through two distinct mechanisms. *The Plant Journal, 26*, 509-522.

Klusener, B., et al. (2002). Convergence of calcium signaling pathways of pathogenic elicitors and abscisic acid in *Arabidopsis* guard cells. *Plant Physiology, 130*, 2152-2163.

Knepper, C., et al. (2011). The role of NDR1 in pathogen perception and plant defense signaling. *Plant Signaling Behavior, 6*, 1114-1116.

Knight, M. R., et al. (1991). Transgenic plant aequorin reports the effects of touch and cold-shock and elicitors on cytoplasmic calcium. *Nature, 352*, 524-526.

Kombrink, E. (2012). Chemical and genetic exploration of jasmonate biosynthesis and signaling paths. *Planta, 236*, 1351-1366.

Kong, X., et al. (2018). PHB3 maintains root stem cell niche identity through ROS-responsive AP2/ERF transcription factors in *Arabidopsis*. *Cell Reports, 22*, 1350-1363.

Koo, A. J., et al. (2014). Endoplasmic reticulum-associated inactivation of the hormone jasmonoyl-L-isoleucine by multiple members of the cytochrome P450 94 family in *Arabidopsis*. *Journal of Biological Chemistry, 289*, 29728-29738.

Koornneef, M., & Meinke, D. (2010). The development of *Arabidopsis* as a model plant. *The Plant Journal, 61*, 909-921.

Koornneef, M., et al. (1983). Linkage map of *Arabidopsis thaliana*. *Journal of Heredity, 74*, 265-272.

Köster, P., et al. (2022). Ca^{2+} signals in plant immunity. *The EMBO Journal, 41*, e110741.

Krämer, U. (2015). Planting molecular functions in an ecological context with *Arabidopsis thaliana*. *eLife, 4*, e06100.

Krasileva, K. V., et al. (2010). Activation of an *Arabidopsis* resistance protein is specified by the in planta association of its leucine-rich repeat domain with the cognate oomycete effector. *The Plant Cell, 22*, 2444-2458.

Krol, E., et al. (2010). Perception of the *Arabidopsis* danger signal peptide 1 involves the pattern recognition receptor *AtPEPR1* and its close homologue *AtPEPR2*. *Journal of Biological Chemistry, 285*, 13471-13479.

Kudla, J., et al. (2010). Calcium signals: the lead currency of plant information processing. *The Plant Cell, 22*, 541-563.

Kudla, J., et al. (2018). Advances and current challenges in calcium signaling. *New Phytologist, 218*, 414-431.

Kumar, K., et al. (2020). *Arabidopsis MAPK* signaling pathways and their cross talks in abiotic stress response. *Journal of Plant Biochemistry Biotechnology, 29*, 700-714.

Kunze, G., et al. (2004). The N Terminus of Bacterial Elongation Factor Tu Elicits Innate Immunity in *Arabidopsis* Plants. *The Plant Cell, 16*, 3496-3507.

Kwaaitaal, M., et al. (2011). Ionotropic glutamate receptor (iGluR)-like channels mediate MAMP-induced calcium influx in *Arabidopsis thaliana*. *Biochemical Journal, 440*, 355-373.

Laibach, F. (1907). Zur Frage nach der Individualität der Chromosomen in Pflanzenreich. *Beihefte zum Botanischen Centralblatt*, 191.

Laibach, F. (1943). *Arabidopsis thaliana (L.) Heynh.* als Objekt für genetische und entwicklungsphysiologische Untersuchungen. *Bot Arch, 44*, 439-455.

Laibach, F. (1951). Summer-and winter-annual races of *A. thaliana*. A contribution to the etiology of flower development. *Beitr. Biol. Pflanzen, 28*, 173-210.

Laurie-Berry, N., et al. (2006). The *Arabidopsis thaliana JASMONATE INSENSITIVE 1* gene is required for suppression of salicylic acid-dependent defenses during infection by *Pseudomonas syringae*. *Molecular Plant-Microbe Interactions, 19*, 789-800.

Lee, D., et al. (2020). Regulation of reactive oxygen species during plant immunity through phosphorylation and ubiquitination of *RBOHD*. *Nature Communications, 11*, 1838.

Lee, D. S., et al. (2017). The *Arabidopsis* cysteine-rich receptor-like kinase *CRK36*

regulates immunity through interaction with the cytoplasmic kinase *BIK1*. *Frontiers in Plant Science, 8*, 1856.

Lemaitre, B., et al. (1996). The dorsoventral regulatory gene cassette spätzle/Toll/cactus controls the potent antifungal response in Drosophila adults. *Cell, 86*, 973-983.

Lemaitre, B., et al. (1997). Drosophila host defense: differential induction of antimicrobial peptide genes after infection by various classes of microorganisms. *Proceedings of the National Academy of Sciences, 94*, 14614-14619.

Lewis, J. D., et al. (2013). The *Arabidopsis ZED1* pseudokinase is required for *ZAR1*-mediated immunity induced by the *Pseudomonas syringae* type III effector *HopZ1a*. *Proceedings of the National Academy of Sciences, 110*, 18722-18727.

Li, J., et al. (2006). *WRKY70* modulates the selection of signaling pathways in plant defense. *The Plant Journal, 46*, 477-491.

Li, J., et al. (2004). The *WRKY70* transcription factor: a node of convergence for jasmonate-mediated and salicylate-mediated signals in plant defense. *The Plant Cell, 16*, 319-331.

Li, N., et al. (2019). Signaling crosstalk between salicylic acid and ethylene/jasmonate in plant defense: do we understand what they are whispering? *International Journal of Molecular Sciences, 20*, 671.

Li, Z., et al. (2023). Resting cytosol Ca^{2+} level maintained by Ca^{2+} pumps affects environmental responses in *Arabidopsis*. *Plant Physiology, 191*, 2534-2550.

Li, J., et al. (2015). Exogenous spermidine is enhancing tomato tolerance to salinity–alkalinity stress by regulating chloroplast antioxidant system and chlorophyll metabolism. *BMC Plant Biology, 15*, 1-17.

Li, L., et al. (2014). The *FLS2*-associated kinase *BIK1* directly phosphorylates the NADPH oxidase *RbohD* to control plant immunity. *Cell Host & Microbe, 15*, 329-338.

Li, F., et al. (2013). Glutamate receptor-like channel 3.3 is involved in mediating glutathione-triggered cytosolic calcium transients, transcriptional changes, and innate immunity responses in *Arabidopsis*. *Plant Physiology, 162*, 1497-1509.

Li, Z., et al. (2016a). The alterations of endogenous polyamines and phytohormones induced by exogenous application of spermidine regulate antioxidant metabolism, metallothionein and relevant genes conferring drought tolerance in white clover. *Environmental Experimental Botany, 124*, 22-38.

Li, P., et al. (2021). The receptor-like cytoplasmic kinase RIPK regulates broad-spectrum ROS signaling in multiple layers of plant immune system. *Molecular Plant, 14*, 1652-1667.

Li, B., et al. (2016b). Transcriptional regulation of pattern-triggered immunity in plants. *Cell Host & Microbe, 19*, 641-650.

Li, C. M., et al. (2002). The Hrp pilus of *Pseudomonas syringae* elongates from its tip and acts as a conduit for translocation of the effector protein HrpZ. *The EMBO Journal*.

Li, L., et al. (2020). Atypical Resistance Protein *RPW8*/HR Triggers Oligomerization of the NLR Immune Receptor *RPP7* and Autoimmunity. *Cell Host & Microbe, 27*, 405-417.

Liang, X., & Zhou, J. M. (2018). Receptor-like cytoplasmic kinases: central players in plant receptor kinase–mediated signaling. *Annual review of plant biology, 69*, 267-299.

Liebrand, T. W., et al. (2014). Two for all: receptor-associated kinases *SOBIR1* and BAK1. *Trends in Plant Science, 19*, 123-132.

Lin, W., et al. (2014). Tyrosine phosphorylation of protein kinase complex *BAK1/BIK1*

mediates *Arabidopsis* innate immunity. *Proceedings of the National Academy of Sciences, 111*, 3632-3637.

Lindermayr, C., et al. (2005). Proteomic identification of S-nitrosylated proteins in *Arabidopsis*. *Plant Physiology, 137*, 921-930.

Liochev, S. I., & Fridovich, I. (2007). The effects of superoxide dismutase on H_2O_2 formation. *Free Radical Biology Medicine, 42*, 1465-1469.

Liu, T., et al. (2014). *Arabidopsis* mutant plants with diverse defects in polyamine metabolism show unequal sensitivity to exogenous cadaverine probably based on their spermine content. *Physiology Molecular Biology of Plants, 20*, 151-159.

Liu, Y., et al. (2019a). Anion channel *SLAH3* is a regulatory target of chitin receptor-associated kinase *PBL27* in microbial stomatal closure. *eLife, 8*, e44474.

Liu, Y., et al. (2020a). Diverse roles of the salicylic acid receptors *NPR1* and *NPR3/NPR4* in plant immunity. *The Plant Cell, 32*, 4002-4016.

Liu, P. P., et al. (2010). Altering expression of benzoic acid/salicylic acid carboxyl methyltransferase 1 compromises systemic acquired resistance and PAMP-triggered immunity in *Arabidopsis*. *Molecular Plant-Microbe Interactions, 23*, 82-90.

Liu, Y., & Zhang, S. (2004). Phosphorylation of 1-aminocyclopropane-1-carboxylic acid synthase by *MPK6*, a stress-responsive mitogen-activated protein kinase, induces ethylene biosynthesis in *Arabidopsis*. *The Plant Cell, 16*, 3386-3399.

Liu, C., et al. (2020b). Putrescine elicits ROS-dependent activation of the salicylic acid pathway in *Arabidopsis thaliana*. *Plant, Cell & Environment, 43*, 2755-2768.

Liu, C., et al. (2019b). The polyamine putrescine contributes to H_2O_2 and *RbohD/F*-dependent positive feedback loop in *Arabidopsis* PAMP-triggered immunity. *Frontiers in Plant Science, 10*, 465182.

Liu, T., et al. (2012). Chitin-induced dimerization activates a plant immune receptor. *Science, 336*(6085), 1160-1164.

Locato, V., et al. (2018). ROS and redox balance as multifaceted players of cross-tolerance: epigenetic and retrograde control of gene expression. *Journal of experimental botany, 69*, 3373-3391.

Lou, Y.-R., et al. (2016). *Arabidopsis NATA1* acetylates putrescine and decreases defense-related hydrogen peroxide accumulation. *Plant Physiology, 171*, 1443-1455.

Lu, D., et al. (2011). Direct ubiquitination of pattern recognition receptor *FLS2* attenuates plant innate immunity. *Science, 332*, 1439-1442.

Lu, H., et al. (2003). *ACD6*, a novel ankyrin protein, is a regulator and an effector of salicylic acid signaling in the *Arabidopsis* defense response. *The Plant Cell, 15*, 2408-2420.

Lu, D., et al. (2010). A receptor-like cytoplasmic kinase, *BIK1*, associates with a flagellin receptor complex to initiate plant innate immunity. *Proceedings of the National Academy of Sciences, 107*, 496-501.

Luan, S., & Wang, C. (2021). Calcium signaling mechanisms across kingdoms. *Annual review of cell developmental biology, 37*, 311-340.

Luna, E., et al. (2011). Callose deposition: a multifaceted plant defense response. *Molecular Plant-Microbe Interactions, 24*, 183-193.

Luo, J., et al. (2007). Convergent evolution in the BAHD family of acyl transferases: identification and characterization of anthocyanin acyl transferases from Arabidopsis thaliana. The Plant Journal, 50(4), 678-695.

Luo, L., et al. (2023). *MYC2*: a master switch for plant physiological processes and specialized metabolite synthesis. *International Journal of Molecular Sciences,*

24, 3511.
Luo, X., et al. (2020). Tyrosine phosphorylation of the lectin receptor-like kinase *LORE* regulates plant immunity. *The EMBO Journal, 39*, e102856.
Ma, Y., et al. (2012). Linking ligand perception by *PEPR* pattern recognition receptors to cytosolic Ca^{2+} elevation and downstream immune signaling in plants. *Proceedings of the National Academy of Sciences, 109*, 19852-19857.
Ma, S., et al. (2020). Direct pathogen-induced assembly of an NLR immune receptor complex to form a holoenzyme. *Science, 370*, eabe3069.
Macho, A. P., & Zipfel, C. (2014). Plant PRRs and the Activation of Innate Immune Signaling. *Molecular Cell, 54*, 263-272.
Maierhofer, T., et al. (2014). Site-and kinase-specific phosphorylation-mediated activation of SLAC1, a guard cell anion channel stimulated by abscisic acid. *Science signaling, 7*, ra86.
Marina, M., et al. (2008). Apoplastic polyamine oxidation plays different roles in local responses of tobacco to infection by the necrotrophic fungus Sclerotinia sclerotiorum and the biotrophic bacterium *Pseudomonas viridiflava*. *Plant Physiology, 147*, 2164-2178.
Martinez, C., et al. (1998). Apoplastic peroxidase generates superoxide anions in cells of cotton cotyledons undergoing the hypersensitive reaction to Xanthomonas campestris pv. malvacearum race 18. *Molecular Plant-Microbe Interactions, 11*, 1038-1047.
Maruta, N., et al. (2022). Structural basis of NLR activation and innate immune signalling in plants. *Immunogenetics, 74*, 5-26.
Mbengue, M., et al. (2016). Clathrin-dependent endocytosis is required for immunity mediated by pattern recognition receptor kinases. *Proceedings of the National Academy of Sciences, 113*, 11034-11039.
Medzhitov, R. (2001). Toll-like receptors and innate immunity. *Nature Reviews Immunology, 1*, 135-145.
Mehler, A. H. (1951). Studies on reactions of illuminated chloroplasts: I. Mechanism of the reduction of oxygen and other hill reagents. *Archives of Biochemistry Biophysics, 33*, 65-77.
Meinke, D. W., et al. (1998). *Arabidopsis* thaliana: a model plant for genome analysis. *Science, 282*, 662-682.
Melotto, M., et al. (2008). Role of stomata in plant innate immunity and foliar bacterial diseases. *Annu. Rev. Phytopathol., 46*, 101-122.
Melotto, M., et al. (2006). Plant stomata function in innate immunity against bacterial invasion. *Cell, 126*, 969-980.
Melotto, M., et al. (2017). Stomatal defense a decade later. *Plant Physiology, 174*, 561-571.
Meng, X., et al. (2013). Phosphorylation of an *ERF* transcription factor by *Arabidopsis MPK3/MPK6* regulates plant defense gene induction and fungal resistance. *The Plant Cell, 25*, 1126-1142.
Meng, X., & Zhang, S. (2013). *MAPK* cascades in plant disease resistance signaling. *Annual Review of Phytopathology, 51*, 245-266.
Meraj, T. A., et al. (2020). Transcriptional factors regulate plant stress responses through mediating secondary metabolism. *Genes, 11*, 346.
Messens, J., & Collet, J.F. (2013). Thiol–disulfide exchange in signaling: disulfide bonds as a switch. *Antioxidants & redox signaling, 18*, 1594–1596.
Meyer, Y., et al. (2012). Thioredoxin and glutaredoxin systems in plants: molecular mechanisms, crosstalks, and functional significance. *Antioxidants Redox*

Signaling, 17, 1124-1160.
Meyerowitz, E. M. (2001). Prehistory and History of *Arabidopsis* Research. *Plant Physiology, 125*, 15-19.
Meyerowitz, E. M., & Pruitt, R. E. (1985). *Arabidopsis* thaliana and Plant Molecular Genetics. *Science, 229*, 1214-1218.
Michael, A. J. (2016). Polyamines in eukaryotes, bacteria, and archaea. *Journal of Biological Chemistry, 291*, 14896-14903.
Miculan, M., et al. (2021). A forward genetics approach integrating genome-wide association study and expression quantitative trait locus mapping to dissect leaf development in maize (*Zea mays*). *The Plant Journal, 107*, 1056-1071.
Miller, G., et al. (2010). Reactive oxygen species homeostasis and signalling during drought and salinity stresses. *Plant, Cell & Environment, 33*, 453-467.
Mishina, T. E., & Zeier, J. (2007). Pathogen-associated molecular pattern recognition rather than development of tissue necrosis contributes to bacterial induction of systemic acquired resistance in *Arabidopsis*. *The Plant Journal, 50*, 500-513.
Mitsuya, Y., et al. (2009). Spermine signaling plays a significant role in the defense response of *Arabidopsis* thaliana to cucumber mosaic virus. *Journal of Plant Physiology, 166*, 626-643.
Mittal, S., & Davis, K. R. (1995). Role of the phytotoxin coronatine in the infection of *Arabidopsis* thaliana by *Pseudomonas syringae pv. tomato*. *MPMI-Molecular Plant Microbe Interactions, 8*, 165-171.
Mittler, R., & Blumwald, E. (2015). The roles of ROS and ABA in systemic acquired acclimation. *The Plant Cell, 27*, 64-70.
Mittler, R., et al. (2022). Reactive oxygen species signalling in plant stress responses. *Nature Reviews Molecular Cell Biology, 23*, 663-679.
Miya, A., et al. (2007). *CERK1*, a LysM receptor kinase, is essential for chitin elicitor signaling in *Arabidopsis*. *Proceedings of the National Academy of Sciences, 104*, 19613-19618.
Mo, H., et al. (2015). Cotton *ACAULIS5* is involved in stem elongation and the plant defense response to Verticillium dahliae through thermospermine alteration. *Plant Cell Reports, 34*, 1975-1985.
Møller, S. G., & McPherson, M. J. (1998). Developmental expression and biochemical analysis of the *Arabidopsis* atao1 gene encoding an H_2O_2-generating diamine oxidase. *The Plant Journal, 13*, 781-791.
Monaghan, J., et al. (2015). The calcium-dependent protein kinase *CPK28* negatively regulates the *BIK1*-mediated PAMP-induced calcium burst. *Plant Signaling Behavior, 10*, e1018497.
Monaghan, J., et al. (2014). The calcium-dependent protein kinase *CPK28* buffers plant immunity and regulates *BIK1* turnover. *Cell Host & Microbe, 16*, 605-615.
Montillet, J.-L., et al. (2013). An abscisic acid-independent oxylipin pathway controls stomatal closure and immune defense in *Arabidopsis*. *PLoS Biology, 11*, e1001513.
Mor, A., et al. (2014). Singlet oxygen signatures are detected independent of light or chloroplasts in response to multiple stresses. *Plant Physiology, 165*, 249-261.
Morales, J., et al. (2016). The *Arabidopsis* NADPH oxidases *RbohD* and *RbohF* display differential expression patterns and contributions during plant immunity. *Journal of experimental botany, 67*, 1663-1676.
Moreau, M., et al. (2012). *EDS1* contributes to nonhost resistance of *Arabidopsis thaliana* against Erwinia amylovora. *Molecular Plant-Microbe Interactions, 25*, 421-430.

Morgan, A. J., & Jacob, R. (1994). Ionomycin enhances Ca^{2+} influx by stimulating store-regulated cation entry and not by a direct action at the plasma membrane. *Biochemical Journal, 300*, 665-672.

Moselhy, S. S., et al. (2016). Spermidine, a polyamine, confers resistance to rice blast. *Journal of pesticide science, 41*, 79-82.

Mousavi, S. A., et al. (2013). GLUTAMATE RECEPTOR-LIKE genes mediate leaf-to-leaf wound signalling. *Nature, 500*, 422-426.

Müller, M., & Munné-Bosch, S. (2015). Ethylene response factors: a key regulatory hub in hormone and stress signaling. *Plant Physiology, 169*, 32-41.

Muñiz, L., et al. (2008). *ACAULIS5* controls *Arabidopsis* xylem specification through the prevention of premature cell death. *Development (Cambridge, England)*, *135*, 2573–2582.

Munné-Bosch, S. (2005). The role of α-tocopherol in plant stress tolerance. *Journal of Plant Physiology, 162*, 743-748.

Mur, L. A., et al. (2006). The outcomes of concentration-specific interactions between salicylate and jasmonate signaling include synergy, antagonism, and oxidative stress leading to cell death. *Plant Physiology, 140*, 249-262.

Mustafavi, S. H., et al. (2018). Polyamines and their possible mechanisms involved in plant physiological processes and elicitation of secondary metabolites. *Acta Physiologiae Plantarum, 40*, 1-19.

Nambeesan, S., et al. (2012). Polyamines attenuate ethylene-mediated defense responses to abrogate resistance to Botrytis cinerea in tomato. *Plant Physiology, 158*, 1034-1045.

Navarro, L., et al. (2004). The transcriptional innate immune response to flg22. Interplay and overlap with Avr gene-dependent defense responses and bacterial pathogenesis. *Plant Physiology, 135*, 1113-1128.

Nawrath, C., et al. (2002). *EDS5*, an essential component of salicylic acid–dependent signaling for disease resistance in *Arabidopsis*, is a member of the MATE transporter family. *The Plant Cell, 14*, 275-286.

Nekrasov, V., et al. (2009). Control of the pattern-recognition receptor *EFR* by an ER protein complex in plant immunity. *The EMBO Journal, 28*, 3428-3438.

Ngou, B. P. M., et al. (2021). Mutual potentiation of plant immunity by cell-surface and intracellular receptors. *Nature, 592*, 110-115.

Ngou, B. P. M., et al. (2024). Evolutionary trajectory of pattern recognition receptors in plants. *Nature Communications, 15*, 308.

Nickstadt, A., et al. (2004). The jasmonate-insensitive mutant jin1 shows increased resistance to biotrophic as well as necrotrophic pathogens. *Molecular Plant Pathology, 5*, 425-434.

Nishimura, M. T., et al. (2017). TIR-only protein *RBA1* recognizes a pathogen effector to regulate cell death in *Arabidopsis*. *Proceedings of the National Academy of Sciences, 114*, E2053-E2062.

Nishimura, M. T., et al. (2003). Loss of a callose synthase results in salicylic acid-dependent disease resistance. *Science, 301*, 969-972.

Noutoshi, Y., et al. (2012). Novel plant immune-priming compounds identified via high-throughput chemical screening target salicylic acid glucosyltransferases in *Arabidopsis*. *The Plant Cell, 24*, 3795-3804.

Nühse, T. S., et al. (2007). Quantitative phosphoproteomic analysis of plasma membrane proteins reveals regulatory mechanisms of plant innate immune responses. *The Plant Journal, 51*, 931-940.

Nuhse, T. S., et al. (2000). Microbial elicitors induce activation and dual

phosphorylation of the *Arabidopsis* thaliana *MAPK6*. *Journal of Biological Chemistry, 275*, 7521-7526.

Nüsslein-Volhard, C. (2022). The Toll gene in Drosophila pattern formation. *Trends in Genetics , 38*, 231-245.

O'Brien, J. A., et al. (2012). A peroxidase-dependent apoplastic oxidative burst in cultured *Arabidopsis* cells functions in MAMP-elicited defense. *Plant Physiology, 158*, 2013-2027.

O'Malley, R. C., et al. (2015). A user's guide to the *Arabidopsis* T-DNA insertion mutant collections. *Plant functional genomics: methods*, 323-342.

Ogasawara, Y., et al. (2008). Synergistic activation of the *Arabidopsis* NADPH oxidase *AtrbohD* by Ca^{2+} and phosphorylation. *Journal of Biological Chemistry, 283*, 8885-8892.

Ono, E., et al. (2020). *RLP23* is required for *Arabidopsis* immunity against the grey mould pathogen Botrytis cinerea. *Scientific Reports, 10*, 13798.

Pál, M., et al. (2021). Unfinished story of polyamines: Role of conjugation, transport and light-related regulation in the polyamine metabolism in plants. *Plant Science, 308*, 110923.

Pandey, S. P., & Somssich, I. E. (2009). The role of *WRKY* transcription factors in plant immunity. *Plant Physiology, 150*, 1648-1655.

Pauwels, L., et al. (2010). *NINJA* connects the co-repressor TOPLESS to jasmonate signalling. *Nature, 464*, 788-791.

Pei, Z.-M., et al. (2000). Calcium channels activated by hydrogen peroxide mediate abscisic acid signalling in guard cells. *Nature, 406*, 731-734.

Peng, Y., et al. (2021). Salicylic acid: biosynthesis and signaling. *Annual review of plant biology, 72*, 761-791.

Perez-Amador, M. A., et al. (2002). Induction of the arginine decarboxylase *ADC2* gene provides evidence for the involvement of polyamines in the wound response in *Arabidopsis*. *Plant Physiology, 130*, 1454-1463.

Peters, J. L., et al. (2003). Forward genetics and map-based cloning approaches. *Trends in Plant Science, 8*, 484-491.

Petit-Houdenot, Y., & Fudal, I. (2017). Complex Interactions between Fungal Avirulence Genes and Their Corresponding Plant Resistance Genes and Consequences for Disease Resistance Management. *Frontiers in Plant Science, 8*, 1072.

Pieterse, C. M., et al. (2012). Hormonal modulation of plant immunity. *Annual Review of Cell Developmental Biology, 28*, 489-521.

Pinto, E., et al. (2003). Heavy metal–induced oxidative stress in algae 1. *Journal of Phycology, 39*(6), 1008-1018.

Planas-Portell, J., et al. (2013). Copper-containing amine oxidases contribute to terminal polyamine oxidation in peroxisomes and apoplast of *Arabidopsis* thaliana. *BMC Plant Biology, 13*, 1-13.

Poltorak, A., et al. (1998). Defective LPS signaling in C3H/HeJ and C57BL/10ScCr mice: mutations in *Tlr4* gene. *Science, 282*, 2085-2088.

Poole, L. B., & Nelson, K. (2008). Discovering mechanisms of signaling-mediated cysteine oxidation. *Current Opinion in Chemical Biology, 12*, 18-24.

Poudel, A. N., et al. (2019). 12-Hydroxy-jasmonoyl-L-isoleucine is an active jasmonate that signals through *CORONATINE INSENSITIVE 1* and contributes to the wound response in *Arabidopsis*. *Plant Cell Physiology, 60*, 2152-2166.

Provart, N. J., et al. (2016). 50 years of *Arabidopsis* research: highlights and future directions. *New Phytologist, 209*, 921-944.

Pruitt, R. N., et al. (2021). The *EDS1–PAD4–ADR1* node mediates *Arabidopsis* pattern-triggered immunity. *Nature, 598*(7881), 495-499.

Pryde, K. R., & Hirst, J. (2011). Superoxide is produced by the reduced flavin in mitochondrial complex I: a single, unified mechanism that applies during both forward and reverse electron transfer. *Journal of Biological Chemistry, 286*, 18056-18065.

Qi, G., et al. (2018a). Pandemonium breaks out: disruption of salicylic acid-mediated defense by plant pathogens. *Molecular Plant, 11*, 1427-1439.

Qi, J., et al. (2018b). Reactive oxygen species signaling and stomatal movement in plant responses to drought stress and pathogen attack. *Journal of integrative plant biology, 60*, 805-826.

Qi, J., et al. (2017). Apoplastic ROS signaling in plant immunity. *Current Opinion in Plant Biology, 38*, 92-100.

Qiu, J. L., et al. (2008). *Arabidopsis* mitogen-activated protein kinase kinases *MKK1* and *MKK2* have overlapping functions in defense signaling mediated by *MEKK1*, *MPK4*, and *MKS1*. *Plant Physiology, 148*, 212-222.

Qu, Y., et al. (2014). Copper amine oxidase and phospholipase D act independently in abscisic acid (ABA)-induced stomatal closure in Vicia faba and *Arabidopsis*. *Journal of Plant Research, 127*, 533-544.

Rady, M. M., & Hemida, K. A. (2015). Modulation of cadmium toxicity and enhancing cadmium-tolerance in wheat seedlings by exogenous application of polyamines. *Ecotoxicology Environmental Safety, 119*, 178-185.

Rafiqi, M., et al. (2009). In the trenches of plant pathogen recognition: Role of NB-LRR proteins. *Seminars in Cell & Developmental Biology, 20*, 1017-1024.

Rahmati Ishka, M., et al. (2021). *Arabidopsis* Ca^{2+}-ATPases 1, 2, and 7 in the endoplasmic reticulum contribute to growth and pollen fitness. *Plant Physiology, 185*, 1966-1985.

Ramel, F., et al. (2012). Chemical quenching of singlet oxygen by carotenoids in plants. *Plant Physiology, 158*, 1267-1278.

Ranf, S., et al. (2014). Microbe-associated molecular pattern-induced calcium signaling requires the receptor-like cytoplasmic kinases, *PBL1* and *BIK1*. *BMC Plant Biology, 14*, 1-15.

Ranf, S., et al. (2011). Interplay between calcium signalling and early signalling elements during defence responses to microbe-or damage-associated molecular patterns. *The Plant Journal, 68*, 100-113.

Ranf, S., et al. (2015). A lectin S-domain receptor kinase mediates lipopolysaccharide sensing in *Arabidopsis* thaliana. *Nature Immunology, 16*, 426-433.

Ranf, S., et al. (2012). Defense-related calcium signaling mutants uncovered via a quantitative high-throughput screen in *Arabidopsis* thaliana. *Molecular Plant, 5*, 115-130.

Reddie, K. G., & Carroll, K. S. (2008). Expanding the functional diversity of proteins through cysteine oxidation. *Current Opinion in Chemical Biology, 12*, 746-754.

Rédei, G. P. (1962). Single locus heterosis. *Zeitschrift für Vererbungslehre, 93*, 164-170.

Rédei, G. P. (1975). *Arabidopsis* as a genetic tool. *Annual Review of Genetics, 9*, 111-127.

Rédei, G. P. (1992). A heuristic glance at the past of *Arabidopsis* genetics. *Methods in Arabidopsis research*, 1-15.

Rekhter, D., et al. (2019). Isochorismate-derived biosynthesis of the plant stress hormone salicylic acid. *Science, 365*, 498-502.

Reth, M. (2002). Hydrogen peroxide as second messenger in lymphocyte activation.

Nature Immunology, 3, 1129-1134.

Robatzek, S., et al. (2006). Ligand-induced endocytosis of the pattern recognition receptor FLS2 in *Arabidopsis*. *Genes Development, 20*, 537-542.

Rossi, F. R., et al. (2015). Role of *ARGININE DECARBOXYLASE* (*ADC*) in *Arabidopsis thaliana* defence against the pathogenic bacterium *Pseudomonas viridiflava. Plant Biology, 17*, 831-839.

Rosso, M. G., et al. (2003). An *Arabidopsis* thaliana T-DNA mutagenized population (GABI-Kat) for flanking sequence tag-based reverse genetics. *Plant molecular biology, 53*, 247-259.

Roux, M., et al. (2011). The *Arabidopsis* leucine-rich repeat receptor–like kinases *BAK1/SERK3* and *BKK1/SERK4* are required for innate immunity to hemibiotrophic and biotrophic pathogens. *The Plant Cell, 23*, 2440-2455.

Roy, M., & Wu, R. (2002). Overexpression of S-adenosylmethionine decarboxylase gene in rice increases polyamine level and enhances sodium chloride-stress tolerance. *Plant Science, 163*, 987-992.

Rui, Y., & Dinneny, J. R. (2020). A wall with integrity: surveillance and maintenance of the plant cell wall under stress. *New Phytologist, 225*, 1428-1439.

Sagi, M., & Fluhr, R. (2001). Superoxide production by plant homologues of the gp91phox NADPH oxidase. Modulation of activity by calcium and by tobacco mosaic virus infection. *Plant Physiology, 126*, 1281-1290.

Sagor, G., et al. (2013). The polyamine spermine protects *Arabidopsis* from heat stress-induced damage by increasing expression of heat shock-related genes. *Transgenic Research, 22*, 595-605.

Sahu, P. K., et al. (2020). Next generation sequencing based forward genetic approaches for identification and mapping of causal mutations in crop plants: A Comprehensive Review. *Plants (Basel, Switzerland)*, *9*, 1355.

Saile, S. C., et al. (2021). *Arabidopsis ADR1* helper NLR immune receptors localize and function at the plasma membrane in a phospholipid dependent manner. *New Phytologist, 232*, 2440-2456.

Sakata, N., & Ishiga, Y. (2023). Prevention of stomatal entry as a strategy for plant disease control against foliar pathogenic *Pseudomonas* species. *Plants, 12*, 590.

Samardakiewicz, S., et al. (2012). Is callose a barrier for lead ions entering Lemna minor L. root cells? *Protoplasma, 249*, 347-351.

Scandalios, J. G. (1993). Oxygen stress and superoxide dismutases. *Plant Physiology, 101*, 7.

Scherzer, S., et al. (2012). Multiple calcium-dependent kinases modulate ABA-activated guard cell anion channels. *Molecular Plant, 5*, 1409-1412.

Schilmiller, A. L., & Howe, G. A. (2005). Systemic signaling in the wound response. *Current Opinion in Plant Biology, 8*, 369-377.

Schulze, B., et al. (2010). Rapid heteromerization and phosphorylation of ligand-activated plant transmembrane receptors and their associated kinase *BAK1*. *Journal of Biological Chemistry, 285*, 9444-9451.

Schweizer, F., et al. (2013). *Arabidopsis* basic helix-loop-helix transcription factors *MYC2*, *MYC3*, and *MYC4* regulate glucosinolate biosynthesis, insect performance, and feeding behavior. *The Plant Cell, 25*, 3117-3132.

Seifi, H. S., et al. (2019). Spermine is a potent plant defense activator against gray mold disease on *Solanum lycopersicum*, *Phaseolus vulgaris,* and *Arabidopsis thaliana*. *Phytopathology*, *109*, 1367-1377.

Sequera-Mutiozabal, M. I., et al. (2016). Global metabolic profiling of *Arabidopsis POLYAMINE OXIDASE 4* (*AtPAO4*) loss-of-function mutants exhibiting

delayed dark-induced senescence. *Frontiers in Plant Science, 7*, 178777.
Serrano, M., et al. (2013). Export of salicylic acid from the chloroplast requires the multidrug and toxin extrusion-like transporter *EDS5*. *Plant Physiology, 162*, 1815-1821.
Sessions, A., et al. (2002). A high-throughput *Arabidopsis* reverse genetics system. *The Plant Cell, 14*, 2985-2994.
Seto, D., et al. (2017). Expanded type III effector recognition by the *ZAR1* NLR protein using *ZED1*-related kinases. *Nature Plants, 3*, 1-4.
Shan, Q., et al. (2013). Targeted genome modification of crop plants using a CRISPR-Cas system. *Nature Biotechnology, 31*, 686-688.
Shang, Y., et al. (2016). BRI1-associated receptor kinase 1 regulates guard cell ABA signaling mediated by open stomata 1 in *Arabidopsis*. *Molecular Plant, 9*, 447-460.
Sharma, P., et al. (2012). Reactive oxygen species, oxidative damage, and antioxidative defense mechanism in plants under stressful conditions. *Journal of Botany, 2012: 217037.*
Sheard, L. B., et al. (2010). Jasmonate perception by inositol-phosphate-potentiated *COI1–JAZ* co-receptor. *Nature, 468*, 400-405.
Sheikh, A. H., et al. (2016). Regulation of *WRKY46* transcription factor function by mitogen-activated protein kinases in *Arabidopsis* thaliana. *Frontiers in Plant Science, 7*, 61.
Shinya, T., et al. (2014). Selective regulation of the chitin-induced defense response by the *Arabidopsis* receptor-like cytoplasmic kinase *PBL 27*. *The Plant Journal, 79*, 56-66.
Shiu, S.-H., & Bleecker, A. B. (2003). Expansion of the receptor-like kinase/pelle gene family and receptor-like proteins in *Arabidopsis Plant Physiology, 132*, 530-543.
Sies, H., et al. (2022). Defining roles of specific reactive oxygen species (ROS) in cell biology and physiology. *Nature Reviews Molecular Cell Biology, 23*, 499-515.
Singh, D. (2022). Juggling with reactive oxygen species and antioxidant defense system–A coping mechanism under salt stress. *Plant Stress, 5*, 100093.
Smirnoff, N., & Arnaud, D. (2019). Hydrogen peroxide metabolism and functions in plants. *New Phytologist, 221*, 1197-1214.
Smith, J. M., et al. (2014). Sensitivity to Flg22 is modulated by ligand-induced degradation and de novo synthesis of the endogenous flagellin-receptor *FLAGELLIN-SENSING2*. *Plant Physiology, 164*, 440-454.
Somerville, C., & Koornneef, M. (2002). A fortunate choice: the history of *Arabidopsis* as a model plant. *Nature Reviews Genetics, 3*, 883-889.
Somssich, M. (2019). A short history of *Arabidopsis thaliana (L.) Heynh. Columbia-0*. *PeerJ Preprints, 7*: e26931v5
Somssich, M. (2022). The dawn of plant molecular biology: how three key methodologies paved the way. *Current Protocols, 2*, e417.
Song, S., et al. (2017). *MYC5* is involved in jasmonate-regulated plant growth, leaf senescence and defense responses. *Plant Cell Physiology, 58*, 1752-1763.
Soyka, S., & Heyer, A. G. (1999). *Arabidopsis* knockout mutation of *ADC2* gene reveals inducibility by osmotic stress. *FEBS Letters, 458*, 219-223.
Spoel, S. H., et al. (2003). *NPR1* modulates cross-talk between salicylate-and jasmonate-dependent defense pathways through a novel function in the cytosol. *The Plant Cell, 15*, 760-770.
St-Pierre, B., & De Luca, V. (2000). Origin and diversification of the BAHD

superfamily of acyltransferases involved in secondary metabolism. *Recent Advances in Phytochemistry*, *34*, 285-315.

Stael, S., et al. (2012). Plant organellar calcium signalling: an emerging field. *Journal of experimental botany, 63*, 1525-1542.

Staswick, P. E., & Tiryaki, I. (2004). The oxylipin signal jasmonic acid is activated by an enzyme that conjugates it to isoleucine in *Arabidopsis*. *The Plant Cell, 16*, 2117-2127.

Steele, J. F. C., et al. (2019). Structural and biochemical studies of an NB-ARC domain from a plant NLR immune receptor. *PloS one, 14*, e0221226.

Strawn, M. A., et al. (2007). *Arabidopsis* isochorismate synthase functional in pathogen-induced salicylate biosynthesis exhibits properties consistent with a role in diverse stress responses. *Journal of Biological Chemistry, 282*, 5919-5933.

Strohm, A. K., et al. (2015). Natural variation in the expression of *ORGANIC CATION TRANSPORTER 1* affects root length responses to cadaverine in *Arabidopsis*. *Journal of experimental botany, 66*, 853-862.

Suarez-Rodriguez, M. C., et al. (2007). *MEKK1* is required for flg22-induced *MPK4* activation in *Arabidopsis* plants. *Plant Physiology, 143*, 661-669.

Sumimoto, H. (2008). Structure, regulation and evolution of Nox-family NADPH oxidases that produce reactive oxygen species. *The FEBS Journal, 275*, 3249-3277.

Sun, T., et al. (2020). Redundant *CAMTA* transcription factors negatively regulate the biosynthesis of salicylic acid and N-hydroxypipecolic acid by modulating the expression of *SARD1* and *CBP60g*. *Molecular Plant, 13*, 144-156.

Sun, L., et al. (2022). TOUCH 3 and *CALMODULIN 1/4/6* cooperate with calcium-dependent protein kinases to trigger calcium-dependent activation of *CAM-BINDING PROTEIN 60-LIKE G* and regulate fungal resistance in plants. *The Plant Cell, 34*, 4088-4104.

Sun, T., & Zhang, Y. (2022). MAP kinase cascades in plant development and immune signaling. *EMBO reports, 23*, e53817.

Sun, T., et al. (2015). ChIP-seq reveals broad roles of *SARD1* and *CBP60g* in regulating plant immunity. *Nature Communications, 6*, 10159.

Sun, W., et al. (2012). Probing the *Arabidopsis* Flagellin Receptor: *FLS2-FLS2* Association and the Contributions of Specific Domains to Signaling Function *The Plant Cell, 24*, 1096-1113.

Sun, Y., et al. (2013). Structural basis for flg22-induced activation of the *Arabidopsis FLS2-BAK1* immune complex. *Science, 342*, 624-628.

Swanson, S., & Gilroy, S. (2010). ROS in plant development. *Physiologia Plantarum, 138*, 384-392.

Szalai, G., et al. (2017). Comparative analysis of polyamine metabolism in wheat and maize plants. *Plant Physiology Biochemistry, 112*, 239-250.

Tada, Y., et al. (2008). Plant immunity requires conformational charges of *NPR1* via S-nitrosylation and thioredoxins. *Science, 321*, 952-956.

Tajti, J., et al. (2018). Comparative study on the effects of putrescine and spermidine pre-treatment on cadmium stress in wheat. *Ecotoxicology Environmental Safety, 148*, 546-554.

Takahashi, Y., et al. (2010). Characterization of five polyamine oxidase isoforms in *Arabidopsis* thaliana. *Plant Cell Reports, 29*, 955-965.

Takahashi, T., & Kakehi, J.-I. (2010). Polyamines: ubiquitous polycations with unique roles in growth and stress responses. *Annals of botany, 105*, 1-6.

Takahashi, Y., et al. (2018). Characterization of the polyamine biosynthetic pathways and salt stress response in Brachypodium distachyon. *Journal of Plant Growth Regulation, 37*, 625-634.

Tameling, W. I. L., et al. (2006). Mutations in the NB-ARC Domain of I-2 That Impair ATP Hydrolysis Cause Autoactivation. *Plant Physiology, 140*, 1233-1245.

Tanaka, K., et al. (2014). Extracellular ATP acts as a damage-associated molecular pattern (DAMP) signal in plants. *Frontiers in Plant Science, 5*, 446.

Tanaka, K., & Heil, M. (2021). Damage-associated molecular patterns (DAMPs) in plant innate immunity: applying the danger model and evolutionary perspectives. *Annual review of phytopathology, 59*, 53-75.

Tang, D., et al. (2017). Receptor kinases in plant-pathogen interactions: more than pattern recognition. *The Plant Cell, 29*, 618-637.

Tanji, T., et al. (2007). Toll and IMD pathways synergistically activate an innate immune response in Drosophila melanogaster. *Molecular and cellular biology, 27*, 4578-4588.

Tassoni, A., et al. (2000). Polyamine content and metabolism in *Arabidopsis thaliana* and effect of spermidine on plant development. *Plant Physiology Biochemistry, 38*, 383-393.

Tavladoraki, P., et al. (2016). Copper-containing amine oxidases and FAD-dependent polyamine oxidases are key players in plant tissue differentiation and organ development. *Frontiers in Plant Science, 7*, 195327.

Tavladoraki, P., et al. (2012). Polyamine catabolism: target for antiproliferative therapies in animals and stress tolerance strategies in plants. *Amino acids, 42*, 411-426.

Tavladoraki, P., et al. (2006). Heterologous expression and biochemical characterization of a polyamine oxidase from *Arabidopsis* involved in polyamine back conversion. *Plant Physiology, 141*, 1519-1532.

Tavormina, P., et al. (2015). The plant peptidome: an expanding repertoire of structural features and biological functions. *The Plant Cell, 27*, 2095-2118.

Taylor, N. L., et al. (2009). Abiotic environmental stress induced changes in the *Arabidopsis* thaliana chloroplast, mitochondria and peroxisome proteomes. *Journal of Proteomics, 72*, 367-378.

The *Arabidopsis* Genome, I. (2000). Analysis of the genome sequence of the flowering plant *Arabidopsis* thaliana. *Nature, 408*, 796-815.

Thines, B., et al. (2007). *JAZ* repressor proteins are targets of the SCFCOI1 complex during jasmonate signalling. *Nature, 448*, 661-665.

Thomas, C. M., & Jones, J. D. (2007). Molecular analysis of *Agrobacterium* T-DNA integration in tomato reveals a role for left border sequence homology in most integration events. *Molecular Genetics and Genomics, 278*(4), 411-420.

Thomma, B. P., et al. (2011). Of PAMPs and effectors: the blurred PTI-ETI dichotomy. *Plant Cell, 23*, 4-15.

Thor, K., et al. (2020). The calcium-permeable channel *OSCA1.3* regulates plant stomatal immunity. *Nature, 585*, 569-573.

Tian, W., et al. (2019). A calmodulin-gated calcium channel links pathogen patterns to plant immunity. *Nature, 572*, 131-135.

Tian, W., et al. (2020). Calcium spikes, waves and oscillations in plant development and biotic interactions. *Nature Plants, 6*, 750-759.

Tiburcio, A. F., et al. (2014). The roles of polyamines during the lifespan of plants: from development to stress. *Planta, 240*, 1-18.

Tilman, D., et al. (2011). Global food demand and the sustainable intensification of

agriculture. *Proceedings of the National Academy of Sciences, 108*, 20260-20264.

Tiwari, M., et al. (2022). Agrobacterium-mediated gene transfer: recent advancements and layered immunity in plants. *Planta, 256*, 37.

Tomar, P. C., et al. (2013). Cadaverine: a lysine catabolite involved in plant growth and development. *Plant Signaling Behavior, 8*(10), e25850.

Torrens-Spence, M. P., et al. (2019). *PBS3* and *EPS1* complete salicylic acid biosynthesis from isochorismate in *Arabidopsis*. *Molecular Plant, 12*, 1577-1586.

Torres, M. A., et al. (2002). *Arabidopsis* gp91phox homologues *AtrbohD* and *AtrbohF* are required for accumulation of reactive oxygen intermediates in the plant defense response. *Proceedings of the National Academy of Sciences, 99*, 517-522.

Torres, M. A., et al. (2005). Pathogen-induced, NADPH oxidase–derived reactive oxygen intermediates suppress spread of cell death in *Arabidopsis* thaliana. *Nature genetics, 37*, 1130-1134.

Torres, M. A., et al. (2006). Reactive oxygen species signaling in response to pathogens. *Plant Physiology, 141*, 373-378.

Torres, M. A., et al. (1998). Six *Arabidopsis* thaliana homologues of the human respiratory burst oxidase (gp91phox). *The Plant Journal, 14*, 365-370.

Toumi, I., et al. (2019). Genetically modified heat shock protein90s and polyamine oxidases in *Arabidopsis* reveal their interaction under heat stress affecting polyamine acetylation, oxidation and homeostasis of reactive oxygen species. *Plants, 8*, 323.

Triantaphylides, C., et al. (2008). Singlet oxygen is the major reactive oxygen species involved in photooxidative damage to plants. *Plant Physiology, 148*, 960-968.

Tsuda, K., et al. (2008). Interplay between MAMP-triggered and SA-mediated defense responses. *The Plant Journal, 53*, 763-775.

Tsuda, K., et al. (2009). Network properties of robust immunity in plants. *PLoS Genetics, 5*, e1000772.

Tsuda, K., & Somssich, I. E. (2015). Transcriptional networks in plant immunity. *New Phytologist, 206*, 932-947.

Tsukagoshi, H., et al. (2010). Transcriptional regulation of ROS controls transition from proliferation to differentiation in the root. *Cell, 143*, 606-616.

Tun, N. N., et al. (2006). Polyamines induce rapid biosynthesis of nitric oxide (NO) in *Arabidopsis* thaliana seedlings. *Plant Cell Physiology, 47*, 346-354.

Urano, K., et al. (2005). *Arabidopsis ADC* genes involved in polyamine biosynthesis are essential for seed development. *FEBS Letters, 579*, 1557-1564.

Urano, K., et al. (2003). Characterization of Arabidopsis genes involved in biosynthesis of polyamines in abiotic stress responses and developmental stages. *Plant, Cell & Environment, 26*, 1917-1926.

Urano, K., et al. (2004). *Arabidopsis* stress-inducible gene for arginine decarboxylase AtADC2 is required for accumulation of putrescine in salt tolerance. *Biochemical Biophysical Research Communications, 313*, 369-375.

Van der Does, D., et al. (2013). Salicylic acid suppresses jasmonic acid signaling downstream of *SCFCOI1-JAZ* by targeting GCC promoter motifs via transcription factor *ORA59*. *The Plant Cell, 25*, 744-761.

Velásquez, A. C., et al. (2018). Plant-pathogen warfare under changing climate conditions. *Current Biology, 28*, R619-r634.

Veronese, P., et al. (2006). The membrane-anchored *BOTRYTIS-INDUCED KINASE 1*

plays distinct roles in *Arabidopsis* resistance to necrotrophic and biotrophic pathogens. *The Plant Cell, 18*, 257-273.

Vincent, T. R., et al. (2017). Interplay of plasma membrane and vacuolar ion channels, together with *BAK1*, elicits rapid cytosolic calcium elevations in *Arabidopsis* during aphid feeding. *The Plant Cell, 29*, 1460-1479.

Wagner, T. A., & Kohorn, B. D. (2001). Wall-associated kinases are expressed throughout plant development and are required for cell expansion. *The Plant Cell, 13*, 303-318.

Walters, D. R. (2003). Polyamines and plant disease. *Phytochemistry, 64*, 97-107.

Wang, C., & Luan, S. (2024). Calcium homeostasis and signaling in plant immunity. *Current Opinion in Plant Biology, 77*, 102485.

Wang, C., et al. (2024). Mechanisms of calcium homeostasis orchestrate plant growth and immunity. *Nature*. *627*, 382–388.

Wang, D., et al. (2006). A genomic approach to identify regulatory nodes in the transcriptional network of systemic acquired resistance in plants. *PLoS Pathogens, 2*, e123.

Wang, G., et al. (2015). The decoy substrate of a pathogen effector and a pseudokinase specify pathogen-induced modified-self recognition and immunity in plants. *Cell Host & Microbe, 18*, 285-295.

Wang, J., et al. (2018a). A regulatory module controlling homeostasis of a plant immune kinase. *Molecular Cell, 69*, 493-504. e496.

Wang, L., et al. (2009a). *Arabidopsis* CaM binding protein *CBP60g* contributes to MAMP-induced SA accumulation and is involved in disease resistance against *Pseudomonas syringae*. *PLoS Pathogens, 5*, e1000301.

Wang, L., et al. (2011b). *CBP60g* and *SARD1* play partially redundant critical roles in salicylic acid signaling. *The Plant Journal, 67*, 1029-1041.

Wang, P., et al. (2023). Identification and analysis of BAHD superfamily related to malonyl ginsenoside biosynthesis in Panax ginseng. *Frontiers in Plant Science*, *14*, 1301084.

Wang, W., et al. (2009b). Specific targeting of the *Arabidopsis* resistance protein RPW8. 2 to the interfacial membrane encasing the fungal haustorium renders broad-spectrum resistance to powdery mildew. *The Plant Cell, 21*, 2898-2913.

Wang, W., et al. (2019). Polyamine catabolism in plants: a universal process with diverse functions. *Frontiers in Plant Science, 10*, 457164.

Wang, W., & Liu, J.H. (2016). *CsPAO4* of Citrus sinensis functions in polyamine terminal catabolism and inhibits plant growth under salt stress. *Scientific Reports, 6*, 31384.

Wang, X., et al. (2013). Salicylic acid regulates plasmodesmata closure during innate immune responses in *Arabidopsis*. *The Plant Cell, 25*, 2315-2329.

Wang, X., et al. (2016). The cytosolic Fe-S cluster assembly component MET18 is required for the full enzymatic activity of ROS1 in active DNA demethylation. *Scientific Reports, 6*, 26443.

Wang, Y., et al. (2018b). A *MPK3/6-WRKY33-ALD1*-pipecolic acid regulatory loop contributes to systemic acquired resistance. *The Plant Cell, 30*, 2480-2494.

Wang, Y., et al. (2021). Regulation and function of defense-related callose deposition in plants. *International Journal of Molecular Sciences, 22*, 2393.

Wang, Z., et al. (2011a). *BON1* interacts with the protein kinases *BIR1* and *BAK1* in modulation of temperature-dependent plant growth and cell death in *Arabidopsis*. *The Plant Journal, 67*, 1081-1093.

Wasternack, C., & Song, S. (2017). Jasmonates: biosynthesis, metabolism, and signaling by proteins activating and repressing transcription. *Journal of Experimental Botany, 68*, 1303-1321.

Waszczak, C., et al. (2018). Reactive oxygen species in plant signaling. *Annual Review of Plant Biology, 69*, 209-236.

Webb, A. A., et al. (1996). Calcium ions as intracellular second messengers in higher plants. *Advances in Botanical Research*, 45-96.

Weckwerth, W., et al. (2020). PANOMICS meets germplasm. *18*(7), 1507-1525.

Wiermer, M., et al. (2005). Plant immunity: the *EDS1* regulatory node. *Current Opinion in Plant Biology, 8*, 383-389.

Wildermuth, M. C., et al. (2001). Isochorismate synthase is required to synthesize salicylic acid for plant defence. *Nature, 414*, 562-565.

Willmann, R., et al. (2011). *Arabidopsis* lysin-motif proteins *LYM1 LYM3 CERK1* mediate bacterial peptidoglycan sensing and immunity to bacterial infection. *Proceedings of the National Academy of Sciences, 108*, 19824-19829.

Wimalasekera, R., et al. (2011a). *COPPER AMINE OXIDASE1 (CuAO1)* of *Arabidopsis* thaliana contributes to abscisic acid-and polyamine-induced nitric oxide biosynthesis and abscisic acid signal transduction. *Molecular Plant, 4*, 663-678.

Wimalasekera, R., et al. (2015). *POLYAMINE OXIDASE 2* of *Arabidopsis* contributes to ABA mediated plant developmental processes. *Plant Physiology Biochemistry, 96*, 231-240.

Wimalasekera, R., et al. (2011b). Polyamines, polyamine oxidases and nitric oxide in development, abiotic and biotic stresses. *Plant Science, 181*, 593-603.

Woodward, A. W., & Bartel, B. (2018). Biology in Bloom: A Primer on the *Arabidopsis* thaliana Model System. *Genetics, 208*, 1337-1349.

Woody, S. T., et al. (2007). The WiscDsLox T-DNA collection: an *Arabidopsis* community resource generated by using an improved high-throughput T-DNA sequencing pipeline. *Journal of Plant Research, 120*, 157-165.

Wrzaczek, M., et al. (2010). Transcriptional regulation of the *CRK/DUF26* group of Receptor-like protein kinases by ozone and plant hormones in *Arabidopsis*. *BMC Plant Biology, 10*, 95.

Wu, D., et al. (2019). A plant pathogen type III effector protein subverts translational regulation to boost host polyamine levels. *Cell Host & Microbe, 26*, 638-649. e635.

Wu, X., & Ye, J. (2020). Manipulation of jasmonate signaling by plant viruses and their insect vectors. *Viruses, 12*, 148.

Wu, Y., et al. (2012). The *Arabidopsis NPR1* protein is a receptor for the plant defense hormone salicylic acid. *Cell Reports, 1*, 639-647.

Wu, B., et al. (2023). Fuels for ROS signaling in plant immunity. *Trends in Plant Science*.

Wu, F., et al. (2020). Hydrogen peroxide sensor *HPCA1* is an LRR receptor kinase in *Arabidopsis*. *Nature, 578*, 577-581.

Xia, X. J., et al. (2015). Interplay between reactive oxygen species and hormones in the control of plant development and stress tolerance. *Journal of experimental botany, 66*, 2839-2856.

Xiao, P.,et al. (2021). Evolution analyses of *CAMTA* transcription factor in plants and its enhancing effect on cold-Tolerance. *Frontiers in Plant Science, 12*, 758187.

Xiao, S., et al. (2001). Broad-spectrum mildew resistance in *Arabidopsis thaliana* mediated by RPW8. *Science, 291*, 118-120.

Xin, X. F., et al. (2018). *Pseudomonas syringae*: what it takes to be a pathogen. *Nature Reviews Microbiology, 16*, 316-328.

Xu, G., et al. (2022). A tale of many families: calcium channels in plant immunity. *The Plant Cell*, 34, 1551-1567.

Xu, S., et al. (2017). Wild tobacco genomes reveal the evolution of nicotine biosynthesis. *Proceedings of the National Academy of Sciences, 114*, 6133-6138.

Yaakoubi, H., et al. (2014). Protective action of spermine and spermidine against photoinhibition of photosystem I in isolated thylakoid membranes. *PloS One, 9*, e112893.

Yamada, K., et al. (2016). The *Arabidopsis CERK 1*-associated kinase *PBL 27* connects chitin perception to *MAPK* activation. *The EMBO Journal, 35*, 2468-2483.

Yamaguchi, K., et al. (2007). A protective role for the polyamine spermine against drought stress in *Arabidopsis*. *Biochemical Biophysical Research Communications, 352*, 486-490.

Yamaguchi, K., et al. (2006a). The polyamine spermine protects against high salt stress in *Arabidopsis* thaliana. *FEBS letters, 580*, 6783-6788.

Yamaguchi, Y., et al. (2010). *PEPR2* is a second receptor for the Pep1 and Pep2 peptides and contributes to defense responses in *Arabidopsis*. *The Plant Cell, 22*, 508-522.

Yamaguchi, Y., et al. (2006b). The cell surface leucine-rich repeat receptor for *AtPep1*, an endogenous peptide elicitor in *Arabidopsis*, is functional in transgenic tobacco cells. *Proceedings of the National Academy of Sciences, 103*, 10104-10109.

Yamaguchi, Y., & Huffaker, A. (2011). Endogenous peptide elicitors in higher plants. *Current Opinion in Plant Biology,* 14, 351-357.

Yamamoto, M., & Takahashi, T. (2017). Thermospermine enhances translation of *SAC51* and *SACL1* in *Arabidopsis*. *Plant Signaling Behavior, 12*, 1583-1592.

Yan, J., et al. (2009). The *Arabidopsis CORONATINE INSENSITIVE 1* protein is a jasmonate receptor. *The Plant Cell, 21*, 2220-2236.

Yang, Y. X., et al. (2015a). Crosstalk among jasmonate, salicylate and ethylene signaling pathways in plant disease and immune responses. *Current Protein Peptide Science, 16*, 450-461.

Yang, C., et al. (2015b). Ethylene signaling in rice and *Arabidopsis*: conserved and diverged aspects. *Molecular Plant, 8*, 495-505.

Yang, D. L., et al. (2017). Calcium pumps and interacting *BON1* protein modulate calcium signature, stomatal closure, and plant immunity. *Plant Physiology, 175*, 424-437.

Yang, F., et al. (2019). A plant immune receptor degraded by selective autophagy. *Molecular Plant, 12*, 113-123.

Yi, S. Y., et al. (2014). The activated SA and JA signaling pathways have an influence on flg22-triggered oxidative burst and callose deposition. *PloS One, 9*, e88951.

Yin, Z. P., et al. (2014). Role of spermidine and spermine in alleviation of drought-induced oxidative stress and photosynthetic inhibition in Chinese dwarf cherry *(Cerasus humilis)* seedlings. *Plant Growth Regulation, 74*, 209-218.

Yu, Z., et al. (2019). Polyamine oxidases play various roles in plant development and abiotic stress tolerance. *Plants, 8*, 184.

Yu, T.Y., et al. (2021). Receptors in the Induction of the Plant Innate Immunity. *Molecular Plant-Microbe Interactions, 34*, 587-601.

Yuan, P., et al. (2017a). Calcium signatures and signaling events orchestrate plant–microbe interactions. *Current Opinion in Plant Biology, 38*, 173-183.

Yuan, H. M., et al. (2017b). *CATALASE2* coordinates SA-mediated repression of both auxin accumulation and JA biosynthesis in plant defenses. *Cell Host & Microbe, 21*, 143-155.

Yuan, M., et al. (2021). Pattern-recognition receptors are required for NLR-mediated plant immunity. *Nature, 592*, 105-109.

Zeier, J. (2021). Metabolic regulation of systemic acquired resistance. *Current Opinion in Plant Biology, 62*, 102050.

Zeiss, D. R., et al. (2021). Hydroxycinnamate amides: Intriguing conjugates of plant protective metabolites. *Trends in Plant Science, 26*, 184-195.

Zhang, J. et al. (2010a). Receptor-like cytoplasmic kinases integrate signaling from multiple plant immune receptors and are targeted by a *Pseudomonas syringae* effector. *Cell Host & Microbe, 7*, 290-301.

Zhang, J. et al. (2007). A *Pseudomonas syringae* effector inactivates *MAPKs* to suppress PAMP-induced immunity in plants. *Cell Host & Microbe, 1*, 175-185.

Zhang, Y., et al. (2010b). Control of salicylic acid synthesis and systemic acquired resistance by two members of a plant-specific family of transcription factors. *Proceedings of the National Academy of Sciences, 107*, 18220-18225.

Zhang, F., et al. (2015). Structural basis of *JAZ* repression of *MYC* transcription factors in jasmonate signalling. *Nature, 525*, 269-273.

Zhang, M. & Zhang, S. (2022). Mitogen-activated protein kinase cascades in plant signaling. *Journal of Integrative Plant Biology, 64*, 301-341.

Zhang, Y., et al. (2017). *S5H/DMR6* encodes a salicylic acid 5-hydroxylase that fine-tunes salicylic acid homeostasis. *Plant Physiology, 175*, 1082-1093.

Zhang, Y., et al. (2023). Cysteine-rich receptor-like protein kinases: emerging regulators of plant stress responses. *Trends in Plant Science*, *28*, 776–794.

Zhao, Z. X., et al. (2021a). *RPW8.1* enhances the ethylene-signaling pathway to feedback-attenuate its mediated cell death and disease resistance in *Arabidopsis*. *The New Phytologist, 229*, 516.

Zhao, T., et al. (2018). Silencing of the *SAMDC* gene decreases resistance of tomato to Cladosporium fulvum. *Physiological molecular plant pathology, 102*, 1-7.

Zhao, C., et al. (2021b). A mis-regulated cyclic nucleotide-gated channel mediates cytosolic calcium elevation and activates immunity in *Arabidopsis*. *New Phytologist, 230*, 1078-1094.

Zheng, X. Y., et al. (2012). Coronatine promotes *Pseudomonas syringae* virulence in plants by activating a signaling cascade that inhibits salicylic acid accumulation. *Cell Host & Microbe, 11*, 587-596.

Zhong, Y., & Cheng, Z. M. (2016). A unique *RPW8*-encoding class of genes that originated in early land plants and evolved through domain fission, fusion, and duplication. *Scientific Reports, 6*, 32923.

Zhou, M. et al. (2018). *WRKY70* prevents axenic activation of plant immunity by direct repression of *SARD1*. *New Phytologist, 217*, 700-712.

Zhou, J., et al. (2020). Differential phosphorylation of the transcription factor *WRKY33* by the protein kinases *CPK5/CPK6* and *MPK3/MPK6* cooperatively regulates camalexin biosynthesis in *Arabidopsis*. *The Plant Cell, 32*, 2621-2638.

Zhou, D., et al. (2014). Reactive oxygen species in normal and tumor stem cells. *Advances in Cancer Research, 122*, 1–67.

Zhu, Z., et al. (2011). Derepression of ethylene-stabilized transcription factors (*EIN3/EIL1*) mediates jasmonate and ethylene signaling synergy in *Arabidopsis*. *Proceedings of the National Academy of Sciences, 108*, 12539-12544.

Zipfel, C., et al. (2006). Perception of the Bacterial PAMP EF-Tu by the Receptor *EFR*

restricts *Agrobacterium*-mediated transformation. *Cell, 125*, 749-760.
Zipfel, C.& Oldroyd, G. E. (2017). Plant signalling in symbiosis and immunity. *Nature, 543*, 328-336.
Zipfel, C., (2014). Plant pattern-recognition receptors. *Trends In Immunology, 35*, 345-351.
Zou, C., et al. (2016). Bulked sample analysis in genetics, genomics and crop improvement. *Plant Biotechnology Journal, 14*, 1941-1955.

ANNEX I

SUPPLEMENTARY DATA

Spermine inhibits PAMP-induced ROS and Ca^{2+} burst and reshapes the transcriptional landscape of PTI in Arabidopsis

Chi Zhang, Kostadin E. Atanasov and Rubén Alcázar*

Department of Biology, Healthcare and Environment. Section of Plant Physiology, Faculty of Pharmacy and Food Sciences, Universitat de Barcelona, Av. Joan XXIII 27-31, 08028 Barcelona, Spain.

*Author for correspondence: ralcazar@ub.edu

SUPPLEMENTARY FIGURES S1 – S22

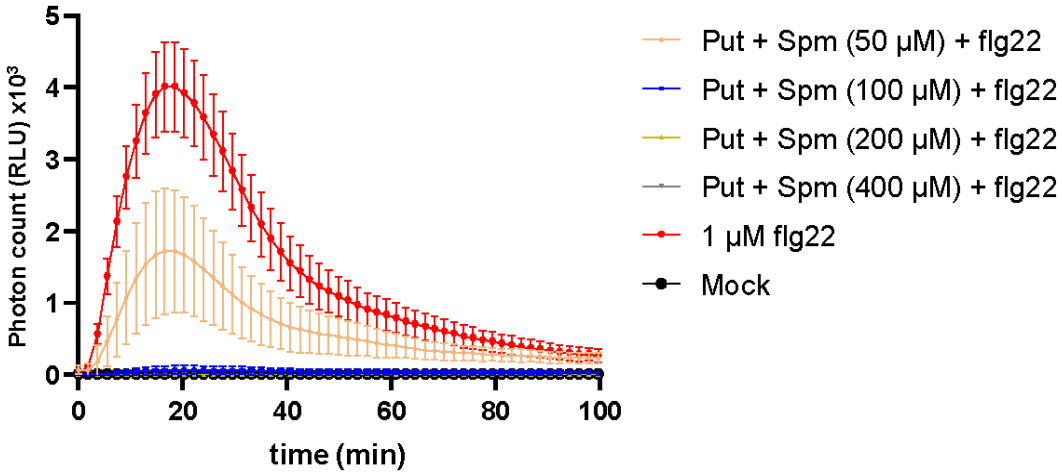

Figure S1. Effect of the Put and Spm cotreatment on flg22-elicited ROS burst. Leaf discs from 5-week-old wild-type plants were treated with flg22 (1 µM), and Put or Spm (50 µM to 400 µM). Values represent the mean ± S.E. from at least twelve replicates per treatment and are expressed in photon counts (relative light units, RLU).

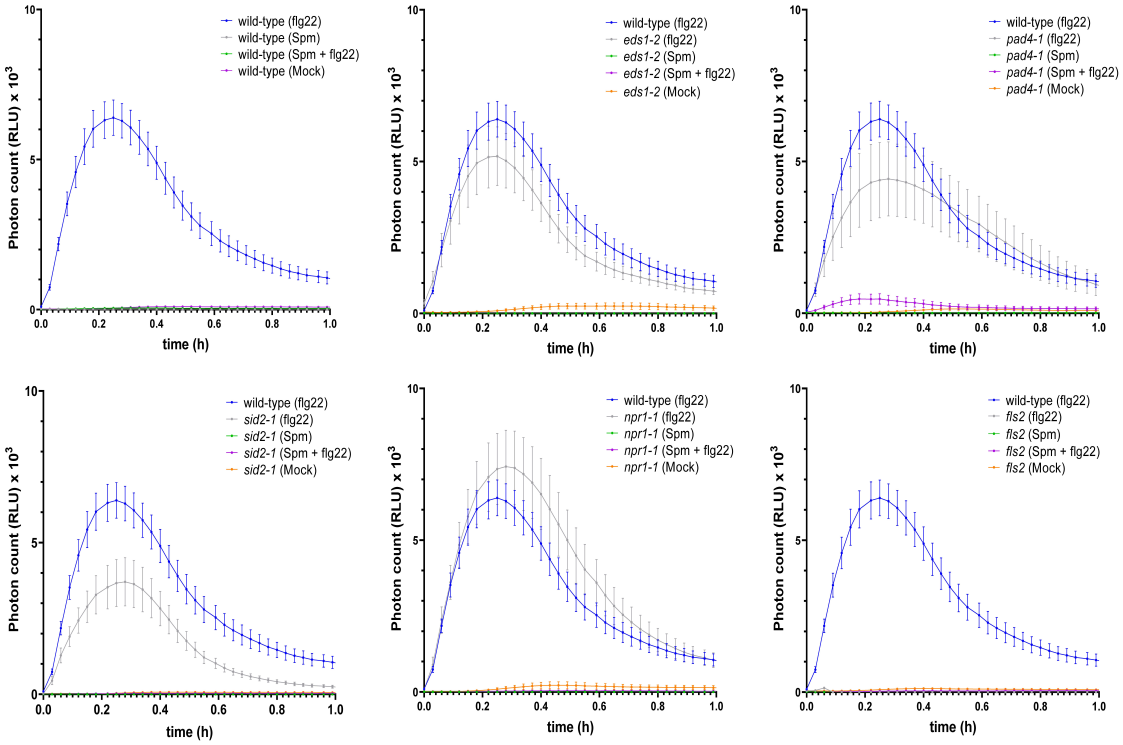

Figure S2. Effect of Spm on flg22-elicited ROS burst in *eds1-2*, *pad4-1*, *sid2-1*, *npr1-1* and *fls2* (negative control) mutants. Leaf discs from 5-week-old plants were treated with flg22 (1 μM), Spm (100 μM), Spm (100 μM) + flg22 (1 μM) or mock (water). Values represent the mean ± S.E. from at least twelve replicates per treatment and are expressed in photon counts (relative light units, RLU).

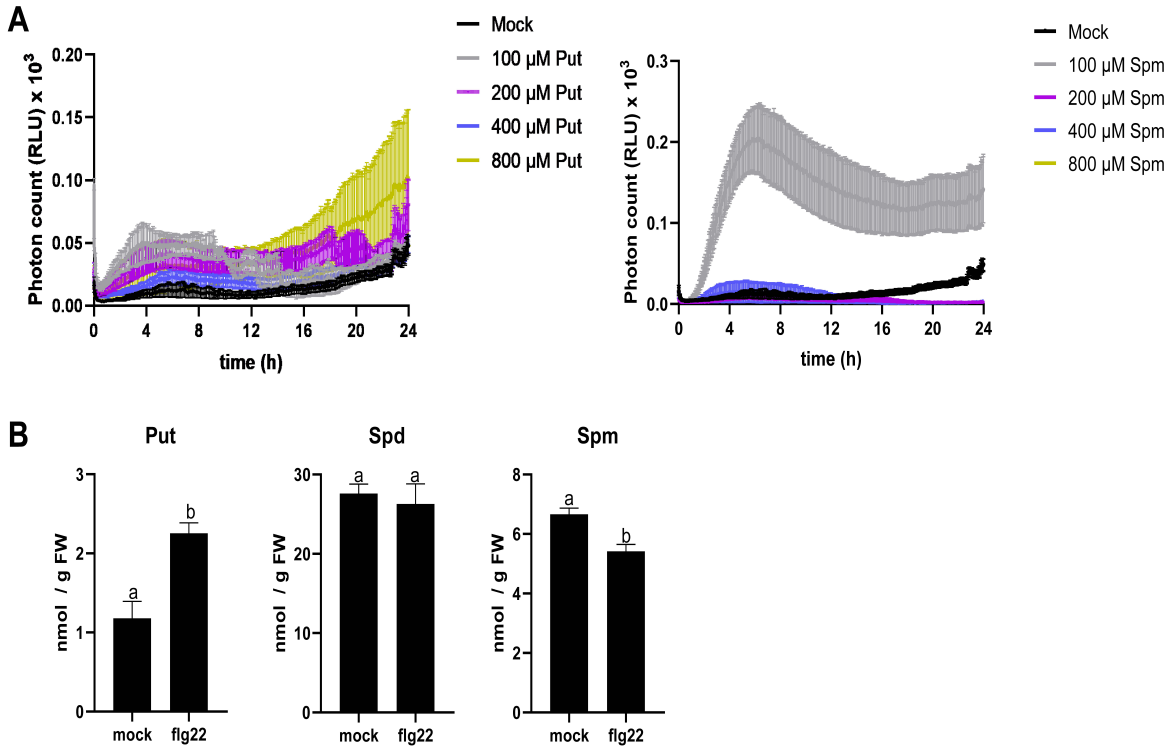

Figure S3. **(A)** ROS produced by Put and Spm treatments. Leaf discs from 5-week-old wild-type plants were incubated with different concentrations (100 µM to 800 µM) of Put, Spm and mock (water). Values represent the mean ± S.E. from at least twelve replicates per treatment and are expressed in photon counts (relative light units, RLU). **(B)** Free Put, Spd and Spm levels in wild-type plants at 24 h of treatment with flg22 (1 µM) or mock (water). Values represent the mean ± S.D. from three biological replicates per treatment. Letters indicate values that are significantly different according to Tukey's HSD test at $P < 0.05$.

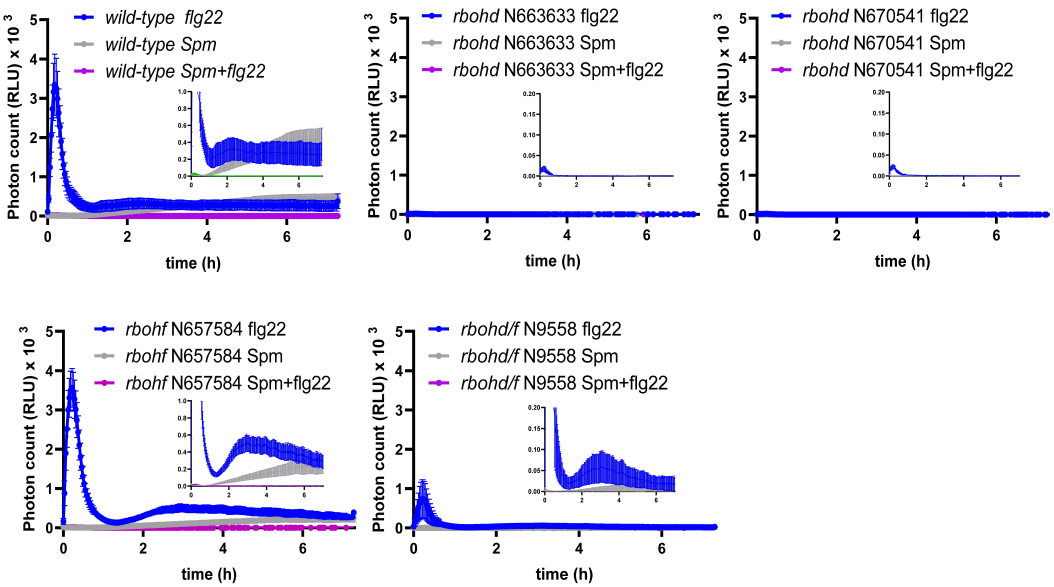

Figure S4. Effect of Spm on flg22-elicited ROS burst in *rbohd* (N663633 and N670541), *rbohf* (N657584) and double *rbohd/f* (N9558) mutants. Leaf discs from 5-week-old wild-type plants and mutants were treated with flg22 (1 µM), Spm (100 µM) or Spm (100 µM) + flg22 (1 µM). Values represent the mean ± S.E. from at least twelve replicates per treatment and are expressed in photon counts (relative light units, RLU).

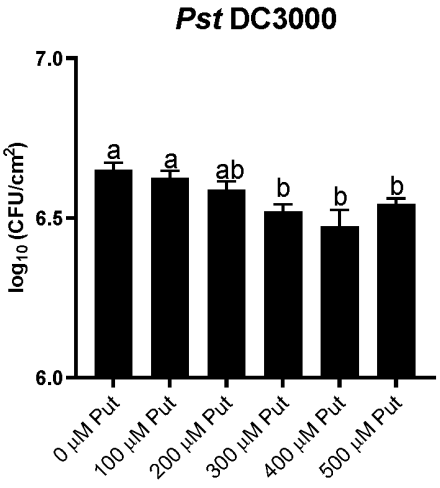

Figure S5. Analysis of *Pst* DC3000 disease resistance phenotypes in wild-type plants locally pretreated with different concentrations of Put (0 µM to 500 µM). Treatments were performed 24 h before *Pst* DC3000 infiltration ($OD_{600\ nm}$= 0.005). Bacterial numbers were assessed at 72 h post-inoculation and expressed as colony forming units (CFU) per cm^2 leaf area. Values are the mean from at least eight biological replicates ± SD. Letters indicate values that are significantly different according to Tukey's HSD test at $P < 0.05$.

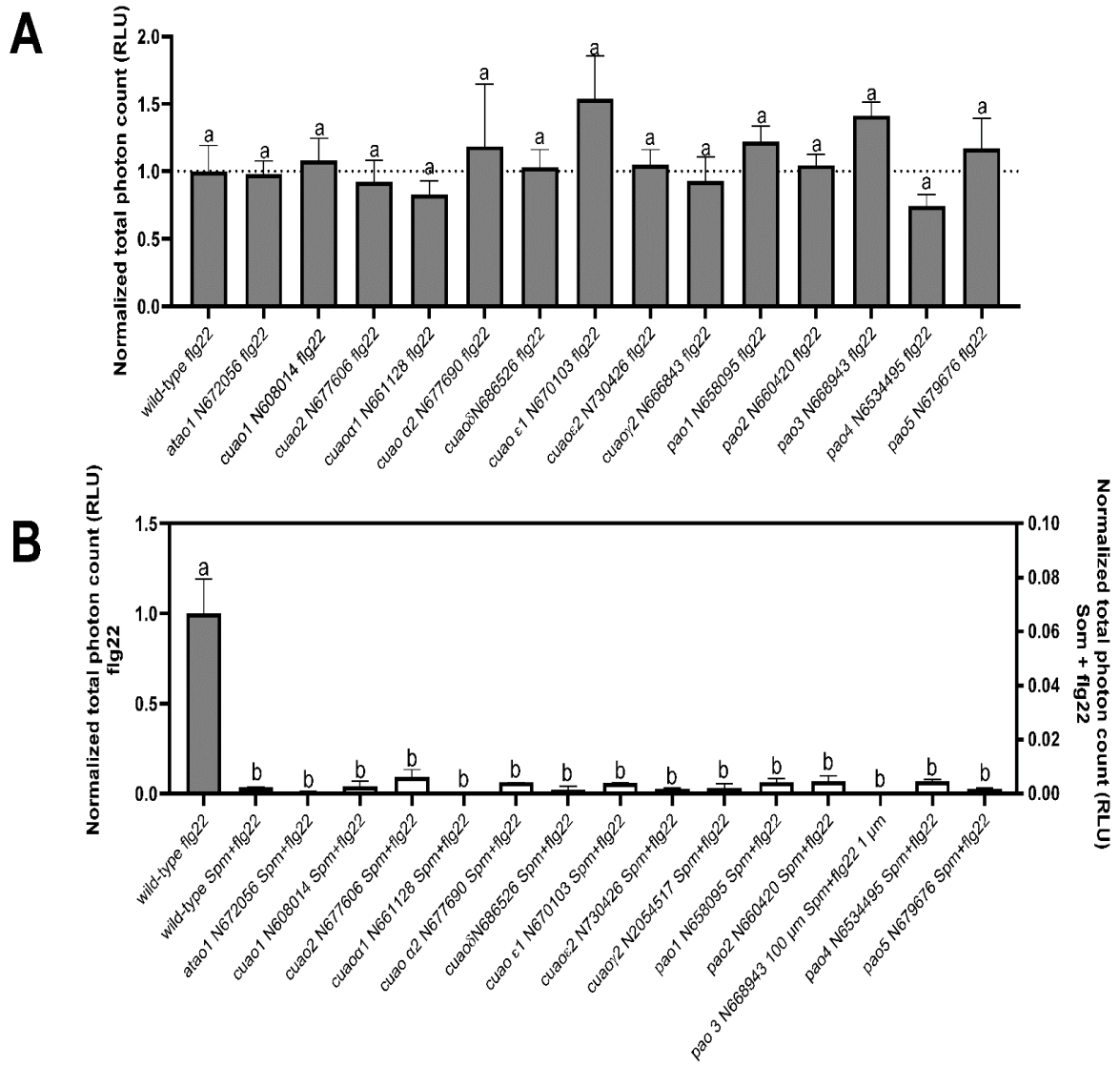

Figure S6. (A) Flg22-elicited ROS and **(B)** effect of Spm on flg22-elicited ROS production in *CuAO* mutants (*atao1*, *cuao1*, *cuao*2, *cuaoa1*, *cuao*a2, *cuao*d, *cuao*e1, *cuao*e2, *cuao*g2) and *PAO* mutants (*pao1*, *pao2*, *pao3*, *pao4* and *pao5*) in comparison to the wild-type. The total sum of RLU (total photon counts) in each genotype was normalized to the total photon counts in the wild-type reference. Values represent the mean ± S.E. of the normalized values from at least twelve replicates per treatment. Letters indicate values that are significantly different according to Tukey's HSD test at $P < 0.05$.

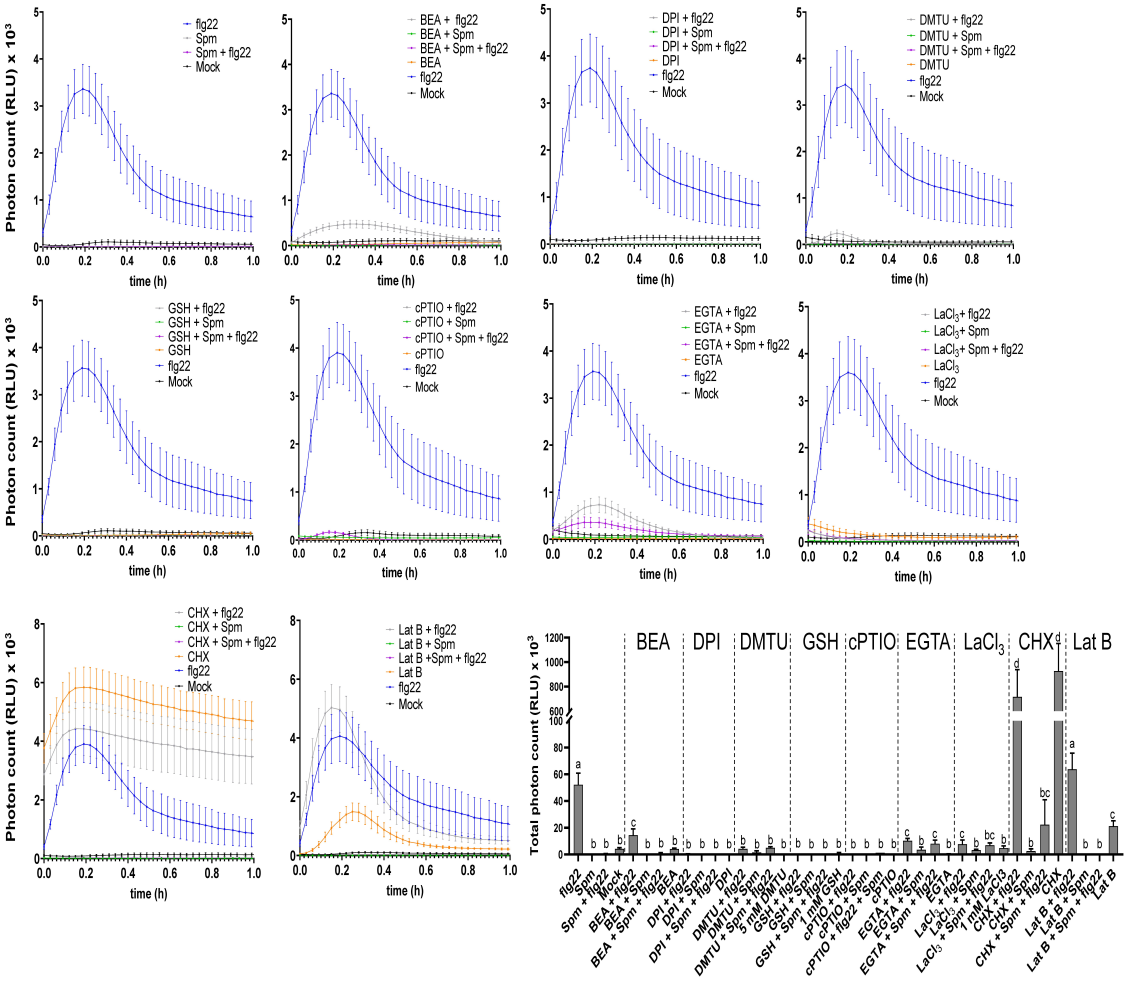

Figure S7. Effect of 2-bromoethylamine BEA (5 mM), diphenyleneiodonium chloride (DPI, 20 µM), dimethylthiourea (DMTU, 5 mM), reduced L-glutathione (GSH, 1 mM), carboxy-PTIO (cPTIO, 100 µM), EGTA (2 mM), $LaCl_3$ (1 mM), cycloheximide (CHX, 300 µM) and Latrunculin B (Lat B, 20 µM) on Spm inhibition of flg22-triggered ROS burst in wild-type plants. Leaf discs from 5-week-old plants were pretreated with the different chemicals 3 h before Spm (100 µM), flg22 (1 µM) and Spm (100 µM) + flg22 (1 µM) elicitation. Photon counts (relative light units, RLU) were determined over time. Values represent the mean ± S.E. from at least twelve replicates per treatment. Letters indicate values that are significantly different according to Tukey's HSD test at $P < 0.05$.

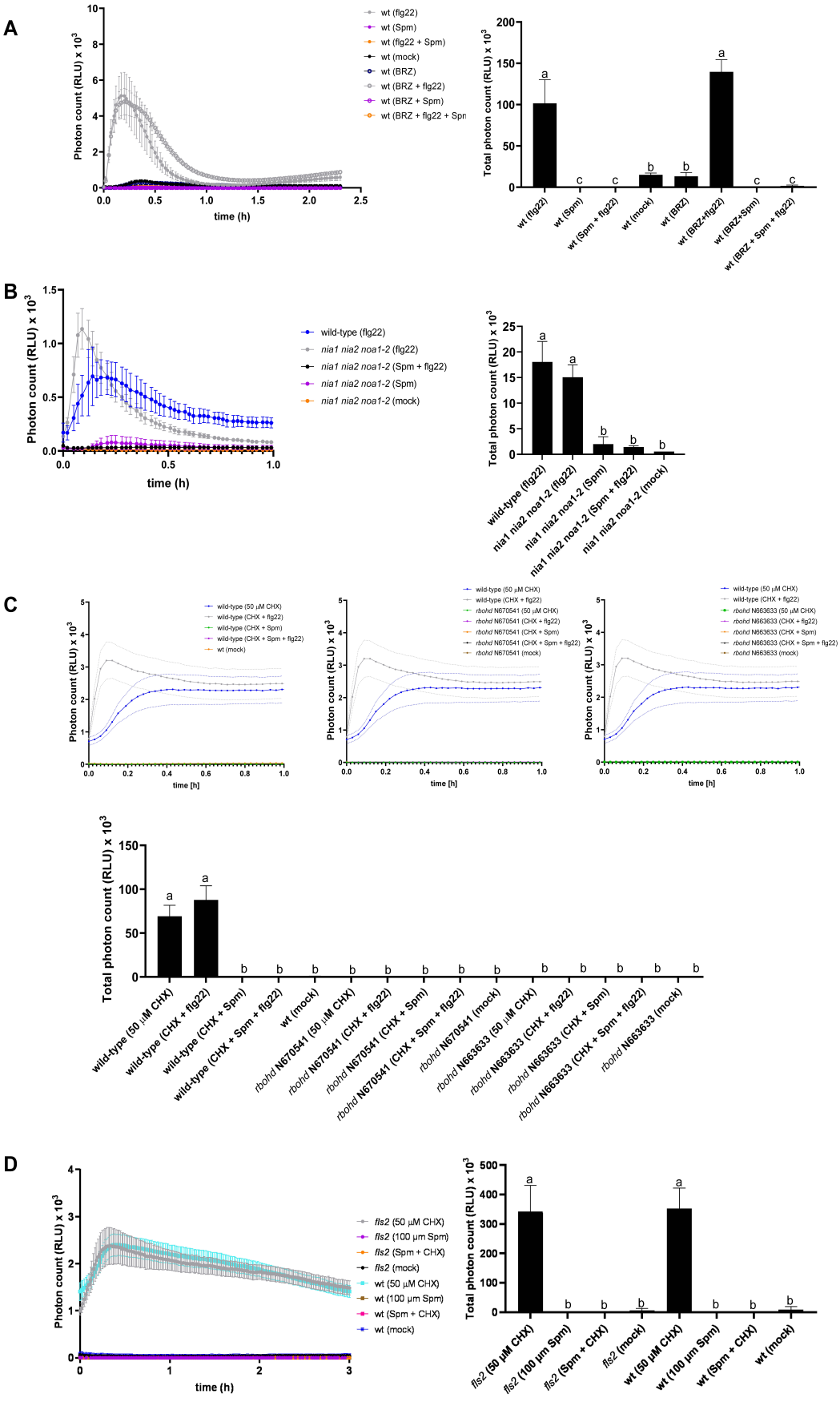
A
Photon count (RLU) x 10³
time (h)
wt (flg22)
wt (Spm)
wt (flg22 + Spm)
wt (mock)
wt (BRZ)
wt (BRZ + flg22)
wt (BRZ + Spm)
wt (BRZ + flg22 + Spm)
Total photon count (RLU) x 10³
wt (flg22)
wt (Spm)
wt (Spm + flg22)
wt (mock)
wt (BRZ)
wt (BRZ+flg22)
wt (BRZ+Spm)
wt (BRZ + Spm + flg22)
B
Photon count (RLU) x 10³
time (h)
wild-type (flg22)
nia1 nia2 noa1-2 (flg22)
nia1 nia2 noa1-2 (Spm + flg22)
nia1 nia2 noa1-2 (Spm)
nia1 nia2 noa1-2 (mock)
Total photon count (RLU) x 10³
wild-type (flg22)
nia1 nia2 noa1-2 (flg22)
nia1 nia2 noa1-2 (Spm)
nia1 nia2 noa1-2 (Spm + flg22)
nia1 nia2 noa1-2 (mock)
C
Photon count (RLU) x 10³
time [h]
wild-type (50 µM CHX)
wild-type (CHX + flg22)
wild-type (CHX + Spm)
wild-type (CHX + Spm + flg22)
wt (mock)
rbohd N670541 (50 µM CHX)
rbohd N670541 (CHX + flg22)
rbohd N670541 (CHX + Spm)
rbohd N670541 (CHX + Spm + flg22)
rbohd N670541 (mock)
rbohd N663633 (50 µM CHX)
rbohd N663633 (CHX + flg22)
rbohd N663633 (CHX + Spm)
rbohd N663633 (CHX + Spm + flg22)
rbohd N663633 (mock)
Total photon count (RLU) x 10³
wild-type (50 µM CHX)
wild-type (CHX + flg22)
wild-type (CHX + Spm)
wild-type (CHX + Spm + flg22)
wt (mock)
rbohd N670541 (50 µM CHX)
rbohd N670541 (CHX + flg22)
rbohd N670541 (CHX + Spm)
rbohd N670541 (CHX + Spm + flg22)
rbohd N670541 (mock)
rbohd N663633 (50 µM CHX)
rbohd N663633 (CHX + flg22)
rbohd N663633 (CHX + Spm)
rbohd N663633 (CHX + Spm + flg22)
rbohd N663633 (mock)
D
Photon count (RLU) x 10³
time (h)
fls2 (50 µM CHX)
fls2 (100 µm Spm)
fls2 (Spm + CHX)
fls2 (mock)
wt (50 µM CHX)
wt (100 µm Spm)
wt (Spm + CHX)
wt (mock)
Total photon count (RLU) x 10³
fls2 (50 µM CHX)
fls2 (100 µm Spm)
fls2 (Spm + CHX)
fls2 (mock)
wt (50 µM CHX)
wt (100 µm Spm)
wt (Spm + CHX)
wt (mock)

Figure S8. (A) Effect of brassinazole (BRZ, 2.5 μM) on Spm inhibition of flg22-triggered ROS burst in the wild-type. **(B)** Effect of Spm on flg22-elicited ROS burst in 3-week-old *nia1 nia2 noa1-2* triple mutant. **(C,D)** Effect of cycloheximide (CHX, 50 μM) on Spm inhibition of flg22-triggered ROS burst in **(B)** wild-type and *rbohd* **(C)** wild-type (wt) and *fls2*. Pharmacological treatments were performed as described in Figure S7. Values represent the mean ± S.E. from at least twelve replicates per treatment and are expressed in photon counts (relative light units, RLU). Letters indicate values that are significantly different according to Tukey's HSD test at $P < 0.05$.

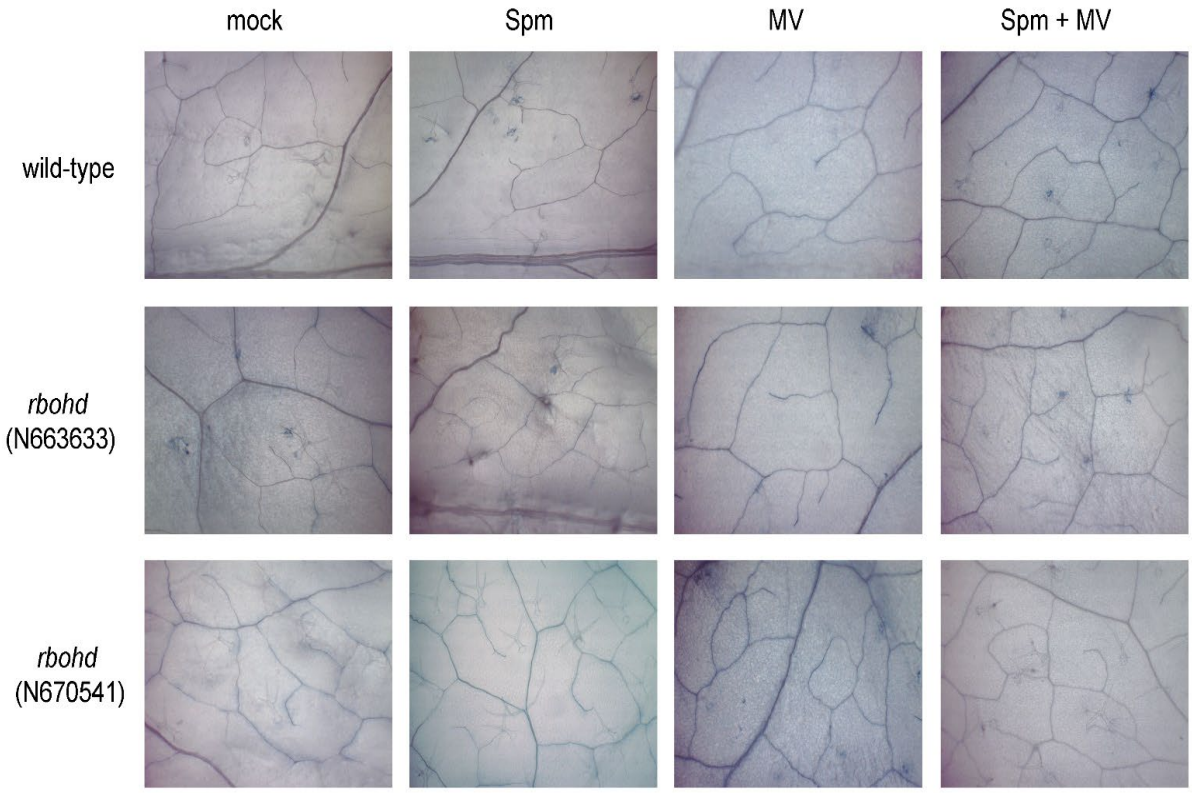

Figure S9. Trypan blue staining of wild-type and *rbohd* leaves infiltrated with Spm (100 μM), methyl viologen (MV, 100 μM) or both (100 μM Spm + 100 μM MV). Staining was performed at 24 h of treatment.

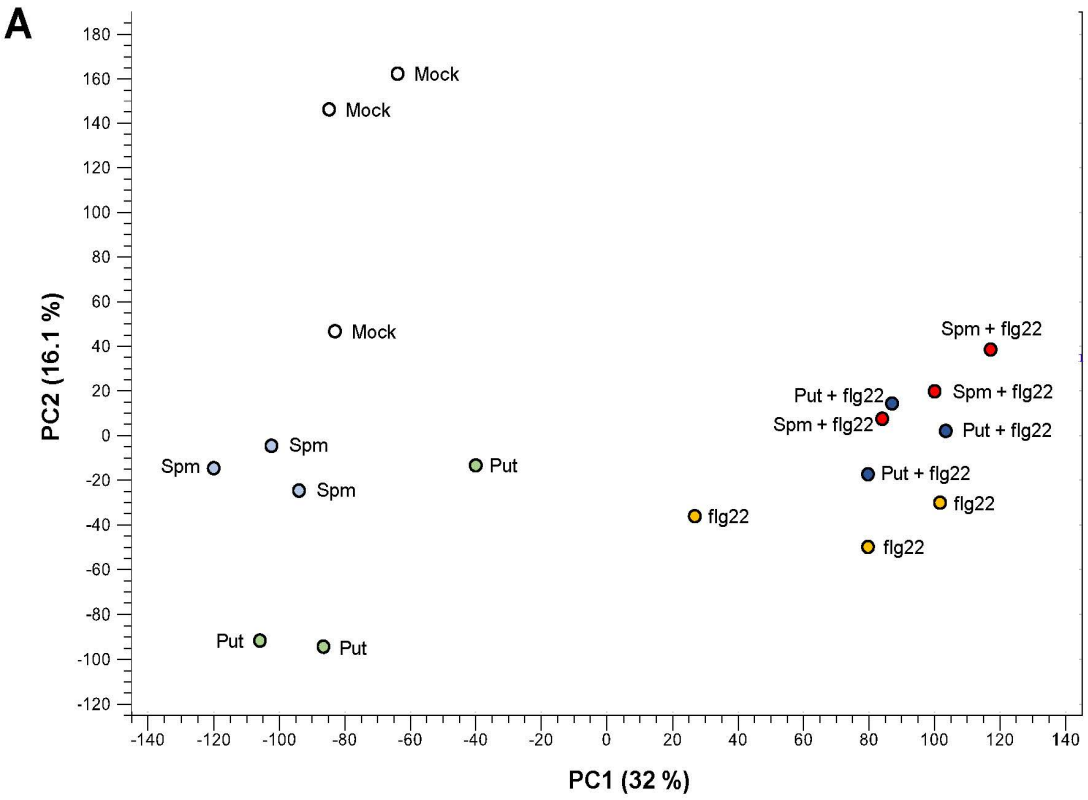
A
PC2 (16.1 %)
PC1 (32 %)
Mock
Mock
Mock
Spm
Spm
Spm
Put
Put
Put
flg22
flg22
flg22
Spm + flg22
Spm + flg22
Spm + flg22
Put + flg22
Put + flg22
Put + flg22

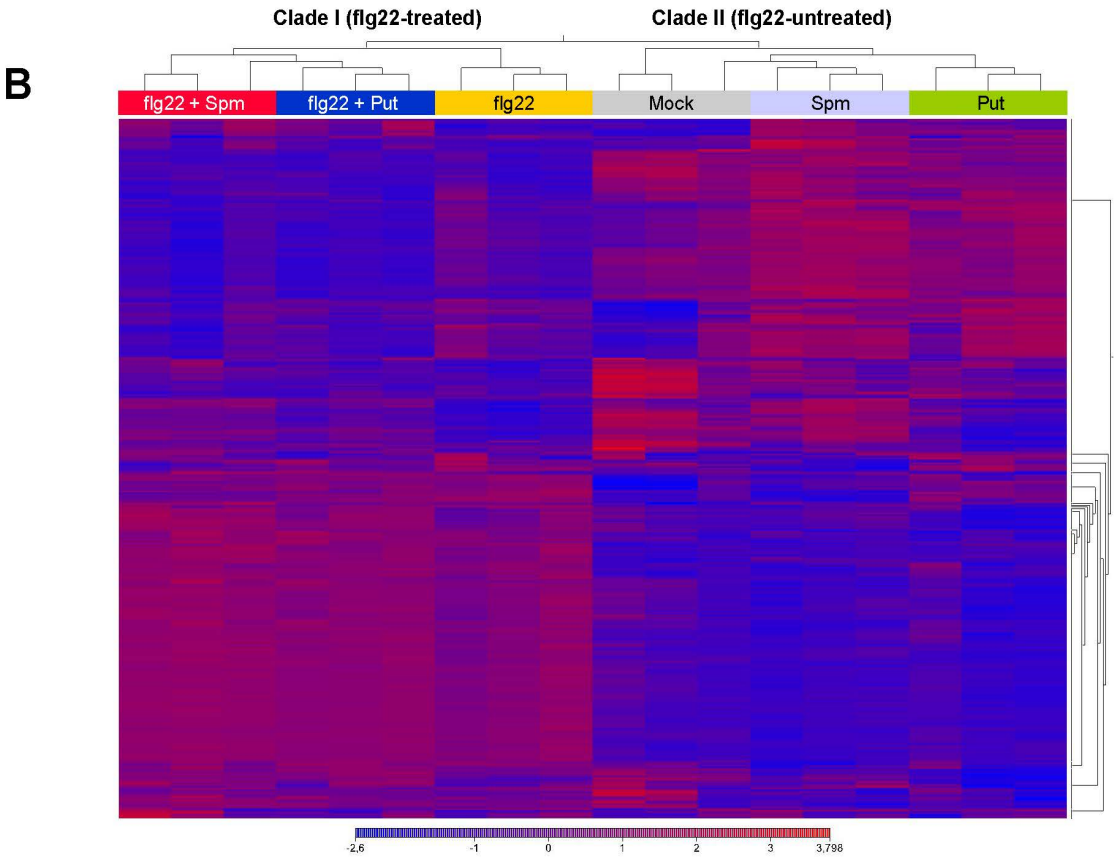
B
Clade I (flg22-treated)
Clade II (flg22-untreated)
flg22 + Spm
flg22 + Put
flg22
Mock
Spm
Put
-2,6
-1
0
1
2
3
3,798

Figure S10. (A) Principal component analysis (PCA) and **(B)** Hierarchical clustering analysis (HCA) of RNA-seq gene expression data obtained from 5-week-old wild-type plants treated with Put (100 μM), Spm (100 μM), flg22 (1 μM), Put (100 μM) + flg22 (1 μM), Spm (100 μM) + flg22 (1 μM) and mock (water) for 24 h. Each treatment was performed in three biological replicates.

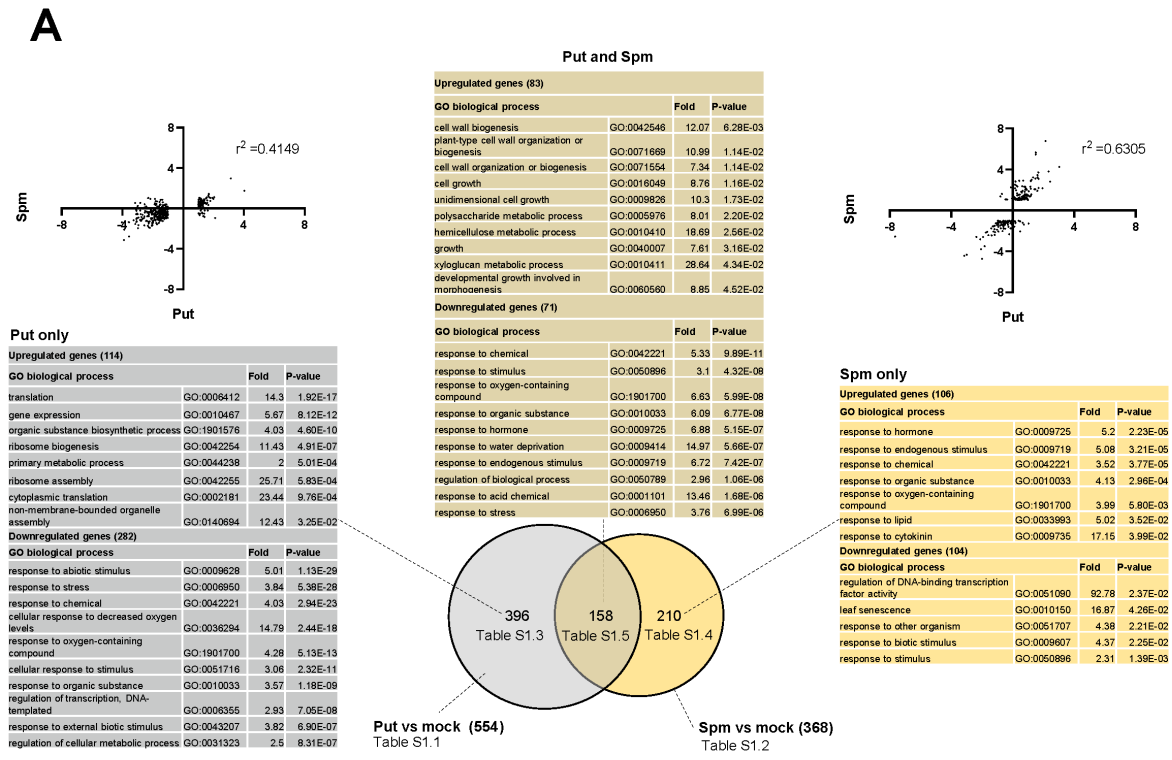
A
Put and Spm
Upregulated genes (83)
GO biological process Fold P-value
cell wall biogenesis GO:0042546 12.07 6.28E-03
plant-type cell wall organization or biogenesis GO:0071669 10.99 1.14E-02
cell wall organization or biogenesis GO:0071554 7.34 1.14E-02
cell growth GO:0016049 8.76 1.16E-02
unidimensional cell growth GO:0009826 10.3 1.73E-02
polysaccharide metabolic process GO:0005976 8.01 2.20E-02
hemicellulose metabolic process GO:0010410 18.69 2.56E-02
growth GO:0040007 7.61 3.16E-02
xyloglucan metabolic process GO:0010411 28.64 4.34E-02
developmental growth involved in morphogenesis GO:0060560 8.85 4.52E-02
Downregulated genes (71)
GO biological process Fold P-value
response to chemical GO:0042221 5.33 9.89E-11
response to stimulus GO:0050896 3.1 4.32E-08
response to oxygen-containing compound GO:1901700 6.63 5.99E-08
response to organic substance GO:0010033 6.09 6.77E-08
response to hormone GO:0009725 6.88 5.15E-07
response to water deprivation GO:0009414 14.97 5.66E-07
response to endogenous stimulus GO:0009719 6.72 7.42E-07
regulation of biological process GO:0050789 2.96 1.06E-06
response to acid chemical GO:0001101 13.46 1.68E-06
response to stress GO:0006950 3.76 6.99E-06
r2 =0.4149
Spm
Put
Put only
Upregulated genes (114)
GO biological process Fold P-value
translation GO:0006412 14.3 1.92E-17
gene expression GO:0010467 5.67 8.12E-12
organic substance biosynthetic process GO:1901576 4.03 4.60E-10
ribosome biogenesis GO:0042254 11.43 4.91E-07
primary metabolic process GO:0044238 2 5.01E-04
ribosome assembly GO:0042255 25.71 5.83E-04
cytoplasmic translation GO:0002181 23.44 9.76E-04
non-membrane-bounded organelle assembly GO:0140694 12.43 3.25E-02
Downregulated genes (282)
GO biological process Fold P-value
response to abiotic stimulus GO:0009628 5.01 1.13E-29
response to stress GO:0006950 3.84 5.38E-28
response to chemical GO:0042221 4.03 2.94E-23
cellular response to decreased oxygen levels GO:0036294 14.79 2.44E-18
response to oxygen-containing compound GO:1901700 4.28 5.13E-13
cellular response to stimulus GO:0051716 3.06 2.32E-11
response to organic substance GO:0010033 3.57 1.18E-09
regulation of transcription, DNA-templated GO:0006355 2.93 7.05E-08
response to external biotic stimulus GO:0043207 3.82 6.90E-07
regulation of cellular metabolic process GO:0031323 2.5 8.31E-07
396
Table S1.3
158
Table S1.5
210
Table S1.4
Put vs mock (554)
Table S1.1
Spm vs mock (368)
Table S1.2
r2 =0.6305
Spm
Put
Spm only
Upregulated genes (106)
GO biological process Fold P-value
response to hormone GO:0009725 5.2 2.23E-05
response to endogenous stimulus GO:0009719 5.08 3.21E-05
response to chemical GO:0042221 3.52 3.77E-05
response to organic substance GO:0010033 4.13 2.96E-04
response to oxygen-containing compound GO:1901700 3.99 5.80E-03
response to lipid GO:0033993 5.02 3.52E-02
response to cytokinin GO:0009735 17.15 3.99E-02
Downregulated genes (104)
GO biological process Fold P-value
regulation of DNA-binding transcription factor activity GO:0051090 92.78 2.37E-02
leaf senescence GO:0010150 16.87 4.26E-02
response to other organism GO:0051707 4.38 2.21E-02
response to biotic stimulus GO:0009607 4.37 2.25E-02
response to stimulus GO:0050896 2.31 1.39E-03
B
Put
Spm
Log2 Fold change
Enzyme
Transcription factor
Ribosome biogenesis or rRNA processing
Cell wall biogenesis
RING/U-box superfamily protein
Transporter
Arabinogalactan protein
Transmembrane protein
ABA-related
Protein kinase
Auxin-related
Defense
F-box protein
Receptor-like kinase
Cytokinin-related
BTB AND TAZ DOMAIN PROTEIN
Calcium/calmodulin binding porotein
Heat shock protein
Receptor-like protein
Carbohydrate metabolism
Lipid metabolism
Amino acids metabolism
Nucleoside/nucleotide metabolism
Proteolysis
Redox homeostasis
Flavonoids metabolism
Glucosinolates metabolism
N-Acetylglucosaminyltransferases
Peroxidases
Polyamine metabolism
Phenylpropanoid metabolism
Phosphatases
Transferase
Nucleoside metabolism
AP2/EREBP
NAC domain
C2H2 zinc finger
C3H zinc finger
Homeobox
MYB
bZIP
WRKY
PLATZ
Heat-shock transcription factor
bHLH
C2C2(Zn) GATA
G2-like
GRAS
TCP
LOB domain-containing
B-box type zinc finger
C3H4 type zinc finger
C2C2(Zn) DOF zinc finger
RAV
MYB
bHLH
Homeobox
NIN-like bZIP
C2C2(Zn) CO-like
C2C2(Zn) GATA
B3
C2H2 zinc finger
Squamosa-promoter binding
TCP

Figure S11. (A) Venn diagram, gene ontology (GO) and expression correlation analyses of genes significantly deregulated (fold-change ≥ 2; Bonferroni corrected *P*-value ≤ 0.05) in response to Put (100 μM) and Spm (100 μM) at 24 h of treatment in the wild-type. **(B)** Molecular functions, main enzymatic activities and TF families of genes differentially expressed in Put and Spm treatments. Bars indicate the mean expression ± S.E. The number of genes within each category are indicated on top of the bar and listed in Tables S1.1 to S1.5.

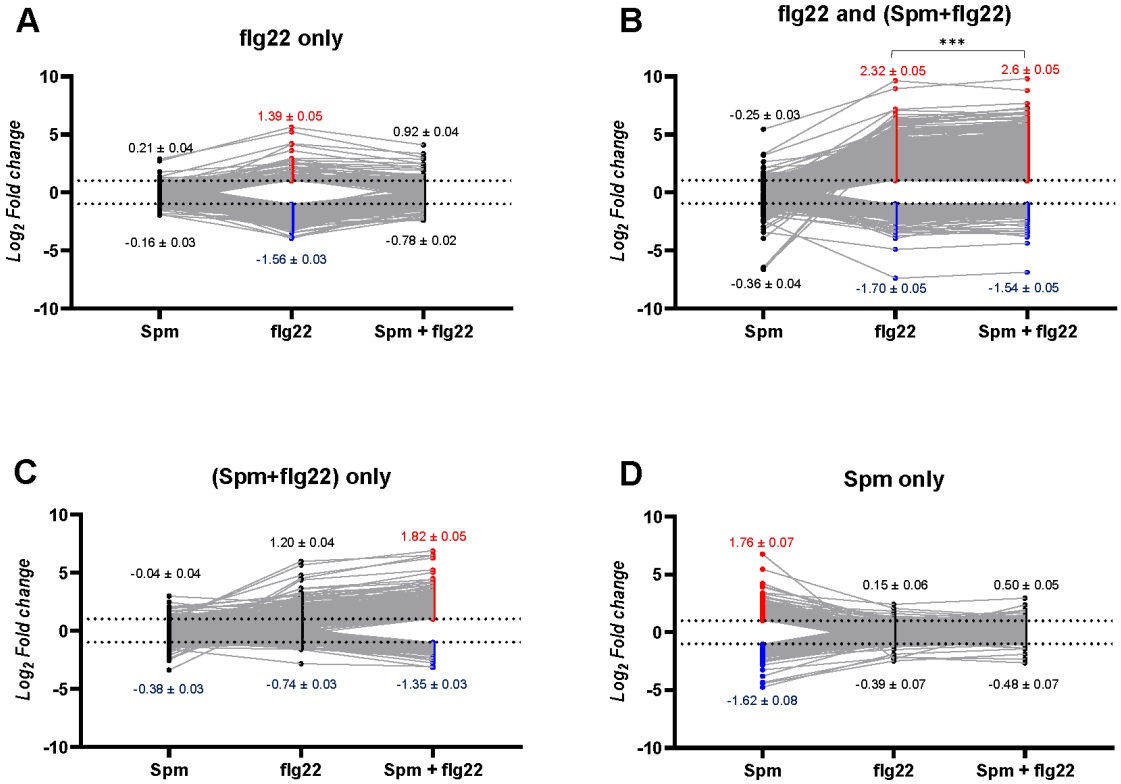
A
flg22 only
Log2 Fold change
10
5
0
-5
-10
1.39 ± 0.05
0.21 ± 0.04
0.92 ± 0.04
-0.16 ± 0.03
-1.56 ± 0.03
-0.78 ± 0.02
Spm
flg22
Spm + flg22
B
flg22 and (Spm+flg22)
***
2.32 ± 0.05
2.6 ± 0.05
-0.25 ± 0.03
-0.36 ± 0.04
-1.70 ± 0.05
-1.54 ± 0.05
C
(Spm+flg22) only
1.20 ± 0.04
1.82 ± 0.05
-0.04 ± 0.04
-0.38 ± 0.03
-0.74 ± 0.03
-1.35 ± 0.03
D
Spm only
1.76 ± 0.07
0.15 ± 0.06
0.50 ± 0.05
-1.62 ± 0.08
-0.39 ± 0.07
-0.48 ± 0.07

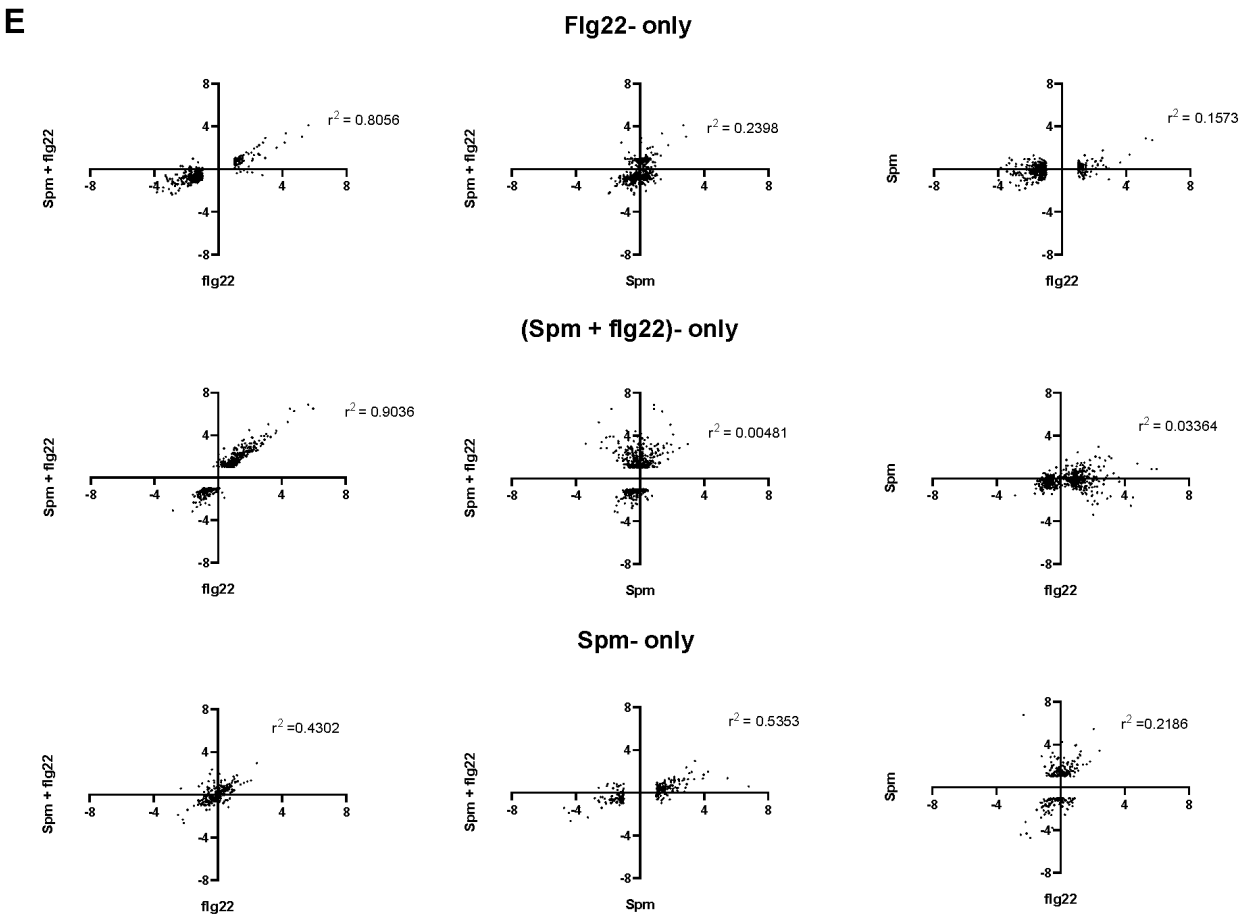
E
Flg22- only
r2 = 0.8056
r2 = 0.2398
r2 = 0.1573
(Spm + flg22)- only
r2 = 0.9036
r2 = 0.00481
r2 = 0.03364
Spm- only
r2 =0.4302
r2 = 0.5353
r2 =0.2186
Spm + flg22
flg22
Spm

Figure S12. Mean expression values and correlation analyses of wild-type (Col-0) plants treated with flg22 (1 µM), Spm (100 µM) and Spm (100 µM) + flg22 (1 µM). **(A)** Genes only significantly deregulated by flg22 treatment. **(B)** Common genes deregulated by flg22 and (Spm + flg22) treatments. **(C)** Genes only deregulated by (Spm + flg22) treatment. **(D)** Genes only deregulated by Spm treatment. Expression values (Log2) are relative to the mock (H_2O). The mean expression ± S.E of upregulated and downregulated genes is shown for each treatment. Asterisks indicate significant differences according to Wilcoxon signed-rank test (***p<0.001). **(E)** Expression correlation between flg22, Spm and (Spm + flg22) treatments.

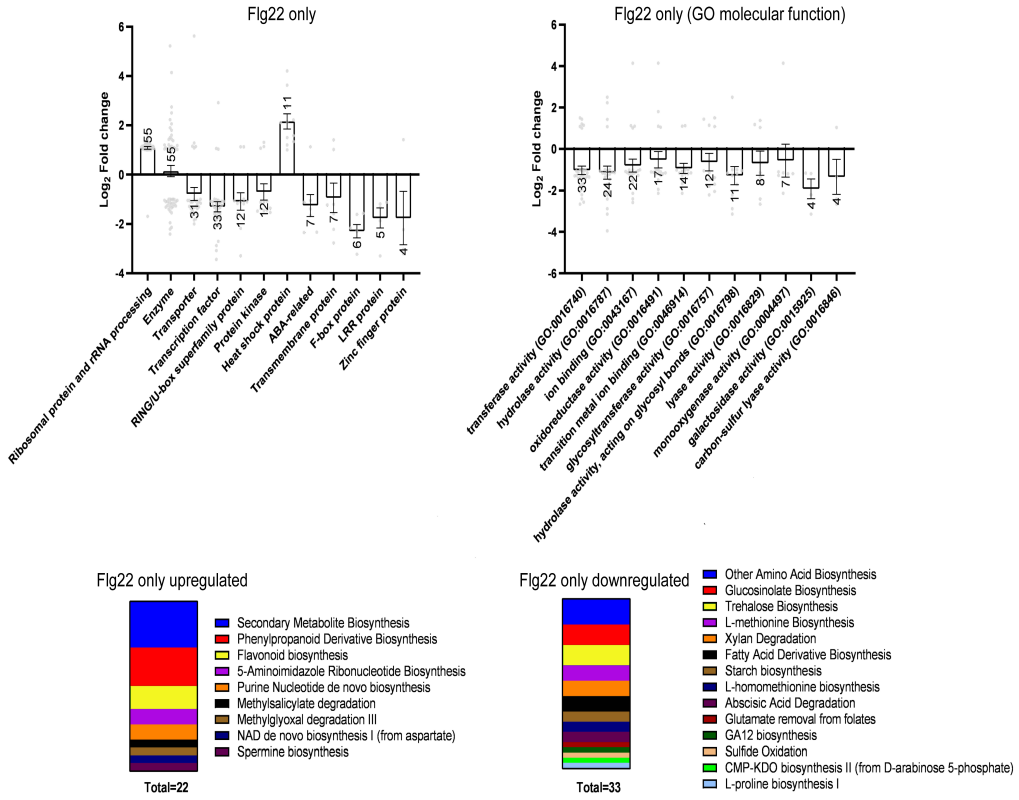

Figure S13. Molecular function categorization and metabolic pathway enrichment analysis of genes only deregulated by flg22 compared to Spm and (Spm + flg22) treatments in the wild-type. Bars indicate the mean expression ± S.E in each category.

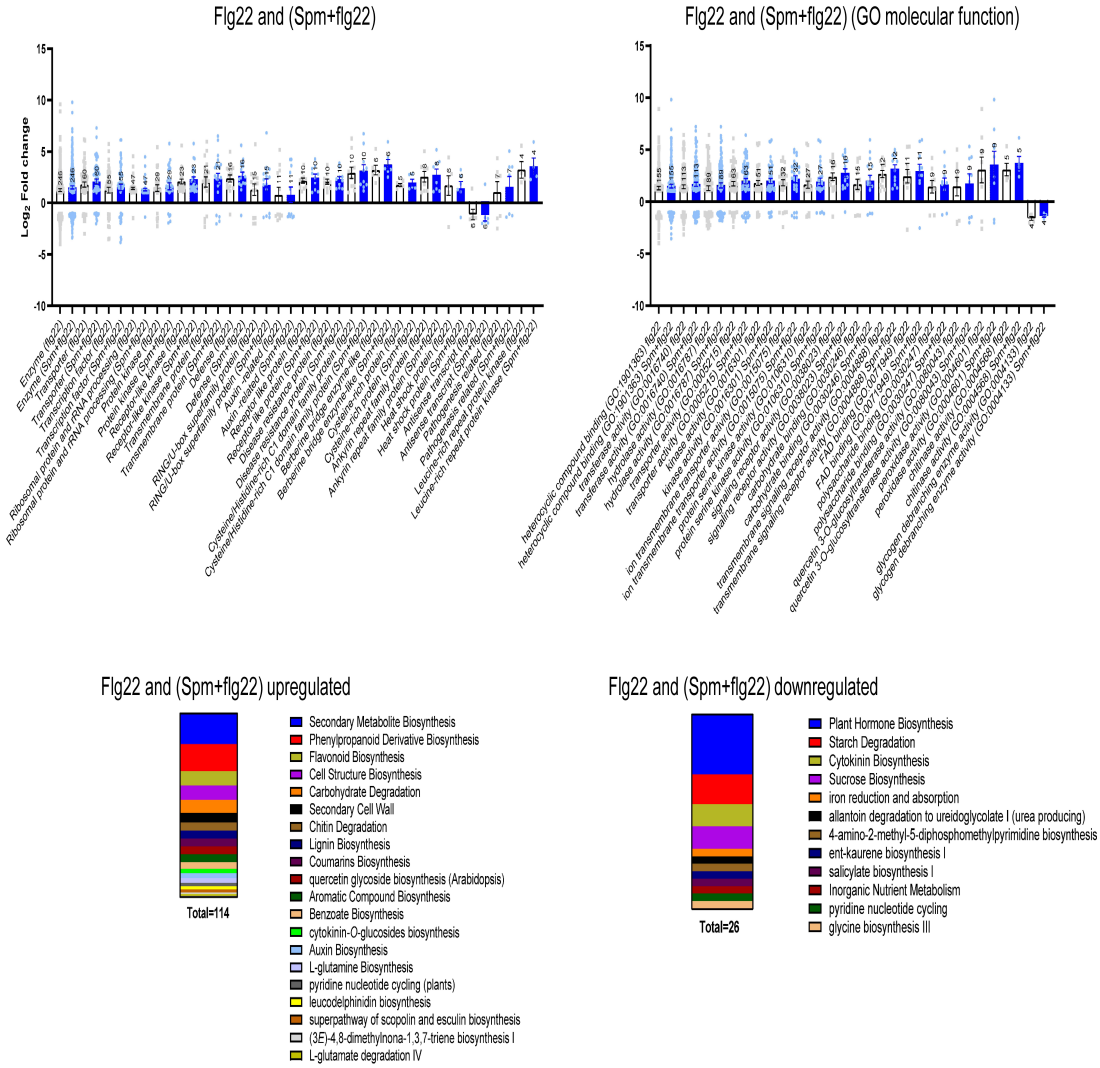

Figure S14. Molecular function categorization and metabolic pathway enrichment analysis of genes commonly deregulated in flg22 and (Spm + flg22) treatments in the wild-type. Bars indicate the mean expression ± S.E in each category.

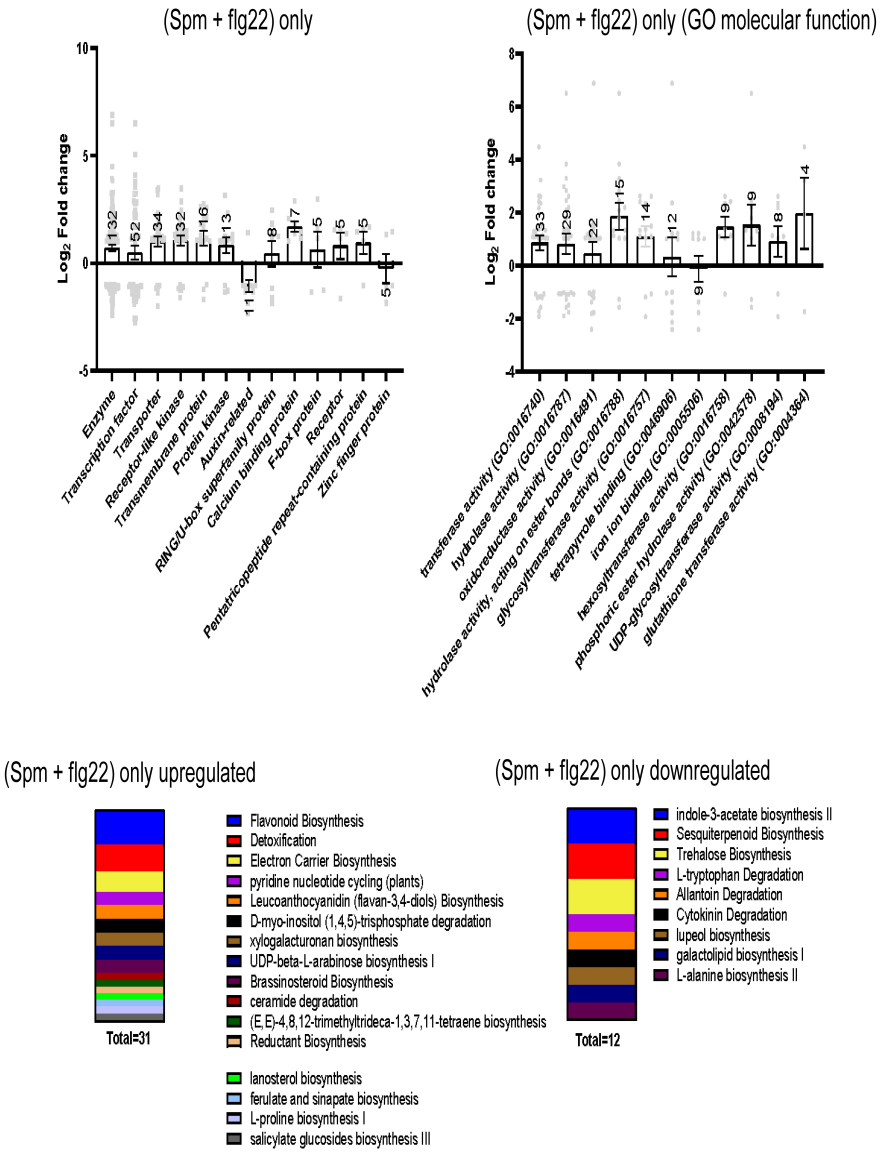

Figure S15. Molecular function categorization and metabolic pathway enrichment analysis of genes only differentially expressed in (Spm + flg22) compared to flg22 and Spm treatments. Bars indicate the mean expression ± S.E in each category.

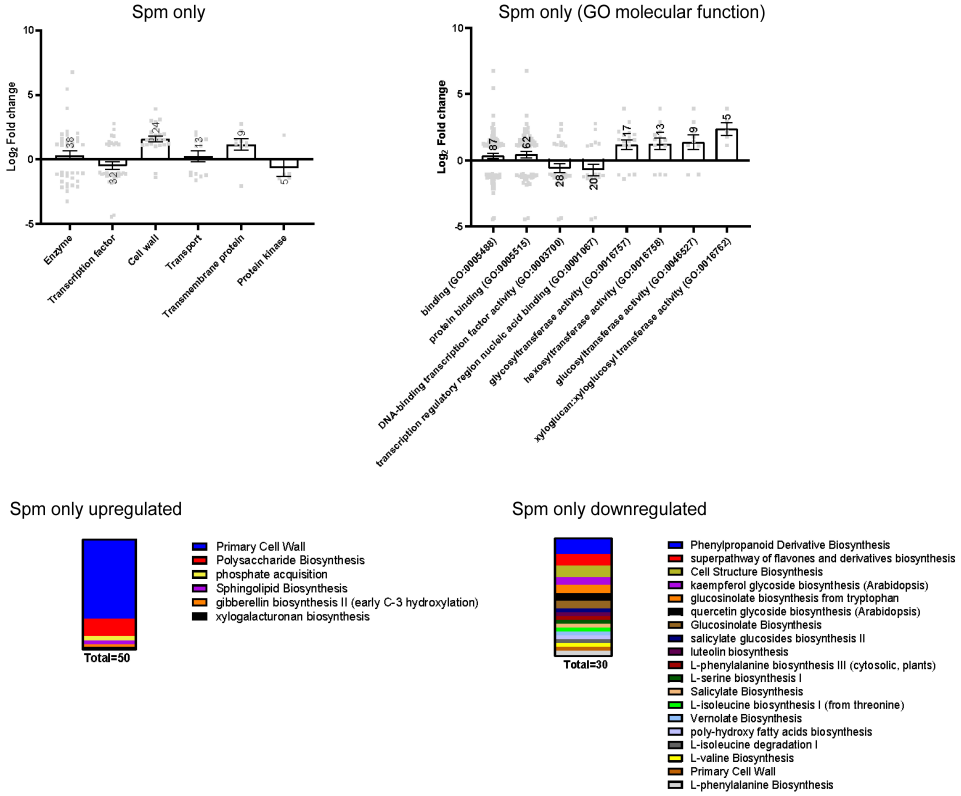

Figure S16. Molecular function categorization and metabolic pathway enrichment analysis of genes only differentially expressed in Spm treatment compared to flg22 and (Spm + flg22) treatments. Bars indicate the mean expression ± S.E in each category.

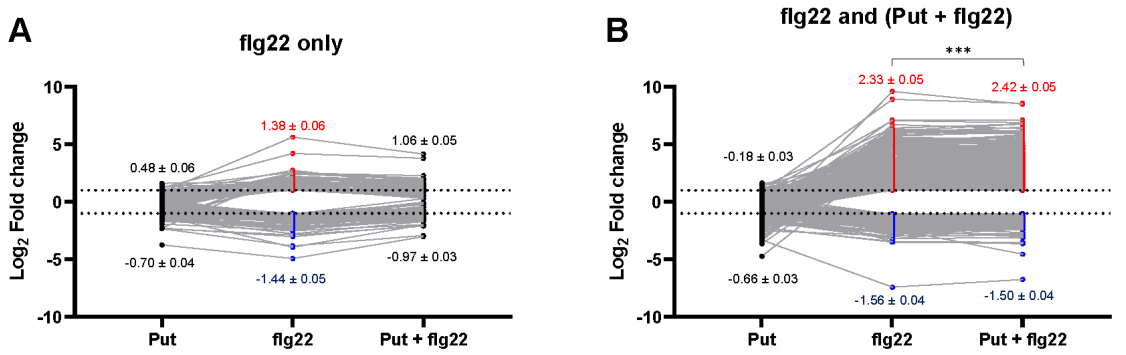
A
flg22 only
Log2 Fold change
10
5
0
-5
-10
1.38 ± 0.06
1.06 ± 0.05
0.48 ± 0.06
-0.70 ± 0.04
-1.44 ± 0.05
-0.97 ± 0.03
Put
flg22
Put + flg22
B
flg22 and (Put + flg22)
***
2.33 ± 0.05
2.42 ± 0.05
-0.18 ± 0.03
-0.66 ± 0.03
-1.56 ± 0.04
-1.50 ± 0.04
Log2 Fold change
Put
flg22
Put + flg22

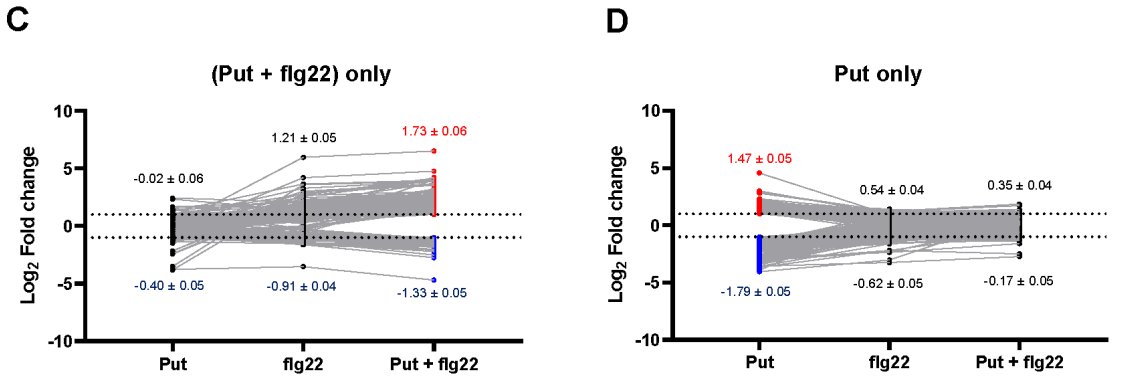
C
(Put + flg22) only
Log2 Fold change
1.21 ± 0.05
1.73 ± 0.06
-0.02 ± 0.06
-0.40 ± 0.05
-0.91 ± 0.04
-1.33 ± 0.05
Put
flg22
Put + flg22
D
Put only
Log2 Fold change
1.47 ± 0.05
0.54 ± 0.04
0.35 ± 0.04
-1.79 ± 0.05
-0.62 ± 0.05
-0.17 ± 0.05
Put
flg22
Put + flg22

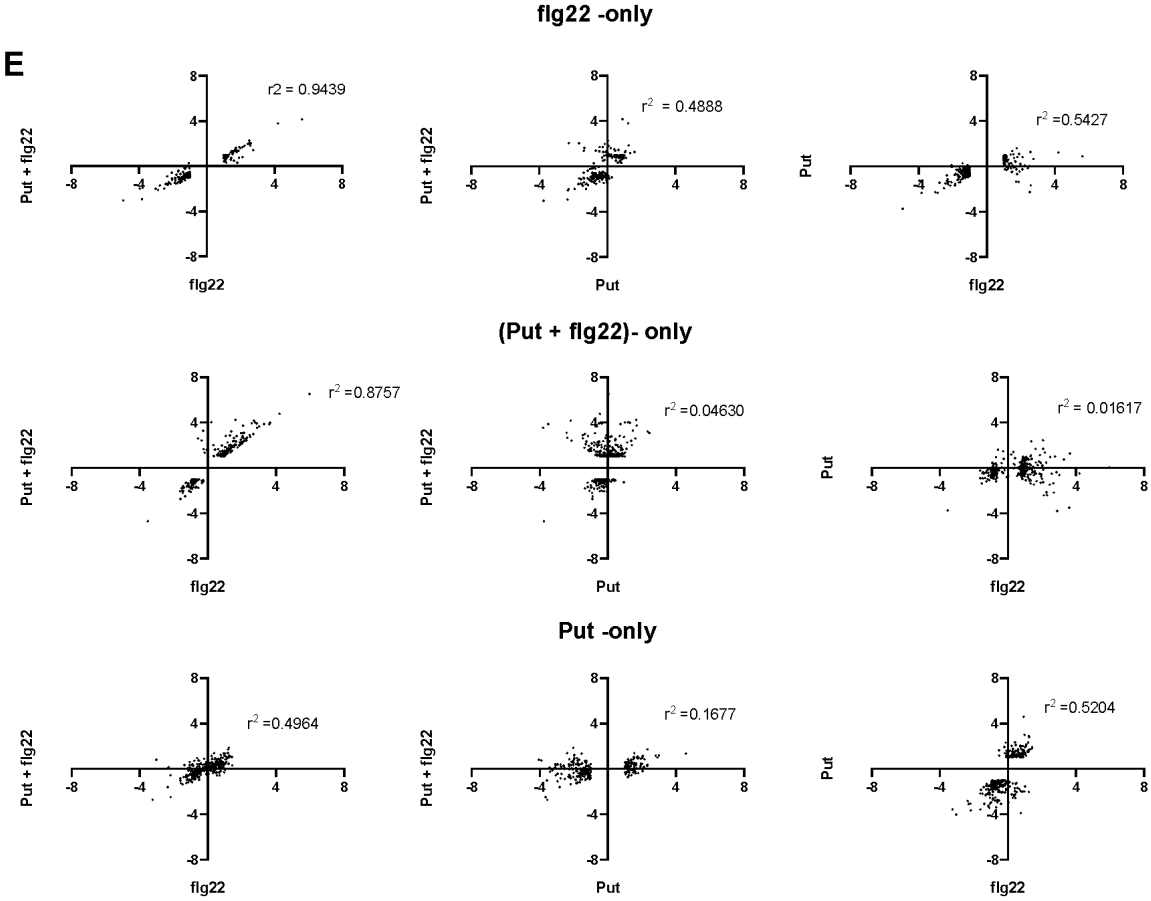
E
flg22 -only
r2 = 0.9439
r2 = 0.4888
r2 =0.5427
Put + flg22
flg22
Put
(Put + flg22)- only
r2 =0.8757
r2 =0.04630
r2 = 0.01617
Put + flg22
Put
flg22
Put -only
r2 =0.4964
r2 =0.1677
r2 =0.5204
Put + flg22
Put
flg22

Figure S17. Mean expression values and correlation analyses of wild-type (Col-0) plants treated with flg22 (1 μM), Put (100 μM) and Put (100 μM) + flg22 (1 μM). **(A)** Genes only significantly deregulated by flg22 treatment. **(B)** Common genes deregulated by flg22 and (Put + flg22) treatments. **(C)** Genes only deregulated by (Put + flg22) treatment. **(D)** Genes only deregulated by Put treatment. Expression values (Log2) are relative to the mock (H_2O). The mean expression ± S.E of upregulated and downregulated genes is shown for each treatment. Asterisks indicate significant differences according to Wilcoxon signed-rank test (***p<0.001). **(E)** Expression correlation between flg22, Put and (Put + flg22) treatments.

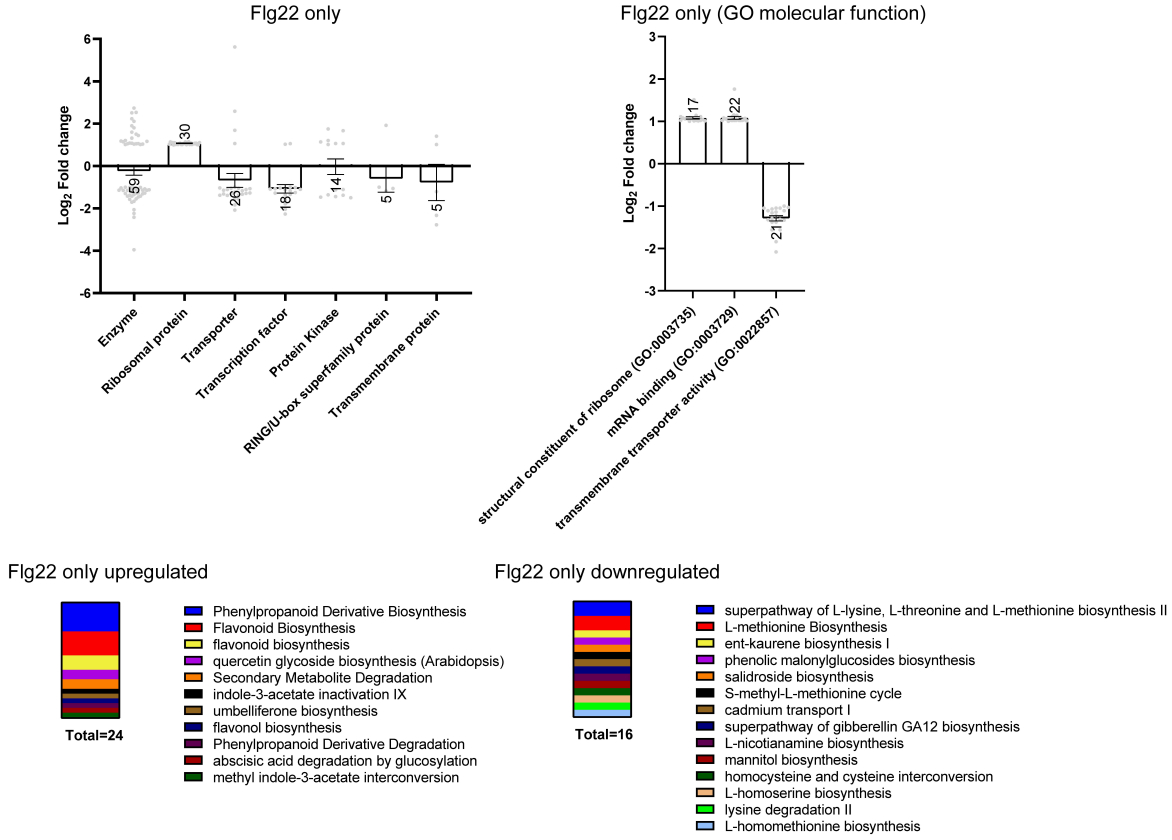

Figure S18. Molecular function categorization and metabolic pathway enrichment analysis of genes only deregulated by flg22 compared to Put and (Put + flg22) treatments. Bars indicate the mean expression ± S.E in each category.

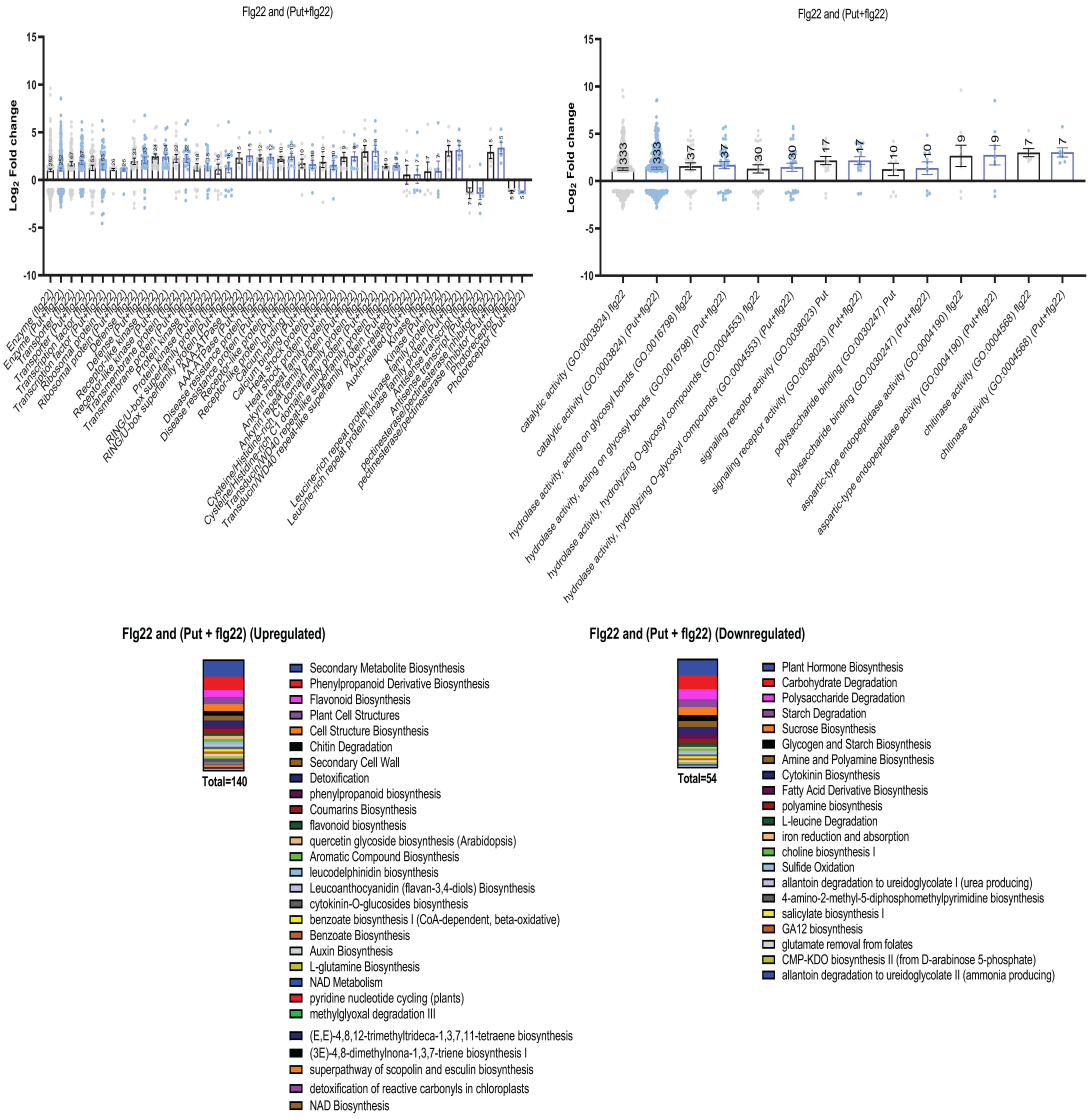

Figure S19. Molecular function categorization and metabolic pathway enrichment analysis of genes commonly deregulated in flg22 and (Put + flg22) treatments in the wild-type. Bars indicate the mean expression ± S.E in each category.

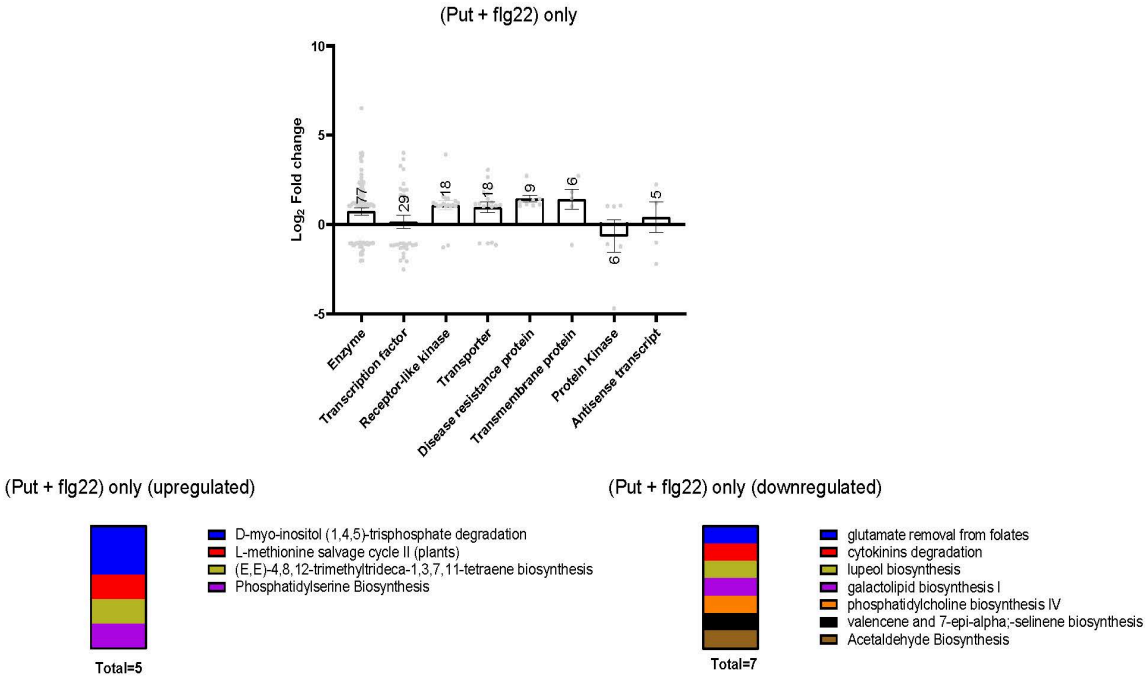

Figure S20. Molecular function categorization and metabolic pathway enrichment analysis of genes only deregulated in (Put + flg22) compared to flg22 and Put treatments. Bars indicate the mean expression ± S.E in each category.

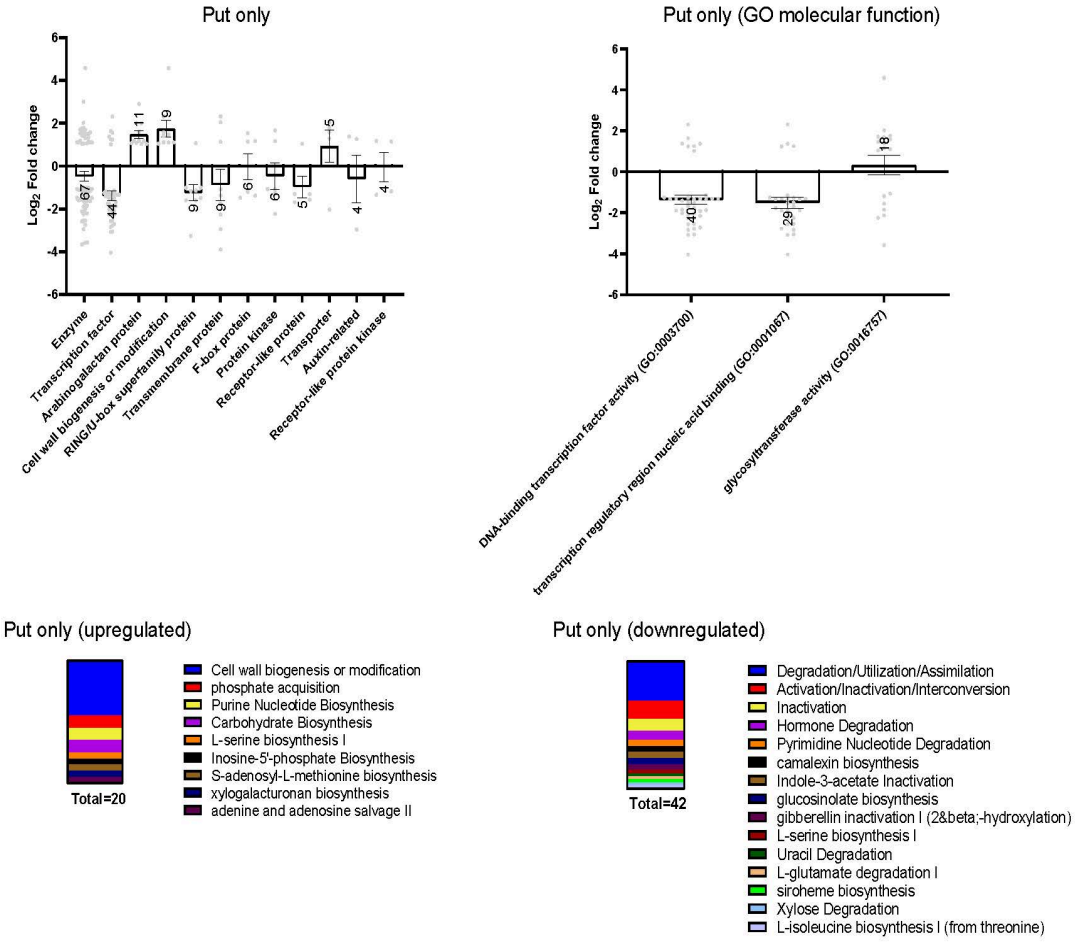

Figure S21. Molecular function categorization and metabolic pathway enrichment analysis of genes only deregulated by Put compared to flg22 and (Put + flg22) treatments. Bars indicate the mean expression ± S.E in each category.

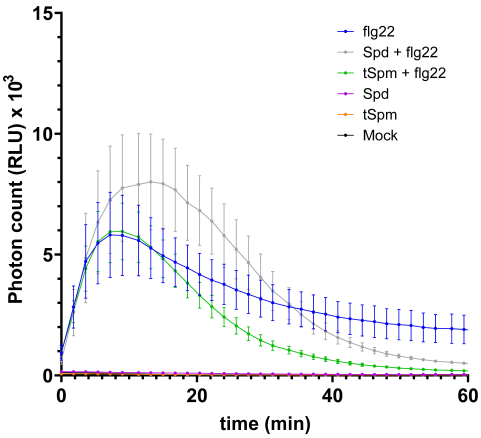

Figure S22. Effect of thermospermine (tSpm, 100 µM) and spermidine (Spd, 100 µM) on flg22-elicited ROS burst in the wild-type (Col-0). Leaf discs from 5-week-old plants were treated with flg22 (1 µM), tSpm (100 µM), Spd (100 µM), tSpm (100 µM) + flg22 (1 µM), Spd (100 µM) + flg22 (1 µM) or mock (water). Values represent the mean ± S.E. from at least twelve replicates per treatment and are expressed in photon counts (relative light units, RLU).

ANNEX II

SUPPORTING INFORMATION

Spermine deficiency shifts the balance between Jasmonic Acid and Salicylic Acid-mediated defense responses in Arabidopsis

Chi Zhang[1], Kostadin E. Atanasov[1], Ester Murillo[1], Vicente Vives-Peris[2], Jiaqi Zhao[1], Cuiyun Deng[3], Aurelio Gómez-Cadenas[2] and Rubén Alcázar[1,*]

[1] Department of Biology, Healthcare and Environment. Section of Plant Physiology, Faculty of Pharmacy and Food Sciences, Universitat de Barcelona, Av. Joan XXIII 27-31, 08028 Barcelona, Spain.
[2] Departamento de Biología, Bioquímica y Ciencias Naturales, Universitat Jaume I, Av. Sos Baynat s/n, 12071 Castelló de la Plana, Spain.
[3] Plant Synthetic Biology and Metabolic Engineering Program, Centre for Research in Agricultural Genomics (CRAG), CSIC-IRTA-UAB-UB, Cerdanyola, 08193 Barcelona, Spain.
* For correspondence (email: ralcazar@ub.edu)

SUPPLEMENTARY FIGURES

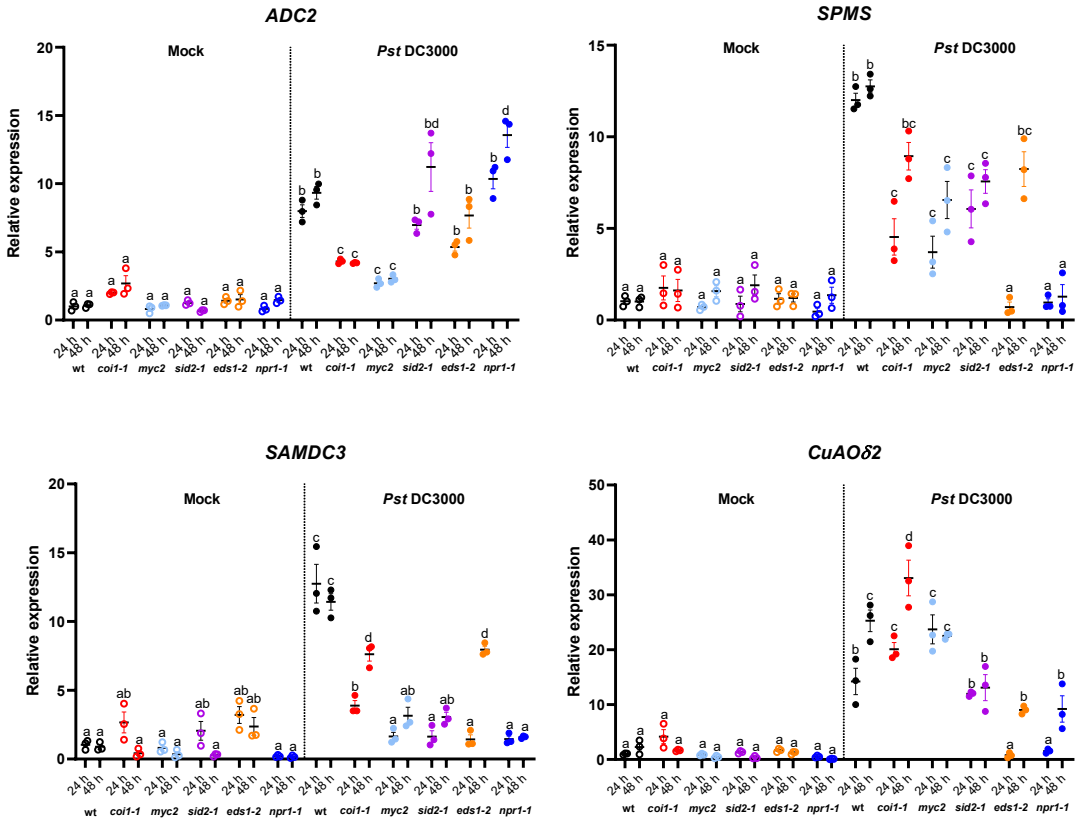

Figure S1. Expression analyses of *ADC2*, *SPMS*, *SAMDC3* and *CuAO*δ2 in wild-type, *coi1-1*, *myc2*, *sid2-1*, *eds1-2* and *npr1-1* mutants in response to *Pst* DC3000 (OD_{600}=0.001) and mock (10 mM $MgCl_2$) infiltration at 24 h and 48 h of treatment. Expression values are relative to wild-type (mock) treatment and represent the mean ± standard deviation from three biological replicates per genotype and treatment. Different letters indicate significant differences ($p<0.05$) according to two-way ANOVA followed by Tukey's post-hoc test.

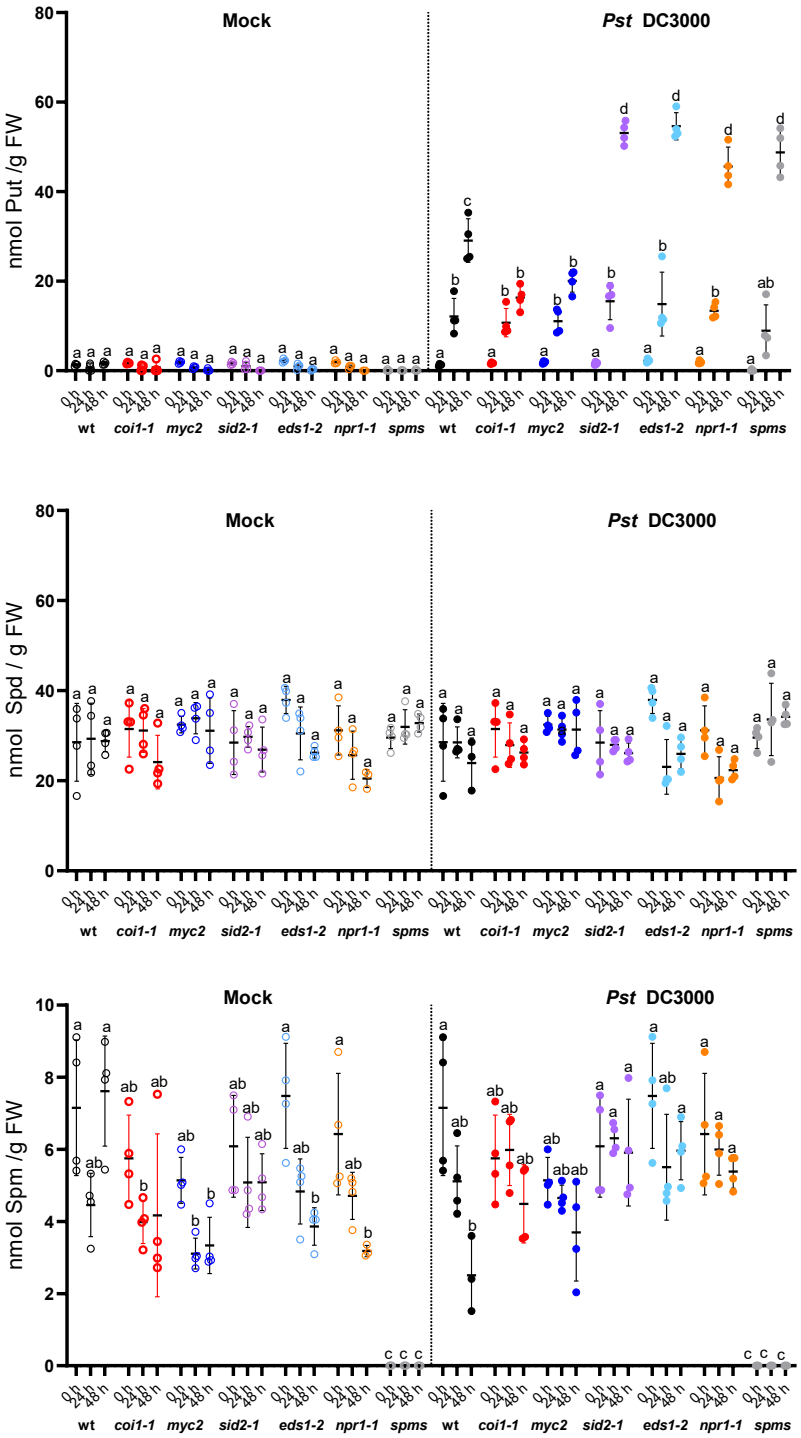

Figure S2. Determination of polyamine contents in wild-type (wt), *coi1-1*, *myc2*, *sid2-1*, *eds1-2* and *npr1-1* mutants in response to *Pst* DC3000 (OD_{600}=0.001) and mock (10 mM $MgCl_2$) infiltration at 0 h, 24 h and 48 h of treatment. Values represent the mean ± standard deviation from four biological replicates per genotype. Different letters indicate significant differences ($p<0.05$) according to two-way ANOVA followed by Tukey's post-hoc test.

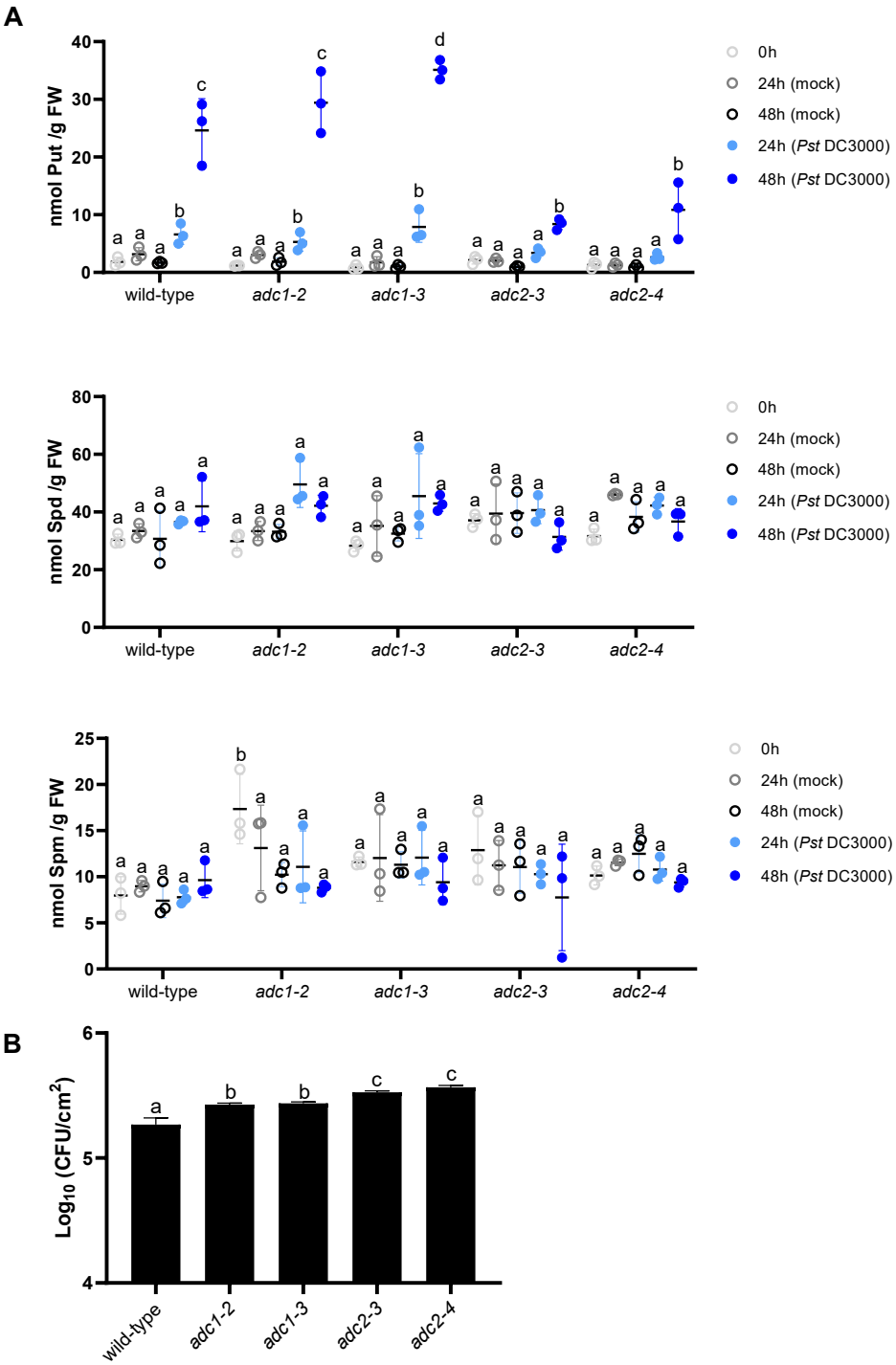

Figure S3. (A) Determination of polyamine contents in wild-type, *adc1-2*, *adc1-3*, *adc2-3* and *adc2-4* mutants in response to *Pst* DC3000 (OD_{600}=0.001) and mock (10 mM $MgCl_2$) infiltration at 0 h, 24 h and 48 h of treatment. Values represent the mean ± standard deviation from three biological replicates per genotype. **(B)** Determination of *Pst* DC3000 growth in wild-type, *adc1* and *adc2* mutants at 48 h of infiltration. Bacterial numbers are expressed as colony forming units (CFU) per cm^2 of leaf area. Values are the mean from six biological replicates ± SD. Different letters indicate significant differences ($p<0.05$) according to two-way ANOVA followed by Tukey's post-hoc test.

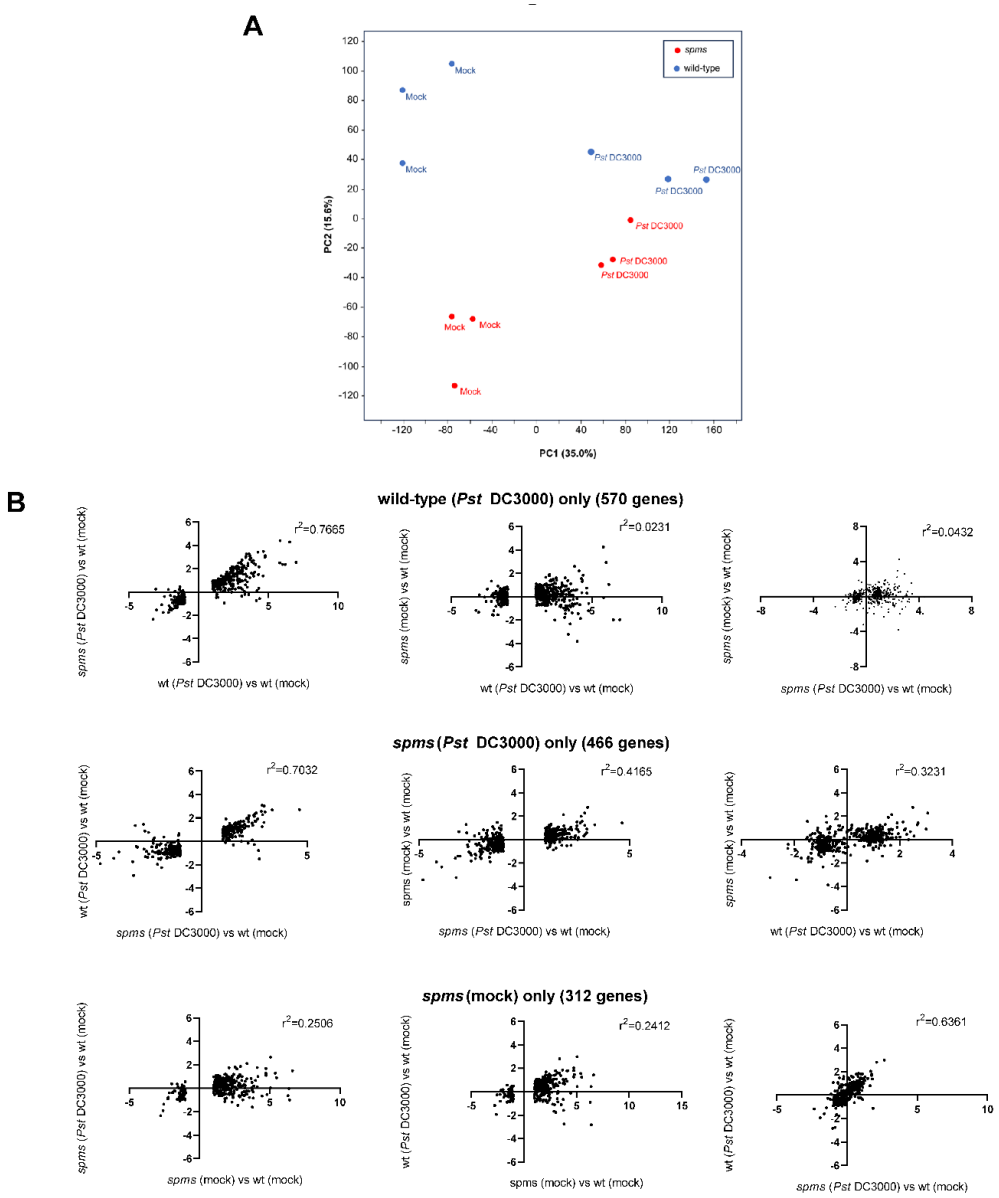

Figure S4. **(A)** Principal component analysis (PCA) of RNA-seq gene expression data at 24 h of *Pst* DC3000 (OD_{600}=0.001) and mock (10 mM $MgCl_2$) inoculation in *spms* and wild-type plants. **(B)** Expression correlation analyses between wild-type (wt) and *spms* in the 'wild-type (*Pst* DC3000) only' sector (genes deregulated only in the comparison between wt *Pst* DC3000 *vs* wt mock), '*spms* (*Pst* DC3000) only' sector (genes deregulated only in the comparison between *spms Pst* DC3000 *vs* wt mock) and '*spms* (mock) only' sector (genes deregulated only in the comparison between *spms* mock *vs* wt mock).

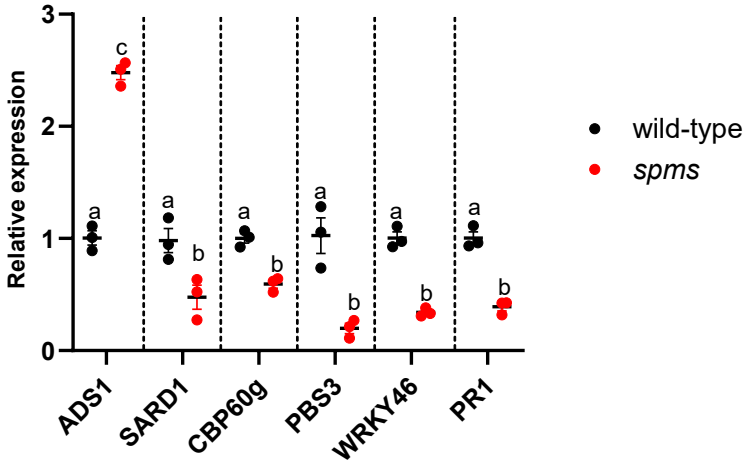

Figure S5. Basal expression of *ADS1*, *SARD1*, *CBP60g*, *PBS3*, *WRKY46* and *PR1* in wild-type and *spms* mutant plants determined by qRT-PCR. Expression values are relative to the wild-type and represent the mean ± standard deviation from three biological replicates per genotype. Different letters indicate significant differences ($p<0.05$) according to two-way ANOVA followed by Tukey's post-hoc test.

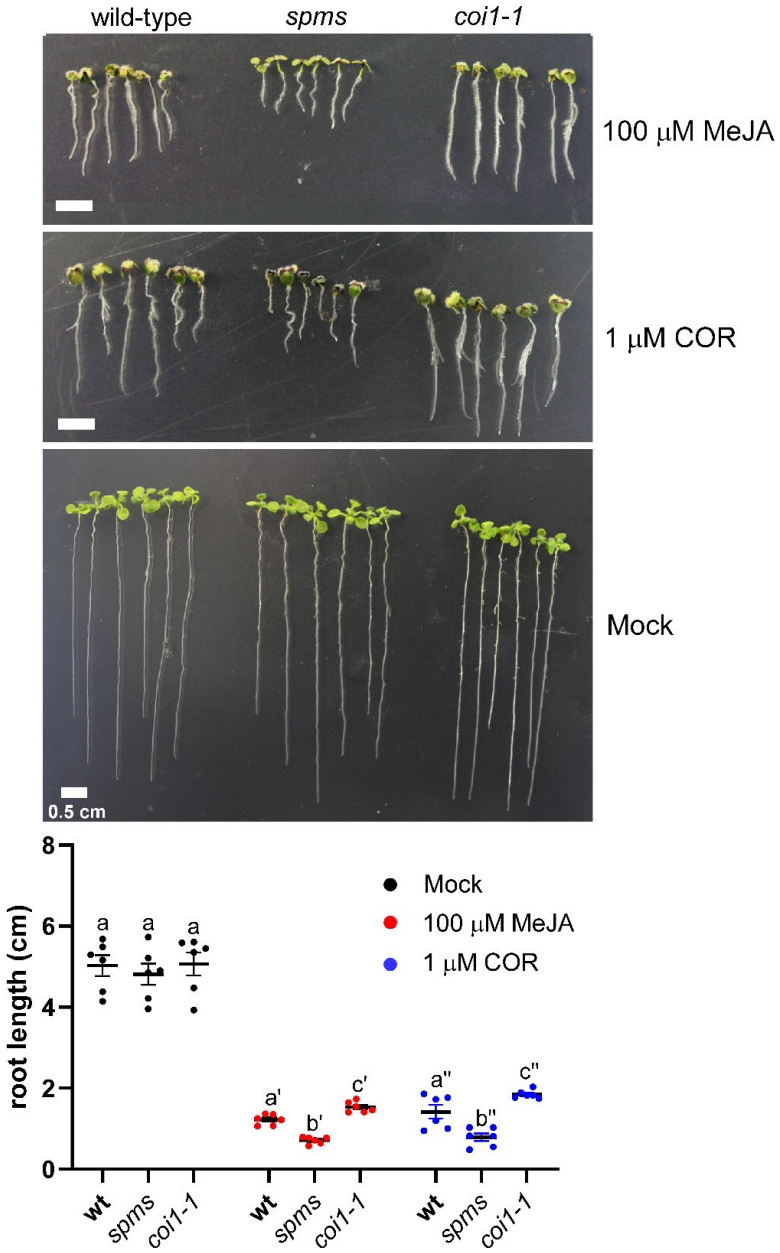

Figure S6. Root growth inhibition assays in response to MeJA and COR. Wild-type (wt), *spms* and *coi1-1* seeds were germinated and grown on vertical plates containing half-strength MS supplemented with 1% sucrose and 100 μM methyl jasmonate (MeJA), 1 μM coronatine (COR) or mock (0.1% DMSO in water) at 16 h light/8 h dark cycles, 20 – 22 °C and 100–125 μmol photons m^{-2} s^{-1} of light intensity. Pictures were taken 12 days after germination for the measurement of the primary root length. Different letters indicate significant differences ($p<0.05$) according to two-way ANOVA followed by Tukey's post-hoc test.

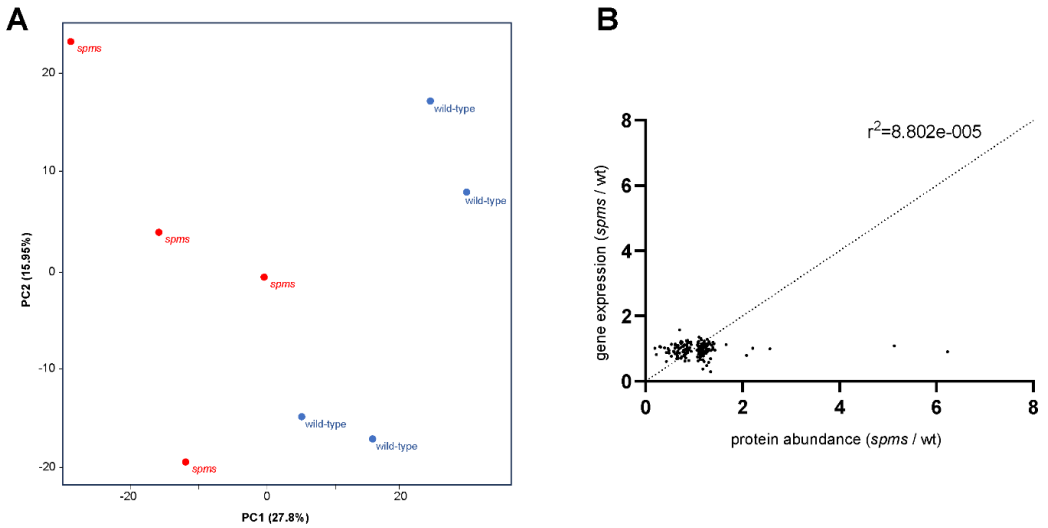

Figure S7. (A) Principal component analysis (PCA) of the proteomics data in *spms* and wild-type under basal conditions. **(B)** Correlation analysis between protein abundance and gene expression in *spms* under basal conditions. Values of proteins exhibiting >1.3-fold difference between *spms* and wild-type are shown.

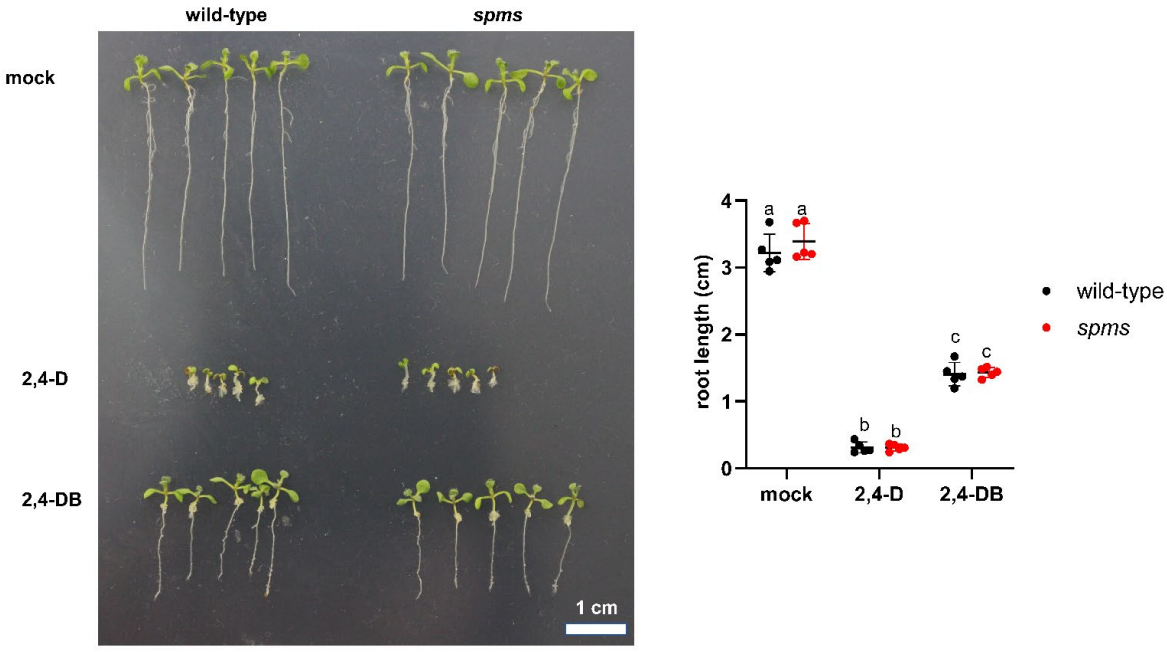

Figure S8. Root growth phenotypes of 12-day-old wild-type and *spms* seedlings germinated and grown on half-strength MS supplemented with 1 % sucrose and 0.05 µg/ml 2,4-dichlorophenoxyacetic acid (2,4-D), 0.2 µg/ml 2,4-dichlorophenoxybutyric acid (2,4-DB) or mock (0.1% DMSO in water). Different letters indicate significant differences ($p<0.05$) according to two-way ANOVA followed by Tukey's post-hoc test.

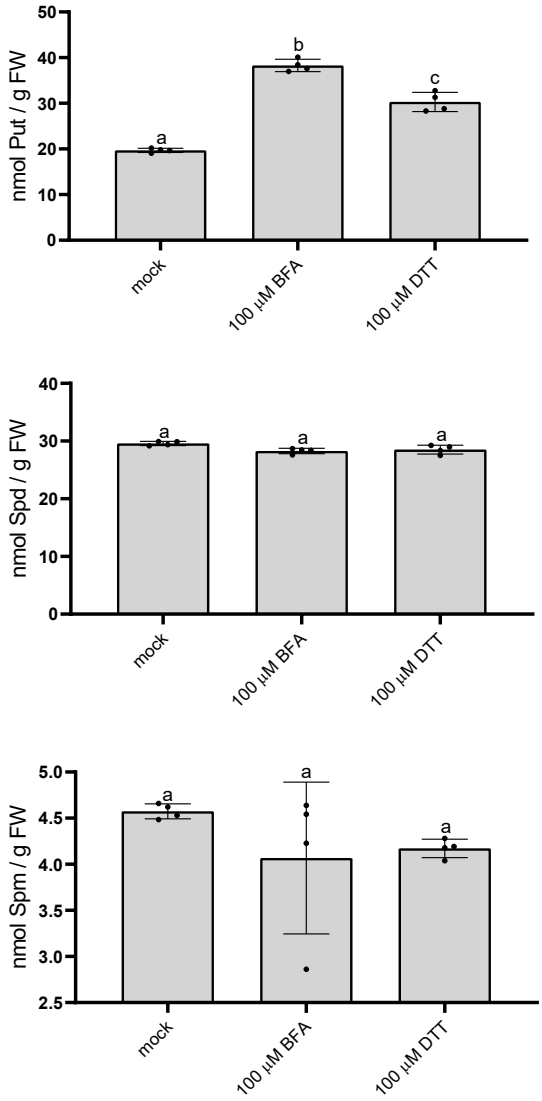

Figure S9. Polyamine levels (Put, putrescine; Spd, spermidine; Spm, spermine) in 10-day-old wild-type seedlings at 6 h of treatment with 100 µM Brefeldin A (BFA), 100 µM DTT (dithiothreitol) or mock (0.1% DMSO in water). Values represent the mean ± standard deviation from four biological replicates per treatment. Different letters indicate significant differences ($p<0.05$) according to two-way ANOVA followed by Tukey's post-hoc test.

ANNEX III

Accession	ecotypeID	native	stockparent	collector	lat	long	country	Mean_SumRLU	Std. Error of Mean	Number of values
cs76089	**1**	ALL1-2	NA	Roux	45.2667	1.48333	France	37.9	15.1	6
cs76158	**96**	LAC-5	NA	Roux	47.7	6.81667	France	28.3	5.15	6
cs76183	**178**	MIB-28	NA	Roux	47.3833	5.31667	France	4.29	0.757	6
cs76189	**242**	MOG-37	NA	Roux	48.6667	-4.06667	France	10.1	4.01	5
cs76092	**5832**	App1-16	NA	Nordborg	56.3333	15.9667	Sweden	0.374	0.23	6
cs76099	**5837**	Bor-1	CS22590	Nordborg	49.4013	16.2326	Czech Republic	56.8	29.8	6
cs76121	**5889**	DraIV 1-7	NA	Nordborg	49.4112	16.2815	Czech Republic	7.17	2.61	6
cs76123	**6005**	DraIV 6-35	NA	Nordborg	49.4112	16.2815	Czech Republic	137	82.4	6
cs76124	**6008**	Duk	<Null>	Nordborg	49.1	16.2	Czech Republic	0.0468	0.0101	6
cs76131	**6019**	FjÃ¤1-2	NA	Nordborg	56.06	14.29	Sweden	3.79	1.89	5
cs76234	**6096**	T1060	NA	Nordborg	55.6472	13.2225	Sweden	9.15	2.15	6
cs76248	**6190**	TDr-3	NA	Nordborg	55.7686	14.1381	Sweden	31.7	9.55	6
cs76250	**6242**	Tomegap-2	NA	Nordborg	55.7	13.2	Sweden	22.9	7.24	6
cs28140	**6727**	CIBC-2	CS22221	Crawley	51.4083	-0.6383	UK	22	10.3	6
cs28141	**6729**	CIBC-4	CS22223	Crawley	51.4083	-0.6383	UK	26.5	4.36	6
cs28142	**6730**	CIBC-5	CS22224	Crawley	51.4083	-0.6383	UK	0.983	0.409	6
cs28550	**6847**	NFC-20	CS22201	Crawley	51.4083	-0.6383	UK	40.9	9.51	6
cs28663	**6953**	Pu2-24	CS22454	Cetl	49.42	16.36	Czech Republic	3.39	3.32	6
cs28013	**6989**	Alst-1	CS22550	Koornneef	54.8	-2.4333	UK	20.7	5.96	6
cs28014	**6990**	Amel-1	CS22526	Koornneef	53.448	5.73	Netherlands	12.1	3.97	6
cs28049	**6994**	Ann-1	CS22520	Koornneef	45.9	6.13028	France	5.61	2.02	6
cs28007	**7000**	Aa-0	CS6600	Kranz	50.9167	9.57073	Germany	23.9	7.79	6
cs28054	**7002**	Baa-1	CS22529	Koornneef	51.3333	6.1	Netherlands	33.2	9.47	6
cs28097	**7004**	Bs-2	CS6628	Kranz	47.5	7.5	Switzerland	0.584	0.217	6
cs28064	**7008**	Benk-1	CS22530	Koornneef	52	5.675	Netherlands	24.8	5.72	6
cs28063	**7011**	Be-1	CS6614	Kranz	49.6803	8.6161	Germany	42.7	19.5	6
cs28053	**7014**	Ba-1	CS6607	Kranz	56.5459	-4.79821	UK	3.28	1.08	6
cs28091	**7026**	Boot-1	CS22551	Koornneef	54.4	-3.2667	UK	20.2	4.78	6
cs28099	**7031**	Bsch-0	CS6630	Kranz	40.0167	8.6667	Germany	18.2	4.78	6
cs28090	**7035**	Blh-2	CS6657	Kranz	48	19	Czech Republic	3.2	0.93	6
cs28108	**7056**	Bu-8	CS6639	Kranz	50.5	9.5	Germany	6.32	3.64	6

cs28128	**7062**	Ca-0	CS6658	Kranz	50.2981	8.26607	Germany	51	13.6	6
cs28133	**7069**	Cha-0	CS6662	Kranz	46.0333	7.1167	Switzerland	250	85.3	6
cs28135	**7071**	Chat-1	CS22521	Koornneef	48.0717	1.33867	France	38.5	16.6	6
cs28158	**7075**	Cit-0	CS1080	Kranz	43.3779	2.54038	France	3.03	2	6
cs28163	**7078**	Co-2	CS6670	Kranz	40.12	-8.25	Portugal	2.86	1.84	6
cs28193	**7092**	Com-1	CS22522	Koornneef	49.416	2.823	France	39.3	11.9	6
cs28200	**7094**	Da-0	CS6676	Kranz	49.8724	8.65081	Germany	7.99	4.61	6
cs28208	**7098**	Di-1	CS6681	Kranz	47	5	France	4.7	1.98	6
cs28202	**7100**	Db-0	CS6677	Kranz	50.3055	8.324	Germany	8.51	2.53	6
cs28210	**7102**	Do-0	CS6683	Kranz	50.7224	8.2372	Germany	13.8	1.55	6
cs28236	**7123**	Ep-0	CS6697	Kranz	50.1721	8.38912	Germany	1.21	0.492	6
cs28243	**7128**	Est-0	CS6700	Kranz	58.3	25.3	Russia	45.3	8.03	6
cs28268	**7135**	Fr-4	CS6710	Kranz	50.1102	8.6822	Germany	8.34	3.1	6
cs28252	**7139**	Fi-1	CS6705	Kranz	50.5	8.0167	Germany	2.13	1.36	6
cs28274	**7141**	Ga-2	CS6715	Kranz	50.3	8	Germany	25.4	5.4	6
cs28279	**7143**	Gel-1	CS22533	Koornneef	51.0167	5.86667	Netherlands	8.4	2.48	6
cs28277	**7145**	Ge-1	CS6718	Kranz	46.5	6.08	Switzerland	43	16	6
cs28280	**7147**	Gie-0	CS6720	Kranz	50.584	8.67825	Germany	0.872	0.49	6
cs28332	**7150**	Gu-1	CS6731	Kranz	50.3	8	Germany	2.49	1.64	6
cs28282	**7151**	Go-0	CS6721	Kranz	51.5338	9.9355	Germany	-0.00273	0.0017	6
cs28326	**7158**	Gr-5	CS6727	Hauser	47	15.5	Austria	6.94	3.68	5
cs28336	**7163**	Ha-0	CS6733	Kranz	52.3721	9.73569	Germany	32.2	7.84	5
cs28343	**7164**	Hau-0	CS6734	Kranz	55.675	12.5686	Denmark	9.19	3.03	6
cs28350	**7165**	Hn-0	CS6739	Kranz	51.3472	8.28844	Germany	25.6	7.2	6
cs28344	**7166**	Hey-1	CS22534	Koornneef	51.25	5.9	Netherlands	0.904	0.427	6
cs28373	**7178**	Jm-1	CS6749	Kranz	49	15	Czech Republic	2.04	0.765	5
cs28364	**7181**	Je-0	CS6742	Kranz	50.927	11.587	Germany	72.4	15.4	6
cs28395	**7186**	Kn-0	CS6762	Kranz	54.8969	23.8924	Lithuania	42.4	4.9	6
cs28382	**7188**	Kelsterbach-2	CS6102	Williams	50.0667	8.5333	Germany	1.48	0.984	6
cs28423	**7205**	Krot-2	CS3888	Clauss	49.631	11.5722	Germany	5.76	3.95	6
cs28420	**7206**	Kro-0	CS6766	Kranz	50.0742	8.96617	Germany	9.18	1.75	5
cs28454	**7224**	Li-3	CS1316	Kranz	50.3833	8.0666	Germany	21.8	2.6	6

cs28457	**7227**	Li-5:2	CS6909	Kranz	50.3833	8.0666	Germany	2.49	1.27	5
cs28495	**7244**	Mnz-0	CS6794	Kranz	50.001	8.26664	Germany	10.8	2.64	6
cs28490	**7252**	Mc-0	CS1362	Kranz	54.6167	-2.3	UK	0.801	0.404	6
cs28492	**7255**	Mh-0	CS6792	Kranz	50.95	7.5	Poland	45.1	12.1	6
cs28573	**7258**	Nw-0	CS6811	Kranz	50.5	8.5	Germany	0.576	0.503	6
cs28575	**7260**	Nw-2	CS6813	Kranz	50.5	8.5	Germany	7.65	3.06	6
cs28578	**7263**	Nz1	CS22661	Campanella	-37.7871	175.283	New Zealand	63.8	23	6
cs28568	**7270**	Nok-1	CS6808	Kranz	52.24	4.45	Netherlands	63.5	19.7	6
cs28564	**7275**	No-0	CS3081	Kranz	51.0581	13.2995	Germany	0.433	0.336	6
cs28583	**7280**	Old-1	CS6820	Kranz	53.1667	8.2	Germany	0.743	0.592	6
cs28587	**7282**	Or-0	CS6822	Kranz	50.3827	8.01161	Germany	7.39	5.69	6
cs28640	**7300**	Pla-0	CS6834	Kranz	41.5	2.25	Spain	18.4	2.19	6
cs28650	**7306**	Pog-0	CS6842	Kranz	49.2655	-123.206	Canada	46.4	5.56	6
cs28645	**7307**	Pn-0	CS6838	Kranz	48.0653	-2.96591	France	3.09	0.861	6
cs28651	**7310**	Pr-0	CS6841	Kranz	50.1448	8.60706	Germany	37.7	10.4	6
cs28685	**7316**	Rhen-1	CS22536	Koornneef	51.9667	5.56667	Netherlands	41.8	10.3	6
cs28734	**7331**	Sh-0	CS6860	Kranz	51.6832	10.2144	Germany	9.53	2.17	6
cs28739	**7337**	Si-0	CS6861	Kranz	50.8738	8.02341	Germany	41.2	13.9	6
cs28725	**7340**	Sav-0	CS6856	Kranz	49.1833	15.8833	Czech Republic	0.044	0.0111	6
cs28743	**7343**	Sp-0	CS6862	Kranz	52.5339	13.181	Germany	4.84	1.81	6
cs28732	**7344**	Sg-1	CS6858	Kranz	47.6667	9.5	Germany	3.66	1.45	5
cs28779	**7372**	Tscha-1	CS22518	Koornneef	47.0748	9.9042	Austria	11.6	3.57	6
cs28788	**7379**	UK-2	CS6881	Kranz	48.0333	7.7667	Germany	0.859	0.269	6
cs28795	**7382**	Utrecht	CS6150	Willemsen	52.0918	5.1145	Netherlands	2.12	0.678	6
cs28800	**7384**	Ven-1	CS22538	Koornneef	52.0333	5.55	Netherlands	46.5	8.13	6
cs28808	**7390**	Wag-3	CS22542	Koornneef	51.9666	5.6666	Netherlands	10.4	4.05	6
cs28809	**7391**	Wag-4	CS22543	Koornneef	51.9666	5.6666	Netherlands	12.9	3.16	6
cs28810	**7392**	Wag-5	CS22544	Koornneef	51.9666	5.6666	Netherlands	13.2	5.09	5
cs28804	**7394**	Wa-1	CS6885	Kranz	52.3	21	Poland	1.25	0.734	6
cs28823	**7397**	Ws	CS915	Kranz	52.3	30	Russia	0.889	0.518	6
cs28814	**7405**	Wc-2	CS6887	Kranz	52.6	10.0667	Germany	1.57	1.44	6
cs28833	**7408**	Wt-3	CS6894	Kranz	52.3	9.3	Germany	37.4	12	6

cs28822	**7411**	Wl-0	CS6920	Kranz	47.9299	10.8134	Germany	131	9.67	6
cs28847	**7418**	Zu-1	CS6903	Kranz	47.3667	8.55	Switzerland	9.87	4.91	5
cs28369	**7424**	Jl-3	CS6745	Kranz	49.2	16.6166	Czech Republic	3.02	1.95	6
cs28527	**7430**	Nc-1	CS6802	Kranz	48.6167	6.25	France	2.91	1.26	6
cs28510	**7446**	N4	CS22482	Savushkin	61.36	34.15	Russia	43	8.08	6
cs28513	**7449**	N7	CS22485	Savushkin	61.36	34.15	Russia	40.1	10.2	6
cs28812	**7477**	WAR	CS8143	Pigliucci	41.7302	-71.2825	USA	30	8.55	6
cs28614	**7483**	PHW-14	CS6061	Williams	51.2878	0.0565	UK	13.3	4.5	6
cs28620	**7490**	PHW-20	CS6071	Williams	51.2878	0.0565	UK	3.78	1.56	6
cs28626	**7496**	PHW-26	CS6081	Williams	50.6728	-3.8404	UK	7.85	3.16	6
cs28631	**7502**	PHW-31	CS6088	Williams	51.4666	-3.2	UK	37.4	12.3	6
cs28633	**7504**	PHW-33	CS6092	Williams	52.25	4.5667	Netherlands	46	8.59	6
cs28635	**7506**	PHW-35	CS6096	Williams	48.6103	2.3086	France	14.4	1.27	6
cs28636	**7507**	PHW-36	CS6098	Williams	48.6103	2.3086	France	0.103	0.043	6
cs28637	**7508**	PHW-37	CS6099	Williams	48.6103	2.3086	France	8.11	1.41	6
cs76212	**8244**	PHW-34	N6034	Williams	48.6103	2.3086	France	0.259	0.213	6
cs76087	**8251**	Ag-0	CS22630	Kranz	45	1.3	France	34	8.84	6
cs76088	**8252**	Alc-0	N1656	Roldan	40.31	-3.22	Spain	19.3	7.62	6
cs76091	**8253**	An-1	CS22626	Kranz	51.2167	4.4	Belgium	0.693	0.433	6
cs76097	**8264**	Bla-1	N971	Kranz	41.6833	2.8	Spain	16.3	6.68	6
cs76098	**8265**	Blh-1	N1031	Kranz	48	19	Czech Republic	59.3	27.7	6
cs76100	**8268**	Bor-4	CS22591	Nordborg	49.4013	16.2326	Czech Republic	2.2	1.31	4
cs76105	**8272**	Bur-0	CS22656	Kranz	54.1	-6.2	Ireland	40.9	12.6	6
cs76127	**8291**	Est-1	CS22629	Kranz	58.3	25.3	Russia	3.15	2.58	5
cs76133	**8295**	Ga-0	CS22634	Kranz	50.3	8	Germany	39.9	9.97	6
cs76137	**8300**	Gr-1	N1199	Hauser	47	15.5	Austria	3.78	1.86	6
cs76140	**8304**	Hi-0	N1227	Kranz	52	5	Netherlands	7.58	2.74	6
cs76147	**8311**	In-0	N1239	Kranz	47.5	11.5	Austria	1.9	0.691	4
cs76203	**8352**	Oy-0	CS22658	Kranz	60.23	6.13	Norway	16.4	8.95	6
cs76210	**8354**	Per-1	N1445	Kranz	58	56.3167	Russia	19.2	11.3	5
cs76211	**8355**	Petergof	N926	Vizir	59	29	Russia	32.1	6.93	6
cs76214	**8360**	Pro-0	CS22649	Bergelson	43.25	-6	Spain	21.4	5.04	6

cs76215	**8361**	Pu2-23	CS22593	Cetl	49.42	16.36	Czech Republic	6.5	2.05	6
cs76222	**8374**	Rsch-4	CS1494	Holub	56.3	34	Russia	87	32.6	6
cs76242	**8389**	Ta-0	N1549	Kranz	49.5	14.5	Czech Republic	10.9	5.63	6
cs76244	**8390**	Tamm-2	CS22604	Savolainen	60	23.5	Finland	10.6	1.68	6
cs76297	**8400**	Van-0	CS22627	Kranz	49.3	-123	Canada	7.43	1.82	6
cs76301	**8404**	Wei-0	CS22622	Holub	47.25	8.26	Switzerland	0.726	0.217	6
cs76304	**8407**	Wt-5	CS22637	Kranz	52.3	9.3	Germany	5.31	2.06	6
cs76306	**8410**	Zdr-6	CS22589	Nordborg	49.3853	16.2544	Czech Republic	11.7	1.81	6
cs76194	**8429**	N13	CS22491	Savushkin	61.36	34.15	Russia	1.47	0.573	6